

NITRIC OXIDE-RELEASING ALGINATES AS A DUAL-ACTION THERAPEUTIC FOR
CYSTIC FIBROSIS

Mona Jasmine R. Ahonen

A dissertation submitted to the faculty at the University of North Carolina at Chapel Hill in partial fulfillment of the requirements for the degree of Doctor of Philosophy in the Department of Chemistry (Polymer/Materials Chemistry).

Chapel Hill
2019

Approved By:

Mark H. Schoenfisch

Wei You

James F. Cahoon

David B. Hill

Camille Ehre

© 2019
Mona Jasmine R. Ahonen
ALL RIGHTS RESERVED

ABSTRACT

Mona Jasmine R. Ahonen: NITRIC OXIDE-RELEASING ALGINATES AS A DUAL-ACTION THERAPEUTIC FOR CYSTIC FIBROSIS
(Under the direction of Mark H. Schoenfisch)

Cystic fibrosis (CF) is an inherited disease characterized by impaired mucociliary clearance of thick mucus and persistent bacterial infection in the lungs. Nitric oxide (NO), an endogenously produced radical with integral roles in the mammalian immune response to foreign pathogens, holds promise as a CF therapy. Inhalation of exogenous NO-releasing biopolymers represents an attractive therapeutic strategy as NO release can be sustained for hours, allowing for near continuous delivery. Alginate is particularly promising for this application due to its water solubility, mucus-altering ability, and biocompatibility. Herein, we evaluated the utility of NO-releasing alginates as a dual-action (i.e., mucolytic and antibacterial) CF therapeutic.

Low (~5 kDa) and high (~300 kDa) molecular weight alginate were first modified with a series of small molecule alkyl amines via carbodiimide chemistry to store and release NO, with release kinetics dependent on the precursor amine structure. The liberated NO showed bactericidal activity against *Pseudomonas aeruginosa* and *Staphylococcus aureus* with pathogen eradication efficiency dependent on both molecular weight and NO-release kinetics. Toxicity against human respiratory epithelial cells proved negligible at NO-releasing alginate concentrations required to achieve biofilm eradication.

The excessive production of thick mucus in CF leads to airway obstruction and provides a suitable environment for bacteria colonization. The impact of NO-releasing alginates on the viscoelasticity of human bronchial epithelial mucus was investigated using parallel plate rheology. The efficacy of the NO-releasing alginates was shown to be dependent on molecular weight, NO-release kinetics, and dose. Nitric oxide-releasing alginates also achieved greater reduction in mucus rheology than both NO-releasing chitosan, a biocompatible cationic polymer, and *N*-acetyl cysteine, a conventional mucolytic agent.

Biofilm-forming pathogens, the major contributor to mortality in CF, are difficult to treat due to additional protection provided by both the biofilm exopolysaccharide matrix and mucus in the airways. The antibiofilm efficacy of NO-releasing alginates were evaluated against *P. aeruginosa*, *Burkholderia cepacia* complex, *S. aureus*, and methicillin-resistant *S. aureus* biofilms under CF-relevant conditions. The NO-releasing alginates were highly antibacterial against the four pathogens, with biocidal efficacy dependent on NO-release kinetics. Relative to tobramycin and vancomycin, the NO-releasing alginates proved to be more effective regardless of growth conditions.

To my mom, whose unconditional love
and endless support continuously inspire me.

ACKNOWLEDGEMENTS

This work would not be possible without the collaborative effort of many people I am deeply grateful for. First, I would like to thank my advisor Mark Schoenfisch, for his guidance and supervision, and for always believing in me and my abilities as a research scientist. Graduate school takes a lot of hard work and a whole lot of luck. I know without a doubt that I was lucky to be your student. Thank you for giving me your trust and for constantly challenging me with the projects you entrusted me with. I have grown a lot these past years and it would not have been possible without a mentor like you. I also thank my undergraduate advisor, Sunghee Lee, for encouraging me to pursue a doctorate degree and cultivating my love for chemistry. I would also like to thank David Hill for all his help and supervision with the rheological studies, and for acting as a second mentor throughout my graduate career. Thank you for expanding my knowledge and understanding of my project, and for the guidance and support in finishing this work.

The research presented in this work was made possible through the contributions of colleagues both inside and outside of the Schoenfisch lab. I would like to thank William Kissner for his help with the rheological studies and for preparing the mucus samples used in the study. Of the previous members of the Schoenfisch group, I thank Katelyn Reighard who helped and guided me in starting out this project, which involved training me on the multiple lab instruments and sending various helpful articles my way as I learned more about cystic fibrosis, antibacterial therapies, mucoadhesion, and rheology. I would also like to thank Brittany Worley for her strict supervision and help in training me to do biological experiments, Dakota Suchyta for his help in

getting the alginate synthesis going, and Robert Soto for his sage advice when dealing with experiment hiccups and for always being there as a big brother for the rest of the lab. I also thank Pedro de Jesus Cruz for his friendship, camaraderie, and help with the chitosan reaction. Lastly, I would like to give special thanks to Micah Brown for not only reading and patiently editing various drafts of this dissertation, but for also being the best friend a girl could ask for over the last few years together in the lab. Thank you for your kindness, sassy and sarcastic humor, and support over the years.

Within the current lab members, I would like to thank Evan Feura, Lei Yang, Jackson Hall, James Taylor, Kaitlyn Rouillard, and Maggie Maloney-Povolny for their years of friendship, witticism, and endless conversations that have made long days in lab go by faster. I would also like to thank Sara Maloney for her friendship and all the coffee runs that seem to be an integral part of the whole graduate school experience for us. I also had the pleasure of mentoring two phenomenal undergraduates, David Zhu and Jamie Dorrier, during my time in the Schoenfish lab. Thank you for all the hard work. Your passion for research and drive will surely aid you in whatever future you decide to pursue.

Finally, I would like to thank my friends and family who have supported me throughout graduate school. To my grandmother, Carmen Rosales, I miss you terribly and I thank you for your sacrifices. I would not make it here if not for that. To my Mommy Thel, thank you for loving me like I was your own daughter and for supporting my education. Lastly, to my mom, thank you for being my rock, my strength, and my source of courage and inspiration over the years. Your unconditional love, supervision, and limitless support has given me the determination to never give up in the pursuit of my dreams. Thank you for being my first mentor and for always continuing the fight with me. I am where I am today because of you.

TABLE OF CONTENTS

LIST OF TABLES	xiv
LIST OF FIGURES	xv
LIST OF ABBREVIATIONS AND SYMBOLS	xx
CHAPTER 1: DESIGNING A NOVEL DUAL-ACTION NITRIC OXIDE-BASED THERAPEUTIC FOR CYSTIC FIBROSIS.....	1
1.1 Cystic fibrosis pathogenesis.....	1
1.1.1 Airway surface liquid in healthy lungs.....	1
1.1.2 Mucus accumulation in CF airways.....	6
1.1.3 Bacterial lung infection in CF.....	6
1.1.4 Inflammation and lung degradation.....	9
1.2 Current treatment methods for cystic fibrosis.....	10
1.2.1 CFTR modulators.....	10
1.2.2 Hypertonic saline and mucolytic agents.....	11
1.2.3 Antibiotics.....	13
1.2.4 Anti-inflammatory agents.....	15
1.2.5 Lung transplantation.....	15
1.3 Nitric oxide as a potential CF therapeutic.....	16
1.3.1 Physiological roles of nitric oxide.....	16

1.3.2	Nitric oxide as an antimicrobial agent	17
1.3.3	Nitric oxide in CF therapy	20
1.4	Nitric oxide delivery.....	23
1.4.1	Small molecule nitric oxide donors	23
1.4.2	Macromolecular scaffolds for nitric oxide delivery.....	25
1.5	The ideal NO-releasing scaffold for CF delivery.....	26
1.5.1	Initial work with nitric oxide-releasing chitosan oligosaccharide	28
1.5.2	Limitations of chitosan oligosaccharides for NO delivery in CF	29
1.6	Alginate in the treatment of cystic fibrosis	30
1.6.1	Alginate as a potential scaffold for NO delivery	30
1.6.2	Alginate in antibacterial applications.....	33
1.6.3	Alginate as a potentiator for antimicrobial activity	34
1.6.4	Alginate as a mucomodulator	35
1.7	Summary of dissertation research	36
	REFERENCES.....	38
	CHAPTER 2: NITRIC OXIDE-RELEASING ALGINATES	52
2.1	Introduction	52
2.2	Experimental Section	54
2.2.1	Materials	54
2.2.2	Instrumentation	55

2.2.3	Oxidative degradation of alginates	55
2.2.4	Synthesis of polyamine-modified alginates (AlgMW-alkyl amine).....	56
2.2.5	Synthesis of NO-releasing alginates	59
2.2.6	Characterization of NO storage and release.....	61
2.2.7	Planktonic bactericidal assay	61
2.2.8	Biofilm eradication assay.....	62
2.2.9	Time-Based Biofilm Eradication Assay	63
2.2.10	In vitro cytotoxicity assay.....	63
2.3	Results and Discussion.....	64
2.3.1	Synthesis of N-diazeniumdiolate-modified biopolymers	65
2.3.2	Antibacterial action against planktonic bacteria	73
2.3.3	Antibiofilm efficacy.....	78
2.3.4	In vitro cytotoxicity against A549 cells	83
2.4	Conclusions	85
	REFERENCES.....	86
CHAPTER 3: RHEOLOGY OF MUCUS TREATED WITH NITRIC OXIDE-RELEASING ALGINATES		91
3.1	Introduction	91
3.2	Experimental Section	93
3.2.1	Materials	93
3.2.2	Instrumentation	94

3.2.3	Oxidative degradation of biopolymers.....	95
3.2.4	Synthesis of polyamine-modified alginates (AlgMW-alkyl amine).....	95
3.2.5	Synthesis of tosylated-aminoethyl Schiff base (TES)	100
3.2.6	Synthesis of ethylamine-modified chitosan oligosaccharides (COS-EA)	100
3.2.7	Synthesis of N-diazeniumdiolate-modified biopolymers	102
3.2.8	Characterization of nitric oxide release	102
3.2.9	Preparation of mucus sample	103
3.2.10	Parallel plate rheology	104
3.2.11	Statistical analysis.....	104
3.3	Results and Discussion.....	105
3.3.1	Synthesis of N-diazeniumdiolate-modified biopolymers	105
3.3.2	Effect of molecular weight on alginate-treated mucus rheology.....	109
3.3.3	Effect of varying functional group and biopolymer charge on mucus.	112
3.3.4	Effect of nitric oxide-release kinetics	116
3.3.5	Dose-dependent effects.....	120
3.3.6	Efficacy compared to N-acetyl cysteine (NAC)	122
3.4	Conclusions	125
	REFERENCES.....	127
CHAPTER 4: ANTIBIOFILM EFFICACY OF NITRIC OXIDE-RELEASING		
ALGINATES AGAINST CYSTIC FIBROSIS BACTERIAL PATHOGENS . 132		
4.1	Introduction	132

4.2	Experimental Section	134
4.2.1	Materials	134
4.2.2	Bacterial strains and media	135
4.2.3	Instrumentation	136
4.2.4	Oxidative degradation of alginate	136
4.2.5	Synthesis of polyamine-modified alginates (AlgMW-alkyl amine).....	136
4.2.6	Synthesis of N-diazeniumdiolate-modified alginates	139
4.2.7	Characterization of nitric oxide release	139
4.2.8	Biofilm eradication assays	140
4.2.9	Time-based biofilm eradication assay	141
4.2.10	Statistical analysis	141
4.3	Results and Discussion.....	141
4.3.1	Nitric oxide release in biological media.	142
4.3.2	Antibiofilm efficacy.....	148
4.3.3	Effect of nitric oxide-release kinetics on antibiofilm efficacy.....	155
4.4	Conclusions	158
	REFERENCES.....	160
	CHAPTER 5: SUMMARY AND FUTURE DIRECTIONS	165
5.1	Summary	165
5.2	Future Directions.....	167

5.2.1	Combination therapy with current CF treatments.....	168
5.2.2	Biophysical characterization of biofilms and CF sputum.....	169
5.2.3	Biopolymeric scaffolds for improved nitric oxide storage and release	170
5.3	Conclusion.....	173
	REFERENCES.....	175
	APPENDIX A: SUPPLEMENTAL INFORMATION FOR CHAPTER 3.....	178

LIST OF TABLES

Table 2.1	Molecular weight of alkyl amine-modified alginate as a function of added alkyl amine ratio. ^a	66
Table 2.2	Elemental (CHN) analysis, zeta potential measurements, and reaction yields for secondary amine-functionalized alginate. ^a	70
Table 2.3	Nitric oxide-release properties of <i>N</i> -diazoniumdiolate-functionalized alginates in PBS (pH 7.4, 37 °C). ^a	74
Table 2.4	Minimum bactericidal concentrations (MBC _{4h}) of NO-releasing alginates against planktonic <i>P. aeruginosa</i> and <i>S. aureus</i> . ^a	76
Table 2.5	Minimum biofilm eradication concentrations (MBEC _{24h}) of NO-releasing alginates against <i>P. aeruginosa</i> and <i>S. aureus</i> biofilms. ^a	80
Table 3.1	Optimization of oxidative degradation of alginate. ^a	96
Table 3.2	Physicochemical characterization for secondary amine-functionalized alginate and chitosan biopolymers. ^a	97
Table 3.3	Nitric oxide-release properties of <i>N</i> -diazoniumdiolate-functionalized biopolymers in PBS at pH 6.5 and 37 °C. ^a	108
Table 3.4	Reduction in elastic and viscous modulus with respect to untreated 3 wt % HBE mucus after treatment for 24 h. ^a	111
Table 3.5	Nitric oxide dose and corresponding reduction in elastic and viscous moduli of 3 wt % HBE mucus after treatment with either NO-releasing alginate or chitosan oligosaccharide. ^a	114
Table 3.6	Reduction in elastic and viscous moduli of 3 wt % HBE mucus after treatment with <i>N</i> -acetylcysteine (NAC). ^a	123
Table 4.1	Nitric oxide-release properties of <i>N</i> -diazoniumdiolate-functionalized biopolymers in PBS (pH 6.5, 37 °C). ^a	143
Table 4.2	Nitric oxide-release properties of NO donor-functionalized alginates in ASM (pH 6.5, 37 °C). ^a	144
Table 4.3	Minimum biofilm eradication concentrations (MBEC _{24h}) of NO-releasing alginates against aerobic biofilms. ^a	150
Table 4.4	Minimum biofilm eradication concentrations (MBEC _{24h}) of NO-releasing alginates against anaerobic biofilms. ^a	154

LIST OF FIGURES

Figure 1.1	The cycle of physiological consequences in the airways resulting from cystic fibrosis.	2
Figure 1.2	The airway surface liquid (ASL), composed of the mucus layer and the periciliary layer in healthy airways. Inhaled particles are trapped within the mucus layer and cleared from the lungs through mechanical clearance by cilia in the PCL.	4
Figure 1.3	Dysregulation of ionic content in ASL impairs mucociliary clearance. In healthy airways, regulation of ionic content is maintained via the epithelial sodium channel (ENaC), which absorbs Na ⁺ , and the calcium-activated Cl ⁻ channel (CaCC) and the CFTR, which secretes Cl ⁻ in the airways. In CF airways, ionic content is dysregulated due to mutations in the CFTR chloride channel and results in the dehydration of both the mucus layer and the PCL. This leads to the collapse of the cilia in the PCL and failure to clear mucus in the lungs.	5
Figure 1.4	The CF microbiome described by pathogen prevalence as a function of age in the US. Reprinted with permission from the 2016 Patient Registry Annual Data Report to the Center Directors (CF Foundation).	7
Figure 1.5	Biofilm-based bacterial colonization in the CF airways. Accumulation of a thick, stagnant mucus layer obstructs the airways and provides a suitable environment for biofilm-based bacterial colonization. Both mucus and the biofilm exopolysaccharide matrix provide additional protection by limiting drug. In addition, slower growth rate and the different biofilm microenvironments reduce efficacy of antibiotics against biofilm-based infections.	14
Figure 1.6	The multi-mechanistic pathways of NO's antibacterial activity. Nitrosative and oxidative stress is exerted by reactive byproducts such as dinitrogen trioxide (N ₂ O ₃) and peroxyxynitrite (ONOO ⁻). Reprinted with permission from Hetrick et al. Copyright 2008, American Chemical Society.	18
Figure 1.7	Formation and subsequent decomposition pathways of (A) <i>S</i> -nitrosothiols and (B) <i>N</i> -diazoniumdiolates.	24
Figure 1.8	Alginate polysaccharide composed of α-L-guluronic acid (G) and β-D-mannuronic acid (M) residues.	32
Figure 2.1	Synthesis of amine-functionalized alginate.	57
Figure 2.2	Synthesis of <i>N</i> -diazoniumdiolate-modified alginates.	60

Figure 2.3	(A) Representative ¹ H NMR spectrum for Alg300, and (B) representative ¹³ C NMR spectrum for Alg300 in D ₂ O. Control ¹³ C NMR of (C) Alg300 with free SPER and (D) SPER-modified Alg300.....	67
Figure 2.4	Representative ¹ H NMR spectra for (A) DETA-, (B) DPTA-, (C) PAPA-; and, (D) SPER-modified Alg5 (top) and Alg300 (bottom) in D ₂ O.	68
Figure 2.5	Representative ¹³ C NMR spectra for (A) DETA-, (B) DPTA-, (C) PAPA-; and, (D) SPER-modified Alg5 (top) and Alg300 (bottom) in D ₂ O.	69
Figure 2.6	Representative UV-vis spectra for (A) DETA-, (B) DPTA-, (C) SPER-; and, (D) PAPA-modified alginates with (dash) and without (solid) <i>N</i> -diazeniumdiolate NO donors.	71
Figure 2.7	(A)Real time NO-release profiles for the first 1 h and (B) plot of total NO release vs. time for NO-releasing DETA- (solid), DPTA- (dash), SPER- (dash-dot); and PAPA- (dot) modified alginates measured via chemiluminescence in pH 7.4 PBS.....	72
Figure 2.8	Antibacterial efficacy of high (square) and low (circle) molecular weight NO-releasing (filled) and control (hollow) (A) DETA-, (B) DPTA-, (C) SPER-; and, (D) PAPA-modified alginates against planktonic <i>P. aeruginosa</i> and <i>S. aureus</i> . Error bars represent standard deviation of the mean viability (CFU/mL). For all measurements, n ≥ 3 pooled experiments.	75
Figure 2.9	Antibiofilm efficacy of high (square) and low (circle) molecular weight NO-releasing (filled) and control (hollow) (A) DETA-, (B) DPTA-, (C) SPER-; and, (D) PAPA-modified alginates against planktonic <i>P. aeruginosa</i> and <i>S. aureus</i> . Error bars represent standard deviation of the mean viability (CFU/mL). For all measurements, n ≥ 3 pooled experiments.	79
Figure 2.10	Time-based bactericidal efficacy of Alg300-DETA/NO (square), Alg300-DPTA/NO (circle), Alg300-SPER/NO (triangle), and Alg300-PAPA/NO (diamond). Comparison of all high molecular weight NO-releasing alginates at equivalent concentrations of 8 mg/mL is presented in (A), and the time-based killing of the fast NO-releasing systems (Alg300-SPER/NO and Alg300-PAPA/NO) at their respective MBEC _{24h} is presented in (B). Studies consisted of at least three experiments with error bars representing the standard deviation.	82

Figure 2.11	Viability of A549 human respiratory epithelial cells exposed to control and NO-releasing (white) and control (dash) alginates at the MBEC _{24h} against (A) <i>P. aeruginosa</i> and (B) <i>S. aureus</i> . Studies consisted of at least three experiments with error bars representing the standard deviation.	84
Figure 3.1	(A) Synthesis of tosyl-modified ethanolamine Schiff base. (B) Synthesis of ethanolamine-modified chitosan oligosaccharides.....	101
Figure 3.2	Representative (A) ¹ H NMR and (B) ¹³ C NMR spectra of Alg5-PAPA-DPTA.	106
Figure 3.3	Elastic and viscous moduli of 3 wt% human bronchial epithelial (HBE) mucus following treatment with 20 mg/mL Alg300 (black solid), Alg10 (black diagonal), Alg5 (gray solid), and Alg1 (gray diagonal). Single asterisks (*) indicate significant differences (p < 0.05) relative to untreated sample (hollow).	110
Figure 3.4	Elastic and viscous moduli of 3 wt% human bronchial epithelial (HBE) mucus following treatment with 20 mg/mL unmodified (solid), modified (horizontal stripe), and NO-releasing (diagonal stripe) (A) Alg5-DETA, (B) Alg5-DPTA, (C) Alg5-PAPA, (D) Alg5-SPER, (E) Alg5-PAPA-DPTA, and (F) COS-EA. Values presented as the mean standard error of the mean for n = 3 experiments. Asterisks (*) indicate significant differences (p < 0.05) relative to untreated sample (hollow).	113
Figure 3.5	Elastic and viscous moduli of 3 wt% HBE mucus following treatment with (A) COS-EA, (B) Alg5-DPTA, (C) Alg5-PAPA, and (D) Alg5-PAPA-DPTA after 1 hour (black solid), 3 hours (black diagonal), 5 hours (gray solid), and 24 hours (gray diagonal) exposure. Asterisks (*) indicate significant differences (p < 0.05) relative to untreated sample (hollow).	117
Figure 3.6	Elastic and viscous moduli of 3 wt% HBE mucus following treatment with (A) COS-EA/NO, (B) Alg5-DPTA/NO, (C) Alg5-PAPA/NO, and (D) Alg5-PAPA-DPTA/NO after 1 hour (black solid), 3 hours (black diagonal), 5 hours (gray solid), and 24 hours (gray diagonal) exposure. Asterisks (*) indicate significant differences (p < 0.05) relative to untreated sample (hollow).	118
Figure 3.7	Elastic (circle) and viscous (square) moduli of 3 wt% HBE mucus following treatment with 20, 40, 60, and 80 mg/mL concentrations of control (hollow) and NO-releasing (solid) (A) Alg5-PAPA-DPTA and (B) COS-EA.	121

Figure 3.8	Elastic and viscous moduli of 3 wt% HBE mucus following treatment with NAC at 0.1 wt% (black solid), 0.2 wt % (black diagonal), 10 wt % (gray solid), and 20 wt% (gray diagonal). Values presented as the mean standard error of the mean for n = 3 experiments. Asterisks (*) indicate significant differences (p < 0.05) relative to untreated sample (hollow).	124
Figure 4.1	(A) Real-time NO-release profiles for the first 1 h and (B) plot of total NO release vs. time for representative biopolymers Alg5-DETA/NO (—), Alg5-DPTA/NO (— —), Alg5-SPER/NO (— ■ ■), Alg5-PAPA/NO (■), and Alg5-PAPA-DPTA/NO (— ■ —) measured via chemiluminescence in ASM pH 6.5.	145
Figure 4.2	Real-time NO-release profiles for the first hour of release for (A) Alg5-DPTA/NO, (B) Alg5-PAPA/NO, and (C) Alg5-PAPA-DPTA/NO in PBS (solid), ASM (dash-dot), mucin (dot), and DNA (dash) solutions buffered at pH 6.5.....	147
Figure 4.3	Antibiofilm efficacy of Alg5-DETA (circle), Alg5-DPTA (triangle), Alg5-SPER (square), Alg5-PAPA (diamond), and Alg5-PAPA-DPTA (cross) against <i>S. aureus</i> biofilms under (A) aerobic and (B) anaerobic conditions. Error bars represent standard deviation of the mean viability (CFU/mL). For all measurements, n ≥ 3 pooled experiments.	149
Figure 4.4	Nitric oxide dose for Alg5-DETA (light gray stripes), Alg5-DPTA/NO (solid light gray), Alg5-SPER/NO (dark gray stripes), Alg5-PAPA/NO (solid dark gray), Alg5-PAPA-DPTA/NO (black stripes) required to treat (A) aerobic and (b) anaerobic biofilms compared to tobramycin (solid black). Studies consisted of at least three experiments with error bars representing the standard deviation.....	153
Figure 4.5	Nitric oxide dose for Alg5-DETA (light gray stripes), Alg5-DPTA/NO (solid light gray), Alg5-SPER/NO (dark gray stripes), Alg5-PAPA/NO (solid dark gray), Alg5-PAPA-DPTA/NO (black stripes) required to treat (A) aerobic and (b) anaerobic biofilms of <i>S. aureus</i> and MRSA. All starting NO doses were compared to vancomycin (solid black). Studies consisted of at least three experiments with error bars representing the standard deviation.	156
Figure 4.6	Time-based bactericidal efficacy of Alg5-DPTA/NO (circle), Alg5-PAPA-DPTA/NO (triangle), Alg5-PAPA/NO (square), and tobramycin (cross). Comparison of all NO-releasing alginates at equivalent concentrations of (A) 4 mg/mL under aerobic conditions and (B) 2 mg/mL under anaerobic conditions. The MBEC _{24h} values under aerobic and anaerobic conditions (2 mg/mL and 4 mg/mL,	

	respectively) were used for tobramycin. Studies consisted of at least three experiments with error bars representing the standard deviation.	157
Figure 5.1	Structures of (A) hyaluronic acid and (B) cyclodextrin biopolymers.....	172
Figure A.1	Representative ¹ H NMR spectra of tosyl-modified ethanolamine Schiff base (TES).....	179
Figure A.2	Representative ¹ H NMR spectra of COS-EA.	179
Figure A.3	Representative UV-vis spectra for secondary amine- (dash) and <i>N</i> -diazoniumdiolate-modified (solid) (for (A) Alg5-DETA, (B) Alg5-DPTA, (C) Alg5-SPER, (D), Alg5-PAPA, (E) Alg5-PAPA-DPTA, and (F) chitosan oligosaccharides (COS-EA).	179
Figure A.4	(A) Real time NO-release profiles for the first 1 h and (B) plot of total NO release vs. time for representative biopolymers Alg5-DETA/NO (—), Alg5-DPTA/NO (— —), Alg5-PAPA-DPTA/NO (— ■ —), Alg5-PAPA/NO (■), Alg5-SPER/NO (— ■ ■), and COS-EA/NO (●) measured via chemiluminescence in PBS pH 6.5.....	179
Figure A.5	Complex viscosity of 3 wt% HBE mucus following treatment with Alg5-DETA (black solid), Alg5-DPTA (black horizontal), Alg5-SPER (black diagonal), Alg5-PAPA (gray solid), Alg5-PAPA-DPTA (gray horizontal), and COS-EA (gray diagonal). Values presented as the mean standard deviation of the mean for n = 3 experiments. Asterisks (*) indicate significant differences (p < 0.05) relative to untreated sample (hollow).	179
Figure A.6	Complex viscosity of 3 wt% HBE mucus following treatment with NAC 0.1 wt% (black solid), NAC 0.2 wt% (black diagonal), NAC 10 wt% (gray solid), and NAC 20 wt% (gray diagonal). Values presented as the mean standard deviation of the mean for n = 3 experiments. Asterisks (*) indicate significant differences (p < 0.05) relative to untreated sample (hollow).	179

LIST OF ABBREVIATIONS AND SYMBOLS

%	percent
~	approximately
<	less than
>	greater than
≤	less than or equal to
≥	greater than or equal to
±	plus or minus
× g	times the force of gravity
°C	degree(s) Celsius
Δ	delta
μg	microgram(s)
μL	microliter(s)
μM	micromolar
μmol	micromole(s)
A549	adenocarcenomic human alveolar epithelial cells
Abs	absorbance
Alg	alginate

ASM	artificial sputum media
Ar	argon
ASL	airway surface liquid
BCC	<i>Burkholderia cepacia</i> complex
¹³ C NMR	carbon nuclear magnetic resonance
CF	cystic fibrosis
CFTR	cystic fibrosis transmembrane regulator
CFU	colony forming units
cGMP	cyclic guanosine monophosphate
cm	centimeter
Cl ⁻	chloride ion
COS	chitosan oligosaccharides
COS-EA	ethanolamine-modified chitosan oligosaccharides
d	day(s)
D ₂ O	deuterium oxide
DETA	diethylenetriamine
DPTA	bis(3-amino)propylamine
DNA	deoxyribonucleic acid

e.g.	exempli gratia (for example)
EDC	1-ethyl-3-(3-(dimethylamino)propyl)-carbodiimide hydrochloride
EDTA	ethylenediaminetetraacetic acid
ENaC	epithelial Na ⁺ (sodium) channel
eNOS	endothelium nitric oxide synthase
EPS	exopolysaccharide
et al.	et alia (and others)
FDA	Food and Drug Administration
g	gram(s)
G	α -L-guluronic acid
¹ H NMR	proton nuclear magnetic resonance
h	hour(s)
<i>H. influenzae</i>	<i>Haemophilus influenzae</i>
H ₂ O	water
HBE	human bronchial epithelial
i.e.	id est (that is)
iNOS	inducible nitric oxide synthase
kDa	kilodalton

LB	Luria Bertani (broth)
M	molar
M	β -D-mannuronic acid
MW	molecular weight
MBC _{4h}	4 h minimum bactericidal concentration
MBEC	minimum biofilm eradication concentration
mg	milligram(s)
MIC	minimum inhibitory concentration
min	minute(s)
mL	milliliter(s)
MRSA	methicillin-resistant <i>Staphylococcus aureus</i>
MSD	mean squared displacement
MTS	3-(4,5-dimethylthiazol-2-yl)-5-(3-carboxymethoxyphenyl)-2-(4-sulfophenyl)-2H-tetrazolium
mV	millivolt
m Ω	miliohm(s)
N ₂	nitrogen
N ₂ O ₃	dinitrogen trioxide
NAC	<i>N</i> -acetylcysteine

NHS	<i>N</i> -hydroxysuccinimide
nM	nanomolar
nm	nanometer(s)
nNOS	neuronal nitric oxide synthase
NO	nitric oxide
NOA	nitric oxide analyzer
O ₂	oxygen
ONOO ⁻	peroxynitrite
<i>P. aeruginosa</i>	<i>Pseudomonas aeruginosa</i>
PAK	<i>Pseudomonas aeruginosa</i> strain K
PAPA	<i>N</i> -propyl-1,3-propanediamine
PAMAM	poly(amidoamine)
PB	phosphate buffered
PBS	phosphate buffered saline
PCL	periciliary layer
PDI	polydispersity index
PEG	polyethylene glycol
pH	-log of proton concentration

PGM	type II pig gastric mucin
PMS	phenazine methosulfate
PLGA	poly lactic-co-glycolic acid
pM	picomolar
ppb	part per billion
ppm	parts per million
PS	penicillin streptomycin
RPMI 1640	Roswell Park Memorial Institute 1640 cell medium
RNS	reactive nitrogen species
ROS	reactive oxygen species
RSNO	<i>S</i> -nitrosothiol
s	second(s)
SPER	spermine
<i>S. aureus</i>	<i>Staphylococcus aureus</i>
SNP	sodium nitroprusside
$t_{1/2}$	half-life
t[NO]	total NO release
t[NO] _{4h}	4 h total NO release

ta	duration of NO release
TES	tosylated ethanolamine Schiff base
TSA	tryptic soy agar
TSB	tryptic soy broth
UNC	University of North Carolina (at Chapel Hill)
US	United States
UV	ultraviolet
vis	visible
vol%	volume to volume ratio
v/v/v	volume to volume to volume ratio
w	weeks
wt%	percent weight per volume

CHAPTER 1: DESIGNING A NOVEL DUAL-ACTION NITRIC OXIDE-BASED THERAPEUTIC FOR CYSTIC FIBROSIS

1.1 Cystic fibrosis pathogenesis

Cystic fibrosis (CF) is a lethal autosomal disorder affecting over 70,000 people worldwide.^{1,2} The disease results from mutations in the CF transmembrane conductance regulator (CFTR), which controls ion (i.e., chloride) transport in epithelial membranes.³⁻⁵ Defects in the CFTR lead to dysregulation of epithelial fluid transport and affect multiple organs, such as the pancreas, liver, kidneys, and the lungs. However, the most debilitating effects are observed in the respiratory tract. In the airways, loss of CFTR function causes dehydration of the airway surface liquid (ASL) and ultimately interferes with mucociliary clearance.⁶⁻⁸ As a result, thick stagnant mucus accumulates and obstructs the airways. Nutrients in mucus foster a suitable environment for the colonization of various bacterial pathogens, including *Pseudomonas aeruginosa*.⁹ *P. aeruginosa* infections in particular lead to significant morbidity and mortality in CF patients. Persistent colonization by pathogens in general elicit a strong host inflammatory response and lung function degradation.¹⁰ This vicious cycle (Figure 1.1) results in respiratory failure that accounts for ~90% of patient mortality.¹⁰⁻¹²

1.1.1 Airway surface liquid in healthy lungs

In healthy lungs, the ASL acts as an innate defense barrier against inhaled particles (e.g., dust, pollen, chemical irritants) and invading pathogens (e.g., bacteria, viruses).^{7,13,14} The ASL is composed of two parts: the mucus layer and the periciliary layer (PCL), the latter separating the

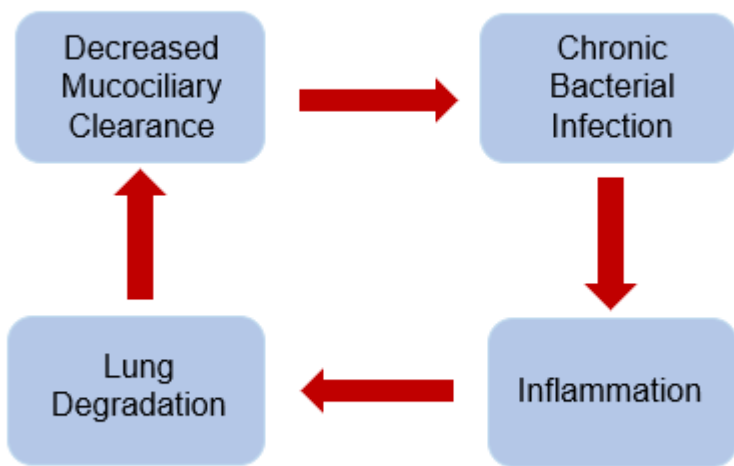


Figure 1.1 The cycle of physiological consequences in the airways resulting from cystic fibrosis.

mucus layer from the epithelial surface of the airways.⁷ Mucus is produced and secreted by different types of cells in the body, with the goblet cells responsible for the production of mucin glycoproteins, the main components of mucus.^{7,15} The mucus layer is composed of 95% water and 2% mucins (the component that dictates its gel-like properties), with the remaining 3% made up of proteins, lipids, and inorganic salts.^{15,16} As a result, mucus is able to entrap inhaled foreign materials and transport them out of the lungs through the motion of ciliated surfaces within the airways.^{7,16} The PCL is $\sim 7 \mu\text{m}$ thick and has a low viscosity and a tightly regulated ionic content; these properties allow the ciliated epithelial cells of the airways to beat unrestricted and propel the mucus layer, a process called mucociliary clearance (Figure 1.2).^{7,17} Epithelial cells are closely packed, forming a dense field of cilia, interrupted only by islands of goblet cells and mucus gland openings.⁷ The PCL thickness allows for optimal contact between cilia and the mucus layer.⁷ The cilia are mostly immersed in the PCL, with only their tips embedded in the mucus layer. The cilia beat in a synchronized, wave-like manner to propel mucus towards the trachea.^{7,18}

To regulate the thickness and volume of the PCL, proper ionic composition of the PCL is required.^{7,18} The necessary ionic concentration is maintained through the absorption of sodium (Na^+) via the epithelial sodium channel (ENaC) and secretion of chloride (Cl^-) in the airways by the calcium-activated Cl^- channel (CaCC) and the CFTR.¹⁹ When the airway surface is dehydrated, water loss first occurs in the mucus layer due to its lower osmotic modulus,⁸ increasing mucin glycoprotein concentration which results in a more viscoelastic layer. Further dehydration leads to water loss in both the mucus layer and the PCL, resulting in compression of the PCL.⁸ The cilia fail to effectively beat, as they are inhibited by the more viscous mucus layer.^{8,16,18,19} (Figure 1.3).¹⁹ The ability to maintain this delicate balance of ion content is essential for normal mucociliary

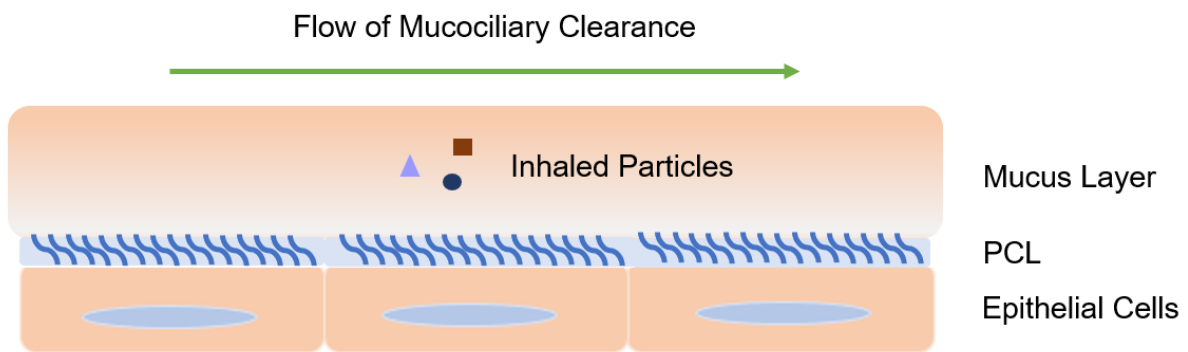


Figure 1.2 The airway surface liquid (ASL), composed of the mucus layer and the periciliary layer in healthy airways. Inhaled particles are trapped within the mucus layer and cleared from the lungs through mechanical clearance by cilia in the PCL.

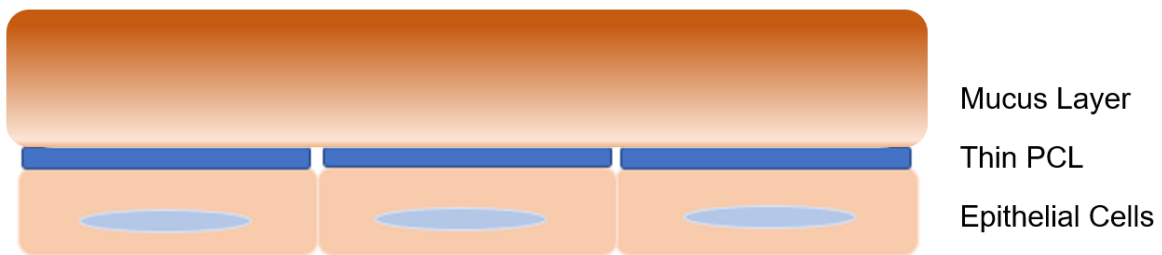


Figure 1.3 Dysregulation of ionic content in ASL impairs mucociliary clearance. In healthy airways, regulation of ionic content is maintained via the epithelial sodium channel (ENaC), which absorbs Na^+ , and the calcium-activated Cl^- channel (CaCC) and the CFTR, which secretes Cl^- in the airways. In CF airways, ionic content is dysregulated due to mutations in the CFTR chloride channel and results in the dehydration of both the mucus layer and the PCL. This leads to the collapse of the cilia in the PCL and failure to clear mucus in the lungs.

clearance. A defect in this mechanism results in pathophysiological changes of the ASL, characteristic of pulmonary diseases such as CF.⁷

1.1.2 *Mucus accumulation in CF airways*

In CF airways, a genetic defect in the CFTR causes chloride and sodium hyperabsorption, which dehydrates the ASL.^{7,16,20,21} Water loss increases mucus viscosity and dehydrates the PCL, resulting in cilia collapse and impaired mucociliary clearance (Figure 1.3).^{16,19} Failure to clear the abnormally thick mucus in the airways coupled with the continuous production of mucins by goblet cells further aggravates this problem.¹⁸ The depletion of the PCL also causes adhesion of the viscous mucus layer to the epithelial surface of the airways, rendering other methods of mechanical clearance (i.e., coughing) ineffective.^{7,18} The inability to remove the accumulated mucus, along with particles and microorganism trapped in it, facilitates chronic infection and inflammatory reactions in the CF lung.

1.1.3 *Bacterial lung infection in CF*

Cystic fibrosis is characterized by persistent bacterial infection. The CF microbiome is diverse, with *Staphylococcus aureus* and *Haemophilus influenzae* being prominent pathogens during infancy and adolescence, with *Pseudomonas aeruginosa*, *Burkholderia cepacia* complex, *Stenotrophomonas maltophilia*, and nontuberculous mycobacteria becoming more prominent during adulthood (Figure 1.4).^{11,12,22,23} Chronic pulmonary infection accounts for ~90% of patient mortality. An understanding of the bacterial colonization within the CF lung is thus essential for the development of novel therapeutic strategies to combat severe infections.

The CF pathogen most associated with patient mortality is *P. aeruginosa*.²⁴ Colonization by *P. aeruginosa* is less common in younger patients, but the likelihood increases with age.^{22,25}

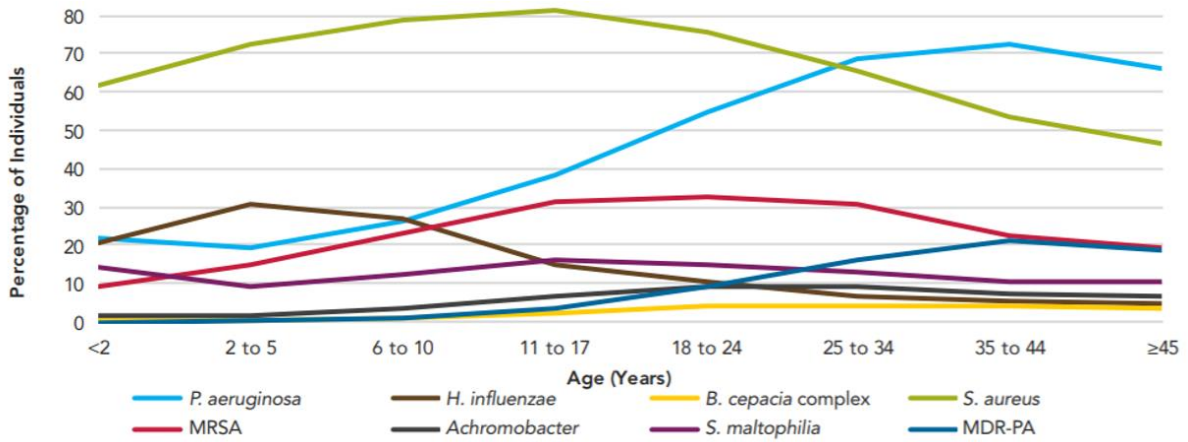


Figure 1.4 The CF microbiome described by pathogen prevalence as a function of age in the US. Reprinted with permission from the 2016 Patient Registry Annual Data Report to the Center Directors (CF Foundation).

Studies have shown that by age 20, ~80% of patients with CF have chronic *P. aeruginosa* infection, with each individual having phenotypically distinct isolates.^{12,22} The ability of this Gram-negative pathogen to genetically adapt to the CF lung microenvironment (e.g., hypoxic or anaerobic conditions present in the mucus layer) allows it to both evade the host immune response and develop resistance to clinically-relevant classes of antibiotics.^{6,26} In addition, *P. aeruginosa* forms biofilms in the lower respiratory tract.^{6,9} Biofilms are cooperative communities of bacteria that produce an exopolysaccharide (EPS) matrix that serves as a capsule to provide additional protection against the host immune response and antibacterial agents.^{6,9,27} A slower growth rate is adapted by bacteria in biofilms to ration limited nutrients, resulting in genetic alterations (e.g., lipopolysaccharide modification on the cell surface, the use of drug efflux pumps) that reduce the efficacy of antibacterial interventions (e.g., antibiotics).²⁸⁻³¹ Despite a reported decline in the prevalence of *P. aeruginosa* over the past 10 years, the occurrence of multi-drug resistant (MDR) strains of *P. aeruginosa* still infects ~17% of patients with CF.²² As a result, the management of *P. aeruginosa* infections have become a critical part of CF treatment strategies.

While colonization by *P. aeruginosa* dominates bacterial infections in the later years of CF patients, the most widespread infection in children is caused by Gram-positive *S. aureus*.¹² A significant increase in the prevalence of *S. aureus* was noted from 2000 to 2010,²² possibly due to improved screening and detection methods, demanding for improved management strategies. Infections with *S. aureus* occur predominantly in the upper respiratory tract which serves as a reservoir for colonizing bacteria, eventually facilitating recurrent infections in the lower airways.¹¹ Similar to *P. aeruginosa*, adaptive strategies allow for the emergence of antibiotic-resistant strains of *S. aureus*, such as methicillin-resistant *S. aureus* (MRSA). Chronic respiratory infections with MRSA have been associated with severe pulmonary function decline in CF patients.³²⁻³⁵

Although less common than *P. aeruginosa* and *S. aureus* colonization, infection with *Burkholderia cepacia* complex (BCC) is associated with high patient mortality in CF.^{12,36,37} The BCC is a group of at least 17 closely related species, with *Burkholderia cenocepacia* and *Burkholderia multivorans* as the best-described causes of pulmonary infection in CF.^{23,38} Treating chronic infection with BCC is difficult, as the Gram-negative bacteria intrinsically demonstrate resistance to most conventional antibiotics.^{12,23} As such, combination therapy (i.e., concurrent treatment with multiple classes of antibiotics) has shown promise in vitro for addressing BCC infections.^{23,39–42} However, a clinical trial demonstrated no improved outcomes for combination therapy, indicating that the success of this type of treatment is still somewhat limited.^{40,43} Due to the severity of BCC infections and the limited potential for their eradication, patients with these infections are ineligible for lung transplantation.^{37,44}

1.1.4 Inflammation and lung degradation

Lung disease in CF is characterized by abnormal, chronic inflammation. Studies have suggested that inflammation occurs very early in the life of a CF patient (even in the absence of infection) as a result of immune dysregulation (e.g., unfolded CFTR stress response, abnormal innate and adaptive immunities).^{45–49} Other reports, however, have not supported this hypothesis and rather show that inflammation occurs as a direct consequence of chronic bacterial infection.^{45,50} Regardless of how the process is initiated, the neutrophil-dominated inflammatory response plays a prominent role in cyclical damage to the airways (Figure 1.1).^{45,51–53} Recruited neutrophils combat invading pathogens through the release of reactive oxygen species (ROS), reactive nitrogen species (RNS), and proteases.^{45,51–53} The overwhelming bacterial load present in CF lungs combined with the formation of biofilms reduces the efficacy of neutrophil phagocytosis, resulting in persistent infection. Consequently, the inflammatory response to the bacterial burden

in the lungs intensifies.^{45,53} The high concentrations of ROS released by the accumulated neutrophils and the influx of proteases, such as neutrophil elastase (NE), cause structural damage to the respiratory epithelium.^{45,51-53} Excessive production of proteases further impairs phagocytosis, allowing infection to persist.^{45,51,52} A self-perpetuating cycle of infection and inflammation initiates and facilitates irreversible lung damage, ultimately leading to lung disease in CF (Figure 1.1).⁵²

1.2 Current treatment methods for cystic fibrosis

To date, there is no cure for cystic fibrosis as any curative treatment for CF must restore function to the impaired CFTR channel. With more than 2,000 known mutations in the CFTR gene found to correlate with CF, only select patients benefit from the use of CFTR modulators for slowing disease progression.²⁵ Instead, most efforts have been directed towards symptomatic treatment of the disease in order to benefit a larger pool of patients. A typical daily regimen for a CF patient includes treatment with hypertonic saline and a combination of mucolytic, antibiotic, and anti-inflammatory agents. These treatments aim to rehydrate the ASL, decrease mucus viscoelasticity, combat infection, and decrease inflammation. Even with these concurrent treatments, normal lung function is not restored. When lung degradation fails to be mitigated, lung transplantation becomes a necessary option. While a cure for CF has yet to be discovered, these treatments have raised the median age of survival from 14 years in 1969 to 40 years in 2016.²²

1.2.1 CFTR modulators

A causative treatment for CF involves the use of CFTR modulators to address the underlying genetic defects associated with the disease. This type of treatment is targeted towards

a specific class of mutations.^{22,25,54} Mutations associated with CF are broken down into classes based on their resulting functional impact. The first class of mutations (Class I) include biosynthetic defects that lead to an absence of functional CFTR protein. Class II mutations, on the other hand, affect intracellular trafficking of the CFTR. In this case, the CFTR protein is present but misfolded, thus keeping it from reaching the cell surface. The Class II mutations also includes F508del, the most common mutation in both U.S. and European patients. Other defects in the CFTR include anomalous gating in the channel that limits ion transport (Class III), abnormal conductance of chloride (Class IV), and splicing mutations, that reduce the level of CFTR gene transcription (i.e., Class V). The U.S. Food and Drug Administration (FDA) approved the first CFTR modulator in 2012 with Ivacaftor (trade name Kalydeco), which targets the G551D mutation falling under Class III. Ivacaftor improves the transport of Cl⁻ through the ion channel by directly binding to the channels to induce a non-conventional mode of gating.⁵⁵ While this mutation is the third most common type worldwide, it is only found in ~4-5% of CF patients.⁵⁶ As of 2012, Ivacaftor has been approved for patients with additional gating mutations, including Class IV R117H mutations and Class II F508del mutations.^{22,25,57} However, with over 2000 mutations for CF, the use of CFTR modulators is still limited only to select CF patients, preventing widespread use of this treatment strategy.²⁵

1.2.2 Hypertonic saline and mucolytic agents

Dehydration of the ASL and impaired mucociliary clearance are major pathological features of CF. These characteristics lead to airway obstruction by accumulated thick mucus in the lungs, persistent colonization of pathogens, and inflammation. As such, one of the crucial components of a patient's regular treatment plan involves therapies focused on reducing mucus accumulation. Hypertonic saline is one of the most common therapies used to improve mucociliary

clearance by rehydrating the ASL.²⁵ Inhalation of a sterile salt solution (typically ~3-7% NaCl) increases water content in the ASL and surface hydration.⁵⁷⁻⁶¹ Increased hydration improves the clearance of stagnant mucus, enhancing overall lung function for CF patients.⁶² This treatment necessitates daily administration and is a part of a patient's regimen.^{25,61}

Mucolytic therapies are also used to improve mucociliary clearance through breakdown of the mucus gel structure, thereby decreasing mucus viscoelasticity.⁶³ Dornase alfa (trade name Pulmozyme) is currently the only FDA-approved mucolytic agent in use for the treatment of CF.^{25,57,63,64} Composed of recombinant human deoxyribonuclease I (rhDNase I), dornase alfa cleaves DNA released by disintegrated neutrophils in CF respiratory secretions. Treatment is administered via nebulization once daily, and a study consisting of over 3,000 patients has shown great improvement in patient health.⁶⁵ Currently, dornase alfa is a highly effective mucolytic agent and one of the most successful CF therapeutics to date.²⁵

An alternative mucolytic agent garnering attention as a potential CF therapeutic is *N*-acetylcysteine (NAC). Inhalation of NAC is believed to reduce mucus viscoelasticity through the reduction of disulfide bonds within mucin glycoproteins, that replace disulfides with sulfhydryl moieties.⁶³ Many in vitro studies have demonstrated the ability of NAC to reduce the viscosity of mucin solutions;^{57,66} however, no data currently supports the clinical efficacy of oral or aerosolized formulations of NAC.^{63,67} As a major obstacle for greater use, NAC has been shown to be incompatible with the aminoglycoside class of antibiotics (e.g., tobramycin).^{63,68} Therefore, NAC is currently not recommended for the treatment of CF but motivates further research toward the identification of alternative mucolytics.^{63,69}

1.2.3 Antibiotics

With chronic airway infections as the leading cause of patient mortality in CF, long-term antibiotic use has become a cornerstone for the treatment of the disease.^{10,70} Current approaches to eradicate the spectrum of CF-relevant bacteria include cycling through different classes of antibiotics to treat specific pathogens (e.g., *P. aeruginosa*, *S. aureus*). With Gram-positive bacteria highly prevalent in pediatric cases, anti-staphylococcal drugs (e.g., flucloxacillin) are commonly used during the early phase of CF.^{12,35} During adulthood, *P. aeruginosa* eradication is the principal focus of CF treatment. Indeed, anti-pseudomonal drugs (e.g., tobramycin, colistin, aztreonam lysine) are employed to treat infections.^{12,25} Inhalation of tobramycin, a U.S. FDA approved aerosolized aminoglycoside, is typically administered by nebulization twice daily at doses of 300 mg.^{12,23,65,69} While the use of this antibiotic is the most recommended single strategy for *P. aeruginosa* managing bacterial infections, combination with other antibiotics (either delivered orally, intravenously, or via inhalation) is a standard regimen for patients with chronic *P. aeruginosa* infections.^{12,25}

The primary setback of persistent bacterial infection and the heavy use of antibiotics is the development of antibiotic resistance.⁷¹ The increased prevalence of multidrug-resistant (MDR) pathogens over the last decade, including MDR *P. aeruginosa* and MRSA, has raised concerns over the effective management of infection in CF.^{12,71} Moreover, the formation of bacterial biofilms poses significant challenges to the management of bacterial infections (Figure 1.5).^{6,9} The development of alternative dosages and methods for delivering different classes of antibiotics (i.e., aminoglycosides, β -lactams, macrolides) have become the main focus of recent research over designing next generation antibacterial treatments.¹² The use of nano- and microparticle-based pulmonary delivery of antibiotics is believed to address the challenges involving targeted delivery

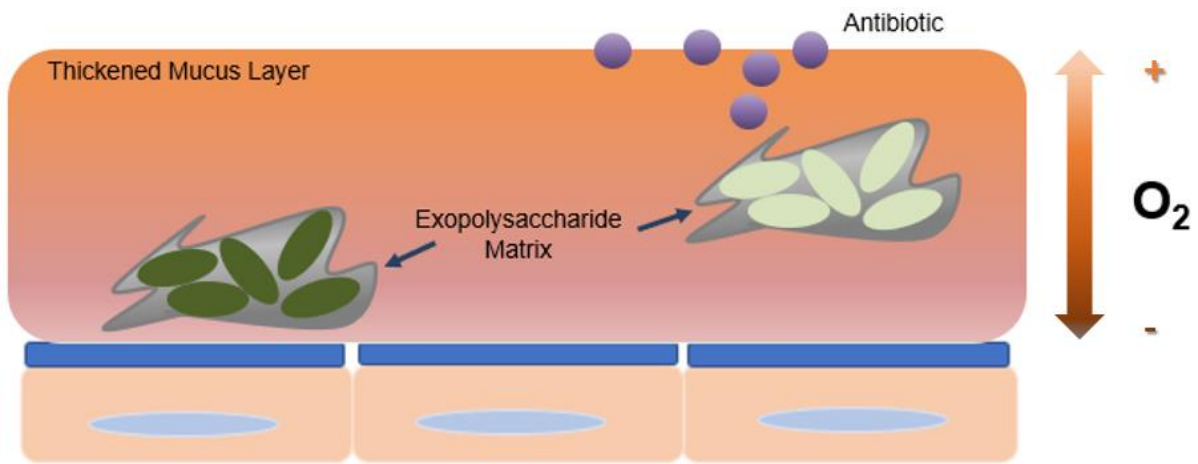


Figure 1.5 Biofilm-based bacterial colonization in the CF airways. Accumulation of a thick, stagnant mucus layer obstructs the airways and provides a suitable environment for biofilm-based bacterial colonization. Both mucus and the biofilm exopolysaccharide matrix provide additional protection by limiting drug. In addition, slower growth rate and the different biofilm microenvironments reduce efficacy of antibiotics against biofilm-based infections.

of antibacterial agents. These systems improve diffusion through the viscous mucus layer by decreasing interactions with mucin glycoproteins, allowing for greater localized antibiotic concentrations and thereby lower overall required antibiotic doses. Studies using targeted drug delivery scaffolds (e.g., liposomes, PLGA microparticles) have demonstrated improved antibacterial efficacy over conventional, molecular antibiotics against common CF pathogens.^{72–76} Despite promising results, innovations in pulmonary delivery still only represent a short-term solution to a broadening problem of antimicrobial resistance. An urgent need remains and necessitates the expansion of research on non-traditional antibacterial agents that can eradicate biofilm-based bacteria.

1.2.4 Anti-inflammatory agents

A persistent and excessive innate inflammatory response as a result of high bacterial burden ultimately causes lung degradation. Chronic inflammation warrants the use of anti-inflammatory therapeutics to mitigate decline in patient lung function and improve survival. Currently, ibuprofen is the only anti-inflammatory agent recommended for long-term treatment of CF airway inflammation.^{51,53,77} Therapies with corticosteroids have also been explored to treat inflammation, but serious, undesirable side-effects (e.g., weight loss, increased use of insulin) have limited their utility.^{46,51,53} Additionally, controlled trials have demonstrated no change in lung function between those treated with corticosteroids versus placebo.⁷⁸

1.2.5 Lung transplantation

Lung transplantation is seen as a last-resort option for CF patients with advanced lung disease. As of 2015, the five-year survival rate for lung transplant patients with CF was about 67%.⁷⁹ The survival rate for adults is generally much better compared to children.⁴⁶ The majority of

CF transplant patient population is typically 30 or above, with only 6.2 % of CF-related lung transplants performed on patients younger than 18 years of age.²² However, lung transplantation is not a permanent cure for CF and only offers a chance of improvement to the patient's health and quality of life. In addition to the risks associated with the surgical procedure and the possibility of organ rejection, immunosuppression is a major concern, with infection as a leading cause of patient mortality. Post-transplantation, the use of immunosuppressive drugs leave patients vulnerable to a host of invading pathogens.^{44,46,80} As such, lung transplants must be contemplated carefully on a case-by-case basis with consideration of associated risks, quality of life, and patient mortality.

1.3 Nitric oxide as a potential CF therapeutic

Nitric oxide (NO) is an endogenous, highly reactive free radical involved in the regulation of several physiological processes, including angiogenesis, vasodilation, neurotransmission, wound healing, and the immune response.⁸¹⁻⁸⁹ The multifaceted roles involving NO has led researchers to investigate its use as a potential therapy for various diseases. In particular, NO's role in the immune response to pathogens has sparked interest in the development of NO-based antibacterial therapeutics. As chronic bacterial infections are a central consideration in designing new CF therapies, this section examines the physiological roles of NO with a particular focus on its antibacterial action. Special attention is also given to recent studies that utilize exogenous NO as a CF therapeutic.

1.3.1 Physiological roles of nitric oxide

In the body, NO is an enzymatic product from the oxidation of L-arginine to L-citrulline via endothelial NO synthase (eNOS), neuronal NOS (nNOS), or inducible NOS (iNOS).⁸²⁻⁸⁵ The

three isoforms catalyze the same reaction, but differ in terms of NO concentration produced, targets, and duration of NO production.^{82,85} The constitutive isoforms, eNOS and nNOS, produce low concentrations (pM-nM) of NO that act in regulatory and signaling functions. In the cardiovascular system, for example, NO produced by eNOS maintains vascular tone and myocardial contractility, regulates proper blood flow and pressure, and promotes antithrombotic effects.⁸² Deficiencies in NO due to endothelial injury can cause cardiovascular pathologies including atherosclerosis, arterial thrombotic disorders, coronary heart disease, hypertension, and stroke.^{81,82} Likewise, NO produced by nNOS acts as a neurotransmitter in the central nervous system, regulating the firing of neurons in the brain, membrane depolarization, and the release of neurotransmitters (e.g., serotonin, acetylcholine).^{85,86} In endothelial, epithelial, and inflammatory cells (e.g., macrophages and neutrophils), larger concentrations (μM) of NO are produced by iNOS as part of the host response against invading pathogens.^{83,85} Nitric oxide's role in the immune system is of great interest in the development of novel antibacterial therapeutics.

1.3.2 Nitric oxide as an antimicrobial agent

Nitric oxide's role as an antimicrobial agent is used by the innate immune response following exposure to foreign pathogens. Nitric oxide is produced via iNOS by proinflammatory cytokines and microbial byproducts (e.g., interleukins, lipopolysaccharides).^{90,91} Nitric oxide exerts both nitrosative and oxidative stresses on invading pathogens through the formation of reactive intermediates as shown in Figure 1.6.⁹²⁻⁹⁴ Nitrosative species, such as dinitrogen trioxide (N_2O_3), deaminates DNA and nitrosates thiols on microbial proteins.^{81,94,95} Meanwhile, the reaction of NO with superoxide results in the formation of peroxynitrite (ONOO^-), causing the oxidative destruction of DNA and protein structures as well as membrane damage via lipid peroxidation.^{94,96} The multi-mechanistic pathways of NO's bactericidal action allow for broad-

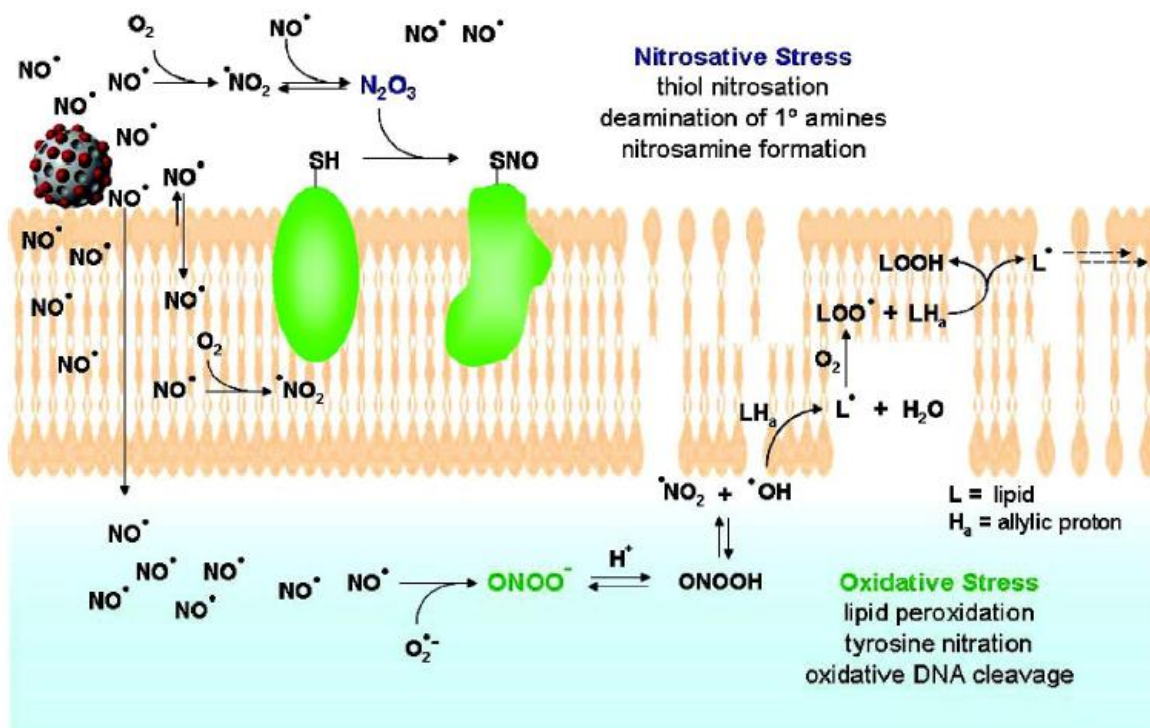


Figure 1.6 The multi-mechanistic pathways of NO's antibacterial activity. Nitrosative and oxidative stress is exerted by reactive byproducts such as dinitrogen trioxide (N₂O₃) and peroxynitrite (ONOO⁻). Reprinted with permission from Hetrick et al. Copyright 2008, American Chemical Society.

spectrum activity against nearly all pathogens, including both Gram-positive and Gram-negative bacteria.^{81,97} Moreover, the multiple molecular targets of NO's antimicrobial activity make it unlikely for bacteria to develop resistance to NO. Indeed, a study by Privett et al. demonstrated that exposure to exogenous NO resulted in a negligible increase in the required inhibitory NO concentration for planktonic species of different bacterial species, including antibiotic-resistant strains, even after several passages (20 d).⁹⁸

In addition to broad-spectrum antibacterial activity against planktonic bacteria, NO also exhibits a dose-dependent effect against bacterial biofilms.^{93,99,100} After biofilm maturation, the dispersal of planktonic bacteria from biofilms is essential for limiting overcrowding of bacteria within the EPS matrix. This purpose also allows for further colonization.¹⁰¹ Biofilm dispersal occurs in three phases: i) detachment of planktonic cells from the mature biofilm, ii) translocation of these planktonic cells, and iii) attachment of planktonic cells to a new substrate. Arora et al. previously reported that NO acts as a signaling molecule to mediate biofilm dispersal at low concentrations (pM-nM).¹⁰⁰ While the mechanism describing or controlling NO's ability to trigger biofilm dispersal remains unclear, a popular hypothesis involves NO's ligation to the cyclic diguanylate (cGMP) signaling molecule, which is involved in the production and maintenance of the biofilm EPS matrix.^{100,102} By initiating biofilm dispersal, NO can be utilized to increase bacterial susceptibility to common antibacterial agents.^{92,93} Barraud et al. reported the pretreatment of *P. aeruginosa* biofilms with sub-eradication concentrations of a low molecular weight NO donor (500 nM for 24 h). This NO pretreatment resulted in enhanced biofilm susceptibility to multiple antibacterial agents (e.g., tobramycin, hydrogen peroxide), allowing for a 2-log reduction in bacterial viability compared to biofilms treated with test agents alone.⁹²

At higher concentrations (μM - mM), complete biofilm eradication is achieved.^{93,103} Although the exact mechanism of NO-mediated biofilm eradication is still unknown, destruction of the biofilm EPS matrix is likely to be a main factor.^{104,105} Within the same concentration range, NO is capable of exerting bactericidal activity, further supporting NO's role in biofilm eradication. A recent study by Neufeld and Reynolds, for example, demonstrated that NO delivered by a low molecular weight donor (1.5 mM NO) was able to decrease the bacterial viability of *P. aeruginosa* biofilms by >1-log after a 12 h exposure.¹⁰³ As such, the development of materials that are capable of storing and releasing large ($\sim\mu\text{M}$) NO concentrations is of great interest for biofilm eradication.

1.3.3 Nitric oxide in CF therapy

The utility of exogenous NO as a CF therapeutic has become appealing due to its broad-spectrum antibacterial activity.^{92,93,106-110} Two main approaches have been investigated for NO-based therapy including the supplementation of L-arginine, NO's biological precursor, and the direct inhalation of NO gas.¹¹¹⁻¹¹⁵ Production of NO is increased in airways diseases with chronic inflammation and bacterial infection (e.g., asthma, COPD). However, the opposite is true for CF, where exhaled NO levels are dramatically lower compared to healthy individuals.¹¹⁶ As such, decreased levels of exhaled NO have been correlated with poor pulmonary health in CF patients.¹¹⁶⁻¹¹⁸ One hypothesis suggests that NO is scavenged by proteins and reactive oxygen species (ROS) in mucus.^{116,117} The thick, viscous mucus layer prevents the diffusion of NO and converts it into stable metabolites (e.g., nitrate, nitrite, and nitrotyrosine).^{116,117} Further, the consumption of NO by pathogens (e.g., *P. aeruginosa*) during anaerobic metabolism is believed to reduce exhaled NO levels.¹¹⁸ Additionally, it is hypothesized that available concentrations of L-arginine are diminished, thereby decreasing NO production.^{119,120} Oral, intravenous, and inhaled administration of L-arginine have been proposed as solutions for this deficiency.^{113-115,121} Of the

different routes of administration, the inhalation of nebulized L-arginine solutions has been found to be most effective. Grasemann and coworkers reported an increase in exhaled NO levels and improved pulmonary function, as characterized by forced air expiratory volume in 1 second (FEV₁) from CF patients following single dose treatments of nebulized L-arginine (7 wt% L-arginine hydrochloride solution).¹¹⁵ In a follow-on study, it was shown that twice daily L-arginine inhalation for two weeks improved exhaled NO levels compared to inhalation of a saline solution over the same treatment period.¹¹⁴ Of note, no improvement in FEV₁ levels were observed over the extended exposure period. Altogether, these studies suggest that L-arginine supplementation is a viable therapeutic to increase exhaled NO levels in CF patients. However, no evidence exists to suggest that this treatment strategy improves pulmonary function for extended periods.

As an alternative therapy, the antibacterial efficacy of directly inhaled gaseous NO has been investigated.¹⁰⁶⁻¹⁰⁹ Webert et al. reported a significant reduction in *P. aeruginosa* colonization in intratracheally injected rats after inhalation of NO gas (40 ppm in air, 24 h, continuous administration).¹⁰⁸ Unfortunately, increasing the length of exposure to 48 h resulted in rat mortality, suggesting that sustained high NO doses are problematic. Jean and coworkers examined the efficacy of lower doses of NO gas (10 ppm in oxygen, 24 h continuous administration).¹⁰⁹ At the lower doses tested, NO gas was only effective at reducing bacterial load when mixed with pure oxygen instead of room air, but this also resulted in an increase in airway inflammation. Miller et al. attempted to improve the bactericidal efficacy of gaseous NO while simultaneously reducing toxicity with the use of intermittent administration of higher NO doses (160 ppm in air, 30 min treatments every 4 h).¹⁰⁶ This periodic treatment method decreased the bacterial load of *P. aeruginosa* in rat lungs. In a more representative study, intermittent treatment with NO gas was administered to eight CF patients.¹¹⁰ Results showed both improved lung function

(increased FEV₁ in patients) and a significant reduction in the bacterial load of multiple microbial pathogens, including *P. aeruginosa*, *S. aureus*, and *Mycobacterium abscessus*.

In addition to antibacterial applications, inhalation of gaseous NO has been proposed as a mucolytic therapy.¹²² Thoroughbred horses with mucus hypersecretion in the airways were subjected to multiple treatment cycles of NO gas (100 breaths, 5,000-10,000 ppm) over several weeks. The treatments resulted in decreased mucus accumulation in the airways and facilitated clearance of non-viscous fluids from the nostrils. While the efficacy of gaseous NO regarding its mucolytic activity was demonstrated in the study, the mechanism by which NO elicits this response has not been systematically characterized. One hypothesis suggests that NO cleaves mucin glycoproteins through *S*-nitrosation of its cysteine residues.^{122,123} Another idea proposes the depolymerization of *O*-linked polysaccharides in the glycosated domains of the glycoprotein to alter intra-mucin interactions.¹⁰⁴ Nitric oxide may also cleave DNA in CF mucus to reduce its viscoelastic properties.¹⁰⁵ Still, factors (e.g., NO dose, delivery method) affecting NO's mucolytic activity and the mechanism by which NO exerts mucolysis remain unclear.

To date, treatments with gaseous NO have demonstrated NO's potential as a dual-action therapeutic that targets both chronic bacterial infection and mucus accumulation in the airways. However, the therapeutic utility of inhaled NO gas is limited by the hazards associated with the use of pressurized cylinders, rapid scavenging of NO in biological media, and toxicity concerns with continuous use at high concentrations.¹²⁴ The need for novel systems designed specifically for administering exogenous NO to the airways remains great.

1.4 Nitric oxide delivery

An alternative to direct inhalation of gaseous NO is the use of donor molecules capable of stable storage and controlled delivery of NO. Several classes of NO donor systems exist, including *N*-diazoniumdiolates, *S*-nitrosothiols (RSNOs), organic nitrates, and metal nitrosyls.¹²⁴ A wide variety of macromolecular NO donor scaffolds, including dendrimers,^{125–130} silica nanoparticles,^{94,131–135} and chitosan,^{136–138} have also been specifically designed for NO delivery for several biomedical applications.^{81,97,139,140} However, not all scaffolds are suitable for delivery of NO to the airways due to scaffold toxicity concerns (e.g., dendrimer secondary amine toxicity), poor water solubility, and ineffective clearance from the lungs. Thus, a more compatible scaffold must be developed for efficient pulmonary NO delivery.

1.4.1 Small molecule nitric oxide donors

Of the multiple classes of NO donors, RSNOs and *N*-diazoniumdiolates have garnered the most interest due to their ability to spontaneously release NO in biological media. *S*-nitrosothiols (e.g., glutathione, nitrosoalbumin) are a class of NO donors that serve as endogenous NO delivery systems.^{124,141} In exogenous preparations, RSNOs are created via the nitrosation of thiols with a nitrosating agent (e.g., nitrous acid, nitrites, nitrogen oxides) under acidic conditions.^{97,124,142} Nitric oxide release from the RSNO is triggered through multiple decomposition pathways (Figure 1.7A), each involving the homolytic cleavage of the S–NO bond.^{124,142,143} Photo and thermal decomposition both result in the formation of a thiyl radical along with the liberation of NO. The thiyl radical can react with another RSNO to yield an additional mole of NO and a disulfide. In the airways, NO release from RSNOs occurs through either thermal decomposition or via reaction with endogenous ascorbic acid, which acts as a reducing agent.¹⁴⁴ Ascorbic acid depletion, however, is a known feature of the ASL in CF, limiting the pathways for potential NO release from

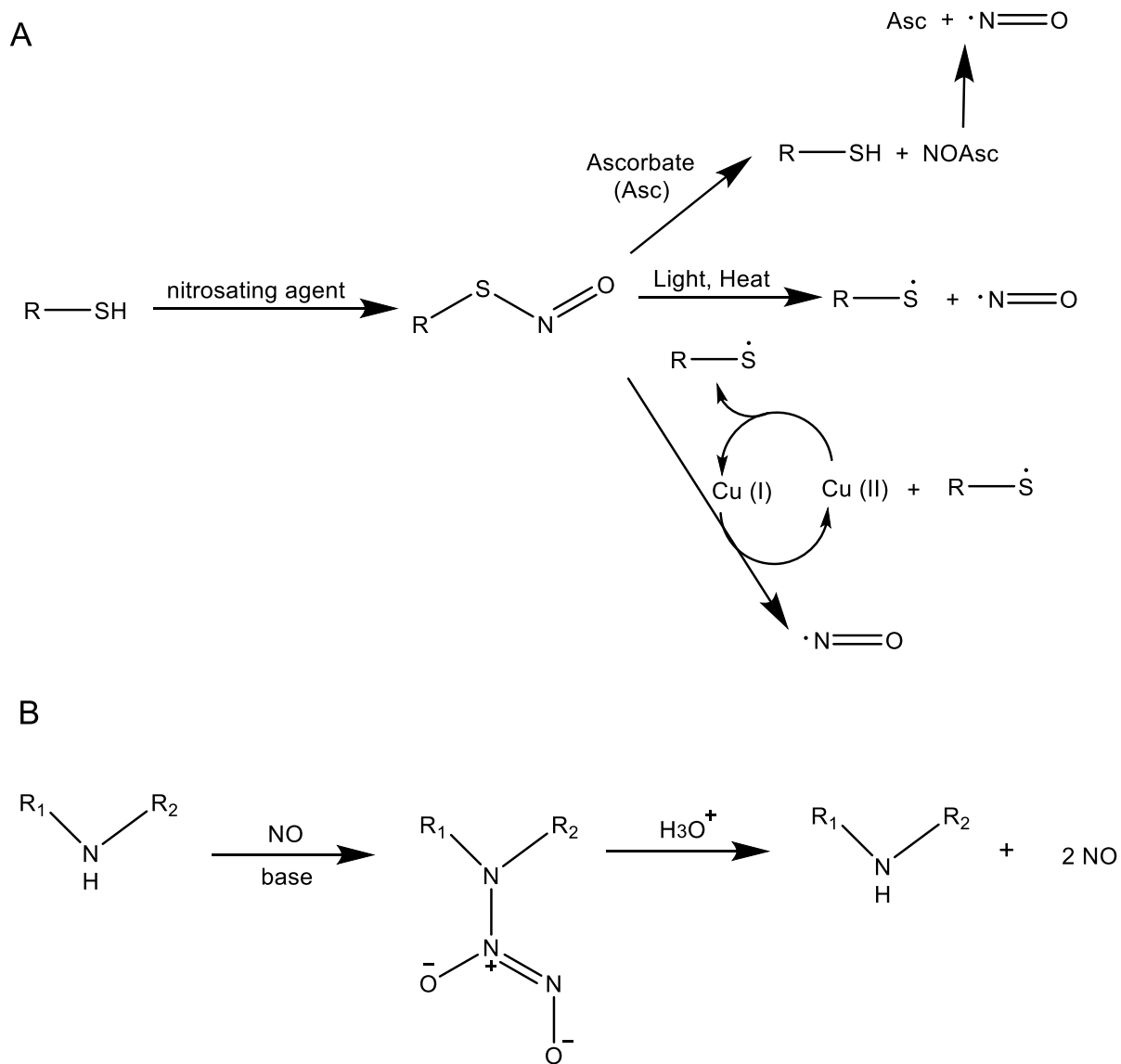


Figure 1.7 Formation and subsequent decomposition pathways of (A) *S*-nitrosothiols and (B) *N*-diazoniumdiolates.

RSNOs.¹⁴⁵ The utility of RSNO-based therapies is thus limited for CF applications necessitating an alternative donor system.

A more suitable NO donor for the development of NO-based CF therapies are *N*-diazoniumdiolates. These donors are prepared via exposure of secondary amine functional groups to high pressures of NO gas under basic conditions (Figure 1.7B).¹²⁴ Proton-mediated decomposition then yields two moles of released NO and the corresponding precursor amine molecule.^{124,146} In addition to temperature and pH, the stability and NO-release kinetics of *N*-diazoniumdiolates are directly affected by the precursor amine structure.^{124,147,148} Nitric oxide-release half-lives under physiological conditions for small or low molecular weight donors typically range from 2 s for cation-stabilized *N*-diazoniumdiolate-modified proline (PROLI/NO) to 20 h for amine-terminated NO-releasing diethylenetriamine (DETA/NO).^{147,148} In the case of DETA/NO, increased stabilization of the *N*-diazoniumdiolate moiety through hydrogen bonding from the terminal primary amine results in the extended NO-release profile.^{147–150} As such, *N*-diazoniumdiolates are a versatile NO donor system with tunable release properties.

1.4.2 *Macromolecular scaffolds for nitric oxide delivery*

While many initial studies have focused on developing small molecule NO donors for the controlled storage and release of exogenous NO as an alternative to gaseous NO, the therapeutic utility of these systems is limited by untargeted NO delivery and precursor toxicity concerns.^{81,124,146} These problems have been addressed through the development of macromolecular NO donor systems.^{97,124,139,140} Modification of macromolecules with NO donors allows for improved localization of NO-release and reduced cytotoxicity. Likewise, the use of macromolecular NO delivery systems enhance NO's efficacy due to potential targeting mechanisms (e.g., incorporation of functional groups that can interact and penetrate the bacterial

wall) and unique NO payloads.^{124,139} Much research has thus focused on the design of NO-releasing macromolecules, including inorganic nanoparticles (e.g. gold, silica), synthetic polymers (e.g., dendrimers), and biopolymers (e.g., chitosan), for a range of biomedical applications.^{81,97,139,140}

1.5 The ideal NO-releasing scaffold for CF delivery

Nitric oxide holds potential as a dual-action (i.e., antibacterial and mucolytic) treatment for CF. To successfully administer exogenous NO using macromolecular structures, certain properties of the delivery scaffold must be taken into consideration. First and foremost, the scaffold must be highly water soluble to allow for direct inhalation of the NO-based treatment into the airways via nebulization. Molecular weight, charge, and functional moieties each influence the water solubility of macromolecules. The same factors also affect other properties desired for an ideal CF therapy, such as its ability to penetrate and release active agents through the highly viscoelastic airway mucus. Both the overall charge and molecular weight dictate a scaffold's ability to electrostatically interact or entangle with the components of the mucus layer. Neutral and negatively charged materials (e.g., poly(ethylene glycol), polylactic-co-glycolic acid, alginate) are found to be advantageous for pulmonary drug delivery due to improved penetration through the mucus layer, minimizing interactions with mucin glycoproteins, for example.^{12,151–156} Positively charged polymers such as chitosan have also garnered great interest for the treatment of bacterial infections in CF patients, as their charge allows for improved localization (e.g., attachment on mucus layer surface) of the administered antibacterial agent.^{12,75,157–161} In this regard, the properties (or the identity) of the biopolymer can influence the efficacy of drug delivery. It may even impact the mucus viscoelasticity with the scaffold's interactions with its components.

The efficacy of NO-based antibacterial agents is also dependent on macromolecule scaffold properties (e.g., size, shape, charge, water solubility) and the associated NO release (e.g., half-lives and total NO payloads).^{129,130,135,162,163} Lu et al. synthesized NO-releasing silica nanorods (SNRs) with diverse NO-release kinetics and particle morphologies.¹⁶² Antibacterial activity of the NO-releasing SNRs were dependent on both the NO-release properties and particle morphology, with a larger NO flux (i.e., instantaneous amount of NO released) and higher aspect ratio (i.e., ratio of length to width of the particle) resulting in more bactericidal action. In a similar study, Slomberg et al., reported on the antibiofilm efficacy of NO-releasing silica particles of different sizes (i.e., 14, 50, and 150 nm) and shapes (i.e., rod-like vs. spherical particles) against *P. aeruginosa* and *S. aureus* biofilms.¹³⁵ Treatment with 14 nm NO-releasing silica particles resulted in enhanced bactericidal activity compared to larger particles (50 and 150 nm), the former allowing for better particle diffusion through the biofilm. Regarding particle shape, rod-like NO-releasing particles were found to have greater antibacterial action compared to spherical particles. The rod-like particles allowed for improved diffusion and greater contact area between the particle and the bacterial membrane, resulting in greater NO delivery (dose).

For dendrimers, Sun et al. demonstrated the antibacterial efficacy of NO-releasing poly(propyleneimine) (PPI) systems against planktonic forms of *P. aeruginosa* and *S. aureus*.¹²⁹ The bactericidal action was reported to be dependent on dendrimer generation (i.e., size), exterior functional groups, and NO-release properties. Dendrimers with hydrophobic terminal groups allowed for increased association with the hydrophobic bacterial cell membrane. On the other hand, larger sizes (i.e., higher generations) allowed for increased functional group density, resulting in greater intercalation with the bacterial cell wall and more efficient NO delivery. Similarly, Lu et al. reported the synthesis of NO-releasing amphiphilic poly(amidoamine)

(PAMAM) dendrimers with enhanced bactericidal activity against both planktonic and biofilm forms of *P. aeruginosa*.¹³⁰ The antibacterial efficacy was dependent on both the identity of the hydrophobic exterior modification and dendrimer generation. While higher dendrimer generations appear to be a desirable feature for enhanced bactericidal action, cytotoxicity was also noted against mammalian cells at the concentrations necessary to achieve biofilm eradication.

For the development of CF therapeutics, the nebulization of water-soluble NO-releasing macromolecular scaffolds that are biocompatible and capable of sustained NO release may represent an attractive strategy for pulmonary NO delivery. Of the various systems potentially available, biopolymers (e.g., chitosan, dextran, alginate) hold the greatest promise due to their biocompatibility and low toxicity, high functionality, and water solubility.⁹⁷

1.5.1 Initial work with nitric oxide-releasing chitosan oligosaccharide

Chitosan is one of the most extensively studied NO-releasing biopolymeric systems to date. Lu et al. first reported on the synthesis of highly water soluble *N*-diazoniumdiolate-modified chitosan oligosaccharides.¹³⁷ By tuning the ratio of 2-methylaziridine grafted onto the chitosan oligosaccharides (COS), a range of secondary amine concentrations and resulting NO payloads (i.e., 0.3-0.8 $\mu\text{mol}/\text{mg}$) were obtained. These NO-releasing chitosan biopolymers (COS/NO) exhibited antibacterial action against both planktonic and biofilm forms of *P. aeruginosa*. Neither control (non-NO-releasing) nor the NO-releasing COS elicited toxicity against mammalian cells at their concentrations required to achieve bactericidal activity.

Reighard et al. evaluated the antibacterial efficacy of NO-releasing chitosan oligosaccharides in the absence and presence of oxygen using nonmucoid, mucoid, and biofilm *P. aeruginosa* phenotypes. It was demonstrated that NO treatment under low oxygen environments

resulted in more effective killing relative to tobramycin, the current standard of care for treating CF infections.¹⁶⁴ In a follow-up study, NO's ability to degrade *P. aeruginosa* biofilms was evaluated using chitosan oligosaccharides with optimized NO-storage capabilities.¹⁶⁵ Treatment with COS/NO resulted in the disruption of the structural integrity of the biofilm EPS. Reighard et al. also reported on NO's potential utility as a mucolytic agent.¹⁶⁶ Modification with ester functional groups reduced the overall charge of the biopolymer and mitigated chitosan's inherent mucoadhesivity (i.e., ability of the biopolymer to adhere to mucus). Secondary amine-modified COS without ester functional groups demonstrated the greatest efficacy at reducing CF sputum's viscoelasticity. The cationic nature of the COS backbone resulted in the aggregation of mucin in sputum samples, while NO release from COS/NO allowed for the degradation of the mucin network. Overall, these studies demonstrate the potential efficacy of positively charged biopolymers for delivering NO for CF applications.

1.5.2 Limitations of chitosan oligosaccharides for NO delivery in CF

While NO's potential utility as a dual-action therapeutic agent holds great promise, the initial studies with chitosan lack a systematic evaluation of how molecular weight, charge, and NO-release properties might influence NO's action. Chitosan is only water soluble up to 10 kDa, limiting the molecular weight range that can be studied.^{137,167} While the NO-releasing biopolymer exhibited a dose-dependent action with biofilm degradation, control chitosan oligosaccharides actually increased biofilm elasticity, suggesting that the non-NO-releasing scaffold may limit NO's efficacy – a potential drawback of using a cationic biopolymer.¹⁶⁵ Further functionalization of the primary amine terminal group of COS with acrylates did not significantly alter the biopolymer's NO-release properties, restricting the scope of the previous study.¹⁶⁶ To fully elucidate the impact of both NO release and scaffold properties (i.e., molecular weight and charge),

expanding the work originally performed with NO-releasing chitosan oligosaccharides using anionic or neutral biopolymers with potential for diverse NO-release properties is warranted.

1.6 Alginate in the treatment of cystic fibrosis

Alginate represents an ideal NO donor biopolymer for use in the CF lung due to its biocompatibility, low toxicity, and water solubility.^{168,169} The hydroxyl and carboxylic acid functional groups of alginate offer sites for straightforward chemical modification. For these reasons, the development of alginate-based therapies has generated great interest across numerous biomedical applications, including wound dressings,^{169–171} drug delivery,^{172–174} potentiators for antimicrobial agents,^{175–177} and more recently, as mucin modifiers for cystic fibrosis.^{151–154} The development of a dual-action antibacterial and mucolytic NO-based therapy using alginate biopolymers is certainly conceivable and potentially attractive.

1.6.1 Alginate as a potential scaffold for NO delivery

As shown in Figure 1.8, alginate is an anionic polysaccharide composed of 1,4-linked β -D-mannuronic acid (M) and α -L-guluronic acid (G) residues.¹⁷³ Commercially available alginates are typically derived from brown algae (*Phaeophyceae*), including *Laminaria hyperborean*, *Ascophyllum nodosum*, and *Macrocystis pyrifera*.^{172,173} Alginate may also be extracted from bacteria including *Azotobacter vinelandii* and *Pseudomonas* species.^{172,173} The composition and residue sequence depend on the source from which the alginate is isolated.¹⁷² Alginate rich in G residues are prepared from stripes of old *L. hyperborean* kelp,^{172,173} whereas alginate with up to 100% M residues are often isolated from *Pseudomonas* strains.^{172,178}

Alginate's molecular weight and composition (i.e., M/G sequence) dictate its viscosity in solution. Commercially available alginates have molecular weights ranging from 32 to 400 kDa.¹⁷³ Higher molecular weight alginates (≥ 100 kDa) containing a high G ($\geq 70\%$) content form hydrogels with enhanced mechanical properties and high stiffness compared to those having decreased G content ($\leq 30\%$).^{173,179,180} The G monomeric units adopt a buckled conformation while the M monomers take the shape of an extended ribbon (Figure 1.8).¹⁸¹ Neighboring G monomers form diamond-shaped holes that are capable of cooperative binding with multivalent cations (e.g., Ca^{2+}), causing gellation.^{172,173,178,179,181} Increasing the G density of alginate has been reported to increase selective binding to alkaline metal ions (e.g., preferential binding with Ca^{2+} compared to Mg^{2+}), whereas M-rich residues and alternating blocks of G and M monomers exhibit relatively low ion selectivity.^{169,182} Alginate undergoes pH-dependent hydrolysis to form "alginic gels" as a result of interactions between the protonated homopolymeric sequences (i.e., repeating units of the same monomer).^{172,174,180,183} Similar to gelation via ionic crosslinking, G monomer residues appear to be most effective for junction formation within the gels, producing gels with high stiffness.^{180,183}

In addition to affecting physical morphology, the overall composition of alginate also affects its biocompatibility and antigenicity.^{172,173} For example, alginate with high G content has been shown to elicit a mild immunological response, while M residue rich alginate was more immunogenic. Alginate with high M content induces cytokine production up to 10-fold greater than G-rich alginate.^{173,184} The alginate backbone offers the ability for straightforward chemical modification at hydroxyl and carboxylic acid functional groups, imparting unique versatility with respect to drug storage and release, and control over solubility, biocompatibility, as well as degradation rates.^{169,173} Alginate is also approved for use by the U.S. Food and Drug Administration (FDA).¹⁷⁹ As a result, alginate and its derivatives are typically used as food

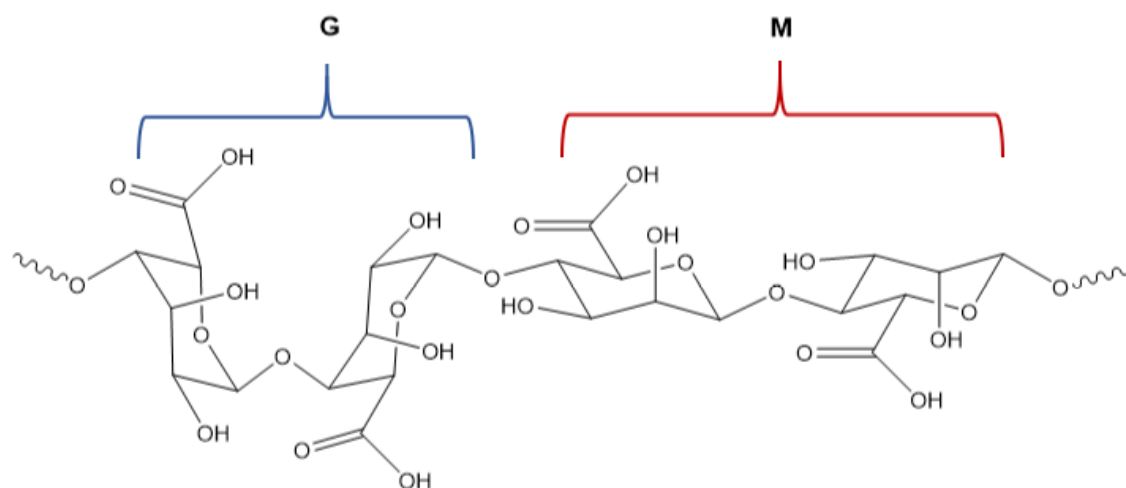


Figure 1.8 Alginate polysaccharide composed of α -L-guluronic acid (G) and β -D-mannuronic acid (M) residues.

additives and have become important biopolymers for a wide range of biomedical applications (e.g., raft-forming formulations for the treatment of heartburn and gastric reflux, protein and cell delivery vehicles in tissue regeneration, and dressings for the treatment of acute and chronic wounds).^{169,179}

1.6.2 Alginate in antibacterial applications

The unique properties of alginate (e.g., water solubility at high molecular weights) make it an excellent scaffold for the delivery of antibacterial agents (e.g., silver and zinc). Traditional use of alginate as a non-woven dressing has sparked interest in developing alginate-based materials imbued with antibacterial properties for wound-healing applications. In a study by Hajial et al., sodium alginate polyethylene oxide nanofibers containing lavender oil (SA-PEO/LO; 5% v/v lavender oil) were used to treat skin burns (induced by midrange ultraviolet radiation) on rats.¹⁸⁵ Bactericidal efficacy was evaluated using *S. aureus*, a common pathogen found in burn wounds. The nanofibers were shown to inhibit growth of *S. aureus* colonies, creating inhibition zones of ~20 mm after 24 h of treatment. In vitro studies showed that the nanofibers were biocompatible, and that both SA-PEO/LO and control SA-PEO nanofibers demonstrated strong anti-inflammatory action, as evidenced by reduced pro-inflammatory cytokine counts. In vivo studies also revealed the ability of these materials to promote wound healing from burn injuries, showing no evident burn marks on the skin of mice treated with control PEO nanofiber dressings. Yang et al. developed nano-silver/sodium alginate (Ag/SA) composite nanoparticles that showed superior antibacterial activity towards *E. coli* and *S. aureus* (MIC values of 0.25 and 0.13 µg/mL, respectively) compared to previously reported silver nanoparticles (0.78-6.25 µg/mL) and pluronic-coated silver nanoprisms (24 µg/mL) following a 24-h exposure.¹⁸⁶⁻¹⁸⁸ The Ag/SA particles demonstrated antibacterial activity against both pathogens after 30 d of exposure to the fiber (MIC of 0.51 µg/mL

for *E.coli* and 0.26 µg/mL for *S. aureus*). Cloth fabrics submerged in a solution of Ag/SA nanoparticles also exhibited antibacterial properties against colonies of *S. aureus*, with inhibition zone diameters improving (1.8-4.8 mm) with increasing concentrations of silver nanoparticles (0.16-0.57 mg/mL).¹⁸⁶ Overall, these studies demonstrate the promise of alginate used in the delivery of antibacterial agents.

1.6.3 Alginate as a potentiator for antimicrobial activity

Current studies highlight alginate's use as a potentiator for antibiotics (e.g. collistin, aztreonam, erythromycin) and as a biofilm dispersant.¹⁷⁵⁻¹⁷⁷ Khan et. al reported on the use of low molecular weight alginate oligosaccharides (OligoG, 2.6 kDa) to treat multi-drug-resistant bacteria, including different strains of *Pseudomonas*, *Acinetobacter*, *Burkholderia* species, and MRSA.¹⁷⁶ Addition of OligoG to liquid cultures reduced bacterial proliferation in a dose-dependent manner, showing a general decrease in percent change in the cell density with respect to control. This effect was particularly evident in the Gram-negative pathogens tested. Imaging PAO1 *P. aeruginosa* biofilms revealed disruption of established biofilms, increased cell death, and decreased cellular density with increasing concentrations (0 to 10%) of OligoG. Treatment with OligoG also improved the efficacy of a range of antibiotics, including macrolides (e.g., azithromycin) by up to 512-fold against Gram-negative MDR pathogens. A similar effect was observed in Gram-positive species, albeit to a lesser extent.

In a subsequent study, the efficacy of OligoG was evaluated against oral biofilms (i.e., *P. gingivalis* and *S. mutans*). Pre-treatment of titanium and polymethylmethacrylate (PMMA) discs with triclosan did not inhibit bacterial attachment. In contrast, triclosan in combination with OligoG resulted in a significant decrease in biofilm attachment for *P. gingivalis*. Bacterial imaging studies with *P. gingivalis* biofilms exposed to high concentrations of OligoG ($\geq 6\%$) revealed a

decrease in cell numbers and increased numbers of non-viable cells. Atomic force microscopy (AFM) studies also revealed that treatment with OligoG resulted in both structural and cellular changes. Similarly, exposure to the same concentrations of OligoG altered *S. mutans* biofilm morphology, producing obvious cellular aggregation and clumping in biofilms and new pores that might improve diffusion of antibacterial agents.¹⁷⁵

Hengzhuang and coworkers recently reported the effect of OligoG treatment in an in vivo murine lung infection model. Biofilm disruption after a 24-h treatment period with OligoG proved dose-dependent, with up to 2.5-log reduction in bacterial viability of *P. aeruginosa* in infected mouse lungs. In vitro assays with OligoG also reduced the required colistin concentrations (512 µg/mL to 8 µg/mL) required to eradicate biofilms after an 8-h exposure.¹⁷⁷ As demonstrated by the above studies, low molecular weight alginate oligosaccharides have utility as potentiators of antibacterial and biofilm dispersal agents.

1.6.4 Alginate as a mucomodulator

The ability of alginate to alter mucus rheology is also an active area of research. Alginate oligosaccharides rich in G units have been shown to decrease both mucus viscosity and elasticity by inhibiting interpolymer crosslinking and intramolecular interactions between mucin glycoproteins.^{151,152} Nordgård and coworkers reported that treatment with alginate oligosaccharides decreased the viscoelastic properties of mucin gels as well as mucin-DNA gels.¹⁵³ Subsequent studies have shown the ability of alginate oligosaccharides to create pores in the mucus network and alter matrix architecture.^{151,154} Treatment with alginate oligomers also led to increased particle diffusion through the mucus layer, indicating the potential for improved drug delivery in the airways. Recent work by Pritchard et al. also demonstrated that at 2 wt% concentration of OligoG managed to reduce the viscoelasticity of CF sputum with comparable efficacy to that of

rhDNAse I.¹⁵¹ Altogether, these studies clearly denote the benefits of developing alginate-based therapies for the treatment of CF, particularly for decreasing the viscoelasticity of mucus in the airways.

1.7 Summary of dissertation research

The goal of my dissertation research was to design NO-releasing alginates as a dual-action mucolytic-antibacterial therapeutic for the future potential treatment of CF. My initial efforts involved first modifying alginate to store and release NO, followed by subsequent examination of NO-release properties. How these amine functional groups and NO-releasing moieties affected alginate's ability to alter the rheological properties of mucus was then examined. Lastly, the antibiofilm efficacy of the NO-releasing alginates against different bacteria under CF-relevant conditions was also determined. In summary, the objectives of my dissertation research included:

1. Synthesis of water-soluble high and low molecular weight alginates with tunable NO storage and release properties;
2. Assessment of the mucolytic efficacy of the NO-releasing alginates on the bulk rheological properties of human bronchial epithelial (HBE) mucus; and,
3. Evaluation of the antibacterial efficacy of the NO-releasing alginate derivatives against bacterial biofilm cultures of CF-relevant pathogens under conditions that mimic diseased airways.

In this chapter, the pathogenesis of CF, a review of current treatment methods for the disease, and the motivations for using NO-based therapeutics were fully described. In particular,

the benefits of designing an alginate-based NO delivery system were introduced. Chapter 2 describes the synthesis of high and low molecular weight alginates functionalized with small molecule alkyl amines to produce anionic NO-releasing biopolymers. The effect of molecular weight and amine precursor structure on total NO storage, NO-release kinetics, toxicity, and antibacterial action under static conditions are discussed. Chapter 3 examines how the physical properties (e.g., molecular weight, scaffold charge), NO-release properties, and concentration of the alginate systems affect mucus viscoelasticity. A comparison with a conventional mucolytic, NAC, was also carried out to assess the potential benefits of the NO-releasing biopolymer. Chapter 4 demonstrates the use of NO-releasing alginate as a bactericidal agent against *P. aeruginosa*, BCC, *S. aureus*, and MRSA under CF-relevant conditions. In addition, NO release under biological conditions and the antibiofilm activity of the alginate systems compared to traditional antibiotics (e.g., tobramycin) were investigated. Lastly, Chapter 5 provides a summary of the dissertation work presented herein and suggests future directions for the evaluation and development of a library of NO-releasing biopolymers as CF therapeutics.

REFERENCES

- (1) Høiby, N. Recent Advances in the Treatment of Pseudomonas Aeruginosa Infections in Cystic Fibrosis. *BMC Med.* **2011**, *9*, 32–39.
- (2) Treggiari, M. M.; Rosenfeld, M.; Retsch-Bogart, G.; Gibson, R.; Ramsey, B. Approach to Eradication of Initial Pseudomonas Aeruginosa Infection in Children with Cystic Fibrosis. *Pediatr. Pulmonol.* **2007**, *42*, 751–756.
- (3) Kerem, B.-S.; Rommens, J. M.; Buchanan, J. A.; Markiewicz, D.; Cox, T. K.; Chakravarti, A.; Buchwald, M.; Tsui, L.-C. Identification of the Cystic Fibrosis Gene: Genetic Analysis. *Science.* **1989**, *245*, 1073–1080.
- (4) Riordan, J. R.; Rommens, J. M.; Kerem, B.; Alon, N.; Rozmahel, R.; Grzelczak, Z.; Zielenski, J.; Lok, S.; Plavsic, N.; Chou, J.-L. Identification of the Cystic Fibrosis Gene: Cloning and Characterization of Complementary DNA. *Science.* **1989**, *245*, 1066–1073.
- (5) Rommens, J. M.; Iannuzzi, M. C.; Kerem, B.; Drumm, M. L.; Melmer, G.; Dean, M.; Rozmahel, R.; Cole, J. L.; Kennedy, D.; Hidaka, N. Identification of the Cystic Fibrosis Gene: Chromosome Walking and Jumping. *Science.* **1989**, *245*, 1059–1065.
- (6) Hassett, D. J.; Cuppoletti, J.; Trapnell, B.; Lyman, S. V.; Rowe, J. J.; Sun Yoon, S.; Hilliard, G. M.; Parvatiyar, K.; Kamani, M. C.; Wozniak, D. J.; et al. Anaerobic Metabolism and Quorum Sensing by Pseudomonas Aeruginosa Biofilms in Chronically Infected Cystic Fibrosis Airways: Rethinking Antibiotic Treatment Strategies and Drug Targets. *Adv. Drug Deliv. Rev.* **2002**, *54*, 1425–1443.
- (7) Samet, J. M.; Cheng, P. W. The Role of Airway Mucus in Pulmonary Toxicology. *Environ. Health Perspect.* **1994**, *102 Suppl*, 89–103.
- (8) Button, B.; Cai, L. H.; Ehre, C.; Kesimer, M.; Hill, D. B.; Sheehan, J. K.; Boucher, R. C.; Rubinstein, M. A Periciliary Brush Promotes the Lung Health by Separating the Mucus Layer from Airway Epithelia. *Science.* **2012**, *337*, 937–941.
- (9) Sriramulu, D. D.; Lünsdorf, H.; Lam, J. S.; Römling, U. Microcolony Formation: A Novel Biofilm Model of Pseudomonas Aeruginosa for the Cystic Fibrosis Lung. *J. Med. Microbiol.* **2005**, *54*, 667–676.
- (10) Ratjen, F. A. Cystic Fibrosis: Pathogenesis and Future Treatment Strategies. *Respir. Care* **2009**, *54*, 595–605.
- (11) Lyczak, J. B.; Cannon, C. L.; Pier, G. B. Lung Infections Associated with Cystic Fibrosis. *Clin. Microbiol. Rev.* **2002**, *15*, 122–194.
- (12) Klinger-Strobel, M.; Lautenschläger, C.; Fischer, D.; Mainz, J. G.; Bruns, T.; Tuchscher, L.; Pletz, M. W.; Makarewicz, O. Aspects of Pulmonary Drug Delivery Strategies for Infections in Cystic Fibrosis – Where Do We Stand? *Expert Opin. Drug Deliv.* **2015**, *12*, 1351–1374.
- (13) Fahy, J. V.; Dickey, B. F. Airway Mucus Function and Dysfunction. *N. Engl. J. Med.* **2010**, *363*, 2233–2247.

- (14) Lamblin, G.; Degroote, S.; Perini, J. M.; Delmotte, P.; Scharfman, A.; Davril, M.; Lo-Guidice, J. M.; Houdret, N.; Dumur, V.; Klein, A.; et al. Human Airway Mucin Glycosylation: A Combinatory of Carbohydrate Determinants Which Vary in Cystic Fibrosis. *Glycoconj. J.* **2001**, *18*, 661–684.
- (15) Bansil, R.; Turner, B. S. Mucin Structure, Aggregation, Physiological Functions and Biomedical Applications. *Curr. Opin. Colloid Interface Sci.* **2006**, *11*, 164–170.
- (16) Quraishi, M. S.; Jones, N. S.; Mason, J. The Rheology of Nasal Mucus: A Review. *Clin. Otolaryngol. Allied Sci.* **2002**, *23*, 403–413.
- (17) Boucher, R. C. New Concepts of the Pathogenesis of Cystic Fibrosis Lung Disease. *Eur. Respir. J.* **2004**, *23*, 146–158.
- (18) Knowles, M. R.; Boucher, R. C. Mucus Clearance as a Primary Innate Defense Mechanism for Mammalian Airways. *J. Clin. Invest.* **2002**, *109*, 571–577.
- (19) Tarran, R.; Button, B.; Boucher, R. C. Regulation of Normal and Cystic Fibrosis Airway Surface Liquid Volume By Phasic Shear Stress. *Annu. Rev. Physiol.* **2006**, *68*, 543–561.
- (20) Tarran, R.; Grubb, B. R.; Gatzky, J. T.; Davis, C. W.; Boucher, R. C. The Relative Roles of Passive Surface Forces and Active Ion Transport in the Modulation of Airway Surface Liquid Volume and Composition. *J. Gen. Physiol.* **2001**, *118*, 223–236.
- (21) Stoltz, D. A.; Meyerholz, D. K.; Welsh, M. J. Origins of Cystic Fibrosis Lung Disease. *N. Engl. J. Med.* **2015**, *372*, 351–362.
- (22) Marshall, B.; Elbert, A.; Petren, K.; Rizvi, S.; Fink, A.; Ostrenga, J.; Sewall, A.; Loeffler, D. Patient Registry: Annual Data Report 2015. *Cyst. Fibros. Found. Patient Regist.* **2016**, 1–94.
- (23) Chmiel, J. F.; Aksamit, T. R.; Chotirmall, S. H.; Dasenbrook, E. C.; Elborn, J. S.; LiPuma, J. J.; Ranganathan, S. C.; Waters, V. J.; Ratjen, F. A. Antibiotic Management of Lung Infections in Cystic Fibrosis. I. The Microbiome, Methicillin-Resistant Staphylococcus Aureus, Gram-Negative Bacteria, and Multiple Infections. *Ann. Am. Thorac. Soc.* **2014**, *11*, 1120–1129.
- (24) Emerson, J.; Rosenfeld, M.; McNamara, S.; Ramsey, B.; Gibson, R. L. Pseudomonas Aeruginosa and Other Predictors of Mortality and Morbidity in Young Children with Cystic Fibrosis. *Pediatr. Pulmonol.* **2002**, *34*, 91–100.
- (25) Spielberg, D. R.; Clancy, J. P. Cystic Fibrosis and Its Management Through Established and Emerging Therapies. *Annu. Rev. Genomics Hum. Genet.* **2016**, *17*, 155–175.
- (26) Worlitzsch, D.; Tarran, R.; Ulrich, M.; Schwab, U.; Cekici, A.; Meyer, K. C.; Birrer, P.; Bellon, G.; Berger, J.; Weiss, T.; et al. Effects of Reduced Mucus Oxygen Concentration in Airway Pseudomonas Infections of Cystic Fibrosis Patients. *J. Clin. Invest.* **2002**, *109*, 317–325.
- (27) Yoon et al., S. S. Pseudomonas Aeruginosa Anaerobic Respiration in Biofilms: Relationships to Cystic Fibrosis Pathogenesis. *Dev. Cell* **2002**, *3*, 593–603.

- (28) Stewart, P. S.; William Costerton, J. Antibiotic Resistance of Bacteria in Biofilms. *Lancet* **2001**, *358*, 135–138.
- (29) Hall-Stoodley, L.; Stoodley, P. Evolving Concepts in Biofilm Infections. *Cell Microbiol.* **2009**, *11*, 1034–1043.
- (30) Donlan, R. M. Biofilm Formation: A Clinically Relevant Microbiological Process. *Clin. Infect. Dis.* **2001**, *33*, 1387–1392.
- (31) Yang, L.; Jelsbak, L.; Molin, S. Microbial Ecology and Adaptation in Cystic Fibrosis Airways. *Environ. Microbiol.* **2011**, *13*, 1682–1689.
- (32) Stone, A.; Saiman, L. Update on the Epidemiology and Management of Staphylococcus Aureus, Including Methicillin-Resistant Staphylococcus Aureus, in Patients with Cystic Fibrosis. *Curr. Opin. Pulm. Med.* **2007**, *13*, 515–521.
- (33) Dasenbrook, E. C.; Merlo, C. A.; Diener-West, M.; Lechtzin, N.; Boyle, M. P. Persistent Methicillin-Resistant Staphylococcus Aureus and Rate of FEV1 Decline in Cystic Fibrosis. *Am. J. Respir. Crit. Care Med.* **2008**, *178*, 814–821.
- (34) Dasenbrook, E.; Checkley, W.; Merlo, C.; Konstan, M.; Lechtzin, N.; Boyle, M. Association between Respiratory Tract Methicillin-Resistant Staphylococcus Aureus and Survival in Cystic Fibrosis. *JAMA* **2010**, *303*, 2386–2392.
- (35) Hurley, M. N. Staphylococcus Aureus in Cystic Fibrosis: Problem Bug or an Innocent Bystander? *Breathe* **2018**, *14*, 87–90.
- (36) Lipuma, J. Update on the Burkholderia Cepacia Complex. *Curr. Opin. Pulm. Med.* **2005**, *11*, 528–533.
- (37) Saiman, L.; Siegel, J. Infection Control Recommendations for Patients With Cystic Fibrosis: Microbiology, Important Pathogens, and Infection Control Practices to Prevent Patient-to-Patient Transmission. *Infect. Control Hosp. Epidemiol.* **2003**, *24*, S6–S52.
- (38) Leitão, J. H.; Sousa, S. A.; Ferreira, A. S.; Ramos, C. G.; Silva, I. N.; Moreira, L. M. Pathogenicity, Virulence Factors, and Strategies to Fight against Burkholderia Cepacia Complex Pathogens and Related Species. *Appl. Microbiol. Biotechnol.* **2010**, *87*, 31–40.
- (39) Speert, D. P. Advances in Burkholderia Cepacia Complex. *Paediatr. Respir. Rev.* **2002**, *3*, 230–235.
- (40) Abbott, F. K.; Milne, K. E. N.; Stead, D. A.; Gould, I. M. Combination Antimicrobial Susceptibility Testing of Burkholderia Cepacia Complex: Significance of Species. *Int. J. Antimicrob. Agents* **2016**, *48*, 521–527.
- (41) El-Halfawy, O. M.; Naguib, M. M.; Valvano, M. A. Novel Antibiotic Combinations Proposed for Treatment of Burkholderia Cepacia Complex Infections. *Antimicrob. Resist. Infect. Control* **2017**, *6*, 120.
- (42) Van Dalem, A.; Herpol, M.; Echahidi, F.; Peeters, C.; Wybo, I.; De Wachter, E.; Vandamme, P.; Piérard, D. In Vitro Susceptibility of Burkholderia Cepacia Complex Isolated from Cystic Fibrosis Patients to Ceftazidime-Avibactam and Ceftolozane-

- Tazobactam. *Antimicrob. Agents Chemother.* **2018**, *62*, e00590-18.
- (43) Aaron, S. D.; Vandemheen, K. L.; Ferris, W.; Fergusson, D.; Tullis, E.; Haase, D.; Berthiaume, Y.; Brown, N.; Wilcox, P.; Yozghatlian, V.; et al. Combination Antibiotic Susceptibility Testing to Treat Exacerbations of Cystic Fibrosis Associated with Multiresistant Bacteria: A Randomised, Double-Blind, Controlled Clinical Trial. *Lancet* **2005**, *366*, 463–471.
- (44) Liou, T. G.; Adler, F. R.; Cox, D. R.; Cahill, B. C. Lung Transplantation and Survival in Children with Cystic Fibrosis. *N. Engl. J. Med.* **2007**, *357*, 2143–2152.
- (45) Cohen-Cymbberknoh, M.; Kerem, E.; Ferkol, T.; Elizur, A. Airway Inflammation in Cystic Fibrosis: Molecular Mechanisms and Clinical Implications. *Thorax* **2013**, *68*, 1157–1162.
- (46) Ratjen, F.; Döring, G. Cystic Fibrosis. *Lancet* **2003**, *361*, 681–689.
- (47) Zahm, J. M.; Gaillard, D.; Dupuit, F.; Hinnrasky, J.; Porteous, D.; Dorin, J. R.; Puchelle, E. Early Alterations in Airway Mucociliary Clearance and Inflammation of the Lamina Propria in CF Mice. *Am. J. Physiol. Physiol.* **1997**, *272*, C853–C859.
- (48) Khan, T. Z.; Wagener, J. S.; Bost, T.; Martinez, J.; Accurso, F. J.; Riches, D. W. Early Pulmonary Inflammation in Infants with Cystic Fibrosis. *Am. J. Respir. Crit. Care Med.* **1995**, *151*, 1075–1082.
- (49) Tirouvanziam, R.; de Bentzmann, S.; Hubeau, C.; Hinnrasky, J.; Jacquot, J.; Péault, B.; Puchelle, E. Inflammation and Infection in Naive Human Cystic Fibrosis Airway Grafts. *Am. J. Respir. Cell Mol. Biol.* **2000**, *23*, 121–127.
- (50) Armstrong, D. S.; Hook, S. M.; Jansen, K. M.; Nixon, G. M.; Carzino, R.; Carlin, J. B.; Robertson, C. F.; Grimwood, K. Lower Airway Inflammation in Infants with Cystic Fibrosis Detected by Newborn Screening. *Pediatr. Pulmonol.* **2005**, *40*, 500–510.
- (51) Cantin, A. M.; Hartl, D.; Konstan, M. W.; Chmiel, J. F. Inflammation in Cystic Fibrosis Lung Disease: Pathogenesis and Therapy. *J. Cyst. Fibros.* **2015**, *14*, 419–430.
- (52) De Rose, V. Mechanisms and Markers of Airway Inflammation in Cystic Fibrosis. *Eur. Respir. J.* **2002**, *19*, 333–340.
- (53) Downey, D. G.; Bell, S. C.; Elborn, J. S. Neutrophils in Cystic Fibrosis. *Thorax* **2009**, *64*, 81–88.
- (54) Rowe, S. M.; Borowitz, D. S.; Burns, J. L.; Clancy, J. P.; Donaldson, S. H.; Retsch-Bogart, G.; Sagel, S. D.; Ramsey, B. W. Progress in Cystic Fibrosis and the CF Therapeutics Development Network. *Thorax* **2012**, *67*, 882–890.
- (55) Sloane, P. A.; Rowe, S. M. Cystic Fibrosis Transmembrane Conductance Regulator Protein Repair as a Therapeutic Strategy in Cystic Fibrosis. *Curr. Opin. Pulm. Med.* **2010**, *16*, 591–597.
- (56) Bobadilla, J. L.; Macek, M.; Fine, J. P.; Farrell, P. M. Cystic Fibrosis: A Worldwide Analysis of CFTR Mutations—correlation with Incidence Data and Application to Screening. *Hum. Mutat.* **2002**, *19*, 575–606.

- (57) Hoffman, L. R.; Ramsey, B. W. Cystic Fibrosis Therapeutics: The Road Ahead. *Chest* **2013**, *143*, 207–213.
- (58) Tarran, R.; Grubb, B. R.; Parsons, D.; Picher, M.; Hirsh, A. J.; Davis, C. W.; Boucher, R. C. The CF Salt Controversy: In Vivo Observations and Therapeutic Approaches. *Mol. Cell* **2001**, *8*, 149–158.
- (59) Ratjen, F. Restoring Airway Surface Liquid in Cystic Fibrosis. *N. Engl. J. Med.* **2006**, *354*, 291–293.
- (60) Wills, P. J.; Hall, R. L.; Chan, W.; Cole, P. J. Sodium Chloride Increases the Ciliary Transportability of Cystic Fibrosis and Bronchiectasis Sputum on the Mucus-Depleted Bovine Trachea. *J. Clin. Invest.* **1997**, *99*, 9–13.
- (61) Daviskas, E.; Robinson, M.; Anderson, S. D.; Bye, P. T. P. Osmotic Stimuli Increase Clearance of Mucus in Patients with Mucociliary Dysfunction. *J. Aerosol Med.* **2002**, *15*, 331–341.
- (62) Elkins, M. R.; Robinson, M.; Rose, B. R.; Harbour, C.; Moriarty, C. P.; Marks, G. B.; Belousova, E. G.; Xuan, W.; Bye, P. T. P. A Controlled Trial of Long-Term Inhaled Hypertonic Saline in Patients with Cystic Fibrosis. *N. Engl. J. Med.* **2006**, *354*, 229–240.
- (63) Henke, M. O.; Ratjen, F. Mucolytics in Cystic Fibrosis. *Paediatr. Respir. Rev.* **2007**, *8*, 24–29.
- (64) Fuchs, H. J.; Borowitz, D. S.; Christiansen, D. H.; Morris, E. M.; Nash, M. L.; Ramsey, B. W.; Rosenstein, B. J.; Smith, A. L.; Wohl, M. E. Effect of Aerosolized Recombinant Human DNase on Exacerbations of Respiratory Symptoms and on Pulmonary Function in Patients with Cystic Fibrosis. *N. Engl. J. Med.* **1994**, *331*, 637–642.
- (65) Mogayzel, P. J.; Naureckas, E. T.; Robinson, K. A.; Mueller, G.; Hadjiliadis, D.; Hoag, J. B.; Lubsch, L.; Hazle, L.; Sadosky, K.; Marshall, B. Cystic Fibrosis Pulmonary Guidelines. *Am. J. Respir. Crit. Care Med.* **2013**, *187*, 680–689.
- (66) Rubin, B. K. Mucus, Phlegm, and Sputum in Cystic Fibrosis. *Respir. Care* **2009**, *54*, 726–732.
- (67) Johnson, K.; McEvoy, C. E.; Naqvi, S.; Wendt, C.; Reilkoff, R. A.; Kunisaki, K. M.; Wetherbee, E. E.; Nelson, D.; Tirouvanziam, R.; Niewoehner, D. E. High-Dose Oral N-Acetylcysteine Fails to Improve Respiratory Health Status in Patients with Chronic Obstructive Pulmonary Disease and Chronic Bronchitis: A Randomized, Placebo-Controlled Trial. *Int. J. Chron. Obstruct. Pulmon. Dis.* **2016**, *11*, 799–807.
- (68) Rodríguez-Beltrán, J.; Cabot, G.; Valencia, E. Y.; Costas, C.; Bou, G.; Oliver, A.; Blázquez, J. N-Acetylcysteine Selectively Antagonizes the Activity of Imipenem in *Pseudomonas Aeruginosa* by an OprD-Mediated Mechanism. *Antimicrob. Agents Chemother.* **2015**, *59*, 3246–3251.
- (69) Flume, P. A.; O’Sullivan, B. P.; Robinson, K. A.; Goss, C. H.; Mogayzel, P. J.; Willey-Courand, D. B.; Bujan, J.; Finder, J.; Lester, M.; Quittell, L. Cystic Fibrosis Pulmonary Guidelines Chronic Medications for Maintenance of Lung Health. *Am. J. Respir. Crit. Care Med.* **2007**, *176*, 957–969.

- (70) Ciofu, O.; Tolker-Nielsen, T.; Jensen, P. Ø.; Wang, H.; Høiby, N. Antimicrobial Resistance, Respiratory Tract Infections and Role of Biofilms in Lung Infections in Cystic Fibrosis Patients. *Adv. Drug Deliv. Rev.* **2015**, *85*, 7–23.
- (71) Høiby Bjarsholt, T., Givskov, M., Molin, S., Ciofu, O., N. Antibiotic Resistance of Bacterial Biofilms. *Int. J. Antimicrob. Agents* **2010**, *35*, 322–332.
- (72) Rytting, E.; Nguyen, J.; Wang, X.; Kissel, T. Biodegradable Polymeric Nanocarriers for Pulmonary Drug Delivery. *Expert Opin. Drug Deliv.* **2008**, *5*, 629–639.
- (73) Makadia, H. K.; Siegel, S. J. Poly Lactic-Co-Glycolic Acid (PLGA) as Biodegradable Controlled Drug Delivery Carrier. *Polymers*. **2011**, *3*, 1377–1397.
- (74) Cu, Y.; Saltzman, W. M. Controlled Surface Modification with Poly(Ethylene)Glycol Enhances Diffusion of PLGA Nanoparticles in Human Cervical Mucus. *Mol. Pharm.* **2009**, *6*, 173–181.
- (75) Ungaro, F.; D’Angelo, I.; Coletta, C.; d’Emmanuele di Villa Bianca, R.; Sorrentino, R.; Perfetto, B.; Tufano, M. A.; Miro, A.; La Rotonda, M. I.; Quaglia, F. Dry Powders Based on PLGA Nanoparticles for Pulmonary Delivery of Antibiotics: Modulation of Encapsulation Efficiency, Release Rate and Lung Deposition Pattern by Hydrophilic Polymers. *J. Control. Release* **2012**, *157*, 149–159.
- (76) Bivas-Benita, M.; Romeijn, S.; Junginger, H. E.; Borchard, G. PLGA–PEI Nanoparticles for Gene Delivery to Pulmonary Epithelium. *Eur. J. Pharm. Biopharm.* **2004**, *58*, 1–6.
- (77) Chmiel, J. F.; Berger, M.; Konstan, M. W. The Role of Inflammation in the Pathophysiology of CF Lung Disease the Excessive Production of the Inflammatory Mediators in the CF Lung, Thereby Slowing the Decline in Lung Function and Improving Survival. *Clin. Rev. Allergy Immunol.* **2002**, *23*, 5–27.
- (78) Balfour-Lynn, I. M.; Lees, B.; Hall, P.; Phillips, G.; Khan, M.; Flather, M.; Elborn, J. S. Multicenter Randomized Controlled Trial of Withdrawal of Inhaled Corticosteroids in Cystic Fibrosis. *Am. J. Respir. Crit. Care Med.* **2006**, *173*, 1356–1362.
- (79) Stephenson, A. L.; Sykes, J.; Berthiaume, Y.; Singer, L. G.; Aaron, S. D.; Whitmore, G. A.; Stanojevic, S. Clinical and Demographic Factors Associated with Post-lung Transplantation Survival in Individuals with Cystic Fibrosis. *J. Hear. Lung Transplant.* **2015**, *34*, 1139–1145.
- (80) Benden, C. Pediatric Lung Transplantation. *J. Thorac. Dis.* **2017**, *9*, 2675–2683.
- (81) Carpenter, A. W.; Schoenfisch, M. H. Nitric Oxide Release: Part II. Therapeutic Applications. *Chem. Soc. Rev.* **2012**, *41*, 3742–3752.
- (82) Loscalzo, J.; Welch, G. Nitric Oxide and Its Role in the Cardiovascular System. *Prog. Cardiovasc. Dis.* **1995**, *38*, 87–104.
- (83) Bogdan, C. Nitric Oxide and the Immune Response. *Nat. Immunol.* **2001**, *2*, 907–916.
- (84) Garthwaite, J.; Boulton, C. L. Nitric Oxide Signaling in the Central Nervous System. *Annu. Rev. Physiol.* **1995**, *57*, 683–706.

- (85) Hill, B. G.; Dranka, B. P.; Bailey, S. M.; Lancaster, J. R.; Darley-Usmar, V. M. What Part of NO Don't You Understand? Some Answers to the Cardinal Questions in Nitric Oxide Biology. *J. Biol. Chem.* **2010**, *285*, 19699–19704.
- (86) Prast, H.; Philippu, A. Nitric Oxide as Modulator of Neuronal Function. *Prog. Neurobiol.* **2001**, *64*, 51–68.
- (87) Rizk, M.; Witte, M. B.; Barbul, A. Nitric Oxide and Wound Healing. *World J. Surg.* **2004**, *28*, 301–306.
- (88) Schäffer, M. R.; Tantry, U.; Gross, S. S.; Wasserkrug, H. L.; Barbul, A. Nitric Oxide Regulates Wound Healing. *J. Surg. Res.* **1996**, *63*, 237–240.
- (89) Witte, M. B.; Barbul, A. Role of Nitric Oxide in Wound Repair. *Am. J. Surg.* **2002**, *183*, 406–412.
- (90) Fang, F. C. Perspectives Series: Host/Pathogen Interactions. Mechanisms of Nitric Oxide-Related Antimicrobial Activity. *J. Clin. Invest.* **1997**, *99*, 2818–2825.
- (91) Jones, M. L.; Ganopolsky, J. G.; Labbé, A.; Wahl, C.; Prakash, S. Antimicrobial Properties of Nitric Oxide and Its Application in Antimicrobial Formulations and Medical Devices. *Appl. Microbiol. Biotechnol.* **2010**, *88*, 401–407.
- (92) Barraud, N.; Hassett, D. J.; Hwang, S. H.; Rice, S. A.; Kjelleberg, S.; Webb, J. S. Involvement of Nitric Oxide in Biofilm Dispersal of *Pseudomonas Aeruginosa*. *J. Bacteriol.* **2006**, *188*, 7344–7353.
- (93) Barraud, N.; Kelso, M. J.; Rice, S. A.; Kjellerberg, S. Nitric Oxide: A Key Mediator of Biofilm Dispersal with Applications in Infectious Diseases. *Curr. Pharm. Des.* **2015**, *21*, 31–42.
- (94) Hetrick, E. M.; Shin, J. H.; Stasko, N. A.; Johnson, C. B.; Wespe, D. A.; Holmuhamedov, E.; Schoenfisch, M. H. Bactericidal Efficacy of Nitric Oxide-Releasing Silica Nanoparticles. *ACS Nano* **2008**, *2*, 235–246.
- (95) Schairer, D. O.; Chouake, J. S.; Nosanchuk, J. D.; Friedman, A. J. The Potential of Nitric Oxide Releasing Therapies as Antimicrobial Agents. *Virulence* **2012**, *3*, 271–279.
- (96) Wink, D. A.; Kasprzak, K. S.; Maragos, C. M.; Elespuru, R. K.; Misra, M.; Dunams, T. M.; Cebula, T. A.; Koch, W. H.; Andrews, A. W.; Allen, J. S.; et al. DNA Deaminating Ability and Genotoxicity of Nitric Oxide and Its Progenitors. *Science*. **1991**, *254*, 1001–1003.
- (97) Yang, L.; Feura, E. S.; Ahonen, M. J. R.; Schoenfisch, M. H. Nitric Oxide-Releasing Macromolecular Scaffolds for Antibacterial Applications. *Adv. Healthc. Mater.* **2018**, *7*, 1800155.
- (98) Privett, B. J.; Broadnax, A. D.; Bauman, S. J.; Riccio, D. A.; Schoenfisch, M. H. Examination of Bacterial Resistance to Exogenous Nitric Oxide. *Nitric Oxide* **2012**, *26*, 169–173.
- (99) Barraud, N.; Storey, M. V; Moore, Z. P.; Webb, J. S.; Rice, S. A.; Kjelleberg, S. Nitric Oxide-Mediated Dispersal in Single-and Multi-Species Biofilms of Clinically and

- Industrially Relevant Microorganisms. *Microb. Biotechnol.* **2009**, *2*, 370–378.
- (100) Arora, D. P.; Hossain, S.; Xu, Y.; Boon, E. M. Nitric Oxide Regulation of Bacterial Biofilms. *Biochemistry* **2015**, *54*, 3717–3728.
- (101) Kaplan, J. B. Biofilm Dispersal: Mechanisms, Clinical Implications, and Potential Therapeutic Uses. *J. Dent. Res.* **2010**, *89*, 205–218.
- (102) Hossain, S.; Nisbett, L.-M.; Boon, E. M. Discovery of Two Bacterial Nitric Oxide-Responsive Proteins and Their Roles in Bacterial Biofilm Regulation. *Acc. Chem. Res.* **2017**, *50*, 1633–1639.
- (103) Neufeld, B. H.; Reynolds, M. M. Critical Nitric Oxide Concentration for *Pseudomonas Aeruginosa* Biofilm Reduction on Polyurethane Substrates. *Biointerphases* **2016**, *11*, 31012.
- (104) Duan, J.; Kasper, D. L. Oxidative Depolymerization of Polysaccharides by Reactive Oxygen/Nitrogen Species. *Glycobiology* **2011**, *21*, 401–409.
- (105) Burney, S.; Caulfield, J. L.; Niles, J. C.; Wishnok, J. S.; Tannenbaum, S. R. The Chemistry of DNA Damage from Nitric Oxide and Peroxynitrite. *Mutat. Res. Mol. Mech. Mutagen.* **1999**, *424*, 37–49.
- (106) Miller, C. C.; Hergott, C. A.; Rohan, M.; Arsenault-Mehta, K.; Döring, G.; Metha, S. Inhaled Nitric Oxide Decreases the Bacterial Load in a Rat Model of *Pseudomonas Aeruginosa* Pneumonia. *J. Cyst. Fibros.* **2013**, *12*, 817–820.
- (107) Miller, C.; McMullin, B.; Ghaffari, A.; Stenzler, A.; Pick, N.; Roscoe, D.; Ghahary, A.; Road, J.; Av-Gay, Y. Gaseous Nitric Oxide Bactericidal Activity Retained during Intermittent High-Dose Short Duration Exposure. *Nitric Oxide* **2009**, *20*, 16–23.
- (108) Webert, K. E.; Vanderzwan, J.; Duggan, M.; Scott, J. A.; McCormack, D. G.; Lewis, J. F.; Mehta, S. Effects of Inhaled Nitric Oxide in a Rat Model of *Pseudomonas Aeruginosa* Pneumonia. *Crit. Care Med.* **2000**, *28*, 2397–2405.
- (109) Jean, D.; Maître, B.; Tankovic, J.; Meignan, M.; Adnot, S.; Brun-Buisson, C.; Harf, A.; Delclaux, C. Beneficial Effects of Nitric Oxide Inhalation on Pulmonary Bacterial Clearance. *Crit. Care Med.* **2002**, *30*, 442–447.
- (110) Deppisch, C.; Herrmann, G.; Graepler-Mainka, U.; Wirtz, H.; Heyder, S.; Engel, C.; Marschal, M.; Miller, C. C.; Riethmüller, J. Gaseous Nitric Oxide to Treat Antibiotic Resistant Bacterial and Fungal Lung Infections in Patients with Cystic Fibrosis: A Phase I Clinical Study. *Infection* **2016**, *44*, 513–520.
- (111) Griffiths, M. J. D.; Evans, T. W. Inhaled Nitric Oxide Therapy in Adults. *N. Engl. J. Med.* **2005**, *353*, 2683–2695.
- (112) Ratjen, F.; Gärtig, S.; Wiesemann, H. G.; Grasemann, H. Effect of Inhaled Nitric Oxide on Pulmonary Function in Cystic Fibrosis. *Respir. Med.* **1999**, *93*, 579–583.
- (113) Grasemann, H.; Grasemann, C.; Kurtz, F.; Tietze-Schillings, G.; Vester, U.; Ratjen, F. Oral L-Arginine Supplementation in Cystic Fibrosis Patients: A Placebo-Controlled Study. *Eur.*

- Respir. J.* **2005**, *25*, 62–68.
- (114) Grasemann, H.; Tullis, E.; Ratjen, F. A Randomized Controlled Trial of Inhaled L-Arginine in Patients with Cystic Fibrosis. *J. Cyst. Fibros.* **2013**, *12*, 468–474.
- (115) Grasemann, H.; Kurtz, F.; Ratjen, F. Inhaled L-Arginine Improves Exhaled Nitric Oxide and Pulmonary Function in Patients with Cystic Fibrosis. *Am. J. Respir. Crit. Care Med.* **2006**, *174*, 208–212.
- (116) de Winter-de Groot, K. M.; van der Ent, C. K. Nitric Oxide in Cystic Fibrosis. *J. Cyst. Fibros.* **2005**, *4*, 25–29.
- (117) Jones, K. L.; Hegab, A. H.; Hillman, B. C.; Simpson, K. L.; Jinkins, P. A.; Grisham, M. B.; Owens, M. W.; Sato, E.; Robbins, R. A. Elevation of Nitrotyrosine and Nitrate Concentrations in Cystic Fibrosis Sputum. *Pediatr. Pulmonol.* **2000**, *30*, 79–85.
- (118) Gaston, B.; Ratjen, F.; Vaughan, J. W.; Malhotra, N. R.; Canady, R. G.; Snyder, A. H.; Hunt, J. F.; Gaertig, S.; Goldberg, J. B. Nitrogen Redox Balance in the Cystic Fibrosis Airway: Effects of Antipseudomonal Therapy. *Am. J. Respir. Crit. Care Med.* **2002**, *165*, 387–390.
- (119) Grasemann, H.; Schwiertz, R.; Grasemann, C.; Vester, U.; Racké, K.; Ratjen, F. Decreased Systemic Bioavailability of L-Arginine in Patients with Cystic Fibrosis. *Respir. Res.* **2006**, *7*, 87–93.
- (120) Grasemann, Hartmut; Ratjen, F. Nitric Oxide and L-Arginine Deficiency in Cystic Fibrosis. *Curr. Pharm. Des.* **2012**, *18*, 726–736.
- (121) Grasemann, H.; Gartig, S. S.; Wiesemann, H. G.; Teschler, H.; Konietzko, N.; Ratjen, F. Effect of L-Arginine Infusion on Airway NO in Cystic Fibrosis and Primary Ciliary Dyskinesia Syndrome. *Eur. Respir. J.* **1999**, *13*, 114–118.
- (122) Miller, C. C.; Hole, D. R.; Murray, B. R.; Perry, B. Use of Inhaled Gaseous Nitric Oxide as a Mucolytic Agent or Expectorant. US8518457, 2013.
- (123) Tsutsumi, N.; Itoh, T.; Ohsawa, A. Cleavage of S-S Bond by Nitric Oxide (NO) in the Presence of Oxygen: A Disproportionation Reaction of Two Disulfides. *Chem. Pharm. Bull. Tokyo* **2000**, *48*, 1524–1528.
- (124) Riccio, D. A.; Schoenfish, M. H. Nitric Oxide Release: Part I. Macromolecular Scaffolds. *Chem. Soc. Rev.* **2012**, *41*, 3731–3741.
- (125) Lu, Y.; Sun, B.; Li, C.; Schoenfish, M. H. Structurally Diverse Nitric Oxide-Releasing Poly (Propylene Imine) Dendrimers. *Chem. Mater.* **2011**, *23*, 4227–4233.
- (126) Stasko, N. A.; Schoenfish, M. H. Dendrimers as a Scaffold for Nitric Oxide Release. *J. Am. Chem. Soc.* **2006**, *128*, 8265–8271.
- (127) Worley, B. V.; Schilly, K. M.; Schoenfish, M. H. Anti-Biofilm Efficacy of Dual-Action Nitric Oxide-Releasing Alkyl Chain Modified Poly(Amidoamine) Dendrimers. *Mol. Pharm.* **2015**, *12*, 1573–1583.
- (128) Worley, B. V.; Slomberg, D. L.; Schoenfish, M. H. Nitric Oxide-Releasing Quaternary

- Ammonium-Modified Poly(Amidoamine) Dendrimers as Dual Action Antibacterial Agents. *Bioconjugate Chem.* **2014**, *25*, 918–927.
- (129) Sun, B.; Slomberg, D. L.; Chudasama, S. L.; Lu, Y.; Schoenfisch, M. H. Nitric Oxide-Releasing Dendrimers as Antibacterial Agents. *Biomacromolecules* **2012**, *13*, 3343–3354.
- (130) Lu, Y.; Slomberg, D. L.; Shah, A.; Schoenfisch, M. H. Nitric Oxide-Releasing Amphiphilic Poly(Amidoamine) (PAMAM) Dendrimers as Antibacterial Agents. *Biomacromolecules* **2013**, *14*, 3589–3598.
- (131) Backlund, C. J.; Worley, B. V.; Sergesketter, A. R.; Schoenfisch, M. H. Kinetic-Dependent Killing of Oral Pathogens with Nitric Oxide. *J. Dent. Res.* **2015**, *94*, 1092–1098.
- (132) Carpenter, A. W.; Slomberg, D. L.; Rao, K. S.; Schoenfisch, M. H. Influence of Scaffold Size on Bactericidal Activity of Nitric Oxide-Releasing Silica Nanoparticles. *ACS Nano* **2011**, *5*, 7235–7244.
- (133) Carpenter, A. W.; Worley, B. V.; Slomberg, D. L.; Schoenfisch, M. H. Dual Action Antimicrobials: Nitric Oxide Release from Quarternary Ammonium-Functionalized Silica Nanoparticles. *Biomacromolecules* **2012**, *13*, 3334–3342.
- (134) Hetrick, E. M.; Shin, J. H.; Paul, H. S.; Schoenfisch, M. H. Anti-Biofilm Efficacy of Nitric Oxide-Releasing Silica Nanoparticles. *Biomaterials* **2009**, *30*, 2782–2789.
- (135) Slomberg, D. L.; Lu, Y.; Broadnax, A. D.; Hunter, R. A.; Carpenter, A. W.; Schoenfisch, M. H. Role of Size and Shape on Biofilm Eradication for Nitric Oxide-Releasing Silica Nanoparticles. *ACS Appl. Mater. Interfaces* **2013**, *5*, 9322–9329.
- (136) Lu, Y.; Shah, A.; Hunter, R. A.; Soto, R. J.; Schoenfisch, M. H. S-Nitrosothiol-Modified Nitric Oxide-Releasing Chitosan Oligosaccharides as Antibacterial Agents. *Acta Biomater.* **2015**, *12*, 62–69.
- (137) Lu, Y.; Slomberg, D. L.; Schoenfisch, M. H. Nitric Oxide-Releasing Chitosan Oligosaccharides as Antibacterial Agents. *Biomaterials* **2014**, *35*, 1716–1724.
- (138) Seabra, A. B.; Durán, N. Nitric Oxide-Releasing Vehicles for Biomedical Applications. *J. Mater. Chem.* **2010**, *20*, 1624–1637.
- (139) Seabra, A. B.; Justo, G. Z.; Haddad, P. S. State of the Art, Challenges and Perspectives in the Design of Nitric Oxide-Releasing Polymeric Nanomaterials for Biomedical Applications. *Biotechnol. Adv.* **2015**, *33*, 1370–1379.
- (140) Wo, Y.; Brisbois, E. J.; Bartlett, R. H.; Meyerhoff, M. E. Recent Advances in Thromboresistant and Antimicrobial Polymers for Biomedical Applications: Just Say Yes to Nitric Oxide (NO). *Biomater. Sci.* **2016**, *4*, 1161–1183.
- (141) Stamler, J. S.; Jaraki, O.; Osborne, J.; Simon, D. I.; Keaney, J.; Vita, J.; Singel, D.; Valeri, C. R.; Loscalzo, J. Nitric Oxide Circulates in Mammalian Plasma Primarily as an S-Nitroso Adduct of Serum Albumin. *Proc. Natl. Acad. Sci.* **1992**, *89*, 7674–7677.
- (142) Wang, P. G.; Xian, M.; Tang, X.; Wu, X.; Wen, Z.; Cai, T.; Janczuk, A. J. Nitric Oxide Donors: Chemical Activities and Biological Applications. *Chem. Rev.* **2002**, *102*, 1091–

1134.

- (143) Hogg, N. The Biochemistry and Physiology of S-Nitrosothiols. *Annu. Rev. Pharmacol. Toxicol.* **2002**, *42*, 585–600.
- (144) Holmes, A. J.; Williams, D. L. H. Reaction of Ascorbic Acid with S-Nitrosothiols: Clear Evidence for Two Distinct Reaction Pathways. *J. Chem. Soc. Perkin Trans. 2* **2000**, 1639–1644.
- (145) Cantin, A. M.; White, T. B.; Cross, C. E.; Forman, H. J.; Sokol, R. J.; Borowitz, D. Antioxidants in Cystic Fibrosis. *Free Radic. Biol. Med.* **2007**, *42*, 15–31.
- (146) Keefer, L. K. Fifty Years of Diazeniumdiolate Research. From Laboratory Curiosity to Broad-Spectrum Biomedical Advances. *ACS Chem. Biol.* **2011**, *6*, 1147–1155.
- (147) Keefer, L. K.; Nims, R. W.; Davies, K. M.; Wink, D. A. Diazeniumdiolates as NO Dosage Forms. *Methods Enzymol.* **1996**, *268*, 281–293.
- (148) Davies, K. M.; Wink, D. A.; Saavedra, J. E.; Keefer, L. K. Chemistry of the Diazeniumdiolates. 2. Kinetics and Mechanism of Dissociation to Nitric Oxide in Aqueous Solution. *J. Am. Chem. Soc.* **2001**, *123*, 5473–5481.
- (149) Hrabie, J. A.; Klose, J. R.; Wink, D. A.; Keefer, L. K. New Nitric Oxide-Releasing Zwitterions Derived from Polyamines. *J. Org. Chem.* **1993**, *58*, 1472–1476.
- (150) Keefer, L. K. Nitric Oxide (NO)- and Nitroxyl (HNO)-Generating Diazeniumdiolates (NONOates): Emerging Commercial Opportunities. *Curr. Top. Med. Chem.* **2005**, *5*, 625–636.
- (151) Pritchard, M. F.; Powell, L. C.; Menzies, G. E.; Lewis, P. D.; Hawkins, K.; Wright, C.; Doull, I.; Walsh, T. R.; Onsøyen, E.; Dessen, A.; et al. A New Class of Safe Oligosaccharide Polymer Therapy to Modify the Mucus Barrier of Chronic Respiratory Disease. *Mol. Pharm.* **2016**, *13*, 863–873.
- (152) Sletmoen, M.; Maurstad, G.; Nordgård, C. T.; Draget, K. I.; Stokke, B. T. Oligoguluronate Induced Competitive Displacement of Mucin-Alginate Interactions: Relevance for Mucolytic Function. *Soft Matter* **2011**, *8*, 8413–8421.
- (153) Nordgård, C. T.; Draget, K. I. Oligosaccharides as Modulators of Rheology in Complex Mucous Systems. *Biomacromolecules* **2011**, *12*, 3084–3090.
- (154) Nordgård, C. T.; Nonstad, U.; Olderø, M. Ø.; Espevik, T.; Draget, K. I. Alterations in Mucus Barrier Function and Matrix Structure Induced by Guluronate Oligomers. *Biomacromolecules* **2014**, *15*, 2294–2300.
- (155) Forier, K.; Messiaen, A.-S.; Raemdonck, K.; Deschout, H.; Rejman, J.; De Baets, F.; Nelis, H.; De Smedt, S. C.; Demeester, J.; Coenye, T. Transport of Nanoparticles in Cystic Fibrosis Sputum and Bacterial Biofilms by Single-Particle Tracking Microscopy. *Nanomedicine* **2012**, *20*, 1–15.
- (156) Wang, Y.; Lai, S. K.; Suk, J. S.; Pace, A.; Cone, R.; Hanes, J. Addressing the PEG Mucoadhesivity Paradox to Engineer Nanoparticles That “Slip” through the Human Mucus

- Barrier. *Angew. Chemie Int. Ed.* **2008**, *47*, 9726–9729.
- (157) Park, J. H.; Jin, H. E.; Kim, D. D.; Chung, S. J.; Shim, W. S.; Shim, C. K. Chitosan Microspheres as an Alveolar Macrophage Delivery System of Ofloxacin via Pulmonary Inhalation. *Int. J. Pharm.* **2013**, *441*, 562–569.
- (158) Jain, D.; Banerjee, R. Comparison of Ciprofloxacin Hydrochloride-Loaded Protein, Lipid, and Chitosan Nanoparticles for Drug Delivery. *J. Biomed. Mater. Res. - Part B Appl. Biomater.* **2008**, *86*, 105–112.
- (159) Osman, R.; Kan, P. L.; Awad, G.; Mortada, N.; EL-Shamy, A.-E.; Alpar, O. Spray Dried Inhalable Ciprofloxacin Powder with Improved Aerosolisation and Antimicrobial Activity. *Int. J. Pharm.* **2013**, *449*, 44–58.
- (160) Grenha, A.; Al-Qadi, S.; Seijo, B.; Remuñán-López, C. The Potential of Chitosan for Pulmonary Drug Delivery. *J. Drug Deliv. Sci. Technol.* **2010**, *20*, 33–43.
- (161) Andrews, G. P.; Laverty, T. P.; Jones, D. S. Mucoadhesive Polymeric Platforms for Controlled Drug Delivery. *Eur. J. Pharm. Biopharm.* **2009**, *71*, 505–518.
- (162) Lu, Y.; Slomberg, D. L.; Sun, B.; Schoenfisch, M. H. Shape- and Nitric Oxide Flux-Dependent Bactericidal Activity of Nitric Oxide-Releasing Silica Nanorods. *Small* **2013**, *9*, 2189–2198.
- (163) Wan, A.; Gao, Q.; Li, H. Effects of Molecular Weight and Degree of Acetylation on the Release of Nitric Oxide from Chitosan-Nitric Oxide Adducts. *J. App. Polm. Sci.* **2010**, *117*, 2183–2188.
- (164) Reighard, K. P.; Schoenfisch, M. H. Antibacterial Action of Nitric Oxide-Releasing Chitosan Oligosaccharides against *Pseudomonas Aeruginosa* under Aerobic and Anaerobic Conditions. *Antimicrob. Agents Chemother.* **2015**, *59*, 6506–6513.
- (165) Reighard, K. P.; Hill, D. B.; Dixon, G. A.; Worley, B. V.; Schoenfisch, M. H. Disruption and Eradication of *P. Aeruginosa* Biofilms Using Nitric Oxide-Releasing Chitosan Oligosaccharides. *Biofouling* **2015**, *31*, 775–787.
- (166) Reighard, K. P.; Ehre, C.; Rushton, Z. L.; Ahonen, M. J. R.; Hill, D. B.; Schoenfisch, M. H. Role of Nitric Oxide-Releasing Chitosan Oligosaccharides on Mucus Viscoelasticity. *ACS Biomater. Sci. Eng.* **2017**, *3*, 1017–1026.
- (167) Chang, K. L. B.; Tai, M.-C.; Cheng, F.-H. Kinetics and Products of the Degradation of Chitosan by Hydrogen Peroxide. *J. Agric. Food Chem.* **2001**, *49*, 4845–4851.
- (168) Nair, L. S.; Laurencin, C. T. Biodegradable Polymers as Biomaterials. *Prog. Polym. Sci.* **2007**, *32*, 762–798.
- (169) Draget, K. I.; Taylor, C. Chemical, Physical and Biological Properties of Alginates and Their Biomedical Implications. *Food Hydrocoll.* **2011**, *25*, 251–256.
- (170) Liakos, I.; Rizzello, L.; Scurr, D. J.; Pompa, P. P. All-Natural Composite Wound Dressing Films of Essential Oils Encapsulated in Sodium Alginate with Antimicrobial Properties. *Int. J. Pharm.* **2014**, *463*, 137–145.

- (171) Paul, W.; Sharma, C. P. Chitosan and Alginate Wound Dressings: A Short Review. *Trends Biomater. Artif. Organs* **2004**, *18*, 18–23.
- (172) Gombotz, W. R.; Wee, S. Protein Release from Alginate Matrices. *Adv. Drug Deliv. Rev.* **1998**, *31*, 267–285.
- (173) Lee, K. Y.; Mooney, D. J. Alginate: Properties and Biomedical Applications. *Prog. Polym. Sci.* **2012**, *37*, 106–126.
- (174) Jain, D.; Bar-Shalom, D. Alginate Drug Delivery Systems: Application in Context of Pharmaceutical and Biomedical Research. *Drug Dev. Ind. Pharm.* **2014**, *40*, 1576–1584.
- (175) Roberts, J. L.; Khan, S.; Emanuel, C.; Powell, L. C.; Pritchard, M. F.; Onsøyen, E.; Myrvold, R.; Thomas, D. W.; Hill, K. E. An in Vitro Study of Alginate Oligomer Therapies on Oral Biofilms. *J. Dent.* **2013**, *41*, 892–899.
- (176) Khan, S.; Tøndervik, A.; Sletta, H.; Klinkenberg, G.; Emanuel, C.; Onsøyen, E.; Myrvold, R.; Howe, R. A.; Walsh, T. R.; Hill, K. E.; et al. Overcoming Drug Resistance with Alginate Oligosaccharides Able To Potentiate the Action of Selected Antibiotics. *Antimicrob. Agents Chemother.* **2012**, *56*, 5134–5141.
- (177) Hengzhuang, W.; Song, Z.; Ciofu, O.; Onsøyen, E.; Rye, P. D.; Høiby, N. OligoG CF-5/20 Disruption of Mucoid Pseudomonas Aeruginosa Biofilm in a Murine Lung Infection Model. *Antimicrob. Agents Chemother.* **2016**, *60*, 2620–2626.
- (178) Skjåk-Bræk, G.; Grasdalen, H.; Larsen, B. Monomer Sequence and Acetylation Pattern in Some Bacterial Alginates. *Carbohydr. Res.* **1986**, *154*, 239–250.
- (179) Sun, J.; Tan, H. Alginate-Based Biomaterials for Regenerative Medicine Applications. *Materials.* **2013**, *6*, 1285–1309.
- (180) Draget, K. I.; Skjåk Bræk, G.; Smidsrød, O. Alginic Acid Gels: The Effect of Alginate Chemical Composition and Molecular Weight. *Carbohydr. Polym.* **1994**, *25*, 31–38.
- (181) George, M.; Abraham, T. E. Polyionic Hydrocolloids for the Intestinal Delivery of Protein Drugs: Alginate and Chitosan — a Review. *J. Control. Release* **2006**, *114*, 1–14.
- (182) Smidsrød, O.; Glover, R. M.; Whittington, S. G. The Relative Extension of Alginates Having Different Chemical Composition. *Carbohydr. Res.* **1973**, *27*, 107–118.
- (183) Andriamanantoanina, H.; Rinaudo, M. Relationship between the Molecular Structure of Alginates and Their Gelation in Acidic Conditions. *Polym. Int.* **2010**, *59*, 1531–1541.
- (184) Moe, S. T.; Skjaak-Braek, G.; Elgsaeter, A.; Smidsroed, O. Swelling of Covalently Crosslinked Alginate Gels: Influence of Ionic Solutes and Nonpolar Solvents. *Macromolecules* **1993**, *26*, 3589–3597.
- (185) Hajiali, H.; Summa, M.; Russo, D.; Armirotti, A.; Brunetti, V.; Bertorelli, R.; Athanassiou, A.; Mele, E. Alginate-Lavender Nanofibers with Antibacterial and Anti-Inflammatory Activity to Effectively Promote Burn Healing. *J. Mater. Chem. B* **2016**, *4*, 1686–1695.
- (186) Yang, J.; Zheng, H.; Han, S.; Jiang, Z.; Chen, X. The Synthesis of Nano-Silver/Sodium Alginate Composites and Their Antibacterial Properties. *RSC Adv.* **2015**, *5*, 2378–2382.

- (187) Jain, J.; Arora, S.; Rajwade, J. M.; Omay, P.; Khandelwal, S.; Paknikar, K. M. Silver Nanoparticles in Therapeutics: Development of an Antimicrobial Gel Formulation for Topical Use. *Mol. Pharm.* **2009**, *6*, 1388–1401.
- (188) Marta, B.; Jakab, E.; Potara, M.; Simon, T.; Imre-Lucaci, F.; Barbu-Tudoran, L.; Popescu, O.; Astilean, S. Pluronic-Coated Silver Nanoprisms: Synthesis, Characterization and Their Antibacterial Activity. *Colloids Surfaces A Physicochem. Eng. Asp.* **2014**, *441*, 77–83.

CHAPTER 2: NITRIC OXIDE-RELEASING ALGINATES

2.1 Introduction

Bacterial infections pose a great challenge to human health in community and hospital settings.¹⁻³ Chronic infections associated with implanted devices,⁴ wounds,^{2,5} and cystic fibrosis^{4,6} are frequently caused by biofilm-forming pathogens, including *Pseudomonas aeruginosa* and *Staphylococcus aureus*.^{4,7} Bacteria in biofilms are particularly challenging to address as they form an exopolysaccharide (EPS) matrix as a protective mechanism from the host immune response and antibiotic interventions. Indeed, eradication of bacteria in biofilms may require up to 1000 times greater antibiotic concentrations relative to those needed to kill planktonic bacteria.⁸ Several factors contribute to such protection, including slower bacterial metabolism, limited diffusion of the antibacterial agent (e.g., antibiotic) through the EPS matrix, and altered microenvironments (e.g., regions of nutrient or oxygen depletion).^{4,7,9} Furthermore, bacteria have developed potential cellular mechanisms (e.g., self-alteration of cell membrane targets and the use of pumps to reduce internal concentration of antibiotics) that minimize the effects of antibiotics. New antibacterial agents that can more effectively penetrate and effectively act on biofilm-based bacterial colonies are greatly needed in the fight against emerging antibiotic-resistant pathogens.¹⁰

Nitric oxide (NO) is an endogenous free radical that plays an integral role in the innate immune response to foreign pathogens. Much of NO's broad-spectrum antibacterial activity is accounted for by its reactive byproducts, including peroxynitrite and dinitrogen trioxide, which exert oxidative and nitrosative damage to microbial DNA and membrane structures.¹¹⁻¹⁵ As a result

of NO's small size and the mechanisms by which it exerts antibacterial action, bacteria are unlikely to foster resistance to NO.¹⁶ The hazards of pressurized cylinders, NO's high reactivity in biological media, and even toxicity concerns have led researchers to develop and study the utility of NO donors – both small molecule and macromolecular systems – as a means for storing and releasing NO under specific environmental conditions.^{12,14,17} *N*-diazeniumdiolate NO donors have garnered much attention due to the spontaneous liberation of NO in aqueous solution at physiological pH.¹⁴ While NO's role in immune cell response to pathogens is clear, developing therapies based on the delivery of NO gas is challenging. Unfortunately, NO payloads for small molecule NO donors can be limited with precursor toxicity risks when larger concentrations are required.¹⁷ To address such concerns, we have focused on the development of macromolecular *N*-diazeniumdiolate NO-release systems with inherently superior NO payloads, control over NO release kinetics, and unique release mechanisms.^{18–24}

Biopolymers such as chitosan, cellulose, and alginate represent attractive potential NO donor scaffolds due to their inherent biodegradability and favorable toxicity profiles.^{25,26} Alginate, a naturally occurring anionic polymer consisting of 1,4-linked α -L-guluronic acid (G) and β -D-mannuronic acid (M) units,^{25,27–30} is water soluble even at high molecular weights (>200 kDa), a critical property for in situ release.^{27,28} As a result of these properties, investigators have studied alginate's utility for a number of biomedical applications including wound dressings,^{30–32} drug delivery,^{5,30,33} potentiators for antimicrobial agents,²⁸ and mucin modifiers for cystic fibrosis.^{29,30,34,35} The alginate backbone offers straightforward chemical modification at hydroxyl and carboxylic acid functional groups, imparting unique versatility with respect to drug storage and release, and control over solubility, biocompatibility, and degradation rates.^{27,36,37}

Herein, we describe the functionalization of both high and low molecular weight alginates with small molecule alkyl amines for subsequent modification with *N*-diazoniumdiolate NO donors to produce anionic NO-releasing biopolymers. The alkyl amine precursors were selected based on prior literature describing diverse NO-release kinetics related to breakdown of the *N*-diazoniumdiolate.^{38,39} The bactericidal action of the alginates was examined with respect to NO-release kinetics, total NO storage, amine precursor structure, and molecular weight.

2.2 Experimental Section

2.2.1 Materials

Alginic acid sodium salt from brown algae (low viscosity), bis(3-aminopropyl) amine (DPTA), diethylenetriamine (DETA), *N*-propyl-1,3-propanediamine (PAPA), spermine (SPER), phenazine methosulfate (PMS), 1-ethyl-3-(3-dimethylaminopropyl)carbodiimide hydrochloride (EDC), *N*-hydroxysuccinimide (NHS), trypsin, penicillin streptomycin (PS), 3-(4,5-dimethylthiazol-2-yl)-5-(3-carboxymethoxyphenyl)-2-(4-sulfophenyl)-2H-tetrazolium inner salt (MTS), were purchased from Sigma-Aldrich (St. Louis, MO). Roswell Park Memorial Institute (RPMI) 1640 cell culture medium and common laboratory salts and solvents were purchased from Fischer Scientific (Fair Lawn, NJ). Unless otherwise specified, all chemicals were used as received without further purification. Tryptic soy broth (TSB) and tryptic soy agar (TSA) were obtained from Becton, Dickinson, and Company (Franklin Lakes, NJ). *Pseudomonas aeruginosa* (*P. aeruginosa*; ATCC #19143), *Staphylococcus aureus* (*S. aureus*; ATCC #29213), and A549 human lung epithelial cells (ATCC CCL-185) were obtained from American Type Tissue Culture Collection (Manassas, VA). Argon (Ar), carbon dioxide (CO₂), nitrogen (N₂), nitric oxide (NO) calibration (25.87 ppm, balance N₂) gas cylinders were purchased from Airgas National Welders

(Raleigh, NC). Pure NO gas (99.5%) was obtained from Praxair (Sanford, NC). Distilled water was purified to a resistivity of 18.2 M Ω .cm and a total organic content of ≤ 6 ppb using a Millipore Milli-Q UV Gradient A10 System (Bedford, MA).

2.2.2 Instrumentation

^1H and ^{13}C nuclear magnetic resonance (NMR) spectra were recorded on a Bruker (600 MHz) spectrometer. Elemental (carbon, hydrogen, and nitrogen; CHN) analysis was performed using a PerkinElmer Elemental Analyzer Series 2400 Instrument (Waltham, MA). Zeta potential measurements were collected in phosphate buffer (10 mM PB; pH 7.4) using a Zetasizer Nano (Malvern Instruments, UK). All absorbance measurements were made in 50 mM sodium hydroxide (NaOH) using a UV-vis Lambda 40 Spectrophotometer (PerkinElmer, Waltham, MA). Gel permeation chromatography measurements were carried out in 0.1 M sodium nitrate using an aqueous GPC-multi-angle light scattering system equipped with a Waters 2414 refractive index detector (Milford, MA) coupled to a Wyatt miniDawn TREOS multi-angle light scattering detector (Santa Barbara, CA).

2.2.3 Oxidative degradation of alginates

Alginate was degraded to lower molecular weight alginate oligosaccharides via oxidative degradation following previously published protocols.^{40,41} Briefly, alginate (2.5 g) was dissolved in 15 wt% hydrogen peroxide (50 mL) and stirred at 85 °C for 1 h. The solution was filtered to remove any insoluble material. The resulting alginate oligosaccharides was precipitated from the filtered solution in ethanol, collected via centrifugation, washed copiously with ethanol, and dried *in vacuo* to yield a white powder. GPC measurements revealed the molecular weight of the starting

alginate material, as received, was 283 kDa with a dispersity (\bar{M}_w/\bar{M}_n) of 1.11. The average molecular weight of the alginate oligosaccharides (Alg5) was 4.68 kDa with a dispersity of 1.20.

2.2.4 Synthesis of polyamine-modified alginates (AlgMW-alkyl amine)

Alginate starting materials were modified with either diethylenetriamine (DETA), bis(3-aminopropyl)amine (DPTA), *N*-propyl-1,3-propanediamine (PAPA), or spermine (SPER) through covalent amide bond formation between the carboxylic acid moieties of alginate and the primary amines of the alkyl amine (Figure 2.1).²⁷ Briefly, alginate (100 mg) was dissolved in 10 mL phosphate buffered saline (PBS; 10 mM, pH 6.5) together with a 2:1 molar ratio to 1-ethyl-3-(3-dimethylaminopropyl)carbodiimide hydrochloride (EDC) and a 2:1 molar ratio of *N*-hydroxysuccinimide (NHS) with respect to the carboxylic moieties of the alginate scaffold. The resulting solution was allowed to mix at room temperature for 30 min before adding a 4:1 molar ratio of the alkyl amine with respect to the carboxylic acid groups of the alginate scaffold to the reaction solution. After 24 h at room temperature, the amine-modified alginates were precipitated in methanol, collected via centrifugation, washed twice with methanol, and dried in vacuo to yield a white solid for each modification.

Representative ¹H NMR of alginate and the polyamine-modified alginates included the following peaks:

Alg300 and Alg5: ¹H NMR (600 MHz, D₂O, δ) 3.60-4.05 (OCHCH(OH)CH(OH)), 4.30 (OCHCH(OH)CH(OH)), 4.50-4.60 (OHCOCH), 4.90 (OCH(CHOH)O).

Alg300-DETA and Alg5-DETA: ¹H NMR (600 MHz, D₂O, δ) 2.30-3.30 (CH₂CH₂NHCH₂CH₂NH₂), 3.60-4.05 (OCHCH(OH)CH(OH)), 4.30 (OCHCH(OH)CH(OH)), 4.50-4.60 (NHCOCH), 4.90 (OCH(CHOH)O).

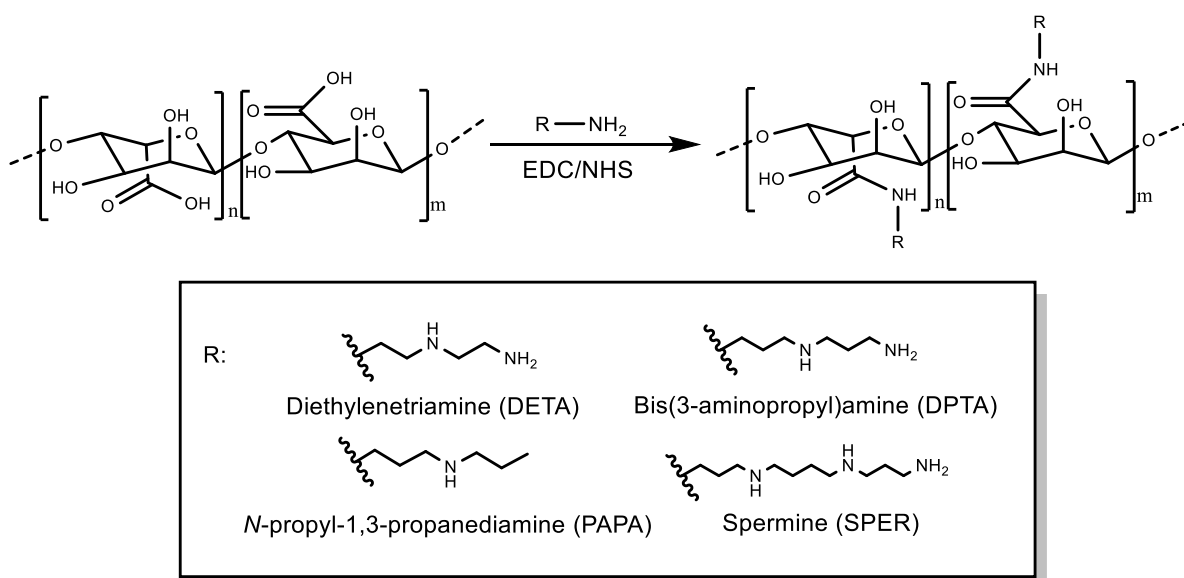


Figure 2.1 Synthesis of amine-functionalized alginate.

Alg300-DPTA and Alg5-DPTA: ^1H NMR (600 MHz, D_2O , δ) 1.60-1.80 ($\text{CH}_2\text{CH}_2\text{CH}_2\text{NHCH}_2\text{CH}_2\text{CH}_2\text{NH}_2$), 2.60-2.30 ($\text{CH}_2\text{CH}_2\text{CH}_2\text{NHCH}_2\text{CH}_2\text{CH}_2\text{NH}_2$), 2.80-3.10 ($\text{CH}_2\text{CH}_2\text{CH}_2\text{NHCH}_2\text{CH}_2\text{CH}_2\text{NH}_2$), 3.60-4.05 ($\text{OCHCH}(\text{OH})\text{CH}(\text{OH})$), 4.30 ($\text{OCHCH}(\text{OH})\text{CH}(\text{OH})$), 4.50-4.60 (NHCOCH), 4.90 ($\text{OCH}(\text{CHOH})\text{O}$).

Alg300-PAPA and Alg5-PAPA: ^1H NMR (600 MHz, D_2O , δ) 0.70-0.80 ($\text{NHCH}_2\text{CH}_2\text{CH}_3$), 1.52 ($\text{NHCH}_2\text{CH}_2\text{CH}_3$), 1.85 ($\text{CH}_2\text{CH}_2\text{CH}_2\text{NHCH}_2\text{CH}_2\text{CH}_3$), 2.80-3.10 ($\text{CH}_2\text{CH}_2\text{CH}_2\text{NHCH}_2\text{CH}_2\text{CH}_3$), 3.60-4.05 ($\text{OCHCH}(\text{OH})\text{CH}(\text{OH})$), 4.30 ($\text{OCHCH}(\text{OH})\text{CH}(\text{OH})$), 4.50-4.60 (NHCOCH), 4.90 ($\text{OCH}(\text{CHOH})\text{O}$).

Alg300-SPER and Alg5-SPER: ^1H NMR (600 MHz, D_2O , δ) 1.13 ($\text{NHCH}_2(\text{CH}_2)_2\text{CH}_2\text{NH}$), 1.56 ($\text{NHCH}_2\text{CH}_2\text{CH}_2\text{NH}$), 1.80 ($\text{C}(\text{O})\text{NHCH}_2\text{CH}_2\text{CH}_2\text{NH}$), 2.20-2.40 ($\text{CH}_2\text{CH}_2\text{CH}_2\text{NH}$, $\text{NHCH}_2(\text{CH}_2)_2\text{CH}_2\text{NH}$, $\text{NHCH}_2\text{CH}_2\text{CH}_2\text{NH}_2$), 2.68 ($\text{NHCH}_2\text{CH}_2\text{CH}_2\text{NH}_2$), 2.80-3.10 ($\text{C}(\text{O})\text{NHCH}_2\text{CH}_2\text{CH}_2\text{NH}$, $\text{NHCH}_2\text{CH}_2\text{CH}_2\text{NH}_2$), 3.60-4.05 ($\text{OCHCH}(\text{OH})\text{CH}(\text{OH})$), 4.30 ($\text{OCHCH}(\text{OH})\text{CH}(\text{OH})$), 4.50-4.60 (NHCOCH), 4.90 ($\text{OCH}(\text{CHOH})\text{O}$).

Representative ^{13}C NMR of alginate and the polyamine-modified alginate included the following peaks:

Alg300 and Alg5: ^{13}C NMR (600 MHz, D_2O , δ) 65.0-80.0 ($\text{OCHCH}(\text{OH})\text{CH}(\text{OH})\text{CH}(\text{OH})\text{CH}(\text{O})$), 100.0 ($\text{OCHCH}(\text{OH})$), 175.0 ($\text{CHC}(\text{O})$).

Alg300-DETA and Alg5-DETA: ^{13}C NMR (600 MHz, D_2O , δ) 39.0-47.0 ($\text{C}(\text{O})\text{NHCH}_2\text{CH}_2\text{NHCH}_2\text{CH}_2\text{NH}_2$), 65.0-80.0 ($\text{OCHCH}(\text{OH})\text{CH}(\text{OH})\text{CH}(\text{OH})\text{CH}(\text{O})$), 100.0 ($\text{OCHCH}(\text{OH})$), 160.0 ($\text{CHC}(\text{O})\text{NH}$), 175.0 ($\text{CHC}(\text{O})$).

Alg300-DPTA and Alg5-DPTA: ^{13}C NMR (600 MHz, D_2O , δ) 26.9-29.5 ($\text{C}(\text{O})\text{NHCH}_2\text{CH}_2\text{CH}_2\text{NH}$, $\text{NHCH}_2\text{CH}_2\text{CH}_2\text{NH}_2$), 37.6-46.0 ($\text{C}(\text{O})\text{NHCH}_2\text{CH}_2\text{CH}_2\text{NH}$,

NHCH₂CH₂CH₂NH₂), 65.0-80.0 (OCHCH(OH)CH(OH)CH(OH)CH(O)), 100.0 (OCHCH(OH)), 160.0 (CHC(O)NH), 175.0 (CHC(O)).

Alg300-PAPA and Alg5-PAPA: ¹³C NMR (600 MHz, D₂O, δ) 10.9 (NHCH₂CH₂CH₃), 20.0 (NHCH₂CH₂CH₃), 31.3-49.0 (C(O)NHCH₂CH₂CH₂NH, NHCH₂CH₂CH₃), 65.0-80.0 (OCHCH(OH)CH(OH)CH(OH)CH(O)), 100.0 (OCHCH(OH)), 160.0 (CHC(O)NH), 175.0 (CHC(O)).

Alg300-SPER and Alg5-SPER: ¹³C NMR (600 MHz, D₂O, δ) 23.2 (NHCH₂(CH₂)₂CH₂NH), 34.8-45.0 (C(O)NHCH₂CH₂CH₂NH), 65.0-80.0 (OCHCH(OH)CH(OH)CH(OH)CH(O)), 100.0 (OCHCH(OH)), 160.0 (CHC(O)NH), 175.0 (CHC(O)).

2.2.5 Synthesis of NO-releasing alginates

To form *N*-diazoniumdiolate NO donors on the alginate scaffolds, polyamine-modified alginate (45 mg) was dissolved in 50 mM NaOH (3 mL) in a 1-dram glass vial (Figure 2.2). The open vials were placed in a stainless steel reactor and stirred continuously using a magnetic stir bar. Oxygen was removed from the vessel by purging with argon (10 s, 7 bar) three times, followed by three additional long purges with argon (10 mins, 7 bar). The vessel was then pressurized to 10 bar with NO gas and allowed to react for 3 d. The same argon purging protocol was then repeated to remove unreacted NO. The NO-releasing alginates were then precipitated in methanol, collected by centrifugation, dried overnight in vacuo, and stored in vacuum sealed bags at -20 °C as a dry powder.

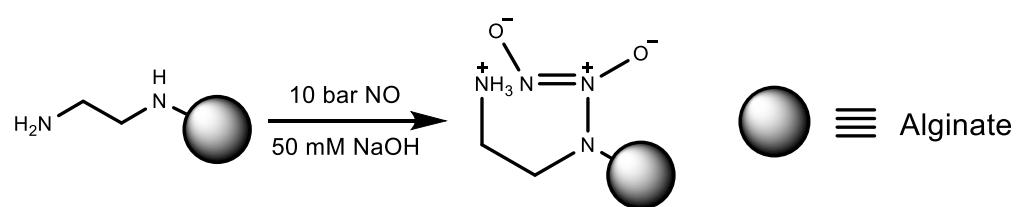


Figure 2.2 Synthesis of *N*-diazeniumdiolate-modified alginates.

2.2.6 Characterization of NO storage and release

Nitric oxide release was evaluated in real-time using a Sievers 280i Chemiluminescence NO analyzer (NOA; Boulder, CO). Each sample was analyzed before use to ensure stability of the stored material. Prior to analysis, the NOA was calibrated with air passed through a NO zero filter (0 ppm NO) and 25.87 ppm of NO standard gas (balance N₂). In a typical measurement, NO-releasing alginates (1 mg) were dissolved in 30 mL of PBS (10 mM, pH 7.4, 37 °C). The solution was purged with nitrogen gas at a flow rate of 70 mL/min to carry liberated NO from the solution to the analyzer. Additional nitrogen flow was supplied to the flask to match the collection rate of the instrument (200 mL/min). Nitric oxide analysis was terminated when NO levels fell below 10 ppb of NO/mg of alginate (the limit of detection of the instrument).

2.2.7 Planktonic bactericidal assay

P. aeruginosa and *S. aureus* bacterial cultures were grown from a frozen (-80 °C) stock overnight in TSB at 37 °C. A 500 µL aliquot of culture was grown in 50 mL of fresh TSB to a concentration of 10⁸ colony forming units per mL (CFU/mL). A working bacterial stock was generated by plating the bacterial suspension on TSA and incubating at 37 °C overnight. The TSA bacterial stocks were prepared weekly and stored at 4 °C. For bactericidal assays, colonies of *P. aeruginosa* and *S. aureus* were taken from the TSA plate, inoculated in 3 mL TSB overnight at 37 °C, and recultured in fresh TSB (50 mL) to a concentration of 10⁸ CFU/mL. These cultures were centrifuged, resuspended in PBS, and diluted to 10⁶ CFU/mL. Weighed samples of NO-releasing alginates and controls (non-NO-releasing alginates) were added to a 1-dram vial. Corresponding volumes of the 10⁶ CFU/mL bacteria were then added to obtain a range of alginate concentrations (0.5 to 16 mg/mL). These solutions were incubated for 4 h at 37 °C. Blanks or untreated bacterial solutions were included in each experiment to ensure bacteria viability over the duration of the

experiment. Following treatment, the bacterial solutions were diluted serially (10- and 100-fold dilutions), spiral plated on TSA using an Eddy Jet spiral plater (IUL; Farmingdale, NY), and incubated overnight at 37 °C. Bacterial viability was determined using a Flash & Go colony counter (IUL; Farmingdale, NY). The minimum bactericidal concentration after a 4-hour exposure period (MBC_{4h}) was defined as the minimum concentration required to achieve a 3-log reduction in bacterial viability relative to untreated cells (i.e., reduced bacterial counts from 10^6 to 10^3 CFU/mL). The limit of detection for this counting method is 2.5×10^3 CFU/mL.⁴² The corresponding NO dose was calculated by multiplying the MBC_{4h} of the alginate samples (mg/mL) with the measured NO released in PBS (pH 7.4; $\mu\text{mol NO/mg alginate}$) over the 4 h experimental window.

2.2.8 *Biofilm eradication assay*

Similar to planktonic experiments, *P. aeruginosa* and *S. aureus* bacterial cultures were grown overnight in TSB at 37 °C and recultured in fresh TSB to a concentration of 10^8 CFU/mL. These solutions were diluted to 10^6 CFU/mL in sterile media (*P. aeruginosa*, TSB; *S. aureus*, TSB + 0.1 % glucose) and grown for 48 h at 37 °C with gentle shaking. The formed biofilms were separated from the growth media by pipetting the biofilm mass. Biofilms (250 μL) were combined with 750 μL of PBS and added to 1-dram vials containing premeasured samples of NO-releasing and control alginates, with final alginate concentrations ranging from 4 to 64 mg/mL. The samples were incubated with gentle shaking for 24 h at 37 °C. Blanks were included in each experiment to ensure bacterial viability over the duration of the experiment. The dispersed biofilms were vortexed, serially diluted (10-, 100-, 1000-, and 10,000-fold dilutions), plated on TSA plates using an Eddy Jet spiral plater, and incubated overnight at 37 °C. Bacterial viability was assessed using a Flash & Go colony counter. The minimum biofilm eradication concentration at 24 h ($MBEC_{24h}$)

was defined as the minimum concentration required to achieve a 5-log reduction in bacterial viability compared to untreated cells (i.e., reduced bacterial counts from 10^8 to 10^3 CFU/mL). The corresponding NO dose was calculated by multiplying the MBEC_{24h} of the alginate samples (mg/mL) with the NO released in PBS (pH 7.4; $\mu\text{mol NO/mg alginate}$) over the testing period.

2.2.9 Time-Based Biofilm Eradication Assay

P. aeruginosa biofilms were grown and treated with NO-releasing alginates (8 mg/mL) following the same protocol as for the biofilm eradication assays. Blanks were included to ensure bacteria viability over the duration of the experiment. The samples were incubated with gentle shaking at 37 °C for 1-24 h before plating on TSA plates using an Eddy Jet spiral plater and incubating overnight at 37 °C. Bacterial viability was assessed using a Flash & Go colony counter. A similar experiment was carried out at the MBEC_{24h} for Alg-PAPA/NO and Alg-SPER/NO for comparison to time-based killing at 8 mg/mL.

2.2.10 In vitro cytotoxicity assay

A549 human respiratory epithelial cells were grown in RPMI 1640 media supplemented with 10 vol% FBS and 1 wt% penicillin streptomycin. Cells were incubated in 5 vol % CO₂ under humidified/aerobic conditions at 37 °C. After reaching 80% confluency, the cells were seeded onto 96-well polystyrene plates at a density of 2×10^3 cells/well, and incubated for 24 h at 37 °C. The supernatant was then aspirated and replaced with 100 μL of alginate in fresh growth medium with a final concentration of test material equivalent to MBEC_{24h} against *P. aeruginosa* or *S. aureus* biofilms. After 24 h incubation at 37 °C, the supernatant was aspirated and the wells containing the cells were washed with PBS. A 100 μL mixture of RPMI 1640/MTS/PMS (105/20/1, v/v/v) was added to each well. After an additional 90 min incubation period (37 °C), the absorbances of the wells were measured at 490 nm using a ThermoScientific Multiskan EX plate reader (Waltham,

MA). A blank mixture of RPMI 1640/MTS/PMS and untreated cells were used as the blank and control, respectively. Cell viability for each sample was calculated as follows:

$$\% \text{ cell viability} = \frac{(Abs_{490} - Abs_{blank})}{(Abs_{control} - Abs_{blank})} \times 100 \quad (\text{eq.1}).$$

2.3 Results and Discussion

Alginates are found in nature as polydisperse, water soluble high molecular weight polymers (200-500 kDa).^{26,27} Prior research has demonstrated the ease by which these polymers undergo oxidative degradation to form lower molecular weight oligosaccharides.^{41,43} To that end, reaction conditions were optimized to yield alginate oligosaccharides with molecular weights of ~5 kDa to compare to previously reported water-soluble NO-releasing biopolymer systems.⁴⁰ The addition of secondary amine-bearing functional groups to the alginate backbone allows for the subsequent formation of *N*-diazoniumdiolate NO donors. This class of NO donor facilitates spontaneous NO release in physiological media. In the present study, a series of small molecule NO donor precursors were linked to the carboxylic acid functional groups of both high molecular weight (~300 kDa) and low molecular weight (~5 kDa) alginates via EDC/NHS reactions (Figure 2.1) to enable tuning of the NO-release kinetics. Of note, pH 6.5 phosphate buffer saline was employed to avoid gelation of alginate.³⁰ The reaction was optimized to maximize alkyl amine modification while minimizing the possibility of crosslinking between the alginate backbone and the diamine functional groups (i.e., DETA, DPTA, SPER). The average molecular weight (Mw) proved to be dependent on the molar excess of the alkyl amine functional group added to the reaction solution (Table 2.1). For example, keeping the molar ratio at 1:1 resulted in a drastic increase in the molecular weight of the alkyl amine-modified alginate (e.g. Alg300-SPER with

Mw ~700 kDa) suggesting possible crosslinking with the biopolymer. Increasing the molar ratio of the diamine functional group minimized this effect (Table 2.1). This trend was observed with the high molecular weight alginate systems and not with the low molecular weight materials. No gel phase was formed at the optimized parameters for the reaction. Polyamine functionalization was also confirmed using ^1H NMR, ^{13}C NMR, and elemental analysis (Figures 2.3, 2.4, and 2.5). The nitrogen content of the alginates increased from 0 to 5-8 wt% with amine modification (Table 2.2). This value translates to ~40-50 % modification of the carboxylic acid functional groups. A positive shift in zeta potential was also noted upon amine modification, corresponding to the formation of protonated amine groups at pH 7.4 (Table 2.2).

2.3.1 *Synthesis of N-diazeniumdiolate-modified biopolymers*

The secondary amine-modified alginates were charged with high pressures of NO (10 bar) in basic aqueous solution (50 mM NaOH) to allow efficient formation of *N*-diazeniumdiolate NO donors (Figure 2.2). The formation of the NO donors was confirmed using UV-vis spectroscopy and the appearance of a characteristic absorbance band at 253 nm (Figure 2.6).

Representative NO-release profiles of the *N*-diazeniumdiolate-functionalized alginates in PBS (pH 7.4) at 37 °C are shown in Figure 2.7. Both high and low molecular weight alginates were found to have similar NO totals that were comparable to other macromolecular NO-releasing biopolymeric scaffolds (0.3-0.6 $\mu\text{mol}/\text{mg}$).^{40,44-47} A broad range of NO-release kinetics was also observed for the alginate scaffolds with Alg300-PAPA/NO and Alg5-PAPA/NO having the shortest NO-release half-lives (~0.5 and ~0.3 h, respectively) or fastest NO donor breakdown. In contrast, the NO release of Alg300-DETA/NO and Alg5-DETA/NO was highly prolonged (NO-release half-lives of ~40 and 29 h, respectively). The NO-release duration varied as a function of amine precursor structure, following trends previously reported for the corresponding small

Table 2.1 Molecular weight of alkyl amine-modified alginate as a function of added alkyl amine ratio.^a

Biopolymer	Molar excess of alkyl amine to -COOH moieties of alginate	Mw (kDa)	PDI
	1	581	1.26
Alg300-DETA	2	409	1.32
	4	388	1.35
	1	548	1.11
Alg300-DPTA	2	439	1.21
	4	397	1.23
	1	335	1.42
Alg300-PAPA	2	324	1.35
	4	323	1.31
	1	711	1.63
Alg300-SPER	2	512	1.60
	4	459	1.45
	1	5	1.50
Alg5-DETA	2	5	1.82
	4	5	2.06
	1	6	1.51
Alg5-DPTA	2	6	1.22
	4	6	1.44
	1	5	1.65
Alg5-PAPA	2	6	1.53
	4	7	1.49
	1	7	1.47
Alg5-SPER	2	7	1.73
	4	8	1.82

^aAverage molecular weight (Mw) and polydispersity index (PDI) was measured using GPC-multi-angle light scattering system.

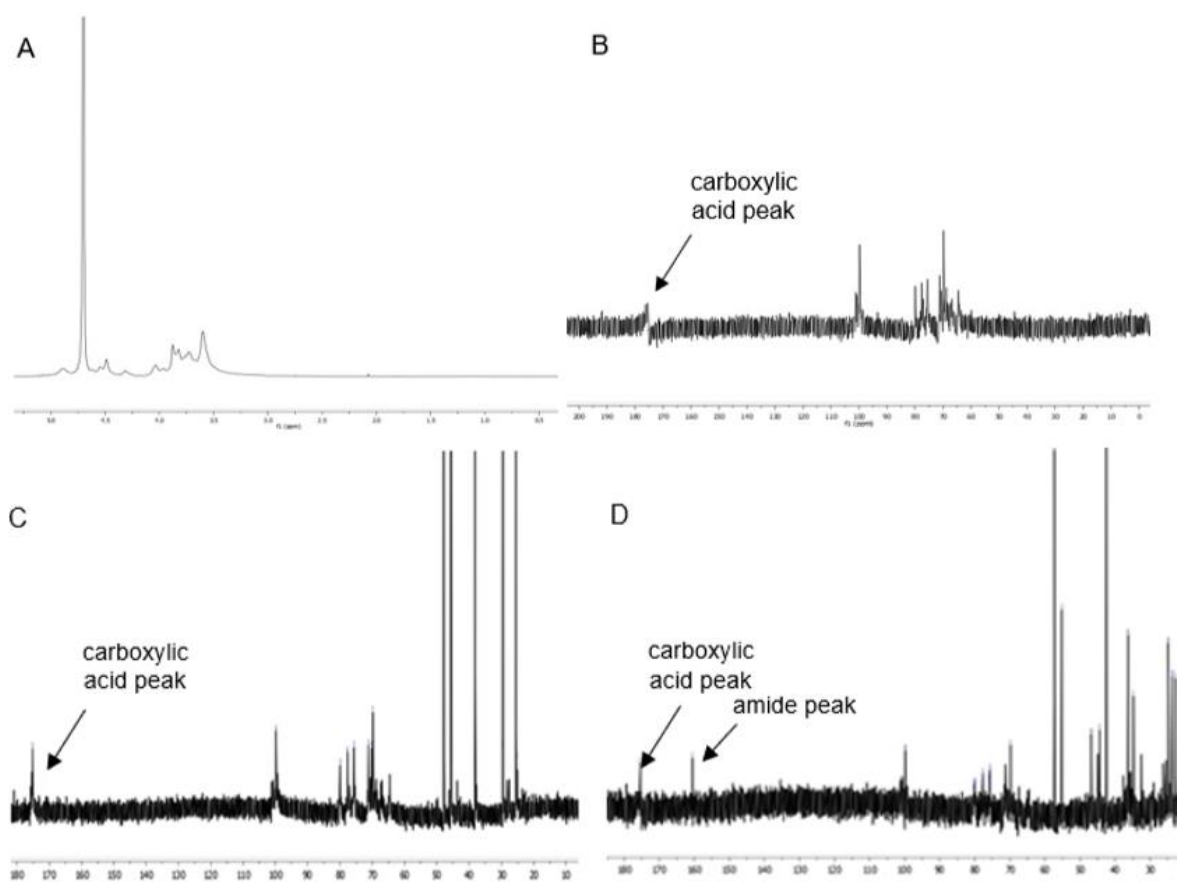


Figure 2.3 (A) Representative ^1H NMR spectrum for Alg300, and (B) representative ^{13}C NMR spectrum for Alg300 in D_2O . Control ^{13}C NMR of (C) Alg300 with free SPER and (D) SPER-modified Alg300.

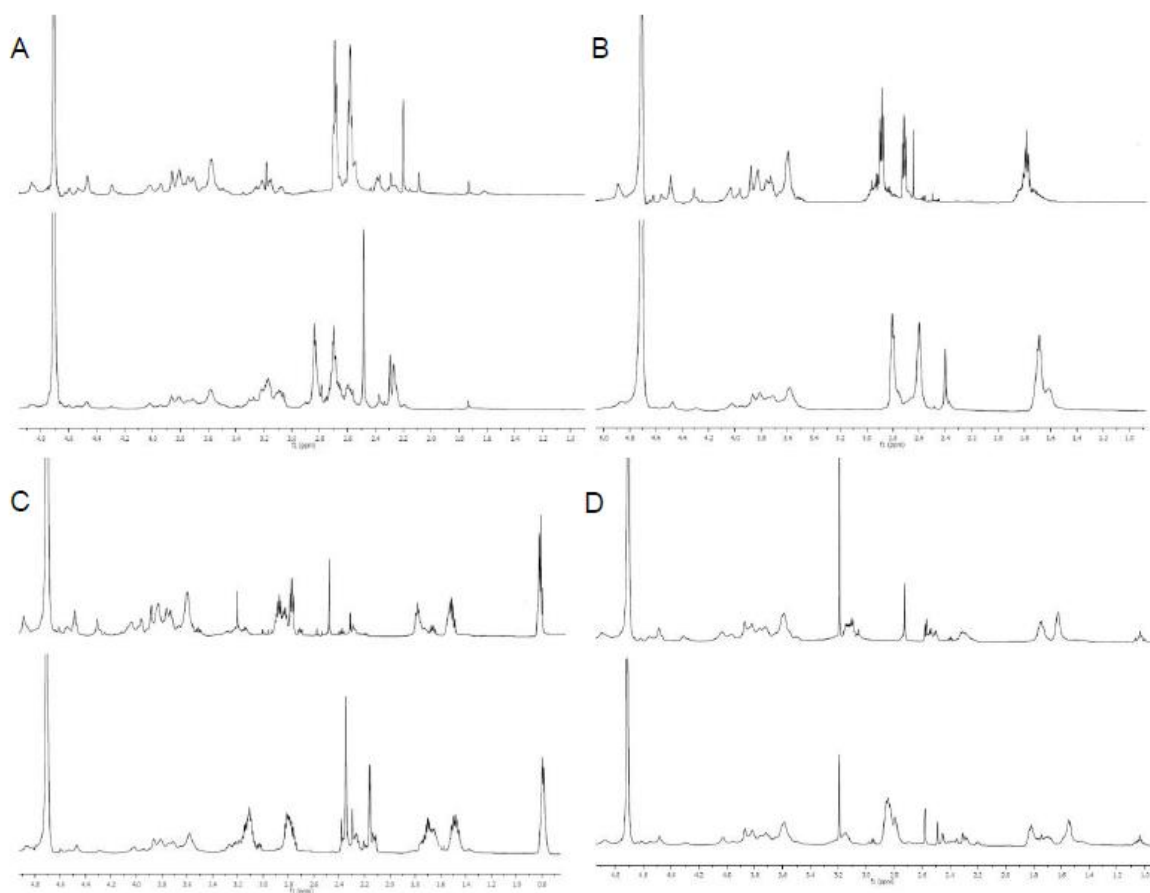


Figure 2.4 Representative ^1H NMR spectra for (A) DETA-, (B) DPTA-, (C) PAPA-; and, (D) SPER-modified Alg5 (top) and Alg300 (bottom) in D_2O .

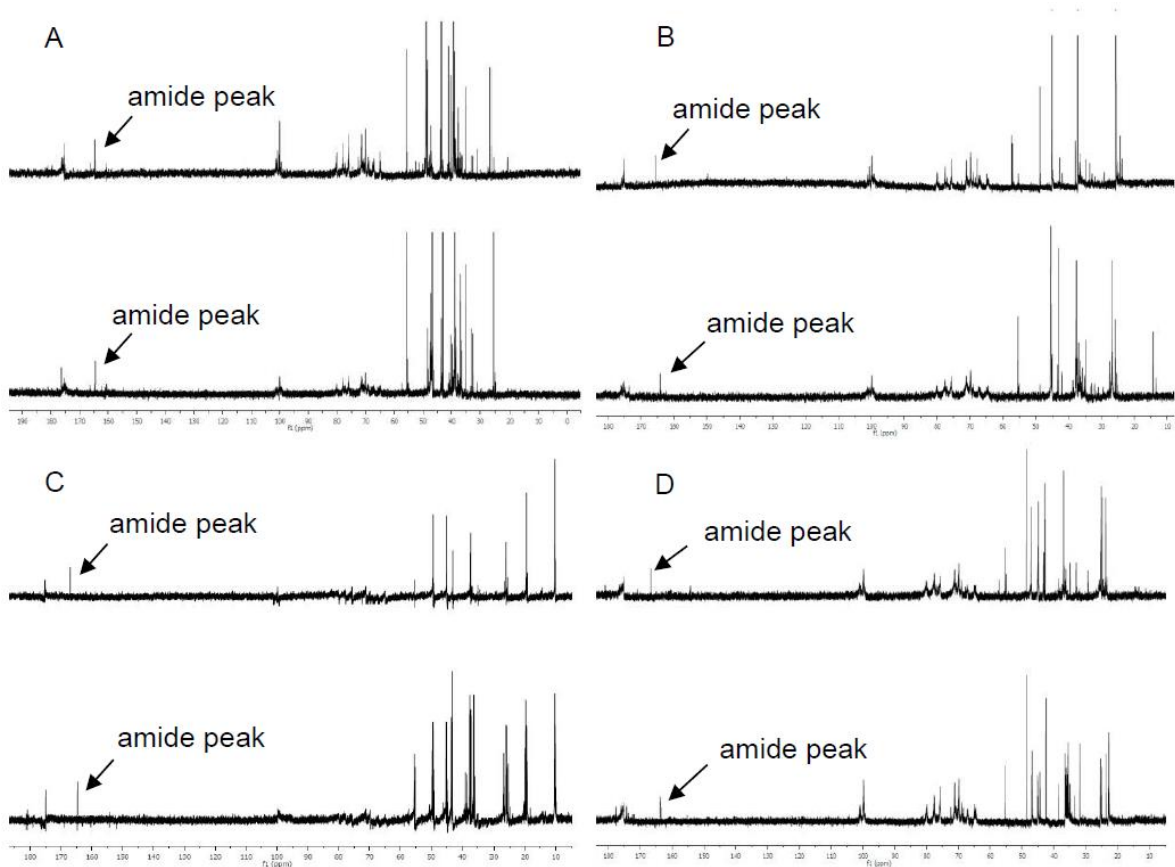


Figure 2.5 Representative ^{13}C NMR spectra for (A) DETA-, (B) DPTA-, (C) PAPA-; and, (D) SPER-modified Alg5 (top) and Alg300 (bottom) in D_2O .

Table 2.2 Elemental (CHN) analysis, zeta potential measurements, and reaction yields for secondary amine-functionalized alginate.^a

Biopolymer	Carbon (%)	Hydrogen (%)	Nitrogen (%)	Zeta Potential (mV)^b	Reaction yield (%)
Alg300	30.4 ± 0.4	4.7 ± 0.4	0.0 ± 0.0	-47.2 ± 2.8	-
Alg300-DETA	35.1 ± 0.5	7.4 ± 0.5	7.6 ± 0.5	-24.2 ± 2.4	92
Alg300-DPTA	34.7 ± 0.6	7.4 ± 0.6	7.5 ± 1.1	-23.1 ± 2.9	89
Alg300-PAPA	34.7 ± 1.1	5.4 ± 0.0	6.7 ± 0.2	-33.4 ± 1.6	86
Alg300-SPER	40.4 ± 2.0	7.6 ± 0.5	8.3 ± 0.1	-13.0 ± 2.5	77
Alg5	29.3 ± 1.3	5.1 ± 0.3	0.0 ± 0.0	-48.0 ± 4.1	-
Alg5-DETA	34.2 ± 0.5	7.6 ± 0.6	7.8 ± 0.8	-23.5 ± 2.7	89
Alg5-DPTA	33.6 ± 0.4	6.4 ± 0.1	6.4 ± 0.2	-20.0 ± 3.5	80
Alg5-PAPA	30.7 ± 0.1	5.3 ± 1.0	4.7 ± 0.7	-28.5 ± 3.3	84
Alg5-SPER	38.2 ± 0.4	7.4 ± 0.2	8.2 ± 1.1	-18.3 ± 3.9	82

^aError represent standard deviation for n ≥ 3 experiments. ^bMeasured in phosphate buffer (pH 7.4).

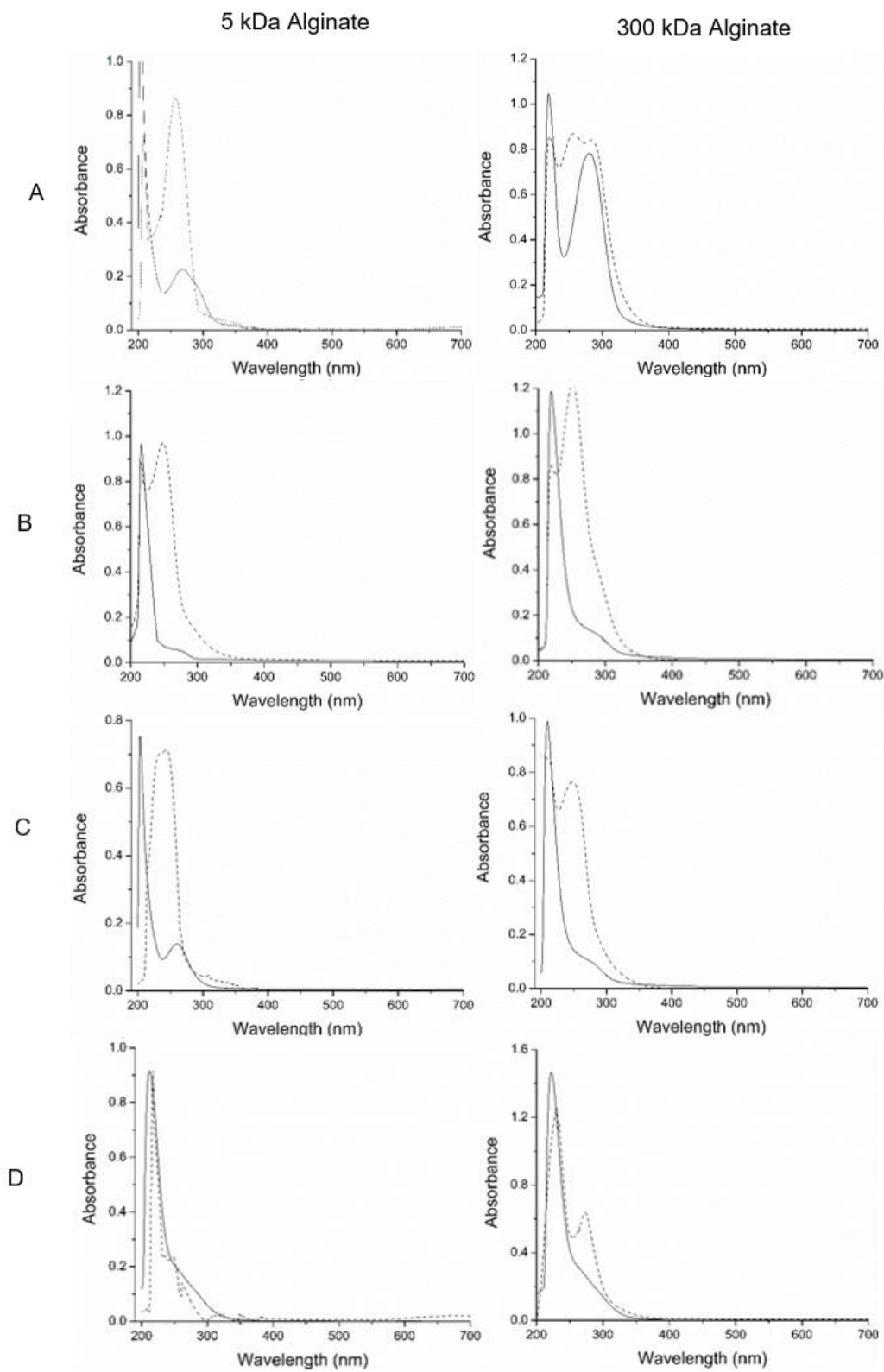


Figure 2.6 Representative UV-vis spectra for (A) DETA-, (B) DPTA-, (C) SPER-; and, (D) PAPA-modified alginates with (dash) and without (solid) *N*-diazeniumdiolate NO donors.

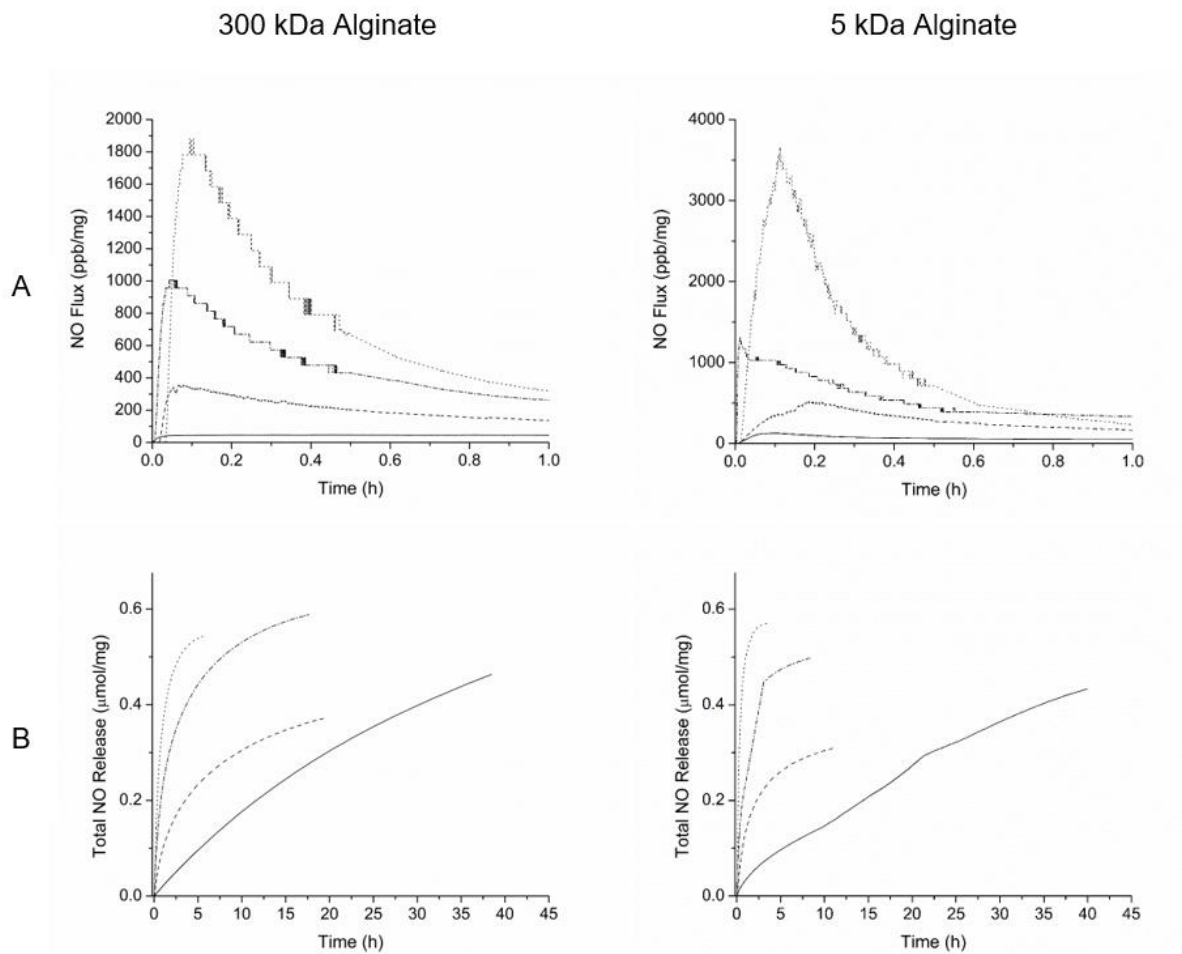


Figure 2.7 (A) Real time NO-release profiles for the first 1 h and (B) plot of total NO release vs. time for NO-releasing DETA- (solid), DPTA- (dash), SPER- (dash-dot); and PAPA- (dot) modified alginates measured via chemiluminescence in pH 7.4 PBS.

molecule NO donors (i.e., DETA, DPTA, PAPA, and SPER).^{48,49} Following previous reports, a decrease in half-life was observed for the NO-releasing alginates as chain length of the alkyl amine functional group increased.^{38,48,49} The positively charged primary amine terminal moiety stabilizes the negative charge of the *N*-diazoniumdiolate NO donor, resulting in an increase in half-life of the anion for DETA-, DPTA-, and SPER-modified alginates compared to that of the PAPA-modified scaffold (Figure 2.2).⁴⁹ The molecular weight of the alginate also dramatically influenced the NO release. For example, the Alg5 oligosaccharides released NO more rapidly than the larger Alg300 analogs modified with the same amine precursor (Table 2.3). In addition, negligible NO release was observed for control alginates modified with ethylenediamine, an alkyl amine lacking secondary amine moieties, suggesting that the primary amines do not react with NO under the reported conditions used for *N*-diazoniumdiolate formation (~0.03 $\mu\text{mol/mg}$ total NO). Overall, these experiments demonstrate exquisite NO-release tunability by simply varying the molecular weight of the scaffold and/or the chemical structure of an amine precursor grafted onto the alginate backbone.

2.3.2 Antibacterial action against planktonic bacteria

The antibacterial activity of control and NO-releasing alginates was evaluated against *P. aeruginosa* and *S. aureus*, two prevalent pathogens associated with infections.^{6,50} Bacterial viability assays were performed under static conditions to extract the minimum bactericidal concentration of the test agent required to elicit a 3-log reduction (i.e., 99.9% killing) in bacterial viability over 4 h (MBC_{4h}). The non-NO-releasing controls did not significantly impact bacterial viability up to 16 mg/mL for both *P. aeruginosa* and *S. aureus* (Figure 2.8). In contrast, low concentrations (< 8mg/mL), led to a 3-log reduction ($\geq 99.9\%$) in bacterial viability for each of the NO-releasing alginate scaffolds (Table 2.4), with the less negatively charged alkyl amine-modified

Table 2.3 Nitric oxide-release properties of *N*-diazoniumdiolate-functionalized alginates in PBS (pH 7.4, 37 °C).^a

Biopolymer	t[NO] ^b (μmol/mg)	[NO] _{max} ^c (ppb/mg)	t _{1/2} ^d (h)	t _d ^e (h)	t[NO] _{4h} ^f (μmol/mg)
Alg300-DETA/NO	0.40 ± 0.04	232 ± 78	13.1 ± 5.8	40.3 ± 14.2	0.10 ± 0.01
Alg300-DPTA/NO	0.42 ± 0.04	428 ± 124	3.4 ± 0.6	16.1 ± 2.9	0.23 ± 0.01
Alg300-PAPA/NO	0.61 ± 0.13	2110 ± 1240	0.5 ± 0.1	6.1 ± 1.0	0.59 ± 0.11
Alg300-SPER/NO	0.65 ± 0.16	1236 ± 240	1.3 ± 0.4	14.6 ± 3.5	0.49 ± 0.11
Alg5-DETA/NO	0.33 ± 0.03	101 ± 30	9.8 ± 0.1	29.3 ± 1.7	0.08 ± 0.03
Alg5-DPTA/NO	0.48 ± 0.02	1157 ± 227	1.2 ± 0.1	8.7 ± 0.5	0.45 ± 0.10
Alg5-PAPA/NO	0.55 ± 0.11	3543 ± 908	0.3 ± 0.0	3.9 ± 0.3	0.55 ± 0.11
Alg5-SPER/NO	0.38 ± 0.03	477 ± 307	1.6 ± 0.2	11.1 ± 0.8	0.25 ± 0.04

^aError represent standard deviation for n ≥ 3 experiments. ^bTotal NO released. ^cMaximum flux of NO release. ^dNO-release half-life. ^eDuration of NO release. ^fTotal NO released after 4 h.

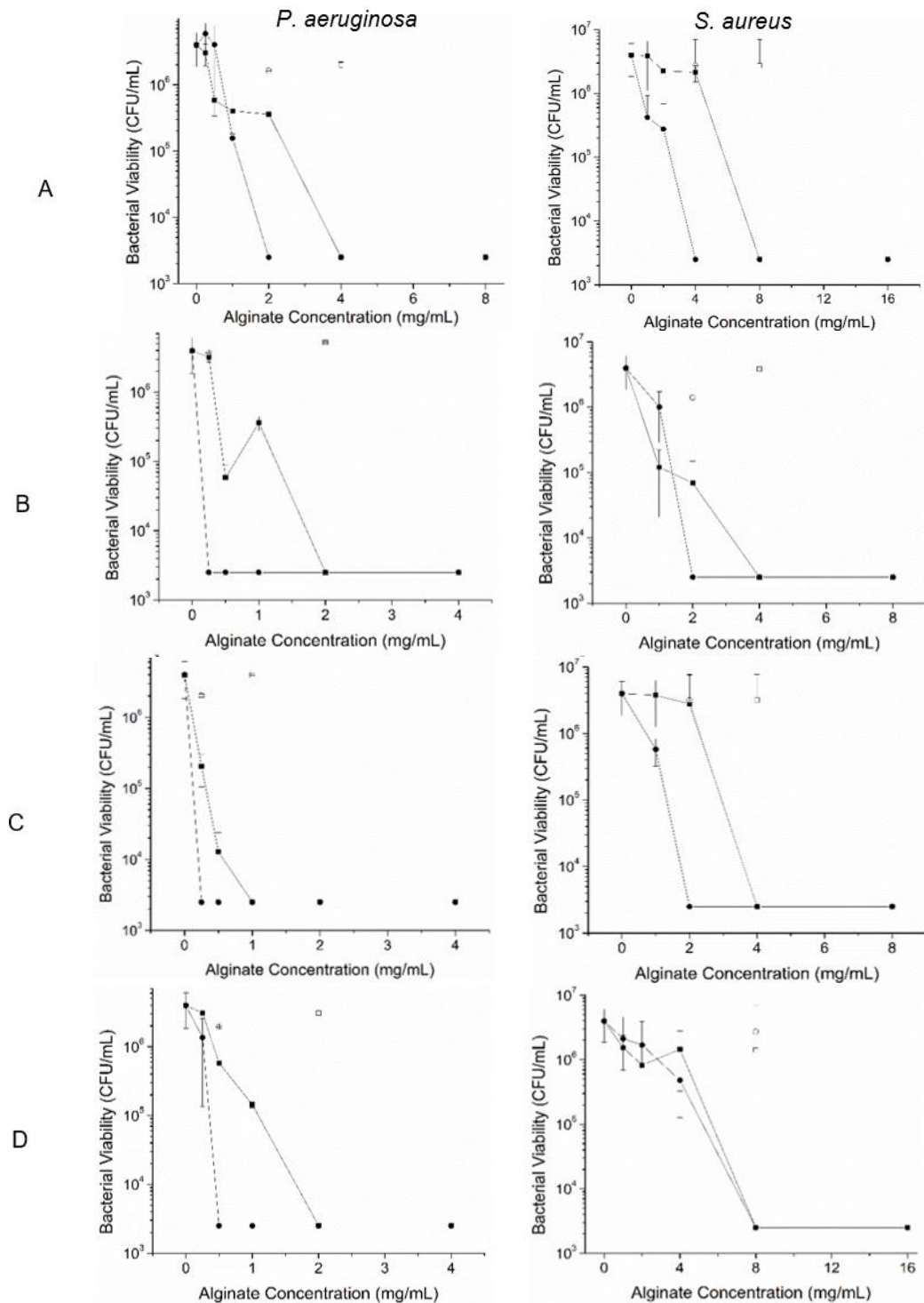


Figure 2.8 Antibacterial efficacy of high (square) and low (circle) molecular weight NO-releasing (filled) and control (hollow) (A) DETA-, (B) DPTA-, (C) SPER-; and, (D) PAPA-modified alginates against planktonic *P. aeruginosa* and *S. aureus*. Error bars represent standard deviation of the mean viability (CFU/mL). For all measurements, $n \geq 3$ pooled experiments.

Table 2.4 Minimum bactericidal concentrations (MBC_{4h}) of NO-releasing alginates against planktonic *P. aeruginosa* and *S. aureus*.^a

Biopolymer	<i>P. aeruginosa</i>		<i>S. aureus</i>	
	MBC _{4h} (mg/mL)	NO dose ^b (μ mol/mL)	MBC _{4h} (mg/mL)	NO dose ^b (μ mol/mL)
Alg300-DETA/NO	4	0.40 \pm 0.04	8	0.80 \pm 0.08
Alg300-DPTA/NO	2	0.45 \pm 0.01	4	0.88 \pm 0.02
Alg300-PAPA/NO	2	1.18 \pm 0.24	8	4.75 \pm 0.95
Alg300-SPER/NO	1	0.49 \pm 0.11	4	1.96 \pm 0.45
Alg5-DETA/NO	2	0.20 \pm 0.02	4	0.40 \pm 0.04
Alg5-DPTA/NO	0.25	0.11 \pm 0.01	2	0.92 \pm 0.01
Alg5-PAPA/NO	0.5	0.30 \pm 0.06	8	4.69 \pm 0.88
Alg5-SPER/NO	0.25	0.07 \pm 0.01	2	0.54 \pm 0.09

^aError represent standard deviation for $n \geq 3$ experiments. ^bNO dose was calculated from NO totals of each tested sample at 4 h in PBS (10 mM, pH 7.4, 37 °C).

alginate requiring the least amount to achieve bactericidal activity (Table 2.2). Other studies have reported that positively charged scaffolds associate more readily with bacteria with a concomitant enhancement in bactericidal action.^{40,51} The alginates herein followed a similar trend, with Alg300-SPER/NO (zeta potential -13.0 mV) eradicating bacteria at the lowest concentration while Alg300-PAPA/NO (-33.4 mV) necessitated the largest (Table 2.2). Nitric oxide-release kinetics also influenced the bactericidal action for the alginate materials, with the fastest (Alg300-PAPA/NO) and slowest (Alg300-DETA/NO) NO-releasing systems requiring greater concentrations relative to alginates with moderate release kinetics. Despite larger overall NO payloads (~0.6 $\mu\text{mol}/\text{mg}$), the faster NO release associated with Alg300-PAPA/NO may liberate NO prematurely prior to the alginate associating with the bacteria, which could then facilitate more efficient delivery of lethal NO doses to the bacteria. Indeed, other macromolecular NO-release systems (e.g., silica) required 20 min to elicit NO build up within *P. aeruginosa* as studied via confocal microscopy.¹⁵ The elevated concentrations of NO-releasing alginates needed for eradication using Alg300-DETA/NO are likewise attributed to insufficient NO released over the 4h MBC assay (~0.10 $\mu\text{mol}/\text{mg}$) compared to the other NO donor modifications (i.e., DPTA, PAPA, SPER).

A similar dependence on NO-release kinetics was observed for the low molecular weight alginates with both Alg5-SPER/NO and Alg5-DPTA/NO having the lowest $\text{MBC}_{4\text{h}}$. Of note, the concentrations of NO-releasing alginate oligosaccharides required to eradicate bacteria were significantly lower than their high molecular weight counterparts. Similar size-dependent effects have been previously reported for NO-releasing silica, albeit silica is a dense (i.e., hard) material.^{20,52} Liu et al. demonstrated similar beneficial antibacterial action as a function of biopolymer molecular weight.⁵³ Our results suggest that the use of lower molecular weight

alginates allows for more efficient NO delivery, in turn reducing the required NO dose for eradicating planktonic bacteria.

For both high and low molecular weight alginates, greater concentrations of NO-releasing derivations were necessary to achieve bactericidal activity against *S. aureus* relative to *P. aeruginosa* (Table 2.4). The thicker peptidoglycan layer of *S. aureus* likely decreases the diffusion of NO into the bacterium, necessitating larger doses of the macromolecule to achieve equivalent killing.⁵⁴ Gram-negative bacteria such as *P. aeruginosa* generally have a more lipid-rich outer membrane and thinner peptidoglycan sheets, increasing their susceptibility to NO and other permeating antimicrobials.⁵⁴

2.3.3 Antibiofilm efficacy

In addition to exhibiting bactericidal action against planktonic bacteria, the NO-releasing alginate scaffolds were also highly effective against *P. aeruginosa* and *S. aureus* biofilms. Similar to the planktonic assays, the concentrations of NO-releasing alginate oligosaccharides were lower for eradicating the biofilms relative to the higher molecular weight systems (Figure 2.9, Table 2.5), further emphasizing the role of NO delivery scaffold on bactericidal action. Greater biocidal action was also noted against *P. aeruginosa* over *S. aureus* biofilms. Worley et al. previously reported reduced penetration of NO-releasing poly(amido amine) dendrimers into *S. aureus* biofilms relative to *P. aeruginosa*.²² Such differences can be attributed to the biofilm architectures. The exopolysaccharide matrix of *S. aureus* biofilms produce greater levels of polysaccharide and extracellular proteins that hinder the diffusion of antibacterial agents such as NO.^{22,55} Coupled with the peptidoglycan differences, these structural advantages account for the lower susceptibility of *S. aureus* biofilms. Nevertheless, the broad-spectrum action of NO is clearly capable of eradicating both Gram-positive and Gram-negative bacterial biofilms.

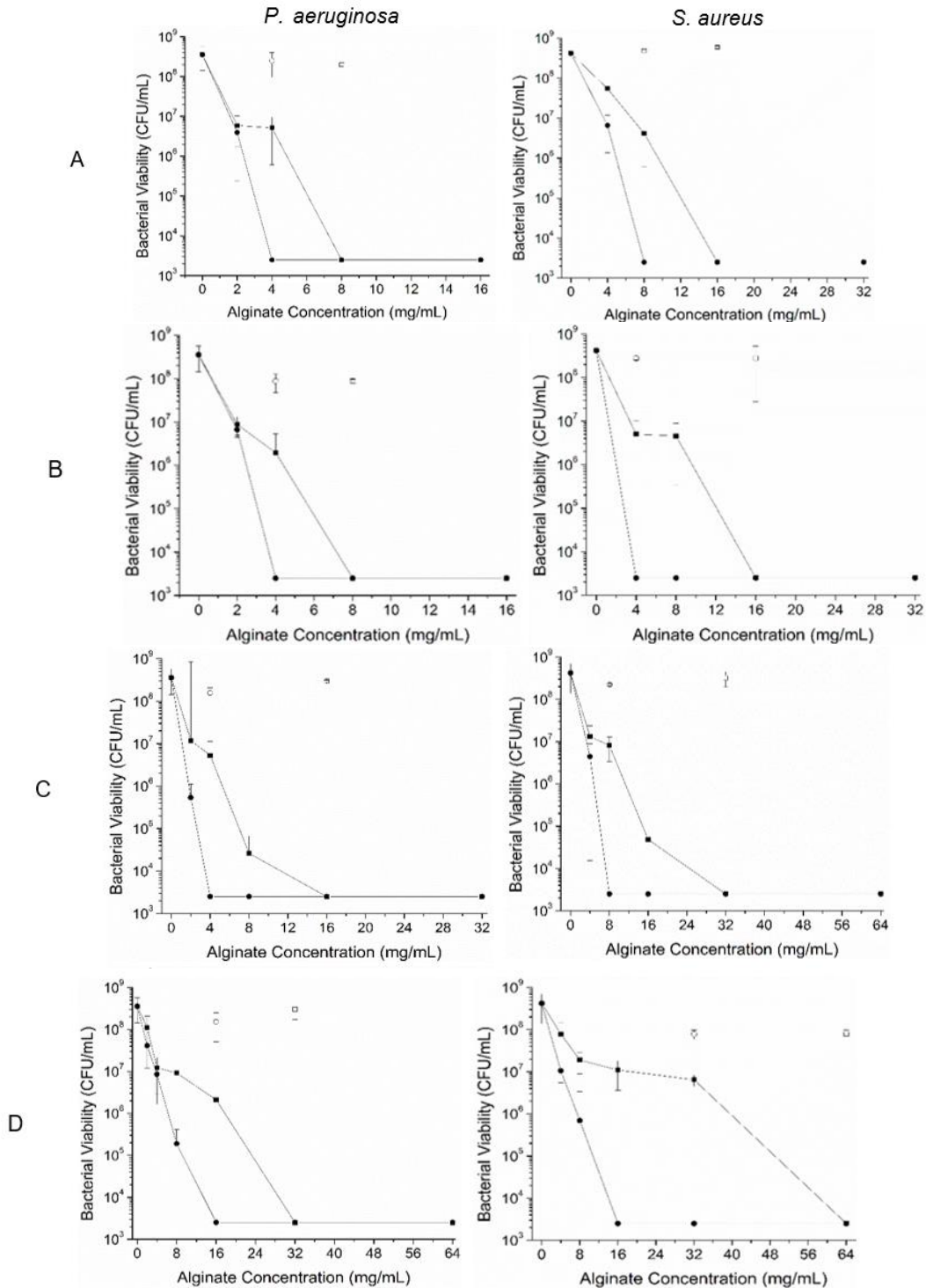


Figure 2.9 Antibiofilm efficacy of high (square) and low (circle) molecular weight NO-releasing (filled) and control (hollow) (A) DETA-, (B) DPTA-, (C) SPER-; and, (D) PAPA-modified alginates against planktonic *P. aeruginosa* and *S. aureus*. Error bars represent standard deviation of the mean viability (CFU/mL). For all measurements, $n \geq 3$ pooled experiments.

Table 2.5 Minimum biofilm eradication concentrations (MBEC_{24h}) of NO-releasing alginates against *P. aeruginosa* and *S. aureus* biofilms.^a

Biopolymer	<i>P. aeruginosa</i>		<i>S. aureus</i>	
	MBEC _{24h} (mg/mL)	NO dose ^b (μ mol/mL)	MBEC _{24h} (mg/mL)	NO dose ^b (μ mol/mL)
Alg300-DETA/NO	8	2.6 \pm 0.5	16	6.2 \pm 0.2
Alg300-DPTA/NO	8	3.4 \pm 0.0	16	6.8 \pm 0.1
Alg300-PAPA/NO	32	19.6 \pm 3.8	64	39.2 \pm 7.6
Alg300-SPER/NO	16	10.3 \pm 1.8	32	20.7 \pm 3.6
Alg5-DETA/NO	4	1.8 \pm 0.5	8	3.6 \pm 1.1
Alg5-DPTA/NO	4	1.7 \pm 0.2	4	1.7 \pm 0.2
Alg5-PAPA/NO	16	9.8 \pm 2.0	16	9.8 \pm 2.0
Alg5-SPER/NO	4	1.3 \pm 0.2	8	2.8 \pm 0.2

^aError represent standard deviation for n \geq 3 experiments. ^bNO dose was calculated from 24 h NO totals of each tested sample in PBS (10 mM, pH 7.4, 37 °C).

Following the size-dependent trend observed in the planktonic studies, the less negatively charged alginate systems required lower alginate concentrations to elicit biocidal activity, with the exception of Alg300-SPER/NO. Despite having the least negative charge of the evaluated alginate systems (Table 2.2), the large NO flux and rapid release half-life for Alg300-SPER/NO (Table 2.3) likely results in undesirable NO donor breakdown similar to that noted for both Alg300-PAPA/NO and Alg5-PAPA/NO. In this respect, the overall biocidal efficacy of the NO-releasing scaffold depends on both the charge of the scaffold and the NO-release kinetics. Alginate scaffolds with moderate to extended NO-release durations ($t_{1/2} \geq 2$ h) consistently require lower alginate concentrations and NO doses to eradicate biofilm-based bacteria, regardless of alginate molecular weight or bacteria Gram class. In this regard, the slower, sustained NO release ensures more effective NO delivery. This result is in agreement with previous studies using different NO-releasing systems.^{20,23,24}

P. aeruginosa biofilms were treated with equal concentrations (8 mg/mL) of each high molecular weight NO-releasing alginate (Figure 2.10A) to study bacterial viability as a function of release kinetics. The high molecular weight alginate scaffolds were selected for this experiment as they demonstrated the largest range in NO-release kinetics. A concentration of 8 mg/mL represented the lowest MBEC_{24h} for the Alg300 systems. At 1 h, treatment with either Alg300-PAPA/NO or Alg300-SPER/NO resulted in a 1- to 2-log reduction in biofilm bacterial viability, as expected based on the NO-release half-lives for the two NO-releasing alginates (~0.5-1.4 h). However, the low NO levels released from the fast NO-releasing alginate at longer durations were insufficient for bacterial killing, with *P. aeruginosa* viability recovering to $\sim 10^8$ CFU/mL after 4 h. In contrast to the fast NO-release systems, the slower NO-releasing alginate scaffolds (~4 and 13 h for Alg300-DPTA/NO and Alg300-DETA/NO, respectively) elicited a more gradual decrease

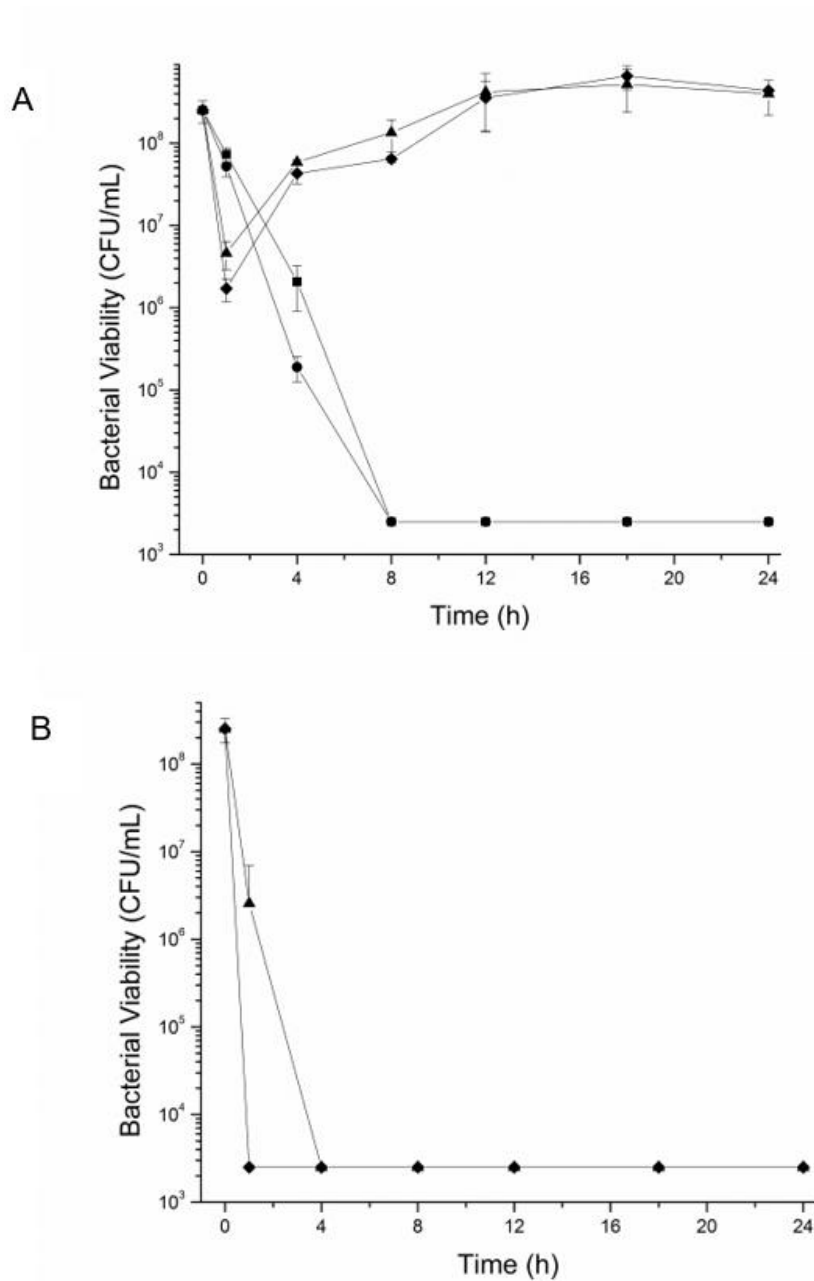


Figure 2.10 Time-based bactericidal efficacy of Alg300-DETA/NO (square), Alg300-DPTA/NO (circle), Alg300-SPER/NO (triangle), and Alg300-PAPA/NO (diamond). Comparison of all high molecular weight NO-releasing alginates at equivalent concentrations of 8 mg/mL is presented in (A), and the time-based killing of the fast NO-releasing systems (Alg300-SPER/NO and Alg300-PAPA/NO) at their respective MBEC_{24h} is presented in (B). Studies consisted of at least three experiments with error bars representing the standard deviation.

in bacteria viability at this same concentration (i.e., 8 mg/mL), eventually leading to a 5-log reduction after 8 h of treatment. At the larger concentrations required to achieve the MBEC_{24h}, both Alg300-PAPA/NO (32 mg/mL) and Alg300-SPER/NO (16 mg/mL) elicited a 5-log reduction in bacterial viability after only 1 and 4 h exposures, respectively, but resulted in observable bacterial growth after 24 h (Figure 2B). The greater alginate (and NO) concentrations improved the antibacterial efficacy of the faster NO-releasing alginates through rapid killing induced by the large initial NO burst. Overall, these results suggest that slower, more sustained NO release is preferred for biofilm eradication at the smaller alginate concentrations.

2.3.4 *In vitro* cytotoxicity against A549 cells

An attractive property of alginates for biomedical applications is the perceived favorable toxicity to mammalian cells. Of course, the influence of the *N*-diazoniumdiolate modification on cytotoxicity might elicit unexpected toxicity. Thus, the cytotoxicity of the alginate scaffolds was evaluated using human respiratory epithelial (A549) cells at the alginate MBECs determined to kill *P. aeruginosa* and *S. aureus*.⁵⁷⁻⁶¹ As shown in Figure 2.11, neither control nor the NO-releasing alginates exhibited significant toxicity (i.e., cell viabilities >70%) against A549 cells at the determined MBEC_{24h} values, regardless of size (i.e., molecular weight) or charge, highlighting the advantage of these biopolymers as antibiofilm agents. The low to negligible toxicity of the NO-releasing alginates at the bactericidal concentrations shows promise for the use of these macromolecules as antibacterial and antibiofilm treatment for wound healing and respiratory infections, for example.

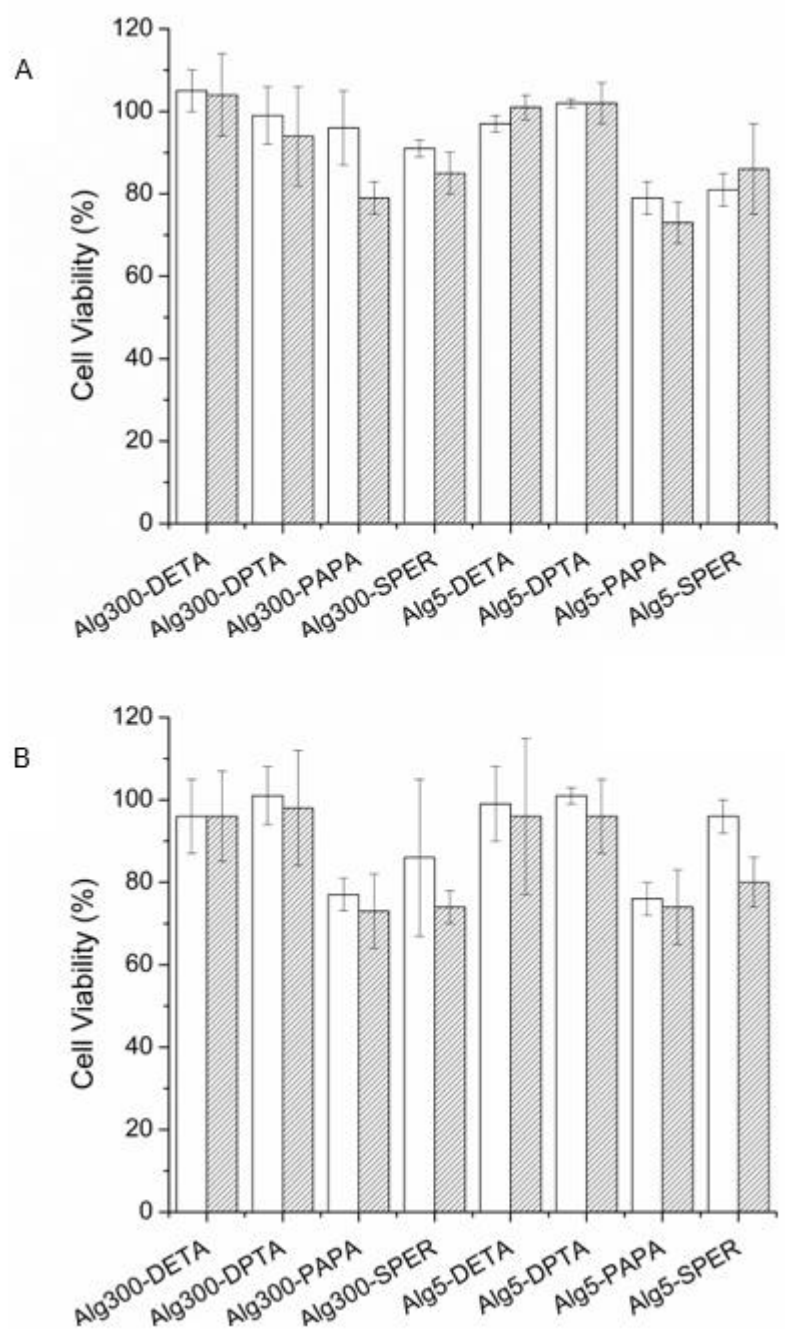


Figure 2.11 Viability of A549 human respiratory epithelial cells exposed to control and NO-releasing (white) and control (dash) alginates at the MBEC_{24h} against (A) *P. aeruginosa* and (B) *S. aureus*. Studies consisted of at least three experiments with error bars representing the standard deviation.

2.4 Conclusions

N-diazoniumdiolate-modified alginate scaffolds were synthesized with diverse NO-release kinetics (0.5-13 h half-lives) and antibacterial properties. The biocidal efficacies of the NO-releasing alginate materials were demonstrated against both planktonic and biofilm-based forms of *P. aeruginosa* and *S. aureus*. Alginate modifications that exhibited slow and sustained NO release (e.g., Alg300-DPTA/NO and Alg300-DETA/NO) proved to be highly effective against bacterial biofilms, requiring lower NO-releasing alginate to elicit eradication. The molecular weight of the scaffold proved important with the oligosaccharides eliciting the greatest bactericidal action. Both amine-modified (control) and NO-releasing alginates exerted minimal toxicity against A549 cells, demonstrating the biocompatible properties of the bare scaffold. Nitric oxide-releasing alginates may prove useful as novel antibacterial agents for treating acute and chronic infections.

REFERENCES

- (1) Levy, S. B.; Marshall, B. Antibacterial Resistance Worldwide: Causes, Challenges and Responses. *Nat. Med.* **2004**, *10*, S122–S129.
- (2) Robson, M. C. Wound Infection: A Failure of Wound Healing Caused by an Imbalance of Bacteria. *Surg. Clin. N. Am.* **1997**, *77*, 637–650.
- (3) Wright, G. D. The Antibiotic Resistome: The Nexus of Chemical and Genetic Diversity. *Nat. Rev. Micro.* **2007**, *5*, 175–186.
- (4) Stewart, P. S.; Costerton, J. W. Antibiotic Resistance of Bacteria in Biofilms. *Lancet* **2001**, *358*, 135–138.
- (5) Pruitt, B. A.; McManus, A. T.; Kim, S. H.; Goodwin, C. W. Burn Wound Infections: Current Status. *World J. Surg.* **1998**, *22*, 135–145.
- (6) Lyczak, J. B.; Cannon, C. L.; Pier, G. B. Lung Infections Associated with Cystic Fibrosis. *Clin. Microbiol. Rev.* **2002**, *15*, 122–194.
- (7) Hall-Stoodley, L.; Stoodley, P. Evolving Concepts in Biofilm Infections. *Cell Microbiol.* **2009**, *11*, 1034–1043.
- (8) Smith, A. W. Biofilms and Antibiotic Therapy: Is There a Role for Combating Bacterial Resistance by the Use of Novel Drug Delivery Systems? *Adv. Drug Deliv. Rev.* **2005**, *57*, 1539–1550.
- (9) Donlan, R. M. Biofilm Formation: A Clinically Relevant Microbiological Process. *Clin. Infect. Dis.* **2001**, *33*, 1387–1392.
- (10) Boucher, H. W.; Talbot, G. H.; Bradley, J. S.; Edwards, J. E.; Gilbert, D.; Rice, L. B.; Scheld, M.; Spellberg, B.; Bartlett, J. Bad Bugs, No Drugs: No ESCAPE! An Update from the Infectious Diseases Society of America. *Clin. Infect. Dis.* **2009**, *48*, 1–12.
- (11) Barraud, N.; Hasset, D. J.; Hwang, S. H.; Rice, S. A.; Kjelleberg, S.; Webb, J. S. Involvement of Nitric Oxide in Biofilm Dispersal of *Pseudomonas Aeruginosa*. *J. Bacteriol.* **2006**, *188*, 7344–7353.
- (12) Carpenter, A. W.; Schoenfisch, M. H. Nitric Oxide Release: Part II. Therapeutic Applications. *Chem. Soc. Rev.* **2012**, *41*, 3742–3752.
- (13) Barraud, N.; Kelso, M. J.; Rice, S. A.; Kjellerberg, S. Nitric Oxide: A Key Mediator of Biofilm Dispersal with Applications in Infectious Diseases. *Curr. Pharm. Des.* **2015**, *21*, 31–42.
- (14) Riccio, D. A.; Schoenfisch, M. H. Nitric Oxide Release: Part I. Macromolecular Scaffolds. *Chem. Soc. Rev.* **2012**, *41*, 3731–3741.
- (15) Hetrick, E. M.; Shin, J. H.; Stasko, N. A.; Johnson, C. B.; Wespe, D. A.; Holmuhamedov, E.; Schoenfisch, M. H. Bactericidal Efficacy of Nitric Oxide-Releasing Silica Nanoparticles. *ACS Nano* **2008**, *2*, 235–246.
- (16) Privett, B. J.; Broadnax, A. D.; Bauman, S. J.; Riccio, D. A.; Schoenfisch, M. H.

Examination of Bacterial Resistance to Exogenous Nitric Oxide. *Nitric Oxide* **2012**, *26*, 169–173.

(17) Keefer, L. K. Fifty Years of Diazeniumdiolate Research. From Laboratory Curiosity to Broad-Spectrum Biomedical Advances. *ACS Chem. Biol.* **2011**, *6*, 1147–1155.

(18) Backlund, C. J.; Worley, B. V.; Sergesketter, A. R.; Schoenfisch, M. H. Kinetic-Dependent Killing of Oral Pathogens with Nitric Oxide. *J. Dent. Res.* **2015**, *94*, 1092–1098.

(19) Lu, Y.; Slomberg, D. L.; Sun, B.; Schoenfisch, M. H. Shape- and Nitric Oxide Flux-Dependent Bactericidal Activity of Nitric Oxide-Releasing Silica Nanorods. *Small* **2013**, *9*, 2189–2198.

(20) Slomberg, D. L.; Lu, Y.; Broadnax, A. D.; Hunter, R. A.; Carpenter, A. W.; Schoenfisch, M. H. Role of Size and Shape on Biofilm Eradication for Nitric Oxide-Releasing Silica Nanoparticles. *ACS Appl. Mater. Interfaces* **2013**, *5*, 9322–9329.

(21) Wo, Y.; Brisbois, E. J.; Bartlett, R. H.; Meyerhoff, M. E. Recent Advances in Thromboresistant and Antimicrobial Polymers for Biomedical Applications: Just Say Yes to Nitric Oxide (NO). *Biomater. Sci.* **2016**, *4*, 1161–1183.

(22) Worley, B. V.; Schilly, K. M.; Schoenfisch, M. H. Anti-Biofilm Efficacy of Dual-Action Nitric Oxide-Releasing Alkyl Chain Modified Poly(Amidoamine) Dendrimers. *Mol. Pharm.* **2015**, *12*, 1573–1583.

(23) Duong, H. T. T.; Jung, K.; Kutty, S. K.; Agustina, S.; Adnan, N. N. M.; Basuki, J. S.; Kumar, N.; Davis, T. P.; Barraud, N.; Boyer, C. Nanoparticle (Star Polymer) Delivery of Nitric Oxide Effectively Negates *Pseudomonas Aeruginosa* Biofilm Formation. *Biomacromolecules* **2014**, *15*, 2583–2589.

(24) Sadrearhami, Z.; Yeow, J.; Nguyen, T.-K.; Ho, K. K. K.; Kumar, N.; Boyer, C. Biofilm Dispersal Using Nitric Oxide Loaded Nanoparticles Fabricated by Photo-PISA: Influence of Morphology. *Chem. Commun.* **2017**, *53*, 12894–12897.

(25) Nair, L. S.; Laurencin, C. T. Biodegradable Polymers as Biomaterials. *Prog. Polym. Sci.* **2007**, *32*, 762–798.

(26) Alnaief, M.; Alzaitoun, M. A.; Garcia-Gonzalez, C. A.; Smirnova, I. Preparation of Biodegradable Nanoporous Microspherical Aerogel Based on Alginate. *Carbohydr. Polym.* **2011**, *84*, 1011–1018.

(27) Bernkop-Schnürch, A.; Kast, C. E.; Richter, M. F. Improvement in the Mucoadhesive Properties of Alginate by the Covalent Attachment of Cysteine. *J. Control. Release* **2001**, *71*, 277–285.

(28) Khan, S.; Tøndervik, A.; Sletta, H.; Klinkenberg, G.; Emanuel, C.; Onsøyen, E.; Myrvold, R.; Howe, R. A.; Walsh, T. R.; Hill, K. E.; et al. Overcoming Drug Resistance with Alginate Oligosaccharides Able To Potentiate the Action of Selected Antibiotics. *Antimicrob. Agents Chemother.* **2012**, *56*, 5134–5141.

(29) Pritchard, M. F.; Powell, L. C.; Menzies, G. E.; Lewis, P. D.; Hawkins, K.; Wright, C.; Doull, I.; Walsh, T. R.; Onsøyen, E.; Dessen, A.; et al. A New Class of Safe Oligosaccharide Polymer Therapy to Modify the Mucus Barrier of Chronic Respiratory Disease. *Mol. Pharm.* **2016**,

13, 863–873.

(30) Draget, K. I.; Taylor, C. Chemical, Physical and Biological Properties of Alginates and Their Biomedical Implications. *Food Hydrocoll.* **2011**, *25*, 251–256.

(31) Liakos, I.; Rizzello, L.; Scurr, D. J.; Pompa, P. P. All-Natural Composite Wound Dressing Films of Essential Oils Encapsulated in Sodium Alginate with Antimicrobial Properties. *Int. J. Pharm.* **2014**, *463*, 137–145.

(32) Paul, W.; Sharma, C. P. Chitosan and Alginate Wound Dressings: A Short Review. *Trends Biomater. Artif. Organs* **2004**, *18*, 18–23.

(33) Matai, I.; Gopinath, P. Chemically Cross-Linked Hybrid Nanogels of Alginate and PAMAM Dendrimers as Efficient Drug Delivery Vehicles. *ACS Biomater. Sci. Eng.* **2016**, *2*, 213–223.

(34) Nordgård, C. T.; Draget, K. I. Oligosaccharides as Modulators of Rheology in Complex Mucous Systems. *Biomacromolecules* **2011**, *12*, 3084–3090.

(35) Nordgård, C. T.; Nonstad, U.; Olderø, M. Ø.; Espevik, T.; Draget, K. I. Alterations in Mucus Barrier Function and Matrix Structure Induced by Guluronate Oligomers. *Biomacromolecules* **2014**, *15*, 2294–2300.

(36) Gombotz, W. R.; Wee, S. Protein Release from Alginate Matrices. *Adv. Drug Deliv. Rev.* **1998**, *31*, 267–285.

(37) Lee, K. Y.; Mooney, D. J. Alginate: Properties and Biomedical Applications. *Prog. Polym. Sci.* **2012**, *37*, 106–126.

(38) Davies, K. M.; Wink, D. A.; Saavedra, J. E.; Keefer, L. K. Chemistry of the Diazeniumdiolates. 2. Kinetics and Mechanism of Dissociation to Nitric Oxide in Aqueous Solution. *J. Am. Chem. Soc.* **2001**, *123*, 5473–5481.

(39) Keefer, L. K.; Nims, R. W.; Davies, K. M.; Wink, D. A. Diazeniumdiolates as NO Dosage Forms. *Methods Enzymol.* **1996**, *268*, 281–293.

(40) Lu, Y.; Slomberg, D. L.; Schoenfisch, M. H. Nitric Oxide-Releasing Chitosan Oligosaccharides as Antibacterial Agents. *Biomaterials* **2014**, *35*, 1716–1724.

(41) Mao, S.; Zhang, T.; Sun, W.; Ren, X. The Depolymerization of Sodium Alginate by Oxidative Degradation. *Pharm. Dev. Technol.* **2012**, *17*, 763–769.

(42) Breed, R. S.; Dotterer, W. D. The Number of Colonies Allowable on Satisfactory Agar Plates. *J. Bacteriol.* **1916**, *1*, 321–331.

(43) Boonthekul, T.; Kong, H.-J.; Mooney, D. J. Controlling Alginate Gel Degradation Utilizing Partial Oxidation and Bimodal Molecular Weight Distribution. *Biomaterials* **2005**, *26*, 2455–2465.

(44) Lu, Y.; Shah, A.; Hunter, R. A.; Soto, R. J.; Schoenfisch, M. H. S-Nitrosothiol-Modified Nitric Oxide-Releasing Chitosan Oligosaccharides as Antibacterial Agents. *Acta Biomater.* **2015**, *12*, 62–69.

- (45) Lutzke, A.; Pegalajar-Jurado, A.; Neufeld, B. H.; Reynolds, M. M. Nitric Oxide-Releasing S-Nitrosated Derivatives of Chitin and Chitosan for Biomedical Applications. *J. Mater. Chem. B* **2014**, *2*, 7449–7458.
- (46) Damodaran, V. B.; Reynolds, M. M. Biodegradable S-Nitrosothiol Tethered Multiblock Polymer for Nitric Oxide Delivery. *J. Mater. Chem.* **2011**, *21*, 5870–5872.
- (47) Wold, K. A.; Damodaran, V. B.; Suazo, L. A.; Bowen, R. A.; Reynolds, M. M. Fabrication of Biodegradable Polymeric Nanofibers with Covalently Attached NO Donors. *ACS Appl. Mater. Interfaces* **2012**, *4*, 3022–3030.
- (48) Keefer, L. K. Nitric Oxide (NO)- and Nitroxyl (HNO)-Generating Diazeniumdiolates (NONOates): Emerging Commercial Opportunities. *Curr. Top. Med. Chem.* **2005**, *5*, 625–636.
- (49) Hrabie, J. A.; Klose, J. R.; Wink, D. A.; Keefer, L. K. New Nitric Oxide-Releasing Zwitterions Derived from Polyamines. *J. Org. Chem.* **1993**, *58*, 1472–1476.
- (50) Bjarnsholt, T.; Kirketerp-Møller, K.; Jensen, P. Ø.; Madsen, K. G.; Phipps, R.; Krogfelt, K.; Høiby, N.; Givskov, M. Why Chronic Wounds Will Not Heal: A Novel Hypothesis. *Wound Repair Regen.* **2008**, *16*, 2–10.
- (51) Sun, B.; Slomberg, D. L.; Chudasama, S. L.; Lu, Y.; Schoenfisch, M. H. Nitric Oxide-Releasing Dendrimers as Antibacterial Agents. *Biomacromolecules* **2012**, *13*, 3343–3354.
- (52) Carpenter, A. W.; Slomberg, D. L.; Rao, K. S.; Schoenfisch, M. H. Influence of Scaffold Size on Bactericidal Activity of Nitric Oxide-Releasing Silica Nanoparticles. *ACS Nano* **2011**, *5*, 7235–7244.
- (53) Liu, N.; Chen, X.-G.; Park, H. J.; Liu, C. G.; Liu, C. S.; Meng, X. H.; Yu, L. J. Effect of MW and Concentration of Chitosan on Antibacterial Activity of Escherichia Coli. *Carbohydr. Polym.* **2006**, *64*, 60–65.
- (54) Beveridge, T. J. Structures of Gram-Negative Cell Walls and Their Derived Membrane Vesicles. *J. Bacteriol.* **1999**, *181*, 4725–4733.
- (55) Hall-Stoodley, L.; Costerton, J. W.; Stoodley, P. Bacterial Biofilms: From the Natural Environment to Infectious Diseases. *Nat. Rev. Micro.* **2004**, *2*, 95–108.
- (56) Reighard, K. P.; Ehre, C.; Rushton, Z. L.; Ahonen, M. J. R.; Hill, D. B.; Schoenfisch, M. H. Role of Nitric Oxide-Releasing Chitosan Oligosaccharides on Mucus Viscoelasticity. *ACS Biomater. Sci. Eng.* **2017**, *3*, 1017–1026.
- (57) Ahmed, M. U.; Velkov, T.; Lin, Y.-W.; Yun, B.; Nowell, C. J.; Zhou, F.; Zhou, Q. T.; Chan, K.; Azad, M. A. K.; Li, J. Potential Toxicity of Polymyxins in Human Lung Epithelial Cells. *Antimicrob. Agents Chemother.* **2017**, *61*, AAC.02690-16.
- (58) Hu, W.; Peng, C.; Luo, W.; Lv, M.; Li, X.; Li, D.; Huang, Q.; Fan, C. Graphene-Based Antibacterial Paper. *ACS Nano* **2010**, *4*, 4317–4323.
- (59) Miller, C.; McMullin, B.; Ghaffari, A.; Stenzler, A.; Pick, N.; Roscoe, D.; Ghahary, A.; Road, J.; Av-Gay, Y. Gaseous Nitric Oxide Bactericidal Activity Retained during Intermittent High-Dose Short Duration Exposure. *Nitric Oxide* **2009**, *20*, 16–23.

- (60) Padmavathi, V.; Sudhakar Reddy, G.; Padmaja, A.; Kondaiah, P.; Ali-Shazia. Synthesis, Antimicrobial and Cytotoxic Activities of 1,3,4-Oxadiazoles, 1,3,4-Thiadiazoles and 1,2,4-Triazoles. *Eur. J. Med. Chem.* **2009**, *44*, 2106–2112.
- (61) Halwani, M.; Yebio, B.; Suntres, Z. E.; Alipour, M.; Azghani, A. O.; Omri, A. Co-Encapsulation of Gallium with Gentamicin in Liposomes Enhances Antimicrobial Activity of Gentamicin against *Pseudomonas Aeruginosa*. *J. Antimicrob. Chemother.* **2008**, *62*, 1291–1297.

CHAPTER 3: RHEOLOGY OF MUCUS TREATED WITH NITRIC OXIDE-RELEASING ALGINATES

3.1 Introduction

Airway mucus represents the first line of defense in the respiratory tract against invading pathogens (e.g., bacteria), dust, spores, pollen, and other chemical irritants.¹⁻³ Mucus is comprised of approximately 95% water, with the balance consisting of proteins, lipids, salts, and mucin glycoproteins (i.e., the main component that determines its gel-like properties).^{4,5} The consistency of mucus is often described in terms of rheological properties, particularly viscosity (resistance to flow) and elasticity (resistance to deformation) due to this complexity.⁵ Excessive, long-term mucus production (i.e., mucus hypersecretion) is a major pathological feature of severe respiratory diseases, such as cystic fibrosis (CF).^{1-3,6} Accumulation of highly viscous and elastic mucus obstructs the airways and provides a suitable environment for the colonization of bacteria.⁷ The presence of persistent chronic infections and impeded mucus clearance leads to a decline in lung function and ultimately patient mortality.

Currently used treatment strategies focused on combining therapies that target bacterial infections (i.e., antibiotics) with those that alter mucus rheology (i.e., mucolytics). Nitric oxide (NO), an endogenously-produced free radical, holds promise as a potential therapeutic agent for treating respiratory diseases due to its broad spectrum antibacterial activity against planktonic and biofilm-based bacteria.⁸⁻¹⁵ Present studies indicated that bacteria are unlikely to foster resistance to NO owing to the multi-mechanistic pathways (e.g., nitrosation of thiols on bacterial proteins)

involved in NO's antibacterial action.^{16,17} While initial studies have demonstrated the efficacy of exogenous NO in the gas form, the hazards associated with the use of pressurized cylinders and NO's high reactivity in biological media has to date limited its therapeutic utility.¹⁸ Research has thus also focused on the development of water soluble macromolecules capable of storing and releasing NO under specific environmental conditions as an alternative to direct NO inhalation.^{18,19} The use of the *N*-diazeniumdiolate NO donor-modified macromolecular scaffolds is particularly attractive due to the NO donor's ability to spontaneously release NO under physiological conditions (e.g., 37 °C, pH 6.5 in CF mucus),^{9,20,21} a property critical for sustained NO delivery in the lungs via intermittent (e.g, twice daily) treatment.¹⁸ Although the activity of NO-releasing macromolecules as antibacterial agents for the treatment of respiratory infections has been well documented,^{8,9} its potential impact on mucus rheology remains uncertain. Initial studies with NO-releasing chitosan have demonstrated NO's ability to damage the three-dimensional mucin network and reduce mucin size.²⁰ While this report indicated NO's potential as a mucolytic, a systematic evaluation of the impact of NO-release properties (e.g., release kinetics) and the effect of the macromolecule properties (e.g., molecular weight) of the material for pulmonary NO delivery is still required for further development of NO as a dual-action (i.e., antibacterial and mucolytic) therapy. Previous reports have characterized the antibacterial properties of NO-releasing materials as a function of macromolecular water solubility, charge, and NO-release kinetics.²²⁻²⁵ We believe that the same properties are likely to influence the mucolytic activity of NO-releasing systems.

Alginate, an anionic biopolymer composed of 1,4-linked α -l-guluronic acid (G) and β -d-mannuronic acid (M) units, holds particular promise as a NO donor scaffold for the development of inhaled NO therapeutics (via nebulization) due to its high water solubility, low toxicity, and

favorable biocompatibility.^{26–30} Previous studies with low molecular weight alginate oligosaccharides demonstrated alginate’s ability to modulate mucin assembly, and reduce the elastic and viscous properties of CF sputum.^{6,31–33} The biopolymer’s ability to alter mucus structure occurs by inhibiting interpolymer crosslinks and interfering with intramolecular interactions between the mucin glycoproteins. We hypothesize that combining alginate with NO’s antibacterial and mucolytic action (by interfering with the disulfide bonds the stitch mucin monomers into long-chain polymers) may result in a favorable dual-action therapeutic for treating obstructive respiratory diseases plagued with chronic infection.^{20,34}

Bulk rheological properties of mucus are tightly correlated to its clearance from the lung.⁵ Therefore, reducing the viscoelastic burden of pathological mucus is important in the treatment of muco-obstructive pulmonary diseases such as CF and COPD. Herein, we evaluated the ability of NO-releasing alginates to alter the bulk viscoelastic properties of human bronchial epithelial (HBE) mucus using parallel plate rheology. Alginate modified with different alkyl amine groups provided a platform to tune NO payloads and release kinetics depending on the precursor amine structure. The effect of NO-release kinetics, alginate concentration, and select biopolymer properties (e.g., molecular weight and charge) on mucus rheology were also examined with similar goals.

3.2 Experimental Section

3.2.1 Materials

Alginic acid sodium salt from brown algae (low viscosity), bis(3-aminopropyl) amine (DPTA), diethylenetriamine (DETA), *N*-propyl-1,3-propanediamine (PAPA), spermine (SPER), 1-ethyl-3-(3-dimethylaminopropyl)carbodiimide hydrochloride (EDC), *N*-hydroxysuccinimide

(NHS), *p*-anisaldehyde, *p*-toluenesulfonyl chloride, ethanolamine and *N*-acetyl cysteine (NAC) were purchased from Sigma-Aldrich (St. Louis, MO). Medium molecular weight chitosan (95% degree of deacetylation) was purchased from Primex (Siglufjordur, Iceland). Common laboratory salts and solvents were purchased from Fisher Scientific (Fair Lawn, NJ). Unless otherwise specified, all chemicals were used as received without further purification. Argon (Ar), carbon dioxide (CO₂), nitrogen (N₂), nitric oxide (NO) calibration (25.87 ppm, balance N₂), and pure NO (99.5%) gas cylinders were purchased from Airgas National Welders (Raleigh, NC). Distilled water was purified to a resistivity of 18.2 MΩ•cm and a total organic content of ≤6 ppb using a Millipore Milli-Q UV Gradient A10 System (Bedford, MA).

3.2.2 Instrumentation

¹H and ¹³C nuclear magnetic resonance (NMR) spectra were recorded on a Bruker (600 MHz) spectrometer. Elemental (carbon, hydrogen, and nitrogen; CHN) analysis was performed using a PerkinElmer Elemental Analyzer Series 2400 Instrument (Waltham, MA). Zeta potential measurements were collected in phosphate buffer (PB; 10 mM; pH 6.5) using a Zetasizer Nano (Malvern Instruments, UK). Rheological measurements were carried out using a TA Discovery Hybrid Rheometer 3 (DHR3; New Castle, DE) with a 20 mm diameter parallel plate set to a gap thickness of 50 mm. Gel permeation chromatography (GPC) measurements were collected out in 0.1 M sodium nitrate using an aqueous GPC-multi-angle light scattering system equipped with a Waters 2414 refractive index detector (Milford, MA) coupled to a Wyatt miniDawn TREOS multi-angle light scattering detector (Santa Barbara, CA).

3.2.3 *Oxidative degradation of biopolymers*

High molecular weight alginate and medium molecular weight chitosan biopolymers were degraded to lower molecular weights following previously published protocols.^{10,25,35} Briefly, the biopolymer (2.5 g) was dissolved in hydrogen peroxide (50 mL) and stirred in an oil bath for 1-4 h. The concentration of the hydrogen peroxide in the solution (15-30 wt% in water), temperature (70-85 °C), and duration of the reaction were varied to obtain alginate oligosaccharides with a range of molecular weights (Table S1). The resulting solution was filtered to remove insoluble material. The alginate oligosaccharides were collected in and washed copiously with ethanol before drying in vacuo to yield a white powder. Alternatively, chitosan was stirred in 15 wt% hydrogen peroxide at 85 °C for 1 h with the resulting oligosaccharides collected in acetone and washed copiously with acetone. The chitosan oligosaccharides (COS) had an average molecular weight of 4.38 kDa and dispersity of 1.2 as determined by GPC measurements (Table 3.2).

3.2.4 *Synthesis of polyamine-modified alginates (AlgMW-alkyl amine)*

The alginate oligosaccharides were modified with either DETA, DPTA, PAPA, or SPER following a previously published protocol.²⁵ Briefly, low molecular weight alginate (100 mg) was dissolved in 10 mL phosphate buffered saline (PBS; 10 mM, pH 6.5) with a 2:1 molar ratio of EDC and a 2:1 molar ratio of NHS with respect to the carboxylic acid moieties on the alginate biopolymer. The reaction was left to stir for 1 h. A 4:1 molar ratio of the alkyl amine with respect to the carboxylic acid groups of the alginate biopolymer was then added dropwise to the mixture. The reaction was allowed to proceed for 24 h at room temperature under constant stirring. The amine-modified alginates were precipitated in methanol and collected by centrifugation, washed twice with methanol, and dried in vacuo to yield a white solid for each modification.

Table 3.1 Optimization of oxidative degradation of alginate.^a

Scaffold	Reaction Time (h)	Concentration of H₂O₂ (wt %)	Temperature (°C)	Mw (kDa)	PDI
Alg10	1 h	15	70	10,980	2.05
Alg5	1 h	15	85	4,680	1.22
Alg1	4 h	30	85	1,447	2.10

^aAverage molecular weight (Mw) and polydispersity index (PDI) were measured using GPC-multi-angle light scattering system.

Table 3.2 Physicochemical characterization for secondary amine-functionalized alginate and chitosan biopolymers.^a

Scaffold	nitrogen^b (%)	Zeta Potential^c (mV)	M_w^d (Da)	PDI^d
Alg300	0.0 ± 0.0	-40.4 ± 3.2	282,000	1.11
Alg10	0.1 ± 0.0	-30.2 ± 5.0	9,184	1.14
Alg5	0.0 ± 0.0	-31.3 ± 0.8	4,680	1.22
Alg5-DETA	7.8 ± 0.8	-17.5 ± 3.4	5,200	2.06
Alg5-DPTA	6.4 ± 0.2	-14.1 ± 1.5	6,000	1.44
Alg5-SPER	8.2 ± 1.1	-12.4 ± 0.7	7,900	1.82
Alg5-PAPA	5.7 ± 0.7	-22.8 ± 2.2	6,700	1.49
Alg5-PAPA-DPTA	11.2 ± 0.7	-15.3 ± 3.1	7,200	1.87
Alg1	0.1 ± 0.1	-22.6 ± 4.5	1,447	1.42
COS	5.2 ± 0.3	1.9 ± 0.3	4,380	1.20
COS-EA	6.3 ± 0.2	5.6 ± 1.3	5,610	1.70

^aError represents standard deviation for n ≥ 3 experiments. ^bMeasured by elemental analysis. ^cMeasured in phosphate buffer (pH 6.5). ^dMeasured using a gel permeation chromatography (GPC)-multiangle light scattering system.

A hybrid alginate system modified with both PAPA and DPTA was also synthesized following similar steps. A 4:1 molar ratio of PAPA with respect to the carboxylic acid groups of alginate were first added dropwise to the solution prior to addition of a 4:1 molar ratio of DPTA with respect to the same groups. The reaction was allowed to proceed for 24 h at room temperature before being collected and copiously washed with methanol to yield a white powder.

Representative ^1H and ^{13}C NMR of alginate and the polyamine modified alginates included the following peaks:

Alg300, Alg 10, Alg5 and Alg1: ^1H NMR (600 MHz, D_2O , δ) 3.60-4.05 (OCHCH(OH)CH(OH)), 4.30 (OCHCH(OH)CH(OH)), 4.50-4.60 (OHCOCH), 4.90 (OCH(CHOH)O). ^{13}C NMR (600 MHz, D_2O , δ) 65.0-80.0 (OCHCH(OH)CH(OH)CH(OH)CH(O)), 100.0 (OCHCH(OH)), 175.0 (CHC(O)).

Alg5-DPTA: ^1H NMR (600 MHz, D_2O , δ) 1.60-1.80 ($\text{CH}_2\text{CH}_2\text{CH}_2\text{NHCH}_2\text{CH}_2\text{CH}_2\text{NH}_2$), 2.60-2.30 ($\text{CH}_2\text{CH}_2\text{CH}_2\text{NHCH}_2\text{CH}_2\text{CH}_2\text{NH}_2$), 2.80-3.10 ($\text{CH}_2\text{CH}_2\text{CH}_2\text{NHCH}_2\text{CH}_2\text{CH}_2\text{NH}_2$), 3.60-4.05 (OCHCH(OH)CH(OH)), 4.30 (OCHCH(OH)CH(OH)), 4.50-4.60 (NHCOCH), 4.90 (OCH(CHOH)O). ^{13}C NMR (600 MHz, D_2O , δ) 26.9-29.5 (C(O)NHCH₂CH₂CH₂NH, NHCH₂CH₂CH₂NH₂), 37.6-46.0 CH₂ (C(O)NHCH₂CH₂CH₂NH, NHCH₂CH₂CH₂NH₂), 65.0-80.0 (OCHCH(OH)CH(OH)CH(OH)CH(O)), 100.0 (OCHCH(OH)), 160.0 (CHC(O)NH), 175.0 (CHC(O)).

Alg5-DETA: ^1H NMR (600 MHz, D_2O , δ) 2.30-3.30 ($\text{CH}_2\text{CH}_2\text{NHCH}_2\text{CH}_2\text{NH}_2$), 3.60-4.05 (OCHCH(OH)CH(OH)), 4.30 (OCHCH(OH)CH(OH)), 4.50-4.60 (NHCOCH), 4.90 (OCH(CHOH)O). ^{13}C NMR (600 MHz, D_2O , δ) 39.0-47.0 (C(O)NHCH₂CH₂NHCH₂CH₂NH₂),

65.0-80.0 (OCHCH(OH)CH(OH)CH(OH)CH(O)), 100.0 (OCHCH(OH)), 160.0 (CHC(O)NH), 175.0 (CHC(O)).

Alg5-PAPA: ^1H NMR (600 MHz, D_2O , δ) 0.70-0.80 ($\text{NHCH}_2\text{CH}_2\text{CH}_3$), 1.52 ($\text{NHCH}_2\text{CH}_2\text{CH}_3$), 1.85 ($\text{CH}_2\text{CH}_2\text{CH}_2\text{NHCH}_2\text{CH}_2\text{CH}_3$), 2.80-3.10 ($\text{CH}_2\text{CH}_2\text{CH}_2\text{NHCH}_2\text{CH}_2\text{CH}_3$), 3.60-4.05 (OCHCH(OH)CH(OH)), 4.30 (OCHCH(OH)CH(OH)), 4.50-4.60 (NHCOCH), 4.90 (OCH(CHOH)O). ^{13}C NMR (600 MHz, D_2O , δ) 10.9 ($\text{NHCH}_2\text{CH}_2\text{CH}_3$), 20.0 ($\text{NHCH}_2\text{CH}_2\text{CH}_3$), 31.3-49.0 (C(O)NHCH₂CH₂CH₂NH, NHCH₂CH₂CH₂), 65.0-80.0 (OCHCH(OH)CH(OH)CH(OH)CH(O)), 100.0 (OCHCH(OH)), 160.0 (CHC(O)NH), 175.0 (CHC(O)).

Alg5-SPER: ^1H NMR (600 MHz, D_2O , δ) 1.13 ($\text{NHCH}_2(\text{CH}_2)_2\text{CH}_2\text{NH}$), 1.56 ($\text{NHCH}_2\text{CH}_2\text{CH}_2\text{NH}$), 1.80 (C(O)NHCH₂CH₂CH₂NH), 2.20-2.40 ($\text{CH}_2\text{CH}_2\text{CH}_2\text{NH}$, $\text{NHCH}_2(\text{CH}_2)_2\text{CH}_2\text{NH}$, $\text{NHCH}_2\text{CH}_2\text{CH}_2\text{NH}_2$), 2.68 ($\text{NHCH}_2\text{CH}_2\text{CH}_2\text{NH}_2$), 2.80-3.10 (C(O)NHCH₂CH₂CH₂NH, $\text{NHCH}_2\text{CH}_2\text{CH}_2\text{NH}_2$), 3.60-4.05 (OCHCH(OH)CH(OH)), 4.30 (OCHCH(OH)CH(OH)), 4.50-4.60 (NHCOCH), 4.90 (OCH(CHOH)O). ^{13}C NMR (600 MHz, D_2O , δ) 23.2 ($\text{NHCH}_2(\text{CH}_2)_2\text{CH}_2\text{NH}$), 34.8-45.0 (C(O)NHCH₂CH₂CH₂NH), 65.0-80.0 (OCHCH(OH)CH(OH)CH(OH)CH(O)), 100.0 (OCHCH(OH)), 160.0 (CHC(O)NH), 175.0 (CHC(O)).

Alg5-PAPA-DPTA: ^1H NMR (600 MHz, D_2O , δ) 0.70-0.80 ($\text{NHCH}_2\text{CH}_2\text{CH}_3$), 1.48 ($\text{NHCH}_2\text{CH}_2\text{CH}_3$), 1.50-1.70 ($\text{CH}_2\text{CH}_2\text{CH}_2\text{NHCH}_2\text{CH}_2\text{CH}_2\text{NH}_2$), 2.30-2.40 ($\text{CH}_2\text{CH}_2\text{CH}_2\text{NHCH}_2\text{CH}_2\text{CH}_2\text{NH}_2$), 2.10 ($\text{CH}_2\text{CH}_2\text{CH}_2\text{NHCH}_2\text{CH}_2\text{CH}_3$), 2.60-3.10 ($\text{CH}_2\text{CH}_2\text{CH}_2\text{NHCH}_2\text{CH}_2\text{CH}_2\text{NH}_2$), 3.60-4.05 (OCHCH(OH)CH(OH)), 4.30 (OCHCH(OH)CH(OH)), 4.50-4.60 (NHCOCH), 4.90 (OCH(CHOH)O). ^{13}C NMR (600 MHz, D_2O , δ) 9.4 ($\text{NHCH}_2\text{CH}_2\text{CH}_3$), 20.0 ($\text{NHCH}_2\text{CH}_2\text{CH}_3$), 26.9-29.5 (C(O)NHCH₂CH₂CH₂NH,

NHCH₂CH₂CH₂NH₂), 31.3-49.0 (C(O)NHCH₂CH₂CH₂NH, NHCH₂CH₂CH₃), 37.6-46.0 CH₂
 (C(O)NHCH₂CH₂CH₂NH, NHCH₂CH₂CH₂NH₂), 65.0-80.0
 (OCHCH(OH)CH(OH)CH(OH)CH(O)), 100.0 (OCHCH(OH)), 160.0 (CHC(O)NH), 175.0
 (CHC(O)).

3.2.5 Synthesis of tosylated-aminoethyl Schiff base (TES)

The aminoethyl Schiff base was first synthesized following a 1:1 molar ratio reaction between ethanolamine and *p*-anisaldehyde for 24 h with strong continuous stirring (Figure 3.1A). The resulting viscous yellow solution was then placed under vacuo to pull off excess water. The aminoethyl Schiff base was subsequently functionalized with a tosyl group. A 1.411 g aliquot of the viscous solution was added in a solution of dichloromethane (5 mL) and pyridine (1.3 mL) with vigorous stirring. The solution was placed in an ice bath and allowed to cool to 0 °C. Tosyl chloride (2.0 g) was dissolved in dichloromethane (10 mL) before adding dropwise to the Schiff base mixture. The reaction was allowed to proceed for 24 h. The product was then precipitated in diethyl ether and collected via vacuum filtration to yield a yellow powder. ¹H NMR (600 MHz, DMSO-d₆, δ) 2.40-2.50 (CH₃C(CHCH)CS), 3.30-3.60 (OCH₂CH₂N), 3.70 (CH₃OC(CHCH)CHCHCCHN), 6.10 (NCHC), 6.90-7.00 (NCHC(CHCH)CHCHCOCH₃), 7.30-7.50 (CH₃C(CHCH)CHCHCS), 7.80-7.90 (NCHC(CHCH)CHCHCOCH₃).

3.2.6 Synthesis of ethylamine-modified chitosan oligosaccharides (COS-EA)

Water-soluble chitosan oligosaccharides were modified with the aminoethyl Schiff base functional group through a tosylate nucleophilic substitution (Figure 3.1B). Briefly, COS (500 mg) was dissolved in 10 mL water and placed in an oil bath at 80°C. The tosylated-aminoethyl Schiff base was then dissolved in dimethyl sulfoxide (DMSO; 12.5 mL) and slowly added dropwise to

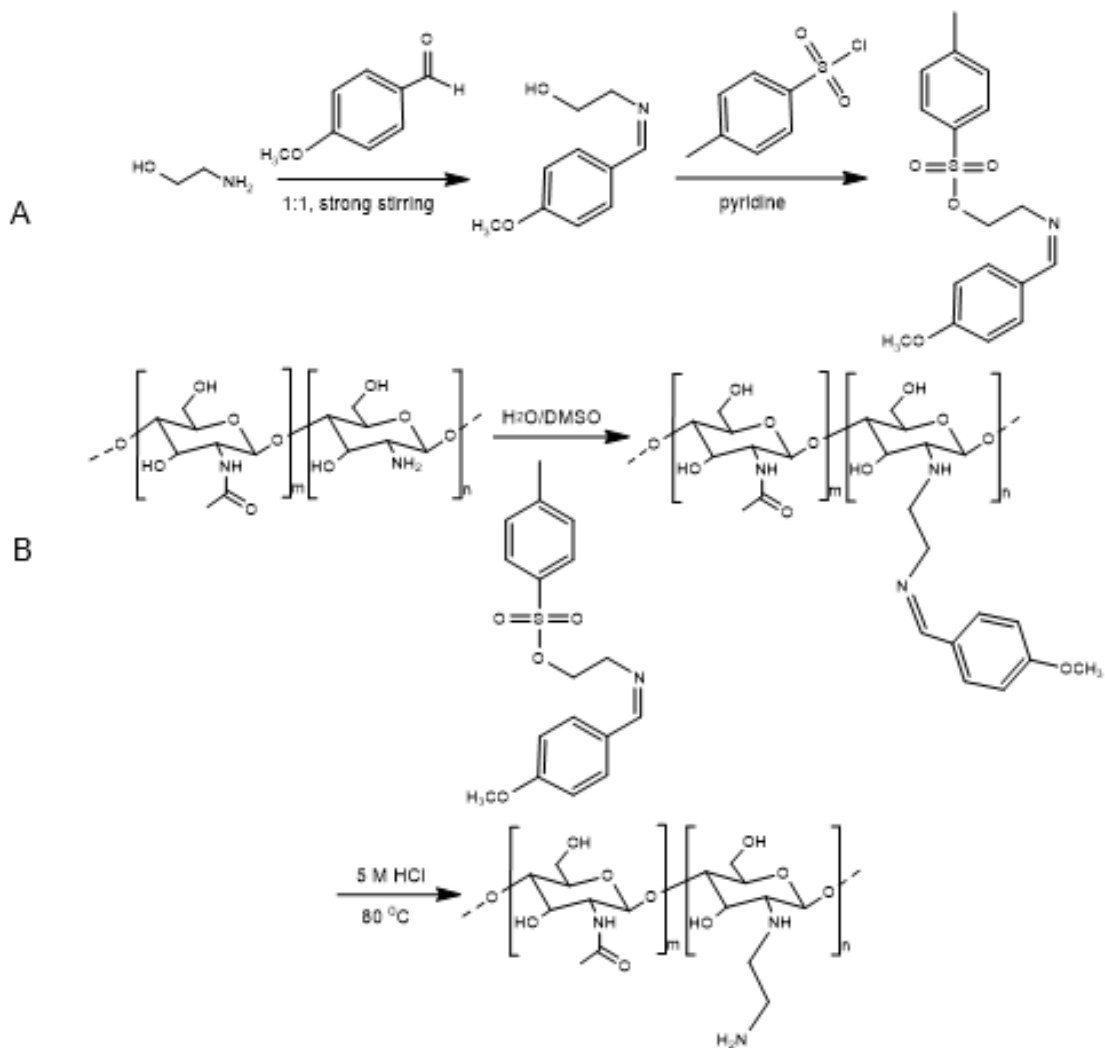


Figure 3.1 (A) Synthesis of tosyl-modified ethanolamine Schiff base. (B) Synthesis of ethanolamine-modified chitosan oligosaccharides.

the chitosan solution. After 1 h, HCl (2 mL; 5 M) was added to the reaction solution. After 18 h, the solution was neutralized with 1 M NaOH before product isolation via precipitation in ethanol, collected via centrifugation, and washed twice with ethanol to yield a brown powder. ^1H NMR (600 MHz, D_2O , δ) 1.90 ($\text{CHNHC}(\text{O})\text{CH}_3$), 2.30-2.90 ($\text{CHNHCH}_2\text{CH}_2\text{NH}_2$), 3.30-4.00 ($\text{OCH}(\text{CH}_2\text{OH})\text{CHCH}(\text{OH})\text{CH}(\text{NH})$), 4.40 ($\text{OCH}(\text{CHNH})\text{O}$).

3.2.7 Synthesis of *N*-diazoniumdiolate-modified biopolymers

Nitric oxide-releasing alginates and chitosan oligosaccharides were synthesized as previously reported.^{10,25} Polyamine-modified alginate (45 mg) was dissolved in 50 mM NaOH solution (3 mL) in a 1-dram glass vial. For the chitosan oligosaccharide sample, COS-EA (45 mg) was dissolved in mixture of water (450 μL), methanol (2.55 mL), and sodium methoxide (5.4 mM in methanol, 75 μL). The open vials were placed in a stainless steel reactor, and solutions stirred continuously via magnetic stirring. Oxygen was removed from the vessel by purging with argon (10 s, 7 bar) three times, followed by three additional long purges with argon (10 min, 7 bar). The vessel was then pressurized to 10 bar with NO gas and allowed to react for 3 d. Afterward, the same argon purging protocol was repeated to remove unreacted NO. The NO-releasing alginates were then precipitated in ethanol, collected by centrifugation, dried overnight in vacuo, and stored at $-20\text{ }^\circ\text{C}$ as a white powder. The NO-releasing COS was collected in acetone via centrifugation and stored similarly as a brown powder.

3.2.8 Characterization of nitric oxide release

Nitric oxide release was evaluated in real-time using a Sievers 280i Chemiluminescence NO analyzer (NOA; Boulder, CO). Measurements were taken before each use to ensure sample stability. Prior to analysis, the NOA was calibrated with air passed through a NO zero filter (0 ppm

NO) and 25.87 ppm of a NO standard gas (balance N₂). In a typical measurement, the NO-releasing biopolymer (1 mg) was dissolved in 30 mL of PBS (10 mM, pH 6.5, 37 °C). Nitrogen was passed through the solution at a flow rate of 70 mL/min to carry the liberated NO from the biopolymer to the analyzer. Additional nitrogen flow was supplied to the flask to match the collection rate of the instrument (200 mL/min) to ensure that water soluble interferents (e.g., nitrite and nitrate) that may be present in the sample flask are not transferred to the reaction cell. Nitric oxide analysis was terminated when NO levels fell to below 10 ppb of NO/mg of biopolymer (the limit of detection of the instrument).^{36,37}

3.2.9 Preparation of mucus sample

Human bronchial epithelial cell culture washings containing mucus were collected from excess surgical tissue (sourced from UNC-Chapel Hill Tissue Core facility). Briefly, primary HBE cells were grown on 0.4 µm pore-sized Millicell cell culture inserts (Millipore; Bedford, MA) coated with collagen in air-liquid interface media (UNC Chapel Hill-Tissue Core Facility) for a minimum of 6 w until the cultures developed cilia, well-defined periciliary liquid (PCL), and mucus layers.³⁸ Mucus was harvested from the cell cultures following previously published protocols.^{39,40} Washings were pooled in 3,500 kDa cut off dialysis tubing (Fisher Scientific; Fairlawn, NJ) and concentrated against Spectra/Gel (Spectrum Labs; Rancho Dominguez, CA) to 3 wt% solids, which served as the minimum mucus concentration for a disease state model.⁴⁰ Subsequently, these washings were treated immediately with either alginate, chitosan, or *N*-acetyl cysteine.

3.2.10 Parallel plate rheology

Concentrated solutions of both control (non-NO-releasing) and NO-releasing biopolymer samples (5 μ L) were added to 50 μ L aliquots of 3 wt% HBE mucus to achieve a final concentration of 20 mg/mL prior to collecting rheological data. Mucus samples were slowly rotated at room temperature for 18 h. The rheological properties of both treated and untreated (blank) mucus samples were measured via amplitude sweep experiments over a stress range of 0.025-50 Pa at a single frequency (1 Hz) using the rheometer equipped with a 20 mm diameter parallel plate set to a gap thickness of 50 μ m. Rheological measurements were performed at 23 $^{\circ}$ C to minimize sample dehydration. The elastic modulus (G') and viscous modulus (G'') were determined from the linear regimes as previously reported.⁴¹

A time-based study with control and NO-releasing biopolymers was conducted following the aforementioned protocol. Rheological data were collected at 1 h, 3 h, and 5 h timepoints using the same parameters. Similarly, a nitric oxide dose-dependence study (20-80 mg/mL) using control and NO-releasing Alg5-PAPA-DPTA, COS-EA, and *N*-acetyl cysteine (1-200 mg/mL) was also carried out following the same protocol.

3.2.11 Statistical analysis

All values either numerically or with error bars are reported as the mean \pm standard deviation of the mean for a minimum of three or more pooled experiments. Statistical significance was determined using the two-tailed Student's *t*-test.

3.3 Results and Discussion

3.3.1 *Synthesis of N-diazeniumdiolate-modified biopolymers*

Alginate oligosaccharides (~5 kDa) with different secondary amine functional groups (i.e., DETA, DPTA, PAPA, and SPER) were prepared via EDC/NHS reactions as reported previously.²⁵ The alkyl amine modification was confirmed via ¹³C NMR by the appearance of the amide bond peak (~160 ppm; Figure 3.2). The nitrogen content for the alkyl amine-modified materials also increased from 0 to 6-11%, providing further evidence of successful modification (Table 3.2).²⁵ The protonated amines at pH 6.5 (Table 3.2) resulted in a positive shift of the zeta potential (from -40 mV to between -12 to -30 mV), making the alkyl amine-modified alginates less negatively charged than the native alginate biopolymer.

In addition to the monosubstituted polymer, a hybrid system was also prepared to design NO-releasing alginate system with potentially high initial NO flux and more sustained NO release by making use of NO donors having both fast and slow NO-release properties. Specifically, the PAPA and DPTA polyamine modifications were selected for the hybrid system based on the reported NO-release half-lives of the small molecule alkyl amines (0.2 and 3.0 h, respectively).⁴² Integration of the peak related to the methyl terminal group of PAPA indicated that the alginate was 43% modified with this functional group. The percent DPTA modification for the hybrid alginate system (50%) was extrapolated from the total nitrogen content of the modified alginate biopolymer, subtracting out the predicted nitrogen contribution from PAPA (calculations provided in Appendix A). These percentages suggest that the two-alkyl amine functional groups have similar alginate modification efficiencies.

The secondary amine-modified alginates were subsequently functionalized with NO donors by exposure to high pressures of NO gas under basic conditions. Formation of the *N*-

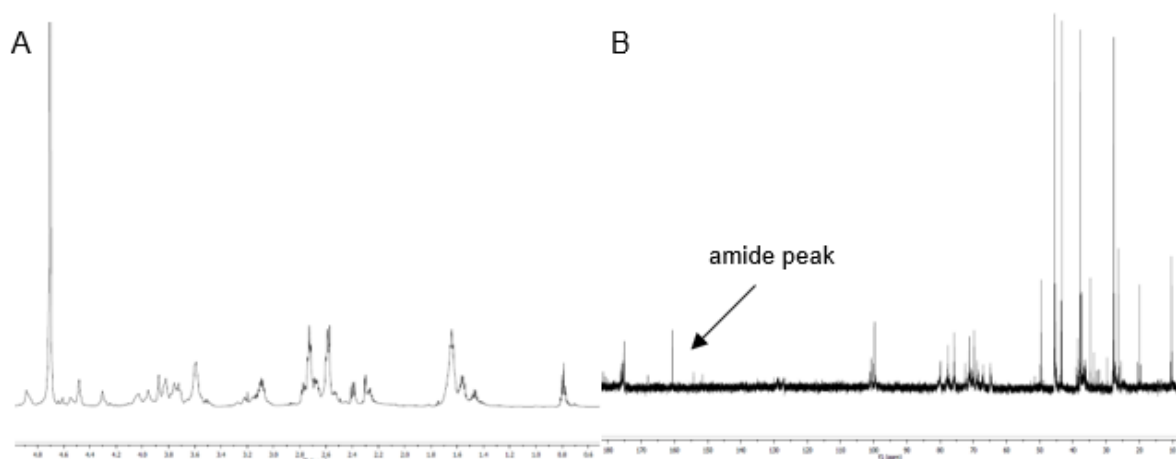


Figure 3.2 Representative (A) ^1H NMR and (B) ^{13}C NMR spectra of Alg5-PAPA-DPTA.

N-diazeniumdiolate NO donors was confirmed by UV-vis spectroscopy and the appearance of a characteristic absorbance band at 253 nm.¹⁶ The resulting *N*-diazeniumdiolate-modified alginates possessed a broad range of NO payloads and release kinetics (Table 3.3), with Alg5-PAPA/NO and Alg5-DETA/NO having the fastest and shortest NO-release half-lives (0.1 and 2.0 h, respectively). Overall, the NO payloads were comparable to that of previously reported water-soluble systems (0.3-0.6 $\mu\text{mol}/\text{mg}$; Table 3.3).^{10,11,25,43-45} While the alginate hybrid system (Alg5-PAPA-DPTA/NO) had a similar NO payload to that of Alg5-PAPA/NO, both the NO-release half-lives and durations resembled Alg5-DPTA/NO. This result was unexpected given the greater number of secondary amine groups for the hybrid system. It is likely that steric hindrance from the crowded functional groups limits *N*-diazeniumdiolate formation.

The NO-release properties of the anionic alginate biopolymers were also compared to chitosan, another naturally derived biopolymer, comprised of repeating units of *N*-acetylglucosamine and d-glucosamine units. To date, chitosan has been used for many biomedical drug delivery applications due to its tolerability (i.e., biocompatibility) and mucoadhesive properties.^{10,11,44-47} Lu et al. reported on the synthesis of low molecular weight (~5 kDa) NO-releasing chitosan oligosaccharides (COS).¹⁰ A similar protocol was adopted in this work to prepare water soluble starting material. The COS primary amines were then modified with ethanolamine via a tosylate nucleophilic substitution reaction (Figure 3.1) to yield secondary amines that could subsequently be functionalized with NO. The resulting NO-donor-modified COS was found to have greater NO payloads than the alginate systems (~0.7 $\mu\text{mol}/\text{mg}$) but comparable NO-release kinetics ($t_{1/2} \sim 0.8$ h). The lower NO payloads for alginate compared to chitosan may be due to the conformation adapted by alginate's monomers. The repeating units of G monomers on the alginate are described to have a buckled conformation resulting in a diamond-

Table 3.3 Nitric oxide-release properties of *N*-diazoniumdiolate-functionalized biopolymers in PBS at pH 6.5 and 37 °C.^a

Biopolymer	t[NO]^b ($\mu\text{mol}/\text{mg}$)	[NO]_{max}^c (ppb/mg)	<i>t</i>_{1/2}^d (h)	<i>t</i>_d^e (h)
Alg5-DETA/NO	0.34 ± 0.15	570 ± 23	2.40 ± 1.37	16.1 ± 3.5
Alg5-DPTA/NO	0.40 ± 0.02	1000 ± 230	2.37 ± 0.10	4.4 ± 0.4
Alg5-SPER/NO	0.39 ± 0.04	2900 ± 330	0.29 ± 0.13	3.0 ± 0.8
Alg5-PAPA/NO	0.57 ± 0.02	11900 ± 3900	0.13 ± 0.06	2.9 ± 0.3
Alg5-PAPA-DPTA/NO	0.53 ± 0.05	4900 ± 1300	0.30 ± 0.08	4.5 ± 1.3
COS-EA/NO	0.74 ± 0.07	1500 ± 300	0.82 ± 0.01	10.2 ± 1.5

^aError represents standard deviation for $n \geq 3$ experiments. ^bTotal NO released. ^cMaximum instantaneous flux of NO release. ^dNO-release half-life. ^eDuration of NO release. All measurements were collected in 10 mM PBS using ~1.0 mg of the biopolymer.

shaped hole while the repeating units of M monomers are described as an extended ribbon, similar to that of chitosan.^{48,49} Both monomeric units can be modified with alkyl amine functional groups via carbodiimide chemistry, however, the conformation adapted by G residues could limit NO donor formation due to steric hindrance.

3.3.2 *Effect of molecular weight on alginate-treated mucus rheology.*

The diffusion of therapeutic agents through mucus depends on both the size and the mucoadhesive properties of the material.⁴ Regardless of charge, low molecular weight polymers (< 10 kDa) usually diffuse through the mucus layer, allowing for more efficient drug delivery to the site of interest (e.g., biofilms embedded in the mucus).⁵⁰ In contrast, larger molecular weight polymers (≥ 10 kDa) have increased interactions with mucins (e.g., chain entanglements, increased H-bonding interactions). These interactions form mucin-polymer aggregates and increase the viscoelastic properties of the mucus.^{46,50} To study the impact of alginate molecular weight on the viscoelasticity of mucus, the elastic (G') and viscous (G'') moduli were measured using parallel plate rheology. Mucus was treated with to 20 mg/mL of bare (unmodified) alginate systems of different molecular weights (1, 5, 10, and 300 kDa) for 24 h. The alginate-treated samples reduced both the elastic and viscous moduli of mucus relative to the untreated blanks (Figure 3.3), with < 5 kDa MW alginates reducing both elasticity and viscosity by 60-70% (Table 3.4 In agreement with previous studies,^{28,31-33} the lower molecular weight materials (Alg1 and Alg5) proved to be the most effective at reducing the viscoelastic properties of the mucus. Alg300 (i.e., the high molecular weight biopolymer) was the least effective, as might have been expected based on size.^{28,31-33} Alginate molecular weight is a crucial factor that controls the biopolymer's gel-forming ability.^{29,30,49} While the Alg300 system still reduced rheological properties, lower molecular weight biopolymers avoid the potential for mucin chain entanglements by having less repeating

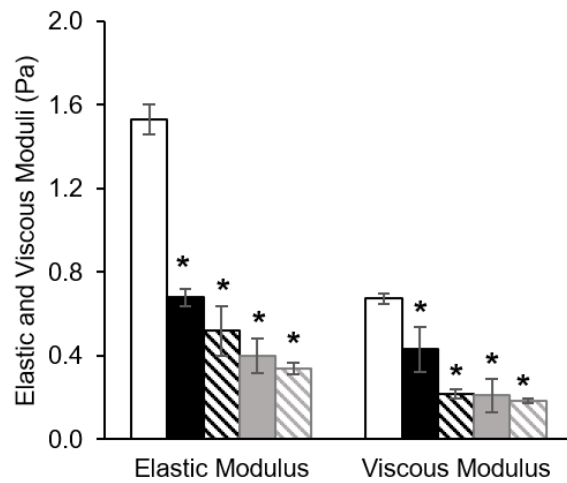


Figure 3.3 Elastic and viscous moduli of 3 wt% human bronchial epithelial (HBE) mucus following treatment with 20 mg/mL Alg300 (black solid), Alg10 (black diagonal), Alg5 (gray solid), and Alg1 (gray diagonal). Single asterisks (*) indicate significant differences ($p < 0.05$) relative to untreated sample (hollow).

Table 3.4 Reduction in elastic and viscous modulus with respect to untreated 3 wt % HBE mucus after treatment for 24 h.^a

Scaffold	% reduction in Elastic Modulus^b	% reduction in Viscous Modulus^b
Alg300	54 ± 4	26 ± 6
Alg10	51 ± 13	42 ± 14
Alg5	73 ± 15	64 ± 21
Alg5-DETA	13 ± 2	14 ± 5
Alg5-DPTA	-8 ± 1	-7 ± 4
Alg5-PAPA-DPTA	14 ± 1	12 ± 1
Alg5-PAPA	14 ± 4	8 ± 3
Alg5-SPER	-17 ± 4	-43 ± 10
Alg1	71 ± 10	77 ± 23
COS	3 ± 1	-49 ± 4
COS-EA	-48 ± 20	-61 ± 40

^aError represents standard deviation for $n \geq 3$ experiments. ^bReduction in both elastic and viscous moduli were calculated from G' (Pa) and G'' (Pa) measured at 10 rad compared to the untreated sample

monomer units and reactive functional groups that would interact with the glycoprotein (Table 3.4).³¹

3.3.3 *Effect of varying functional group and biopolymer charge on mucus.*

In addition to size and chain entanglement, the mucoadhesivity of the biopolymer (impacted most directly by the electrostatic interactions between charged pendant chains of mucins and the polymers) will clearly influence drug diffusion through the mucus layer.⁵¹ Positively charged biopolymers, including chitosan, are generally mucoadhesive, an advantageous property for facilitating localized drug delivery to mucus-coated regions as in the lungs.⁵²⁻⁵⁵ However, studies have also shown that increased mucoadhesivity may promote the formation of polymer-mucin aggregates that, in turn, increase the viscoelastic properties of the mucus layer and limit drug diffusion.⁵³ Neutral and negatively charged polymers (e.g., polyethylene glycol, alginate) reported to exhibit mucus layer penetration are being considered as alternatives for drug delivery in mucus coated regions.^{32,50,53} Amine modification on alginate imparts a positive charge on the biopolymer that could influence its mucoadhesive property. Thus, the impact of these functional groups on the elastic and viscous properties of the mucus might prove equally relevant.

The effect of biopolymer charge was studied after modifying Alg5 with different alkyl amine functional groups (i.e., DETA, DPTA, PAPA, and SPER). The Alg5 systems were selected for this study to allow for a direct comparison with the previously developed NO-releasing chitosan biopolymers with a similar molecular weight. As expected, modification of the alginate backbone with alkyl amine functional groups resulted in a distinct positive charge (Table 3.2), although increases noted in the viscoelastic properties of mucus treated with amine-modified alginates were not statistically significant with respect to the untreated sample (Figure 3.4). Alkyl

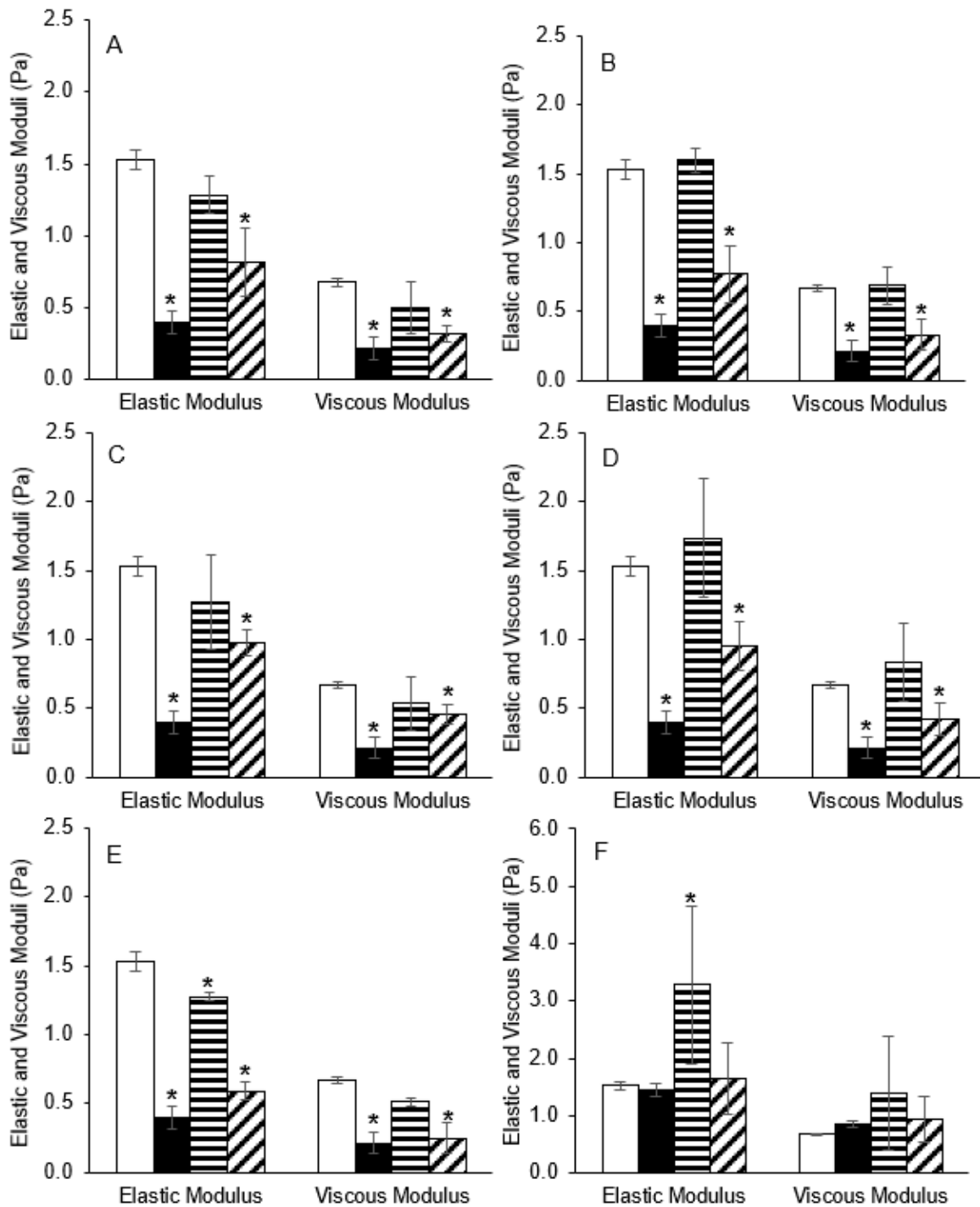


Figure 3.4 Elastic and viscous moduli of 3 wt% human bronchial epithelial (HBE) mucus following treatment with 20 mg/mL unmodified (solid), modified (horizontal stripe), and NO-releasing (diagonal stripe) (A) Alg5-DETA, (B) Alg5-DPTA, (C) Alg5-PAPA, (D) Alg5-SPER, (E) Alg5-PAPA-DPTA, and (F) COS-EA. Values presented as the mean standard error of the mean for $n = 3$ experiments. Asterisks (*) indicate significant differences ($p < 0.05$) relative to untreated sample (hollow).

Table 3.5 Nitric oxide dose and corresponding reduction in elastic and viscous moduli of 3 wt % HBE mucus after treatment with either NO-releasing alginate or chitosan oligosaccharide.^a

Scaffold	NO Dose^b ($\mu\text{mol/mL}$)	% reduction in Elastic Modulus^c	% reduction in Viscous Modulus^c
Alg5-DETA/NO	8 \pm 3	45 \pm 13	45 \pm 8
Alg5-DPTA/NO	8 \pm 2	48 \pm 10	46 \pm 6
Alg5-PAPA-DPTA/NO	11 \pm 1	60 \pm 7	57 \pm 10
Alg5-PAPA/NO	11 \pm 0	34 \pm 4	22 \pm 4
Alg5-SPER/NO	8 \pm 1	36 \pm 7	28 \pm 8
COS-EA/NO	15 \pm 1	-11 \pm 4	-61 \pm 26

^aEach parameter was determined from multiple replicates ($n \geq 3$). ^bNO dose calculated from NO totals in PBS (10 mM, pH 6.5). ^cReduction in both elastic and viscous moduli were calculated from G' (Pa) and G'' (Pa) measured at 10 rad compared to the untreated sample.

amine-modified alginates with a less negative zeta potential (e.g., Alg5-SPER) increased both the mucus elasticity and viscosity (~17 and 43%, respectively; Figure 3.4 and Table 3.4). Negligible changes to the mucus was observed with more negatively charged alginate (i.e., Alg5-PAPA) compared to the reductive effect of the unmodified biopolymer. The increase in both elasticity and viscosity for Alg5-SPER, Alg5-DPTA, Alg5-DETA biopolymers suggests that the addition of amine-based chemical modification resulting in cationic ammonium groups at physiological pH, facilitates interaction with the net negatively charged mucin glycoproteins via electrostatic interactions.^{4,56}

Treatment of mucus with the NO-releasing biopolymers resulted in a decrease in both the elastic (~30-60%) and viscous (~20-60%) moduli, with reductive ability dependent on the NO donor (Table 3.5). Of the different alginate modifications, the hybrid Alg5-PAPA-DPTA/NO biopolymer resulted in the greatest reduction among the different alginate systems (~60% for both elastic and viscous moduli). The enhanced action of the hybrid alginate biopolymers suggests that the mucolytic ability of the alginates depends on both the NO payloads and the NO-release kinetics, with higher NO totals and slower release resulting in greater reduction in the elastic and viscous moduli. While addition of the secondary amine-bearing functional groups counteracts the effect of the alginate biopolymer, the NO release and NO's mucolytic activity influences the mucus to the greatest extent. As such, the results suggest the potential of using alginate biopolymers as an attractive biopolymer for NO storage and delivery through the mucus-coated airways.

Relative to unmodified Alg5, native COS did not significantly change mucus rheology (Figure 3.4). However, the elasticity and viscosity of mucus treated with COS-EA increased by ~40 and 60%, respectively (Table 3.4). These results re-emphasize the effect of biopolymer charge on mucus rheology. In contrast, NO-releasing chitosan decreased both the elastic and viscous

moduli to that of the mucus treated with the unmodified COS. Similarly, Reighard et al. reported a reduction in the size of mucin multimers after treatment with NO-releasing COS compared to treatment with blank buffer or COS controls (non-NO-releasing).²⁰

While the results of this study indicate that NO has potential as a mucolytic agent, the charge of the delivery system may further influence mucus rheology. Interactions between the biopolymer and mucin glycoproteins can enhance NO delivery, as reported for mucoadhesive COS.²⁰ However, electrostatic interactions between highly charged biopolymers and mucin might facilitate unfavorable results (i.e., greater viscoelasticity). For NO-releasing therapeutics, the positive charge of the secondary amine-modified biopolymer has the potential to mitigate NO's effect as a mucolytic by promoting the formation of chitosan-mucin aggregates. The use of a net negatively charged biopolymer, such as alginate, may more favorably act on mucus to improve mucociliary clearance in diseased airways. Of course, such hypothesis must be further evaluated pre-clinically and clinically in human trials.

3.3.4 Effect of nitric oxide-release kinetics

Previous reports demonstrated the importance of NO-release kinetics on the antibacterial activity of macromolecular NO-release systems.²²⁻²⁵ For example, slow and sustained NO-releasing alginate oligosaccharides were proved most favorable for eradicating bacterial biofilms at low (≤ 8 mg/mL) biopolymer concentrations.²⁵ In a similar mode, NO's ability to alter mucus may also depend on NO-release kinetics. To evaluate this hypothesis, mucus samples were treated with equal concentrations (20 mg/mL) of Alg5-DPTA, Alg5-PAPA-DPTA, and Alg5-PAPA biopolymers, selected based on their diverse NO-release kinetics.

As anticipated, the secondary amine-modified oligosaccharides did not alter the viscoelastic properties of the mucus samples regardless of exposure time, with COS-EA being the

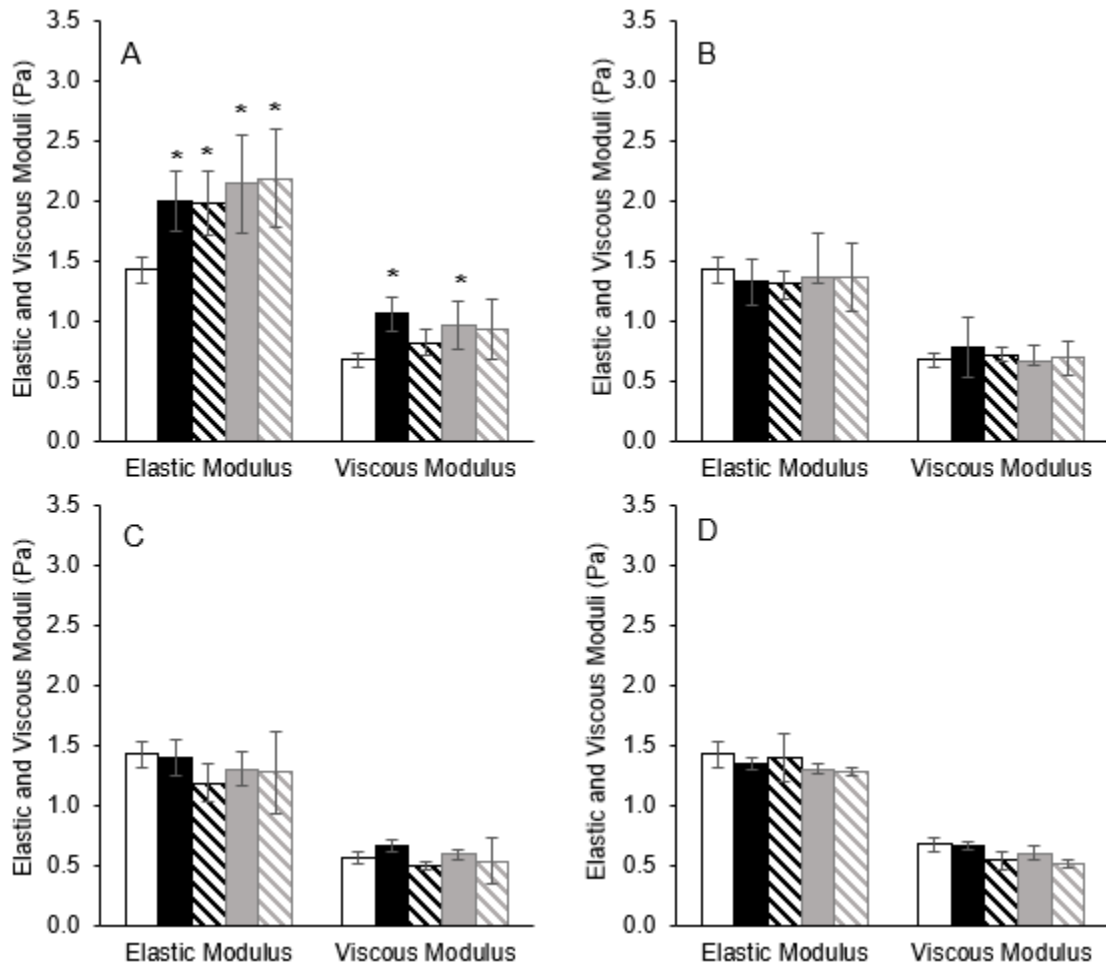


Figure 3.5 Elastic and viscous moduli of 3 wt% HBE mucus following treatment with (A) COS-EA, (B) Alg5-DPTA, (C) Alg5-PAPA, and (D) Alg5-PAPA-DPTA after 1 hour (black solid), 3 hours (black diagonal), 5 hours (gray solid), and 24 hours (gray diagonal) exposure. Asterisks (*) indicate significant differences ($p < 0.05$) relative to untreated sample (hollow).

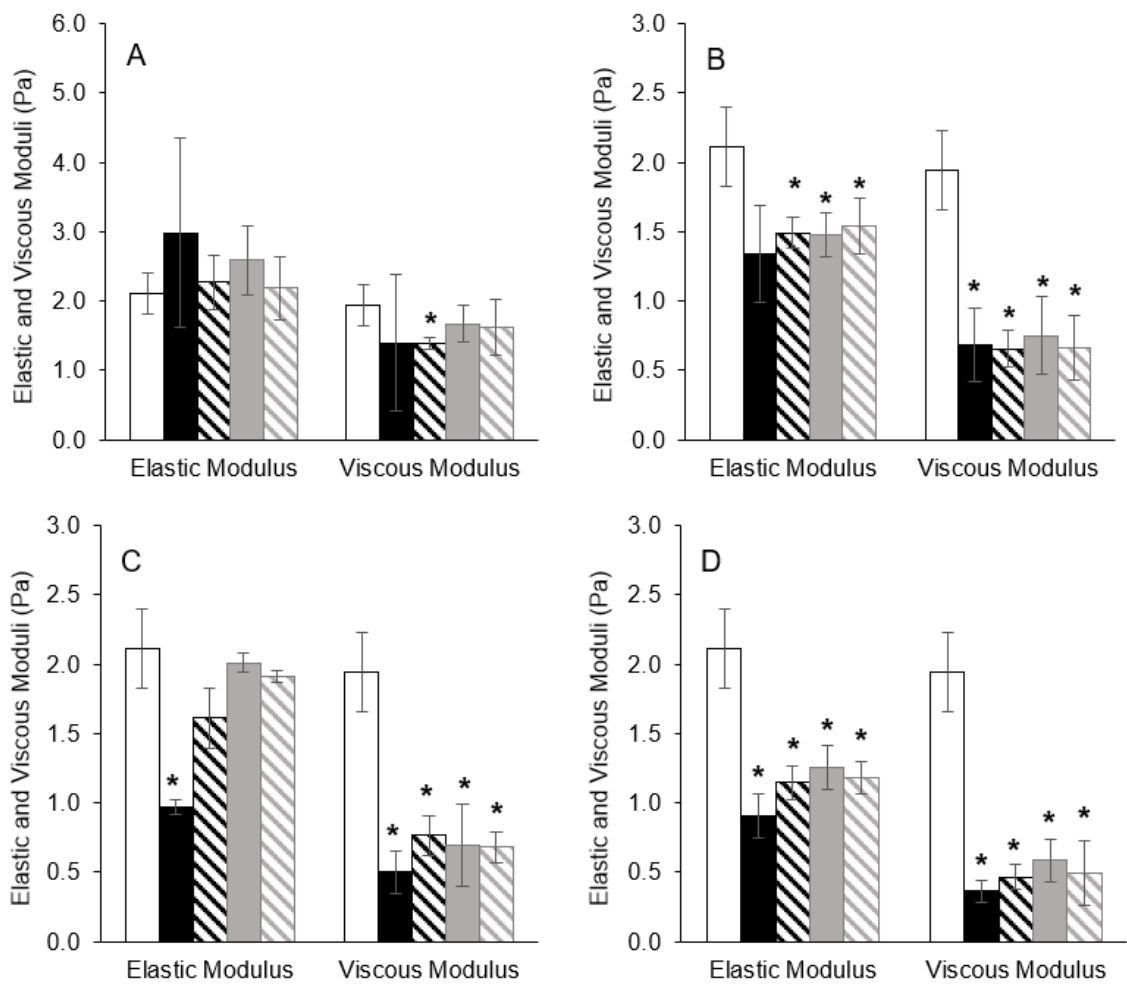


Figure 3.6 Elastic and viscous moduli of 3 wt% HBE mucus following treatment with (A) COS-EA/NO, (B) Alg5-DPTA/NO, (C) Alg5-PAPA/NO, and (D) Alg5-PAPA-DPTA/NO after 1 hour (black solid), 3 hours (black diagonal), 5 hours (gray solid), and 24 hours (gray diagonal) exposure. Asterisks (*) indicate significant differences ($p < 0.05$) relative to untreated sample (hollow).

only exception. Treatment with COS-EA resulted in an increase in the elastic and viscous moduli starting at 1 h (Figure 3.5). The mucus viscoelasticity remained constant even upon treatment with COS-EA/NO, regardless of the exposure time (Figure 3.6), suggesting that treatment with COS-EA/NO has no overall impact on mucus rheology.

The greatest initial reductions in both elasticity and viscosity were observed after 1 h following treatment with the Alg5-PAPA/NO and Alg5-PAPA-DPTA/NO biopolymers (60- 70% and 70-80%, respectively). The large initial NO fluxes characteristic of these materials compared to the slower NO-releasing biopolymers (i.e., Alg5-DPTA/NO and COS-EA/NO), induced mucolysis via delivery of a large NO dose (Table 3.3). However, the faster NO-releasing system (Alg5-PAPA/NO, half-life ~0.1 h) had a depleted NO payload (i.e., NO levels were below the limit of detection of the NOA) at longer exposure times (e.g., 3 and 5 h post exposure), causing the mucus viscoelasticity to return to pre-treatment levels. The biopolymers remained in the mucus sample without NO release capacity with potential for charge-based mucus interactions facilitated by the positively charged Alg5-PAPA and the negatively charged residues of mucin glycoproteins.^{4,56}

In contrast, samples treated with Alg5-PAPA-DPTA/NO did not significantly vary across treatment exposure periods (Figure 3.6). The slower NO-release properties of the hybrid alginate biopolymer enabled by the DPTA modification allowed for near continuous NO release through 5 h (Table 3.3). Even after 24 h, when NO was depleted, the rheological properties of the mucus were comparable to that observed at 1 h, resulting in a significant reduction in viscoelasticity compared to the non-NO-releasing control. Similarly, the slower sustained NO release from Alg5-DPTA/NO (half-life ~0.4 h) maintained the initial reduction in elasticity and viscosity (~50 and 60%, respectively) over the course of the experiment (Figure 3.6). Similar to the controls, no

additional changes were observed up to 24 h once Alg5-DPTA/NO and Alg5-PAPA-DPTA/NO were both depleted of NO. For both Alg5-PAPA-DPTA/NO and Alg5-DPTA/NO, two competing mechanisms occur as NO is released by the biopolymer. Electrostatic interactions between amine groups of the modified alginates can potentially interact with the mucins over the treatment period. However, the release of NO is steady over this same period, thereby acting as a mucolytic. Overall, these results suggest that while a large initial NO flux is favorable for greater reduction in mucus viscoelasticity, slower and more sustained NO release is required to maintain a mucolytic effect over extended exposure periods.

3.3.5 Dose-dependent effects

A range of concentrations using both control and NO-releasing biopolymers were used to treat mucus samples to evaluate dosing effects. The alginate system selected for this study was Alg5-PAPA-DPTA due to its ability to greatly reduce mucus rheology. For comparison, we also evaluated COS-EA at varying concentrations.

Both control and NO-releasing Alg5-PAPA-DPTA biopolymers reduced the rheological moduli of mucus linearly as a function of concentration (Figure 3.7). At the lowest concentration tested (20 mg/mL), Alg5-PAPA-DPTA/NO was able to achieve a greater reduction in elasticity and viscosity (60 and 80 %, respectively) compared to the Alg5-PAPA-DPTA control (~10% for both elastic and viscous moduli), clearly demonstrating the enhanced mucolytic activity with NO. At the greatest concentration (80 mg/mL), the control biopolymer reduced the elasticity and viscosity up to 90 and 80%. The NO-releasing form was able to further decrease these moduli nearly 100%, suggesting an additive effect between the biopolymer and NO for the alginate system that could allow for greatly improved mucociliary clearance in mucus producing respiratory disorders.

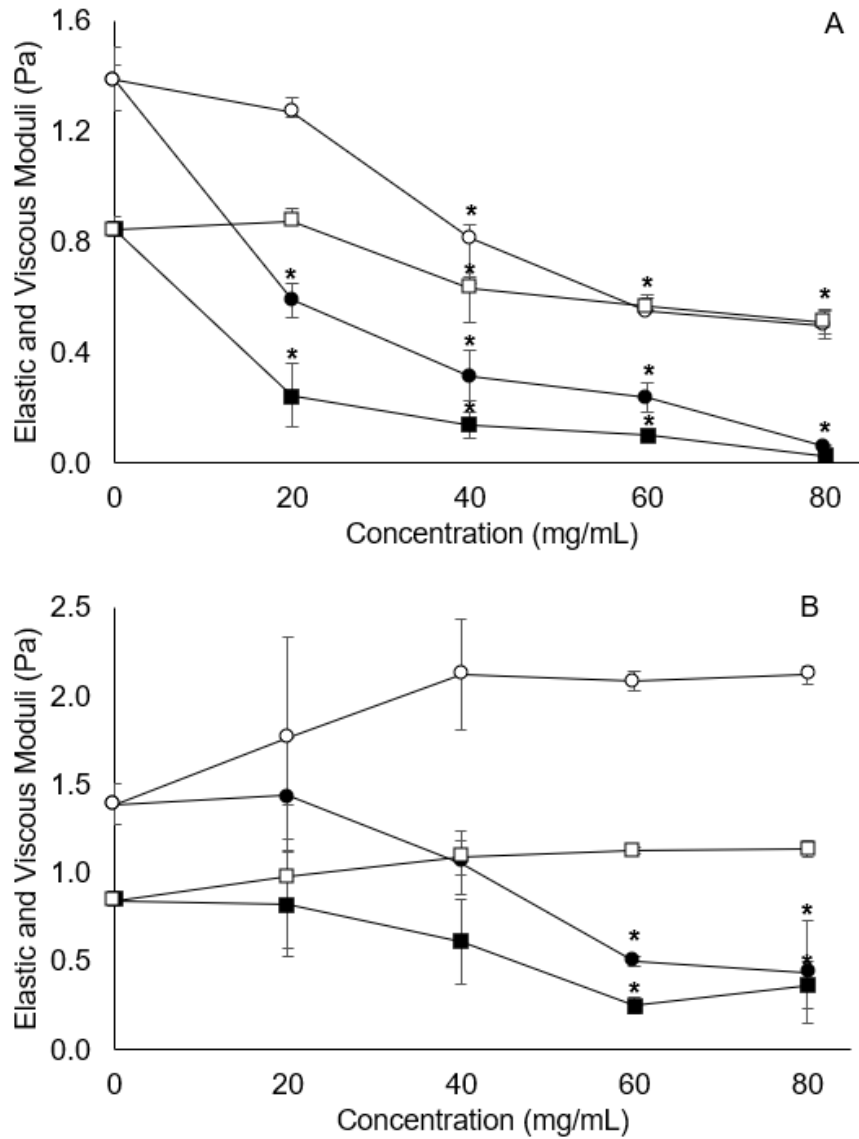


Figure 3.7 Elastic (circle) and viscous (square) moduli of 3 wt% HBE mucus following treatment with 20, 40, 60, and 80 mg/mL concentrations of control (hollow) and NO-releasing (solid) (A) Alg5-PAPA-DPTA and (B) COS-EA.

Treatment of mucus with COS-EA controls showed an increase in both elasticity and viscosity from 20-40 mg/mL, but then less effect above 40 mg/mL (Figure 3.7). Previous reports have indicated that COS concentrations above 4.5 mg/mg mucin (i.e., the COS to mucin ratio at 40 mg/mL) lead to disaggregated chitosan-mucin complexes.^{20,46} Imparting NO-release capabilities minimized the impact of chitosan's attractive interaction with mucus at lower concentrations (i.e., 20-40 mg/mL). At concentrations greater than 40 mg/mL, the NO-releasing COS-EA reduced the mucus elasticity and viscosity up to 70 and 80%, respectively (Figure 3.7). These results suggest that at larger COS-EA/NO concentrations, NO overcomes the electrostatic effects between the positively charged chitosan biopolymer and negatively charged mucin glycoproteins, resulting in a therapeutic action similar to that of the NO-releasing alginate systems. Regardless, the additive effect of the alginate biopolymer with NO at increasing doses, combined with the lower concentrations required to achieve substantial reduction in mucus rheology demonstrates an advantage for NO-releasing alginates over chitosan oligosaccharides with respect to mucolytic action.

3.3.6 Efficacy compared to *N*-acetyl cysteine (NAC)

While the mucolytic action of NO-releasing alginate materials was demonstrated, a comparison of relative efficacy with conventional mucolytic drugs such as *N*-acetylcysteine (NAC) is necessary to fully evaluate its potential as a therapeutic.⁵⁷⁻⁶⁰ For this work, the effect of NAC on mucus rheology was evaluated at comparable doses to the lowest NO dose delivered by the oligosaccharide biopolymers (1-2 mg/mL or 8-16 μ mol/mL NAC) and currently nebulized therapeutic doses (100-200 mg/mL or 613-1220 μ mol/mL NAC).^{57,58,60} At equivalent doses to NO, NAC reduced the mucus elasticity by ~2-8%, which is minimal compared to that observed using any of the NO-releasing alginate systems (~40-60%; Table 3.6). At the inhaled therapeutic dose

Table 3.6 Reduction in elastic and viscous moduli of 3 wt % HBE mucus after treatment with *N*-acetylcysteine (NAC).^a

Sample	Drug Dose ($\mu\text{mol/mL}$)	% reduction in Elastic Modulus^b	% reduction in Viscous Modulus^b
NAC 0.1 wt%	8	2 ± 1	2 ± 1
NAC 0.2 wt %	16	8 ± 2	-23 ± 7
NAC 10 wt %	613	41 ± 3	-39 ± 4
NAC 20 wt %	1220	44 ± 4	-38 ± 12

^aEach parameter was determined from multiple replicates ($n \geq 3$). ^bReduction in both elastic and viscous moduli were calculated from G' (Pa) and G'' (Pa) measured at 10 rad compared to the untreated sample.

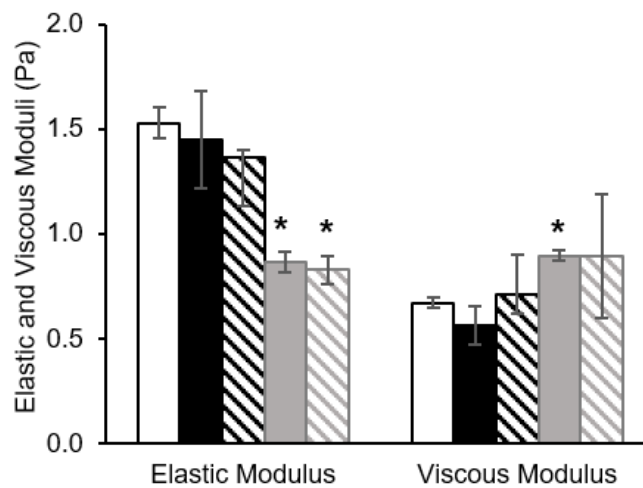


Figure 3.8 Elastic and viscous moduli of 3 wt% HBE mucus following treatment with NAC at 0.1 wt% (black solid), 0.2 wt % (black diagonal), 10 wt % (gray solid), and 20 wt% (gray diagonal). Values presented as the mean standard error of the mean for $n = 3$ experiments. Asterisks (*) indicate significant differences ($p < 0.05$) relative to untreated sample (hollow).

of NAC, the small molecule mucolytic reduced mucus elasticity at an equivalent level to the lowest concentration of alginate (~40%) but at the expense of increasing viscosity (Figure 3.8). As a mucolytic, NAC reduces disulfide bonds of high molecular weight mucins (resulting in sulfhydryl groups).^{61,62} We hypothesize that the thiol-bearing small molecule at high concentrations may cause undesirable entanglement within the mucin network through interactions with the mucin disulfide bonds (i.e., inducing both inter- and intra- mucin disulfide bond formation), resulting in greater viscosity over the 24-h exposure period.^{4,56} Despite an overall positive effect on mucus viscoelasticity (Figure A5), the result of this study indicates that above a threshold NAC concentration, the mucolytic action becomes limited (i.e., increased viscosity despite decreasing elasticity), leading to no discernable change with respect to the untreated sample. The opposite appears true for the NO-releasing alginates. Indeed, the mucolytic action of both control and NO-releasing alginate is dose dependent. Moreover, lower NO-releasing alginate concentrations are needed to exhibit the same reductive effect as that of high concentrations of NAC. Combined with the previously reported antibacterial properties of the NO-releasing alginates,²⁵ the results of this study highlight the potential utility of these materials as dual-action therapeutic agents for the treatment of chronic respiratory diseases such as cystic fibrosis.

3.4 Conclusions

Low molecular weight (5 kDa) alginate oligosaccharides having high initial NO fluxes and sustained NO-release (e.g., Alg5-PAPA-DPTA/NO) greatly reduced both the elasticity and viscosity of mucus, suggesting a high potential utility for improving mucociliary clearance in diseased lungs. Regardless of chemical modifications, each alginate biopolymer investigated was more efficacious relative to the cationic biopolymer chitosan, indicating that a negatively charged

scaffold is beneficial for reducing mucus viscoelasticity. As the NO-releasing dose of the alginate oligosaccharides required is even lower than that of current standard of care mucolytic agents (NAC) and the levels of NO released are antibacterial,²⁴ this work highlights the utility of NO-releasing alginates as a highly unique therapeutic agent for treating chronic respiratory diseases such as cystic fibrosis. While the exact mechanism through which NO alters the rheological properties is yet to be elucidated, the results present herein suggest the addition of NO increases the mucolytic potency of our scaffolds.

REFERENCES

- (1) Cohn, L. Mucus in Chronic Airway Diseases: Sorting out the Sticky Details. *J. Clin. Invest.* **2006**, *116*, 306–308.
- (2) Shale, D. J.; Ionescu, A. A. Mucus Hypersecretion: A Common Symptom, a Common Mechanism? *Eur. Respir. J.* **2004**, *23*, 797–798.
- (3) Rogers, D. F.; Barnes, P. J. Treatment of Airway Mucus Hypersecretion. *Ann. Med.* **2006**, *38*, 116–125.
- (4) Bansil, R.; Turner, B. S. Mucin Structure, Aggregation, Physiological Functions and Biomedical Applications. *Curr. Opin. Colloid Interface Sci.* **2006**, *11*, 164–170.
- (5) Lai, S. K.; Wang, Y. Y.; Wirtz, D.; Hanes, J. Micro- and Macrorheology of Mucus. *Adv. Drug Deliv. Rev.* **2009**, *61*, 86–100.
- (6) Pritchard, M. F.; Powell, L. C.; Menzies, G. E.; Lewis, P. D.; Hawkins, K.; Wright, C.; Doull, I.; Walsh, T. R.; Onsøyen, E.; Dessen, A.; et al. A New Class of Safe Oligosaccharide Polymer Therapy to Modify the Mucus Barrier of Chronic Respiratory Disease. *Mol. Pharm.* **2016**, *13*, 863–873.
- (7) Hassett, D. J.; Cuppoletti, J.; Trapnell, B.; Lyman, S. V.; Rowe, J. J.; Sun Yoon, S.; Hilliard, G. M.; Parvatiyar, K.; Kamani, M. C.; Wozniak, D. J.; et al. Anaerobic Metabolism and Quorum Sensing by *Pseudomonas Aeruginosa* Biofilms in Chronically Infected Cystic Fibrosis Airways: Rethinking Antibiotic Treatment Strategies and Drug Targets. *Adv. Drug Deliv. Rev.* **2002**, *54*, 1425–1443.
- (8) Reighard, K. P.; Hill, D. B.; Dixon, G. A.; Worley, B. V.; Schoenfisch, M. H. Disruption and Eradication of *P. Aeruginosa* Biofilms Using Nitric Oxide-Releasing Chitosan Oligosaccharides. *Biofouling* **2015**, *31*, 775–787.
- (9) Reighard, K. P.; Schoenfisch, M. H. Antibacterial Action of Nitric Oxide-Releasing Chitosan Oligosaccharides against *Pseudomonas Aeruginosa* under Aerobic and Anaerobic Conditions. *Antimicrob. Agents Chemother.* **2015**, *59*, 6506–6513.
- (10) Lu, Y.; Slomberg, D. L.; Schoenfisch, M. H. Nitric Oxide-Releasing Chitosan Oligosaccharides as Antibacterial Agents. *Biomaterials* **2014**, *35*, 1716–1724.
- (11) Lu, Y.; Shah, A.; Hunter, R. A.; Soto, R. J.; Schoenfisch, M. H. S-Nitrosothiol-Modified Nitric Oxide-Releasing Chitosan Oligosaccharides as Antibacterial Agents. *Acta Biomater.* **2015**, *12*, 62–69.
- (12) Miller, C.; McMullin, B.; Ghaffari, A.; Stenzler, A.; Pick, N.; Roscoe, D.; Ghahary, A.; Road, J.; Av-Gay, Y. Gaseous Nitric Oxide Bactericidal Activity Retained during Intermittent High-Dose Short Duration Exposure. *Nitric Oxide* **2009**, *20*, 16–23.
- (13) Sadrearhami, Z.; Yeow, J.; Nguyen, T.-K.; Ho, K. K. K.; Kumar, N.; Boyer, C. Biofilm Dispersal Using Nitric Oxide Loaded Nanoparticles Fabricated by Photo-PISA: Influence of Morphology. *Chem. Commun.* **2017**, *53*, 12894–12897.

- (14) Brisbois, E. J.; Bayliss, J.; Wu, J.; Major, T. C.; Xi, C.; Wang, S. C.; Bartlett, R. H.; Handa, H.; Meyerhoff, M. E. Optimized Polymeric Film-Based Nitric Oxide Delivery Inhibits Bacterial Growth in a Mouse Burn Wound Model. *Acta Biomater.* **2014**, *10*, 4136–4142.
- (15) Hetrick, E. M.; Shin, J. H.; Paul, H. S.; Schoenfisch, M. H. Anti-Biofilm Efficacy of Nitric Oxide-Releasing Silica Nanoparticles. *Biomaterials* **2009**, *30*, 2782–2789.
- (16) Hetrick, E. M.; Shin, J. H.; Stasko, N. A.; Johnson, C. B.; Wespe, D. A.; Holmuhamedov, E.; Schoenfisch, M. H. Bactericidal Efficacy of Nitric Oxide-Releasing Silica Nanoparticles. *ACS Nano* **2008**, *2*, 235–246.
- (17) Privett, B. J.; Broadnax, A. D.; Bauman, S. J.; Riccio, D. A.; Schoenfisch, M. H. Examination of Bacterial Resistance to Exogenous Nitric Oxide. *Nitric Oxide* **2012**, *26*, 169–173.
- (18) Riccio, D. A.; Schoenfisch, M. H. Nitric Oxide Release: Part I. Macromolecular Scaffolds. *Chem. Soc. Rev.* **2012**, *41*, 3731–3741.
- (19) Carpenter, A. W.; Schoenfisch, M. H. Nitric Oxide Release: Part II. Therapeutic Applications. *Chem. Soc. Rev.* **2012**, *41*, 3742–3752.
- (20) Reighard, K. P.; Ehre, C.; Rushton, Z. L.; Ahonen, M. J. R.; Hill, D. B.; Schoenfisch, M. H. Role of Nitric Oxide-Releasing Chitosan Oligosaccharides on Mucus Viscoelasticity. *ACS Biomater. Sci. Eng.* **2017**, *3*, 1017–1026.
- (21) Garland, A. L.; Walton, W. G.; Coakley, R. D.; Tan, C. D.; Gilmore, R. C.; Hobbs, C. A.; Tripathy, A.; Clunes, L. A.; Bencharit, S.; Stutts, M. J.; et al. Molecular Basis for PH-Dependent Mucosal Dehydration in Cystic Fibrosis Airways. *Proc. Natl. Acad. Sci.* **2013**, *110*, 15973–15978.
- (22) Worley, B. V.; Schilly, K. M.; Schoenfisch, M. H. Anti-Biofilm Efficacy of Dual-Action Nitric Oxide-Releasing Alkyl Chain Modified Poly(Amidoamine) Dendrimers. *Mol. Pharm.* **2015**, *12*, 1573–1583.
- (23) Backlund, C. J.; Worley, B. V.; Sergesketter, A. R.; Schoenfisch, M. H. Kinetic-Dependent Killing of Oral Pathogens with Nitric Oxide. *J. Dent. Res.* **2015**, *94*, 1092–1098.
- (24) Slomberg, D. L.; Lu, Y.; Broadnax, A. D.; Hunter, R. A.; Carpenter, A. W.; Schoenfisch, M. H. Role of Size and Shape on Biofilm Eradication for Nitric Oxide-Releasing Silica Nanoparticles. *ACS Appl. Mater. Interfaces* **2013**, *5*, 9322–9329.
- (25) Ahonen, M. J. R.; Suchyta, D. J.; Zhu, H.; Schoenfisch, M. H. Nitric Oxide-Releasing Alginates. *Biomacromolecules* **2018**, *19*, 1189–1197.
- (26) Nair, L. S.; Laurencin, C. T. Biodegradable Polymers as Biomaterials. *Prog. Polym. Sci.* **2007**, *32*, 762–798.
- (27) Alnaief, M.; Alzaitoun, M. A.; Garcia-Gonzalez, C. A.; Smirnova, I. Preparation of Biodegradable Nanoporous Microspherical Aerogel Based on Alginate. *Carbohydr. Polym.* **2011**, *84*, 1011–1018.
- (28) Draget, K. I.; Taylor, C. Chemical, Physical and Biological Properties of Alginates and Their Biomedical Implications. *Food Hydrocoll.* **2011**, *25*, 251–256.
- (29) Sun, J.; Tan, H. Alginate-Based Biomaterials for Regenerative Medicine Applications.

Materials. **2013**, *6*, 1285–1309.

(30) Lee, K. Y.; Mooney, D. J. Alginate: Properties and Biomedical Applications. *Prog. Polym. Sci.* **2012**, *37*, 106–126.

(31) Nordgård, C. T.; Draget, K. I. Oligosaccharides as Modulators of Rheology in Complex Mucous Systems. *Biomacromolecules* **2011**, *12*, 3084–3090.

(32) Nordgård, C. T.; Nonstad, U.; Olderø, M. Ø.; Espevik, T.; Draget, K. I. Alterations in Mucus Barrier Function and Matrix Structure Induced by Gyluronate Oligomers. *Biomacromolecules* **2014**, *15*, 2294–2300.

(33) Sletmoen, M.; Maurstad, G.; Nordgård, C. T.; Draget, K. I.; Stokke, B. T. Oligogyluronate Induced Competitive Displacement of Mucin-Alginate Interactions: Relevance for Mucolytic Function. *Soft Matter* **2011**, *8*, 8413–8421.

(34) Tsutsumi, N.; Itoh, T.; Ohsawa, A. Cleavage of S-S Bond by Nitric Oxide (NO) in the Presence of Oxygen: A Disproportionation Reaction of Two Disulfides. *Chem. Pharm. Bull. Tokyo* **2000**, *48*, 1524–1528.

(35) Mao, S.; Zhang, T.; Sun, W.; Ren, X. The Depolymerization of Sodium Alginate by Oxidative Degradation. *Pharm. Dev. Technol.* **2012**, *17*, 763–769.

(36) Hetrick, E. M.; Schoenfisch, M. H. Analytical Chemistry of Nitric Oxide. *Annu. Rev. Anal. Chem.* **2009**, *2*, 409–433.

(37) Coneski, P. N.; Schoenfisch, M. H. Nitric Oxide Release Part III. Measurement and Reporting. *Chem. Soc. Rev.* **2012**, *41*, 3753–3758.

(38) Fulcher, M. L.; Randell, S. H. Human Nasal and Tracheo-Bronchial Respiratory Epithelial Cell Culture BT - Epithelial Cell Culture Protocols: Second Edition; Randell, S. H., Fulcher, M. L., Eds.; Humana Press: Totowa, NJ, 2013; pp 109–121.

(39) Hill, D. B.; Button, B. Establishment of Respiratory Air–Liquid Interface Cultures and Their Use in Studying Mucin Production, Secretion, and Function BT - Mucins: Methods and Protocols; McGuckin, M. A., Thornton, D. J., Eds.; Humana Press: Totowa, NJ, 2012; pp 245–258.

(40) Hill, D. B.; Vasquez, P. A.; Mellnik, J.; McKinley, S. A.; Vose, A.; Mu, F.; Henderson, A. G.; Donaldson, S. H.; Alexis, N. E.; Boucher, R. C.; et al. A Biophysical Basis for Mucus Solids Concentration as a Candidate Biomarker for Airways Disease. *PLoS One* **2014**, *9*, e87681.

(41) Seagrave, J.; Albrecht, H. H.; Hill, D. B.; Rogers, D. F.; Solomon, G. Effects of Guaifenesin, N-Acetylcysteine, and Ambroxol on MUC5AC and Mucociliary Transport in Primary Differentiated Human Tracheal-Bronchial Cells. *Respir. Res.* **2012**, *13*, 98.

(42) Keefer, L. K.; Nims, R. W.; Davies, K. M.; Wink, D. A. Diazeniumdiolates as NO Dosage Forms. *Methods Enzymol.* **1996**, *268*, 281–293.

(43) Lutzke, A.; Pegalajar-Jurado, A.; Neufeld, B. H.; Reynolds, M. M. Nitric Oxide-Releasing S-Nitrosated Derivatives of Chitin and Chitosan for Biomedical Applications. *J. Mater. Chem. B* **2014**, *2*, 7449–7458.

- (44) Damodaran, V. B.; Reynolds, M. M. Biodegradable S-Nitrosothiol Tethered Multiblock Polymer for Nitric Oxide Delivery. *J. Mater. Chem.* **2011**, *21*, 5870–5872.
- (45) Wold, K. A.; Damodaran, V. B.; Suazo, L. A.; Bowen, R. A.; Reynolds, M. M. Fabrication of Biodegradable Polymeric Nanofibers with Covalently Attached NO Donors. *ACS Appl. Mater. Interfaces* **2012**, *4*, 3022–3030.
- (46) Sogias, I. A.; Williams, A. C.; Khutoryanskiy, V. V. Why Is Chitosan Mucoadhesive? *Biomacromolecules* **2008**, *9*, 1837–1842.
- (47) Dash, M.; Chiellini, F.; Ottenbrite, R. M.; Chiellini, E. Chitosan—A Versatile Semi-Synthetic Polymer in Biomedical Applications. *Prog. Polym. Sci.* **2011**, *36*, 981–1014.
- (48) George, M.; Abraham, T. E. Polyionic Hydrocolloids for the Intestinal Delivery of Protein Drugs: Alginate and Chitosan — a Review. *J. Control. Release* **2006**, *114*, 1–14.
- (49) Draget, K. I.; Skjåk Bræk, G.; Smidsrød, O. Alginic Acid Gels: The Effect of Alginate Chemical Composition and Molecular Weight. *Carbohydr. Polym.* **1994**, *25*, 31–38.
- (50) Wang, Y.; Lai, S. K.; Suk, J. S.; Pace, A.; Cone, R.; Hanes, J. Addressing the PEG Mucoadhesivity Paradox to Engineer Nanoparticles That “Slip” through the Human Mucus Barrier. *Angew. Chemie Int. Ed.* **2008**, *47*, 9726–9729.
- (51) Andrews, G. P.; Laverty, T. P.; Jones, D. S. Mucoadhesive Polymeric Platforms for Controlled Drug Delivery. *Eur. J. Pharm. Biopharm.* **2009**, *71*, 505–518.
- (52) Grenha, A.; Al-Qadi, S.; Seijo, B.; Remuñán-López, C. The Potential of Chitosan for Pulmonary Drug Delivery. *J. Drug Deliv. Sci. Technol.* **2010**, *20*, 33–43.
- (53) Klinger-Strobel, M.; Lautenschläger, C.; Fischer, D.; Mainz, J. G.; Bruns, T.; Tuchscher, L.; Pletz, M. W.; Makarewicz, O. Aspects of Pulmonary Drug Delivery Strategies for Infections in Cystic Fibrosis – Where Do We Stand? *Expert Opin. Drug Deliv.* **2015**, *12*, 1351–1374.
- (54) Jain, D.; Bar-Shalom, D. Alginate Drug Delivery Systems: Application in Context of Pharmaceutical and Biomedical Research. *Drug Dev. Ind. Pharm.* **2014**, *40*, 1576–1584.
- (55) Park, J. H.; Jin, H. E.; Kim, D. D.; Chung, S. J.; Shim, W. S.; Shim, C. K. Chitosan Microspheres as an Alveolar Macrophage Delivery System of Ofloxacin via Pulmonary Inhalation. *Int. J. Pharm.* **2013**, *441*, 562–569.
- (56) Lieleg, O.; Vladescu, I.; Ribbeck, K. Characterization of Particle Translocation through Mucin Hydrogels. *Biophys. J.* **2010**, *98*, 1782–1789.
- (57) Rodríguez-Beltrán, J.; Cabot, G.; Valencia, E. Y.; Costas, C.; Bou, G.; Oliver, A.; Blázquez, J. N-Acetylcysteine Selectively Antagonizes the Activity of Imipenem in *Pseudomonas Aeruginosa* by an OprD-Mediated Mechanism. *Antimicrob. Agents Chemother.* **2015**, *59*, 3246–3251.
- (58) Szkudlarek, U.; Zdziechowski, A.; Witkowski, K.; Kasielski, M.; Luczyńska, M.; Luczyński, R.; Sarniak, A.; Nowak, D. Effect of Inhaled N-Acetylcysteine on Hydrogen Peroxide Exhalation in Healthy Subjects. *Pulm. Pharmacol. Ther.* **2004**, *17*, 155–162.
- (59) Johnson, K.; McEvoy, C. E.; Naqvi, S.; Wendt, C.; Reilkoff, R. A.; Kunisaki, K. M.;

Wetherbee, E. E.; Nelson, D.; Tirouvanziam, R.; Niewoehner, D. E. High-Dose Oral N-Acetylcysteine Fails to Improve Respiratory Health Status in Patients with Chronic Obstructive Pulmonary Disease and Chronic Bronchitis: A Randomized, Placebo-Controlled Trial. *Int. J. Chron. Obstruct. Pulmon. Dis.* **2016**, *11*, 799–807.

(60) Dube, K. M.; Ditch, K. L.; Hills, L. Use of Nebulized Heparin, Nebulized N-Acetylcysteine, and Nebulized Epoprostenol in a Patient With Smoke Inhalational Injury and Acute Respiratory Distress Syndrome. *J. Pharm. Pract.* **2016**, *30*, 663–667.

(61) Perez-Vilar, J.; Boucher, R. C. Reevaluating Gel-Forming Mucins' Roles in Cystic Fibrosis Lung Disease. *Free Radic. Biol. Med.* **2004**, *37*, 1564–1577.

(62) Henke, M. O.; Ratjen, F. Mucolytics in Cystic Fibrosis. *Paediatr. Respir. Rev.* **2007**, *8*, 24–29.

CHAPTER 4: ANTIBIOFILM EFFICACY OF NITRIC OXIDE-RELEASING ALGINATES AGAINST CYSTIC FIBROSIS BACTERIAL PATHOGENS

4.1 Introduction

Cystic fibrosis (CF) is an autosomal disease caused by mutations in the cystic fibrosis transmembrane conductance regulator (CFTR) gene. These mutations cause a deficiency in chloride secretion from the epithelial cells in the airways and ultimately interfere with the mucociliary clearance of inhaled microorganisms.^{1,2} As a result, a thick stagnant mucus layer accumulates, obstructing airways in the CF lung. Nutrients in the mucus foster a suitable environment for the colonization of bacterial pathogens. As the mucus layer thickens, it protects the bacteria from antibiotic treatments.^{3,4} Bacterial biofilms are cooperative communities of bacteria encapsulated by a self-secreted exopolysaccharide matrix that provides additional protection from the host immune response and antibiotics. These combined protective mechanisms further complicate efforts to eradicate pathogens, even in the age of antibiotics.^{3,4} Additionally, the efficacy of antibiotics are minimized by the altered microenvironments in biofilms (e.g., lower oxygen concentrations, nutrient depletion) and slower bacterial metabolism.⁵⁻⁹ Persistent colonization of multiple pathogens, including *Pseudomonas aeruginosa*, *Burkholderia cepacia* complex (BCC), *Staphylococcus aureus*, and methicillin-resistant *S. aureus* (MRSA), elicits a chronic inflammatory response that ultimately degrade lung function to the point of respiratory failure.⁹⁻¹² The need for non-conventional antibacterial agents to eradicate biofilm-based bacteria is great.¹³⁻¹⁵

Nitric oxide (NO) is an endogenously produced broad-spectrum antibacterial free radical capable of eradicating both planktonic bacteria and biofilms. Nitric oxide and its reactive byproducts (e.g., peroxynitrite and dinitrogen trioxide) chemically alter bacterial proteins, DNA, and metabolic enzymes, disrupting vital cellular functions and structures to induce killing.^{16–19} While early studies demonstrated the efficacy of NO as an antibacterial agent via direct gaseous administration, the therapeutic utility of inhaled gas is limited by NO's high reactivity and short lifetime in biological media, and the hazards associated with high pressure gas cylinders.¹⁷ The use of NO donors (e.g., *N*-diazoniumdiolates) for NO storage and triggered release under physiological conditions (pH 7.4, 37 °C) is an alternative to direct inhalation.^{16,17} *N*-diazoniumdiolates undergo proton-initiated decomposition, with NO-release kinetics controlled by factors such as pH, temperature, and the chemical structure of the precursor amine. Unfortunately, the utility of small molecule *N*-diazoniumdiolate NO donors is limited by the toxicity of the precursor structure when larger NO payloads are required.^{16,17,20} This shortcoming has been addressed through the development of macromolecular scaffolds with tunable NO release capabilities. These NO donors facilitate better control over NO-release kinetics and enhanced bacterial killing (i.e., require lower scaffold concentrations).^{16,17,20,21}

Inhalation of NO-releasing macromolecular biopolymers may represent an attractive therapeutic strategy because of extended NO release durations (i.e., several hours), allowing for expanded NO delivery via intermittent (once or twice daily) treatment. Alginate, a biopolymer composed of 1,4-linked α -l-guluronic acid (G) and β -d-mannuronic acid (M) units,^{22–24} holds particular promise as a macromolecular NO donor system for inhalation applications due to its favorable biocompatibility and unprecedented water solubility.^{22,25–28} Recent studies have demonstrated the ability of low molecular weight alginate oligosaccharides to potentiate the

antibacterial efficacy of conventional antibiotics by altering biofilm morphology and mucin assembly, reducing mucus viscoelasticity and enhancing (antibiotic) delivery.^{23,29–31}

Herein, we report on the antibiofilm action of NO-releasing alginate oligosaccharides against multiple CF-relevant pathogens.^{10,32–34} Selection of specific NO donor precursors to modify the alginate allowed for tunable NO-release properties (e.g., total NO payload, NO-release half-lives).^{35–37} As pathogens are able to genetically adapt to the hypoxic or anaerobic conditions in the CF lung microenvironment, allowing it to develop resistance against conventionally used antibiotics, the efficacy of the NO-releasing alginates were tested against biofilms grown under aerobic (with oxygen) and anaerobic (little to no oxygen) conditions.⁴ The effect of NO release on antibacterial action was examined as a function of alginate biopolymer chemical modification. Bactericidal activity of the NO-releasing alginates was also compared to tobramycin and vancomycin, two antibiotics commonly used for the treatment of infections in CF, to assess therapeutic potential relative to current standard of care practice.

4.2 Experimental Section

4.2.1 Materials

Alginic acid sodium salt from brown algae (low viscosity), bis(3-aminopropyl)amine (DPTA), diethylenetriamine (DETA), *N*-propyl-1,3-propanediamine (PAPA), spermine (SPER), 1-ethyl-3-(3-dimethylaminopropyl)carbodiimide hydrochloride (EDC), *N*-hydroxysuccinimide (NHS), casamino acids, tobramycin, vancomycin hydrochloride, and pig gastric mucin (PGM) type II were purchased from Sigma-Aldrich (St. Louis, MO). Deoxyribonucleic acid (DNA) sodium salt, egg yolk enrichment, and common laboratory salts and solvents were purchased from Fischer Scientific (Fair Lawn, NJ). Unless otherwise specified, all chemicals were used as received

without further purification. Argon (Ar), carbon dioxide (CO₂), nitrogen (N₂), nitric oxide (NO) calibration (25.87 ppm balance N₂), and pure NO (99.5%) gas cylinders were purchased from Airgas National Welders (Raleigh, NC). Distilled water was purified to a resistivity of 18.2 MΩ•cm and a total organic content of ≤6 ppb using a Millipore Milli-Q UV Gradient A10 System (Bedford, MA).

4.2.2 Bacterial strains and media

The laboratory *Pseudomonas aeruginosa* strain K (PAK) and the *Burkholderia cepacia* complex (BCC) clinical strain were a gift from Matthew Wolfgang from the Department of Microbiology and Immunology at the University of North Carolina at Chapel Hill (Chapel Hill, NC). *Staphylococcus aureus* (ATCC #29213) and methicillin-resistant *S. aureus* (MRSA; ATCC #33591) were obtained from American Type Tissue Culture Collection (Manassas, VA). Luria-Bertani (LB) broth and Tryptic Soy Agar (TSA) plates were obtained from Becton, Dickinson, and Company (Franklin Lakes, NJ). Artificial sputum media (ASM) was prepared following a previously published protocol.^{3,38} Briefly, DNA (4 g), pig gastric mucin type II (5 g), casamino acids (5 g), diethylenetriaminepentaacetic acid (DTPA; 5.9 mg), sodium chloride (NaCl; 5 g), and potassium chloride (KCl; 2.2 g) were dissolved in 800 mL of sterile water. A 5-mL aliquot of egg yolk emulsion was added to the resulting solution as a source of lecithin. The pH of the solution was adjusted to 6.5 with 1 M Tris (pH 8.5) and the volume brought up to 1 L with sterile water before being sterilized via filtration using Millipore Steritop filter units (Burlington, MA). The filtered ASM was stored in the dark at 4 °C with each stock solution used within a month. For anaerobic growth, ASM was supplemented with 150 mM potassium nitrate (KNO₃).³⁹

4.2.3 Instrumentation

^1H and ^{13}C nuclear magnetic resonance (NMR) spectra were recorded on a Bruker (600 MHz) spectrometer. A PerkinElmer Elemental Analyzer Series 2400 Instrument (Waltham, MA) was used for elemental (carbon, hydrogen, and nitrogen; CHN) analysis. Zeta potential measurements were taken in phosphate buffer (10 mM PB; pH 6.5) using a Zetasizer Nano (Malvern Instruments, UK). Gel permeation chromatography (GPC) measurements were carried out in 0.1 M sodium nitrate (NaNO_3) using an aqueous GPC system equipped with a Waters 2414 refractive index detector (Milford, MA) coupled to a Wyatt miniDawn TREOS multi-angle light scattering detector (Santa Barbara, CA).

4.2.4 Oxidative degradation of alginate

High molecular weight alginate biopolymers were degraded to lower molecular weight oligosaccharides following previously published protocols.^{37,40} Briefly, the biopolymer (2.5 g) was dissolved in 15 wt% hydrogen peroxide (50 mL) and stirred in an oil bath for 1 h at 80 °C. The resulting solution was filtered to remove insoluble material. The alginate oligosaccharides were collected and washed copiously with ethanol before drying in vacuo to yield a white powder.

4.2.5 Synthesis of polyamine-modified alginates (AlgMW-alkyl amine)

Monofunctional alginate materials used in this study were modified with diethylenetriamine (DETA), bis(3-aminopropyl)amine (DPTA), *N*-propyl-1,3-propanediamine (PAPA), or spermine (SPER) following a previously published protocol.³⁷ Briefly, alginate (100 mg) was dissolved in 10 mL phosphate buffered saline (PBS; 10 mM, pH 6.5) with a 2:1 molar ratio of 1-ethyl-3-(3-dimethylaminopropyl)carbodiimide hydrochloride (EDC) and a 2:1 molar ratio of *N*-hydroxysuccinimide (NHS) with respect to the carboxylic acid moieties of alginates.

The reaction was left to stir for 1 h. After 1 h, a 4:1 molar ratio of the alkyl amine with respect to the carboxylic acid groups of the alginates was added dropwise to the mixture. The reaction was allowed to proceed for 24 h at room temperature under constant stirring. The amine-modified alginates were precipitated in methanol and collected via centrifugation, washed twice with methanol, and dried in vacuo to yield a white solid for each modification. A hybrid system modified with PAPA and DPTA functional groups was also synthesized following the same procedure, with the PAPA moiety first added dropwise at a 4:1 molar ratio of the alkyl amine with respect to alginate carboxylic acids followed by addition of a 4:1 molar ratio of DPTA with respect to the same groups. The representative ^1H and ^{13}C NMR peaks for unmodified and alkyl amine-modified alginates are listed below:

Alg5: ^1H NMR (600 MHz, D_2O , δ) 3.60-4.05 (OCHCH(OH)CH(OH)), 4.30 (OCHCH(OH)CH(OH)), 4.50-4.60 (OHCOCH), 4.90 (OCH(CHOH)O). ^{13}C NMR (600 MHz, D_2O , δ) 65.0-80.0 (OCHCH(OH)CH(OH)CH(OH)CH(O)), 100.0 (OCHCH(OH)), 175.0 (CHC(O)).

Alg5-DPTA: ^1H NMR (600 MHz, D_2O , δ) 1.60-1.80 ($\text{CH}_2\text{CH}_2\text{CH}_2\text{NHCH}_2\text{CH}_2\text{CH}_2\text{NH}_2$), 2.60-2.30 ($\text{CH}_2\text{CH}_2\text{CH}_2\text{NHCH}_2\text{CH}_2\text{CH}_2\text{NH}_2$), 2.80-3.10 ($\text{CH}_2\text{CH}_2\text{CH}_2\text{NHCH}_2\text{CH}_2\text{CH}_2\text{NH}_2$), 3.60-4.05 (OCHCH(OH)CH(OH)), 4.30 (OCHCH(OH)CH(OH)), 4.50-4.60 (NHCOCH), 4.90 (OCH(CHOH)O). ^{13}C NMR (600 MHz, D_2O , δ) 26.9-29.5 (C(O)NHCH₂CH₂CH₂NH, NHCH₂CH₂CH₂NH₂), 37.6-46.0 CH₂ (C(O)NHCH₂CH₂CH₂NH, NHCH₂CH₂CH₂NH₂), 65.0-80.0 (OCHCH(OH)CH(OH)CH(OH)CH(O)), 100.0 (OCHCH(OH)), 160.0 (CHC(O)NH), 175.0 (CHC(O)).

Alg5-DETA: ^1H NMR (600 MHz, D_2O , δ) 2.30-3.30 ($\text{CH}_2\text{CH}_2\text{NHCH}_2\text{CH}_2\text{NH}_2$), 3.60-4.05 (OCHCH(OH)CH(OH)), 4.30 (OCHCH(OH)CH(OH)), 4.50-4.60 (NHCOCH), 4.90

(OCH(CHOH)O). ^{13}C NMR (600 MHz, D_2O , δ) 39.0-47.0 (C(O)NHCH₂CH₂NHCH₂CH₂NH₂), 65.0-80.0 (OCHCH(OH)CH(OH)CH(OH)CH(O)), 100.0 (OCHCH(OH)), 160.0 (CHC(O)NH), 175.0 (CHC(O)).

Alg5-PAPA: ^1H NMR (600 MHz, D_2O , δ) 0.70-0.80 (NHCH₂CH₂CH₃), 1.52 (NHCH₂CH₂CH₃), 1.85 (CH₂CH₂CH₂NHCH₂CH₂CH₃), 2.80-3.10 (CH₂CH₂CH₂NHCH₂CH₂CH₃), 3.60-4.05 (OCHCH(OH)CH(OH)), 4.30 (OCHCH(OH)CH(OH)), 4.50-4.60 (NHCOCH), 4.90 (OCH(CHOH)O). ^{13}C NMR (600 MHz, D_2O , δ) 10.9 (NHCH₂CH₂CH₃), 20.0 (NHCH₂CH₂CH₃), 31.3-49.0 (C(O)NHCH₂CH₂CH₂NH, NHCH₂CH₂CH₃), 65.0-80.0 (OCHCH(OH)CH(OH)CH(OH)CH(O)), 100.0 (OCHCH(OH)), 160.0 (CHC(O)NH), 175.0 (CHC(O)).

Alg5-SPER: ^1H NMR (600 MHz, D_2O , δ) 1.13 (NHCH₂(CH₂)₂CH₂NH), 1.56 (NHCH₂CH₂CH₂NH), 1.80 (C(O)NHCH₂CH₂CH₂NH), 2.20-2.40 (CH₂CH₂CH₂NH, NHCH₂(CH₂)₂CH₂NH, NHCH₂CH₂CH₂NH₂), 2.68 (NHCH₂CH₂CH₂NH₂), 2.80-3.10 (C(O)NHCH₂CH₂CH₂NH, NHCH₂CH₂CH₂NH₂), 3.60-4.05 (OCHCH(OH)CH(OH)), 4.30 (OCHCH(OH)CH(OH)), 4.50-4.60 (NHCOCH), 4.90 (OCH(CHOH)O). ^{13}C NMR (600 MHz, D_2O , δ) 23.2 (NHCH₂(CH₂)₂CH₂NH), 34.8-45.0 (C(O)NHCH₂CH₂CH₂NH), 65.0-80.0 (OCHCH(OH)CH(OH)CH(OH)CH(O)), 100.0 (OCHCH(OH)), 160.0 (CHC(O)NH), 175.0 (CHC(O)).

Alg5-PAPA-DPTA: ^1H NMR (600 MHz, D_2O , δ) 0.70-0.80 (NHCH₂CH₂CH₃), 1.48 (NHCH₂CH₂CH₃), 1.50-1.70 (CH₂CH₂CH₂NHCH₂CH₂CH₂NH₂), 2.30-2.40 (CH₂CH₂CH₂NHCH₂CH₂CH₂NH₂), 2.10 (CH₂CH₂CH₂NHCH₂CH₂CH₃), 2.60-3.10 (CH₂CH₂CH₂NHCH₂CH₂CH₂NH₂), 3.60-4.05 (OCHCH(OH)CH(OH)), 4.30 (OCHCH(OH)CH(OH)), 4.50-4.60 (NHCOCH), 4.90 (OCH(CHOH)O). ^{13}C NMR (600 MHz,

D₂O, δ) 9.4 (NHCH₂CH₂CH₃), 20.0 (NHCH₂CH₂CH₃), 26.9-29.5 (C(O)NHCH₂CH₂CH₂NH, NHCH₂CH₂CH₂NH₂), 31.3-49.0 (C(O)NHCH₂CH₂CH₂NH, NHCH₂CH₂CH₃), 37.6-46.0 CH₂ (C(O)NHCH₂CH₂CH₂NH, NHCH₂CH₂CH₂NH₂), 65.0-80.0 (OCHCH(OH)CH(OH)CH(OH)CH(O)), 100.0 (OCHCH(OH)), 160.0 (CHC(O)NH), 175.0 (CHC(O)).

4.2.6 *Synthesis of N-diazeniumdiolate-modified alginates*

Nitric oxide donor-modified alginates were synthesized as previously reported.³⁷ Briefly, polyamine-modified alginate (45 mg) was dissolved in 50 mM NaOH solution (3 mL) in a 1-dram glass vial. The (open) vials were placed in a stainless steel reactor with continuous magnetic stirring. Oxygen was removed from the vessel by purging with argon (10 s, 7 bar) three times. The vessel was then pressurized to 10 bar with NO gas and allowed to react for 3 d. Afterward, the same argon purging protocol was repeated to remove unreacted NO. The NO-releasing alginate oligosaccharides were then precipitated in ethanol, collected by centrifugation, dried overnight in vacuo, and stored at -20 °C as a white powder.

4.2.7 *Characterization of nitric oxide release*

Nitric oxide release was evaluated in real-time using a Sievers 280i Chemiluminescence NO analyzer (NOA; Boulder, CO).^{41,42} Measurements were taken before each biofilm experiment to ensure sample stability. Prior to analysis, the NOA was calibrated with air passed through a NO zero filter (0 ppm NO) and 25.87 ppm of NO standard gas (balance N₂). In a typical measurement, NO-releasing alginate oligosaccharide (~1 mg) was dissolved in 30 mL of either PBS (10 mM, pH 6.5), mucin (4 wt%, pH 6.5), DNA (4 wt%, pH 6.5), or ASM (pH 6.5). Nitrogen was flowed through the solution at a flow rate of 70 mL/min to carry the liberated NO from the biopolymer to

the analyzer. Additional nitrogen flow was supplied to the flask to match the collection rate of the instrument (200 mL/min) to remove water soluble interferents (e.g., nitrite and nitrate).^{41,42} Nitric oxide analysis was terminated when NO levels fell below 10 ppb of NO/mg of alginate (the limit of detection of the instrument).

4.2.8 *Biofilm eradication assays*

P. aeruginosa, BCC, *S. aureus* and MRSA bacterial cultures were grown overnight in LB (pH 6.5) at 37 °C and recultured in fresh LB to a concentration of 10⁸ CFU/mL. These solutions were diluted to 10⁶ CFU/mL in sterile media (*P. aeruginosa* and BCC in ASM; *S. aureus* and MRSA in ASM with 0.25% glucose) and grown for 48 h at 37 °C with gentle shaking.^{3,38,43} Biofilms in ASM were treated with premeasured samples of NO-releasing alginates, control alginates, or antibiotic (i.e., tobramycin, vancomycin) dissolved in ASM (100 µL), with final concentrations ranging from 2 to 64 mg/mL. Treatment was for 24 h at 37 °C in either aerobic (with oxygen) and anaerobic (low oxygen) conditions. All anaerobic biofilm growth and exposures were conducted in a Coy anaerobic chamber equipped with an oxygen and hydrogen monitor (Coy Laboratory Products; Grass Lake, MI). For the anaerobic chamber, oxygen levels were consistently maintained at 0 ppm throughout the experiment. Untreated controls (blanks) were included in each experiment to ensure bacterial viability over the duration of the experiment. The dispersed biofilms were then pipetted out of the wells, serially diluted (10-, 100-, 1000-, and 10,000-fold dilutions), vortexed, plated on TSA plates using an Eddy Jet spiral plater (IUL; Farmingdale, NY), and incubated overnight at 37 °C. Bacterial viability was assessed using a Flash & Go colony counter (IUL; Farmingdale, NY). The minimum biofilm eradication concentration at 24 h (MBEC_{24h}) was defined as the minimum concentration required to achieve a 5-log reduction in bacterial viability compared to untreated cells (i.e., reduced bacterial counts from 10⁸ to ≤10³ CFU/mL). The limit

of detection of this method is 2.5×10^3 CFU/mL.⁴⁴ The NO dose ($\mu\text{g NO/mL}$) was derived from the MBEC_{24h} of the alginate samples (mg/mL) with the NO released measured in ASM (pH 6.5; $\mu\text{mol NO/mg alginate}$) over the testing period.

4.2.9 Time-based biofilm eradication assay

P. aeruginosa biofilms were grown aerobically and anaerobically, and treated with either Alg5-PAPA-DPTA/NO, Alg5-PAPA/NO, and Alg5-DPTA/NO (4 and 2 mg/mL, respectively) following the same protocol as for the biofilm eradication assays. Untreated controls were included to ensure bacteria viability over the duration of the experiment. The samples were incubated with gentle shaking at 37 °C for 2, 4, and 6 h before plating on TSA plates using an Eddy Jet spiral plater and incubating overnight at 37 °C. Bacterial viability was assessed using a Flash & Go colony counter.

4.2.10 Statistical analysis

All values either numerically or with error bars are reported as the mean \pm standard deviation of the mean for a minimum of three or more pooled experiments. Statistical significance was determined using the two-tailed Student's *t*-test.

4.3 Results and Discussion

Alginate oligosaccharides (~5 kDa) with different secondary amine functional groups (e.g., DETA, DPTA, PAPA, and SPER) were prepared via EDC/NHS reactions following previously published protocols.³⁷ Alkyl amine modification was confirmed via ¹³C NMR with the observation of an amide bond peak (~160 ppm) and elemental analysis (monitoring the increase in nitrogen

content from 0 to 6-11 wt%).³⁷ The alkyl amine-modified systems were subsequently functionalized with *N*-diazoniumdiolates via exposure to high pressures (i.e., 10 bar) of NO in basic aqueous solution.³⁷ Formation of NO donors was confirmed using UV-Vis spectroscopy and the appearance of a characteristic absorbance band at 253 nm.²¹ The resulting NO-releasing alginates possessed a broad range of NO-release kinetics when measured in phosphate buffered saline (PBS) at pH 6.5, with the PAPA- and DETA-modified alginates having the fastest (~0.1 h) and slowest (~2.0 h) NO-release half-lives, respectively (Table 4.1). In buffer, the biopolymers were characterized as having NO totals comparable to other previously reported NO-releasing biopolymers (0.3-0.6 $\mu\text{mol}/\text{mg}$; Table 4.1).^{37,45-49}

4.3.1 Nitric oxide release in biological media.

The NO-release properties of the alginate materials were measured in artificial sputum media (ASM, pH 6.5) to determine the total amount of NO available in environments that more closely mimic those in the CF airway.^{3,50-52} As expected, the NO payloads were slightly lower (0.2-0.3 $\mu\text{mol}/\text{mg}$) when measured in ASM compared to in PBS due to the rapid scavenging of NO by reactive oxygen species (ROS) and proteins in biological media (Table 4.2; Figure 4.1).^{39,41} Nevertheless, a range of NO-release kinetics for the alginates was still observed in ASM, with Alg5-DETA/NO maintaining the longest NO-release half-life (~40 min) and Alg5-PAPA/NO the fastest (~4 min), following the same order observed in PBS (Table 4.1). In ASM, a decrease in the NO flux (i.e., maximum instantaneous amount of NO released) was observed for both Alg5-PAPA/NO and Alg5-SPER/NO, again suggesting NO scavenging.³⁹ In contrast, both Alg5-DETA/NO and Alg5-DPTA/NO systems were characterized with an elevated NO flux (i.e., maximum instantaneous NO being released) in media relative to buffer. Previous work has pointed to the positively charged terminal primary amines of the DETA and DPTA modification stabilizing

Table 4.1 Nitric oxide-release properties of *N*-diazoniumdiolate-functionalized biopolymers in PBS (pH 6.5, 37 °C).^a

Biopolymer	t[NO]^b ($\mu\text{mol/mg}$)	[NO]_{max}^c (ppb/mg)	<i>t</i>_{1/2}^d (h)	<i>t</i>_a^e (h)
Alg5-DETA/NO	0.36 ± 0.10	590 ± 20	2.40 ± 1.40	16.0 ± 3.9
Alg5-DPTA/NO	0.42 ± 0.03	1000 ± 230	0.40 ± 0.11	4.5 ± 0.2
Alg5-SPER/NO	0.37 ± 0.06	2890 ± 330	0.30 ± 0.10	3.3 ± 0.9
Alg5-PAPA/NO	0.60 ± 0.03	12100 ± 3800	0.10 ± 0.05	2.7 ± 0.1
Alg5-PAPA-DPTA/NO	0.55 ± 0.04	4890 ± 1300	0.35 ± 0.09	4.8 ± 1.4

^aError represents standard deviation for $n \geq 3$ experiments. ^bTotal NO released. ^cMaximum flux of NO release. ^dNO-release half-life. ^eDuration of NO release.

Table 4.2 Nitric oxide-release properties of NO donor-functionalized alginates in ASM (pH 6.5, 37 °C).^a

Biopolymer	t[NO]^b ($\mu\text{mol}/\text{mg}$)	[NO]_{max}^c (ppb/mg)	<i>t</i>_{1/2}^d (mins)	<i>t</i>_d^e (h)
Alg5-DETA/NO	0.18 ± 0.04	670 ± 160	43.0 ± 10.9	5.0 ± 0.3
Alg5-DPTA/NO	0.19 ± 0.06	3420 ± 960	14.0 ± 1.2	3.1 ± 0.4
Alg5-SPER/NO	0.27 ± 0.09	2370 ± 1750	5.4 ± 1.6	1.7 ± 0.2
Alg5-PAPA/NO	0.28 ± 0.05	5990 ± 1480	3.8 ± 0.9	1.2 ± 0.8
Alg5-PAPA-DPTA/NO	0.29 ± 0.04	4750 ± 1100	8.4 ± 0.6	3.0 ± 0.6

^aError represent standard deviation for n ≥ 3 separate syntheses. ^bTotal NO released.

^cMaximum flux of NO release. ^dNO-release half-life. ^eDuration of NO release.

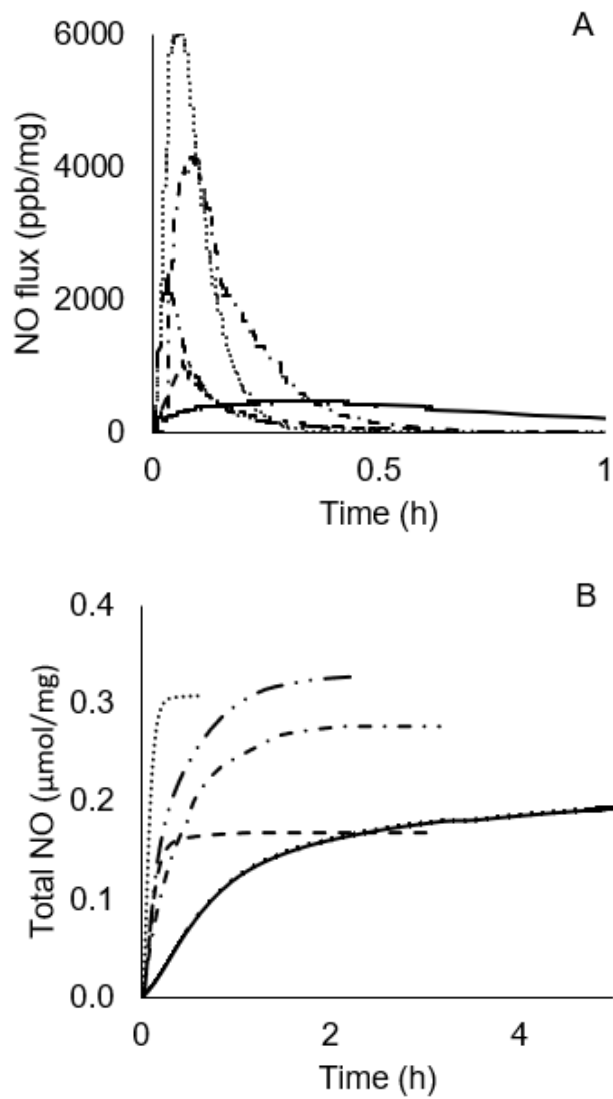


Figure 4.1 (A) Real-time NO-release profiles for the first 1 h and (B) plot of total NO release vs. time for representative biopolymers Alg5-DETA/NO (—), Alg5-DPTA/NO (---), Alg5-SPER/NO (- · - ·), Alg5-PAPA/NO (· · ·), and Alg5-PAPA-DPTA/NO (- · - -) measured via chemiluminescence in ASM pH 6.5.

the negatively charged *N*-diazoniumdiolates, with concomitant prolonged NO release (i.e., lower initial NO flux and longer half-lives) under static conditions.^{53,54} In the case of NO release in ASM, the potential electrostatic interactions between the alginate biopolymers and primary components of the media (i.e., mucins and DNA) may destabilize the *N*-diazoniumdiolate NO donor allowing for a larger initial NO amount released and shorter NO-release half-life.^{3,50,52}

To further elucidate how ASM components may influence the NO-release properties of alginates in media, NO-release measurements were collected in mucin and DNA, two of the main components of ASM. Alg5-PAPA/NO and Alg5-DPTA/NO biopolymers were selected for this study as they represent fast and slow NO-releasing alginates. The hybrid biopolymer containing PAPA and DPTA (Alg5-PAPA-DPTA/NO) was also studied as it represents a combination of the two systems. As expected, NO release in each of the three biological media (i.e., ASM, mucin, and DNA) resulted in a decreased NO flux for the fast releasing Alg5-PAPA/NO in the presence of species capable of scavenging NO (Figure 4.2). However, an increase in NO flux was observed in both ASM and mucin for Alg5-DPTA/NO. The similarity of the NO-release profiles for Alg5-DPTA/NO in the two media clearly reflects destabilization of the *N*-diazoniumdiolate NO donor by enhanced electrostatic interactions between the protonated amine groups on alginate and the negatively charged moieties on the mucin glycoprotein (i.e., sialic acid residues).^{32,53–57} The NO-release profile of the hybrid alginate was unaltered in all media, enabling near constant NO-release kinetics despite a decrease in NO totals in the biological media. The combined, enhanced NO flux for DPTA and decreased flux for PAPA *N*-diazoniumdiolates accounts for this phenomenon, virtually cancelling the changes related to the biological media altogether. In this regard, the Alg5-PAPA-DPTA/NO can mitigate drastic changes in NO-release kinetics due to the biological media.

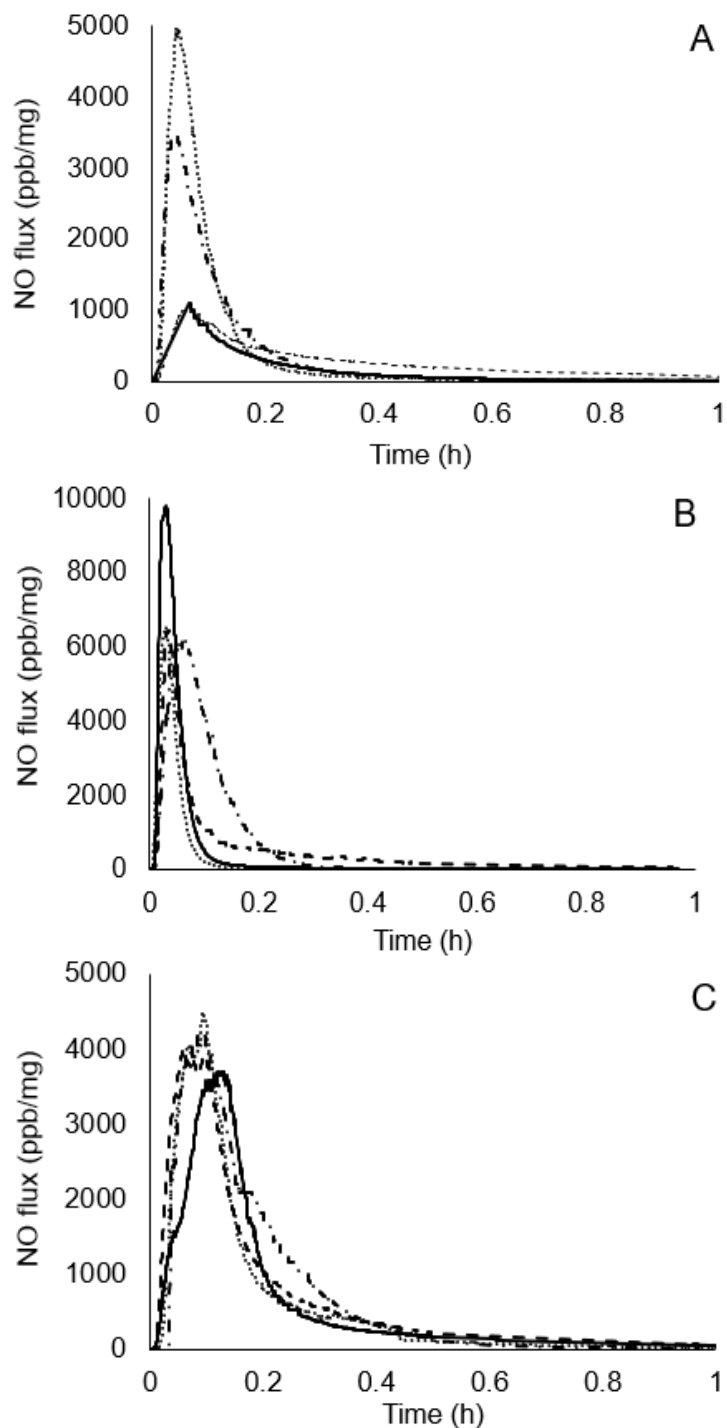


Figure 4.2 Real-time NO-release profiles for the first hour of release for (A) Alg5-DPTA/NO, (B) Alg5-PAPA/NO, and (C) Alg5-PAPA-DPTA/NO in PBS (solid), ASM (dash-dot), mucin (dot), and DNA (dash) solutions buffered at pH 6.5.

4.3.2 Antibiofilm efficacy

Persistent colonization of biofilm-forming pathogens in the airways accounts for ~90% of CF patient mortality.^{10,34} The presence of thick mucus in the CF airways, the EPS matrix, and other unique environmental-related factors (e.g., lower oxygen levels) provide additional protection to biofilm-based bacteria by limiting the diffusion and action of traditional antibiotics.^{3,4,58} Indeed, slower growth due to viscoelasticity of mucus and the unique biofilm microenvironment (e.g., the presence of an oxygen gradient in the mucus that leads to bacteria adaptation to anaerobic microenvironments) contributes to the demonstrated resistance of bacteria by these biofilms.⁸ It is thus imperative to evaluate the antibiofilm activity of new therapeutics under conditions that mimic CF more accurately (i.e., in ASM under both aerobic and anaerobic conditions).

The antibiofilm activity of control and NO-releasing alginates was evaluated against both aerobic and anaerobic biofilms of four CF-relevant pathogens: *P. aeruginosa*, BCC, *S. aureus*, and MRSA.^{33,34} The minimum concentration of antibacterial agent required to achieve a 5-log reduction in viability after 24 h (MBEC_{24h}) was evaluated for each of the alginate compositions. At equivalent concentrations to the MBEC_{24h}, control (non-NO-releasing) alginates did not alter the bacterial viability of the biofilms (Figure 4.3). In contrast, treatment with the NO-releasing biopolymers led to a 5-log reduction ($\geq 99.999\%$) in bacterial viability for each of the NO-releasing alginates regardless of NO-release properties, implicating NO as the required bactericidal agent (Table 4.3).

Alg5-DPTA/NO, Alg5-SPER/NO, and Alg5-PAPA/NO achieved 5-log biocidal activity at 16 mg/mL against both *P. aeruginosa* and BCC under aerobic conditions. The Alg5-DETA/NO and Alg5-PAPA-DPTA/NO derivatives deviated from this trend, with the DETA-modified and hybrid alginate systems requiring greater and lower concentrations, respectively. We previously

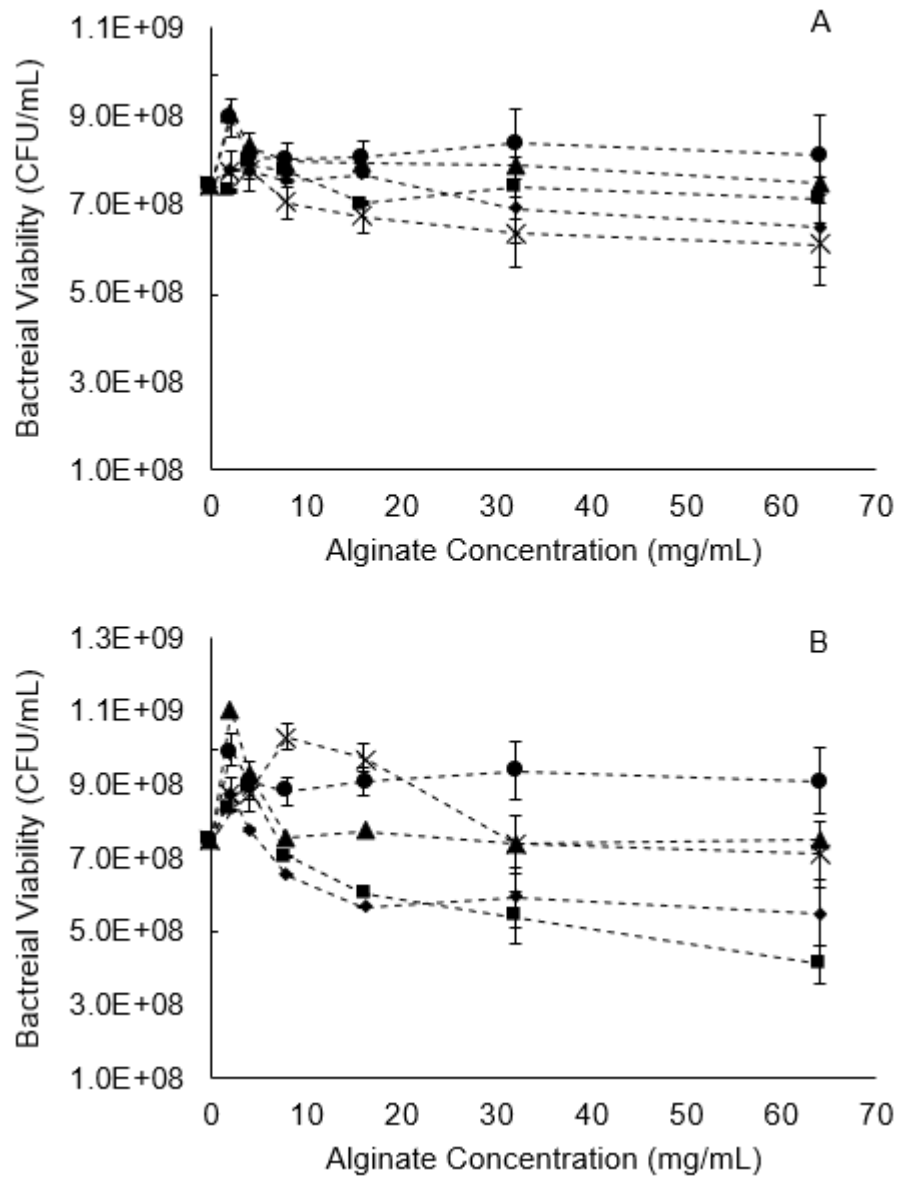


Figure 4.3 Antibiofilm efficacy of Alg5-DETA (circle), Alg5-DPTA (triangle), Alg5-SPER (square), Alg5-PAPA (diamond), and Alg5-PAPA-DPTA (cross) against *S. aureus* biofilms under (A) aerobic and (B) anaerobic conditions. Error bars represent standard deviation of the mean viability (CFU/mL). For all measurements, $n \geq 3$ pooled experiments.

Table 4.3 Minimum biofilm eradication concentrations (MBEC_{24h}) of NO-releasing alginates against aerobic biofilms.^a

Sample	MBEC _{24h} (mg/mL) ^a			
	<i>P. aeruginosa</i>	BCC	<i>S. aureus</i>	MRSA
Alg5-DETA/NO	32	32	64	64
Alg5-DPTA/NO	16	16	32	64
Alg5-SPER/NO	16	16	32	64
Alg5-PAPA/NO	16	16	64	32
Alg5-PAPA-DPTA/NO	4	4	16	16
Tobramycin	2	2	16	>64

^aMBEC_{24h} determined from n ≥ 3 experiments.

reported that under static (i.e., PBS with 1 vol% broth) conditions, the slower, sustained NO-releasing alginates (e.g., Alg5-DETA/NO) facilitated greater biocidal efficacy against biofilms compared to faster NO-releasing systems (e.g., Alg5-PAPA/NO).³⁷ With NO scavenging (e.g., NO release in ASM), however, the combination of lower NO totals (~0.2 $\mu\text{mol}/\text{mg}$) and slower NO release might result in insufficient delivery of the required lethal dose of NO. In this regard, Alg5-DETA/NO proved to be less effective. Indeed, larger alginate concentrations (32 mg/mL for both *P. aeruginosa* and BCC and 64 mg/mL for both *S. aureus* and MRSA) were required to achieve comparable NO doses and bacteria eradication. With the hybrid Alg5-PAPA-DPTA/NO, the slightly higher NO payload (~0.3 $\mu\text{mol}/\text{mg}$), larger NO flux (~5000 ppb/mg), and sustained release ($t_d \sim 3$ h) allowed for a more lethal NO delivery and lower MBEC_{24h} values (4 mg/mL for both *P. aeruginosa* and BCC and 16 mg/mL for both *S. aureus* and MRSA) compared to each of the monosubstituted alginates.

Similar to previous reports,^{37,59,60} greater concentrations of NO-releasing alginates were needed to achieve biocidal action against *S. aureus* and MRSA biofilms (Table 4.3). The thicker peptidoglycan layer, and increased production of polysaccharides and extracellular proteins of Gram-positive species in general likely hinder NO diffusion (into the biofilm), necessitating larger NO fluxes from the biopolymer to achieve killing.⁶⁰ These structural differences are hypothesized to account for the lower susceptibility of both *S. aureus* and MRSA biofilms.

The efficacy of the alginate biopolymers to eradicate the four pathogens was also compared to tobramycin. Under similar conditions, both *P. aeruginosa* and BCC were eradicated at lower tobramycin concentrations than those of the NO-releasing alginates (Table 4.3). However, greater tobramycin concentrations were required to eradicate Gram-positive bacterial biofilms. Against *S. aureus*, the required tobramycin dose for biocidal action equaled that of Alg5-PAPA-DPTA/NO.

Each of the NO-releasing alginates were more efficacious against MRSA, as the Gram-positive bacteria showed resistance to tobramycin up to 64 mg/mL. With NO as the implicated bactericidal agent, tobramycin concentration was also compared to the NO dose delivered during the bacteria killing assay. The NO dose required to achieve antibiofilm activity was derived from both the MBEC_{24h} of the alginate samples and the measured total NO released in ASM to compare the efficacy of NO to the antibiotic under aerobic conditions (Figure 4.4A). Against each of the four pathogens studied, lower initial NO doses relative to the antibiotic were required to achieve biocidal activity, demonstrating NO's potent antimicrobial activity.

Anaerobically grown biofilms required lower alginate and NO concentrations to achieve killing compared to aerobic biofilms (Table 4.4, Figure 4.4B). In contrast, greater tobramycin concentrations were necessary to achieve biocidal action under anaerobic versus aerobic conditions, following previous reports describing diminished antibiotic activity in low-oxygen environments.^{39,61,62} For *S. aureus* and MRSA, lower concentrations of the NO-releasing biopolymers were also required compared to tobramycin, demonstrating superior antibiofilm efficacy compared to the aminoglycoside antibiotic. Analogous to the trends observed under aerobic conditions, Alg5-PAPA-DPTA/NO was most effective, achieving a 5-log reduction in biofilm bacterial viability at an alginate concentration of only 2 mg/mL against the four pathogens. Reighard et al. reported similar results with NO-releasing chitosan oligosaccharides, attributing the larger concentration for aerobic conditions to NO scavenging by oxygen and other ROS.³⁹ Analogously, lower starting NO doses ($\leq 140 \mu\text{g/mL}$) were needed to treat the anaerobic biofilms (Figure 4.4B).

With tobramycin's poor activity against *S. aureus* and MRSA, the antibiofilm activity of the NO-releasing alginates was also compared to vancomycin, the antibiotic traditionally used to

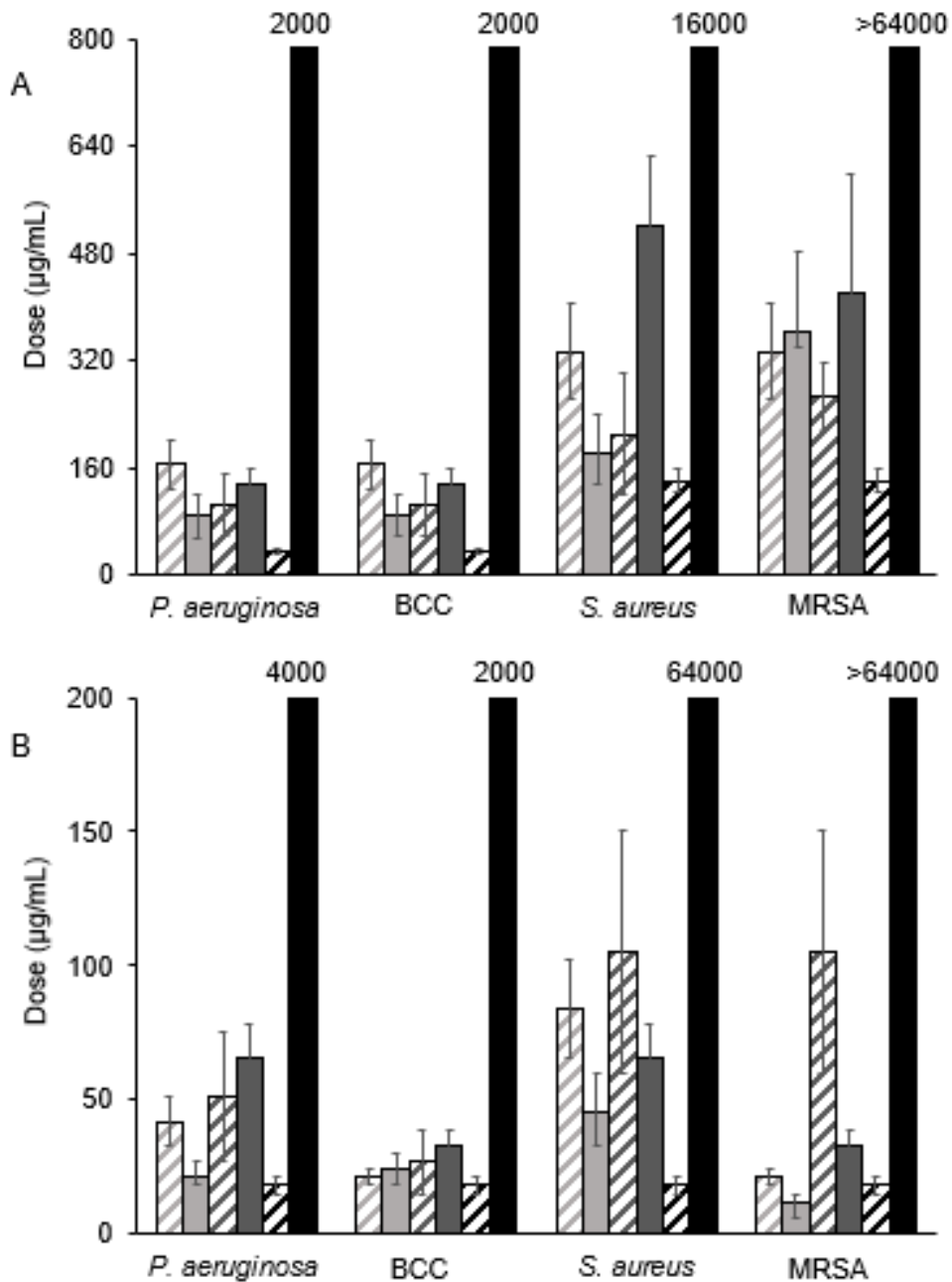


Figure 4.4 Nitric oxide dose for Alg5-DETA (light gray stripes), Alg5-DPTA/NO (solid light gray), Alg5-SPER/NO (dark gray stripes), Alg5-PAPA/NO (solid dark gray), Alg5-PAPA-DPTA/NO (black stripes) required to treat (A) aerobic and (b) anaerobic biofilms compared to tobramycin (solid black). Studies consisted of at least three experiments with error bars representing the standard deviation.

Table 4.4. Minimum biofilm eradication concentrations (MBEC_{24h}) of NO-releasing alginates against anaerobic biofilms.^a

Sample	MBEC _{24h} (mg/mL) ^a			
	<i>P. aeruginosa</i>	BCC	<i>S. aureus</i>	MRSA
Alg5-DETA/NO	8	4	16	4
Alg5-DPTA/NO	4	4	8	2
Alg5-SPER/NO	2	2	2	2
Alg5-PAPA/NO	8	4	8	4
Alg5-PAPA-DPTA/NO	8	4	16	16
Tobramycin	4	2	64	>64

^aMBEC_{24h} determined from n ≥ 3 experiments.

treat infections by Gram-positive bacteria.⁶³ Similar to tobramycin, greater concentrations of vancomycin were required to eradicate anaerobic versus aerobic biofilms (Figure 4.5), indicating a reduced efficacy under low-oxygen conditions. The doses of NO required to eradicate the biofilms were lower for both oxygen levels compared to vancomycin, demonstrating NO's unique ability to remain active as an antimicrobial regardless of oxygen availability.

4.3.3 Effect of nitric oxide-release kinetics on antibiofilm efficacy

Biofilm eradication was also studied as a function of NO-release kinetics. *P. aeruginosa* biofilms were treated with equal concentrations of either Alg5-DPTA/NO, Alg5-PAPA/NO, or Alg5-PAPA-DPTA/NO at 2 and 4 mg/mL for anaerobic and aerobic growth, respectively (Figure 4.6). The selected concentrations represent the lowest MBEC_{24h} for the Alg5 systems (i.e., the MBEC_{24h} of Alg5-PAPA-DPTA/NO against *P. aeruginosa* biofilms). Under both aerobic and anaerobic conditions, one-time treatment at 2 h with Alg5-DPTA/NO and Alg5-PAPA/NO resulted in a 1- and 2-log reduction in biofilm bacterial viability, respectively. Bacteria viability recovered up to $\sim 10^8$ CFU/mL at longer exposure durations for both the PAPA- and DPTA-modified NO-releasing alginates. The greater total NO of Alg5-PAPA/NO at 2 h resulted in a greater viability reduction initially, but the low NO levels released (i.e., below the limit of detection of the instrument) thereafter proved insufficient for maintaining lower viability (i.e., killing). On the other hand, the low NO totals associated with Alg5-DPTA/NO in ASM led to insufficient NO doses after the one-time treatment to achieve any appreciable bacterial killing, thus requiring a larger concentration (i.e., 16 mg/mL) to eradicate the biofilm. The results, however, suggest the possibility of using multiple treatments with lower concentrations (e.g., 2 or 4 mg/mL) to supplement the initial reductions observed for the monosubstituted alginates as an alternative to

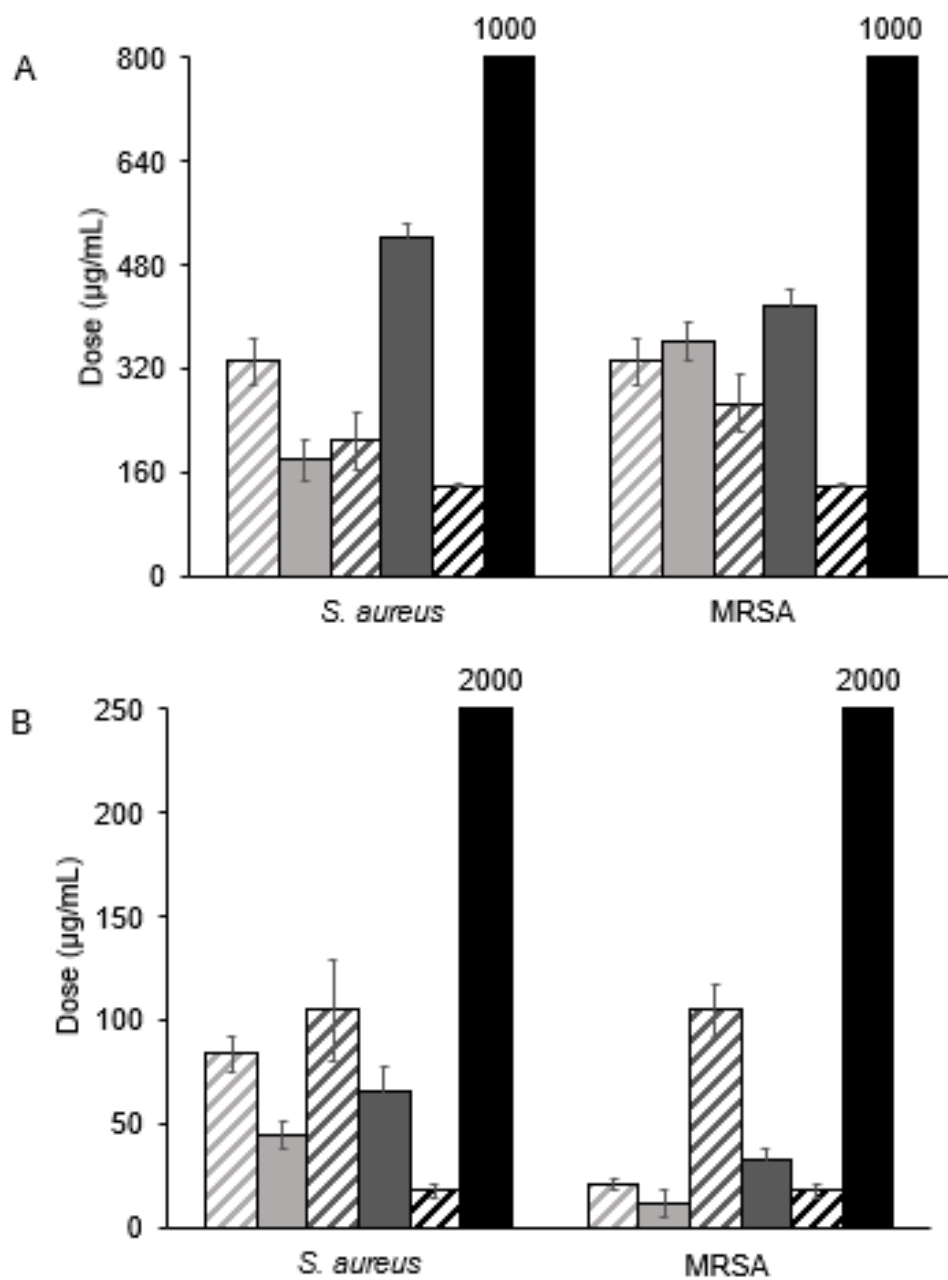


Figure 4.5 Nitric oxide dose for Alg5-DETA (light gray stripes), Alg5-DPTA/NO (solid light gray), Alg5-SPER/NO (dark gray stripes), Alg5-PAPA/NO (solid dark gray), Alg5-PAPA-DPTA/NO (black stripes) required to treat (A) aerobic and (b) anaerobic biofilms of *S. aureus* and MRSA. All starting NO doses were compared to vancomycin (solid black). Studies consisted of at least three experiments with error bars representing the standard deviation.

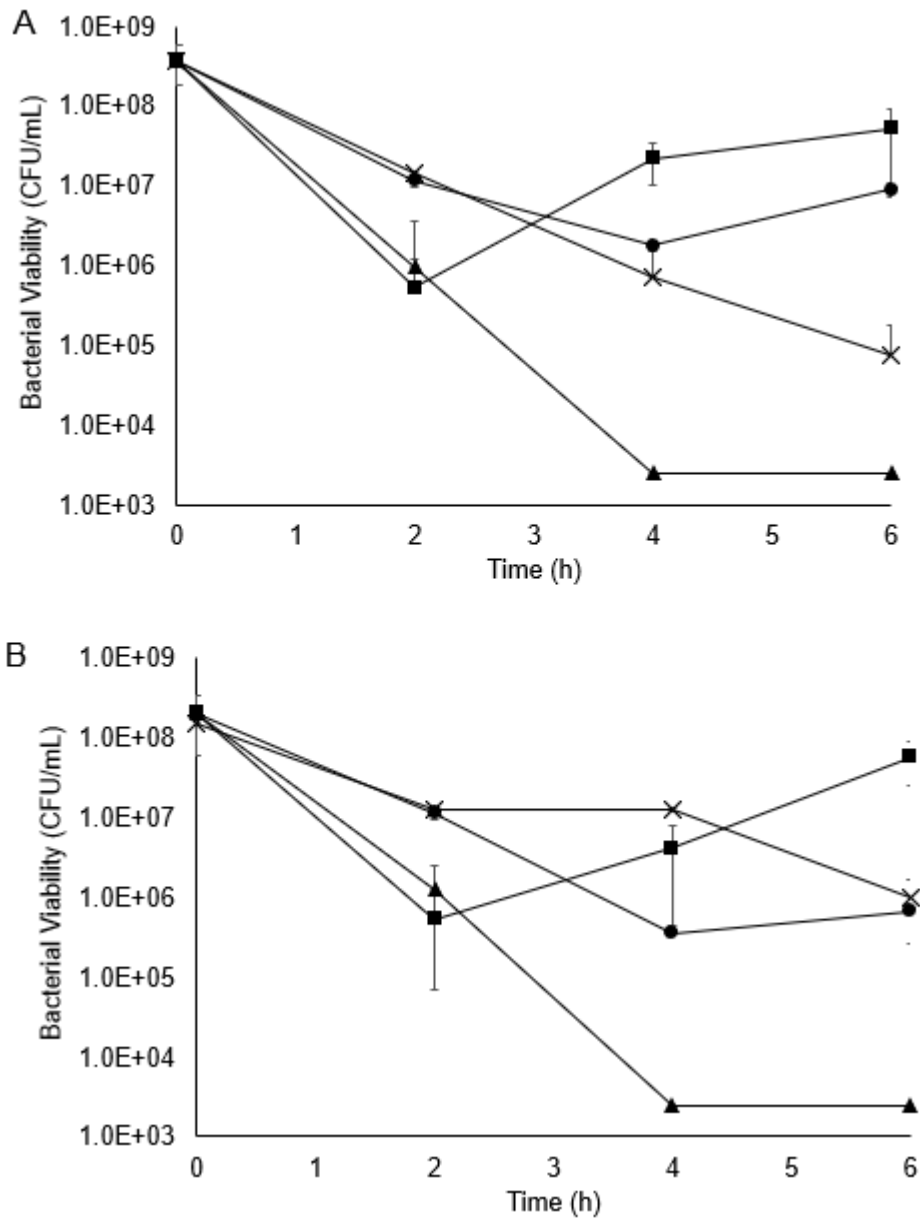


Figure 4.6 Time-based bactericidal efficacy of Alg5-DPTA/NO (circle), Alg5-PAPA-DPTA/NO (triangle), Alg5-PAPA/NO (square), and tobramycin (cross). Comparison of all NO-releasing alginates at equivalent concentrations of (A) 4 mg/mL under aerobic conditions and (B) 2 mg/mL under anaerobic conditions. The MBEC_{24h} values under aerobic and anaerobic conditions (2 mg/mL and 4 mg/mL, respectively) were used for tobramycin. Studies consisted of at least three experiments with error bars representing the standard deviation.

the larger concentration required for one-time treatment. Of course, such a hypothesis must be further evaluated pre-clinically and clinically in future work.

In contrast to both Alg5-PAPA/NO and Alg5-DPTA/NO, the hybrid alginate system (Alg5-PAPA-DPTA/NO) elicited an initial 2-log reduction in bacterial viability at the same concentration after 2 h for both aerobic and anaerobic biofilms. The combination of greater NO totals in ASM (~0.3 $\mu\text{mol/mg}$) coupled with the sustained NO release (~3 h) by using the hybrid biopolymer led to a 5-log reduction after 4 h. Over the same period, tobramycin at its aerobic MBEC_{24h} (2 mg/mL) only achieved a 2-log reduction (with an overall 3-log reduction over the course of 6 h) suggesting a slower biocidal action mechanism. Similarly, anaerobic biofilms treated with tobramycin at the antibiotic's anaerobic MBEC_{24h} achieved a 2-log reduction over the 6-hour treatment period – albeit more slowly. Collectively, the results of this study suggest that the combination of a high initial NO flux and sustained NO release is preferred for biofilm eradication. Moreover, Alg5-PAPA-DPTA/NO exhibited greater potency against the *P. aeruginosa* biofilms grown in ASM under the two conditions, achieving a 5-log reduction in bacterial viability faster than conventional antibiotics.

4.4 Conclusions

The antibiofilm action of NO-releasing alginates were clearly demonstrated against the four tested, CF-relevant pathogens. Of the different alginate systems, Alg5-PAPA-DPTA/NO exhibited the greatest antibacterial action against the test pathogens regardless of biofilm growth conditions (MBEC_{24h} starting NO dose of $\leq 520 \mu\text{g/mL NO}$). The NO-based hybrid alginate therapeutic also exhibited enhanced efficacy compared to tobramycin and vancomycin, demonstrating Alg5-PAPA-DPTA/NO's promise as an alternative to conventional antibiotics for

treating chronic CF infections. Combined with the ability of alginate oligosaccharides to decrease mucus viscoelasticity,^{24,59-61} these results suggest the utility of NO-releasing alginates as a dual-action CF therapeutic. In particular, NO release may hold great promise for eradicating biofilms deeply embedded in the mucus layer where low oxygen concentrations reduce the efficacy of currently employed antibiotics.

REFERENCES

- (1) Høiby, N. Recent Advances in the Treatment of Pseudomonas Aeruginosa Infections in Cystic Fibrosis. *BMC Med.* **2011**, *9*, 32–39.
- (2) Button, B.; Cai, L. H.; Ehre, C.; Kesimer, M.; Hill, D. B.; Sheehan, J. K.; Boucher, R. C.; Rubinstein, M. A Periciliary Brush Promotes the Lung Health by Separating the Mucus Layer from Airway Epithelia. *Science.* **2012**, *337*, 937–941.
- (3) Sriramulu, D. D.; Lünsdorf, H.; Lam, J. S.; Römling, U. Microcolony Formation: A Novel Biofilm Model of Pseudomonas Aeruginosa for the Cystic Fibrosis Lung. *J. Med. Microbiol.* **2005**, *54*, 667–676.
- (4) Hassett, D. J.; Cuppoletti, J.; Trapnell, B.; Lymar, S. V; Rowe, J. J.; Sun Yoon, S.; Hilliard, G. M.; Parvatiyar, K.; Kamani, M. C.; Wozniak, D. J.; et al. Anaerobic Metabolism and Quorum Sensing by Pseudomonas Aeruginosa Biofilms in Chronically Infected Cystic Fibrosis Airways: Rethinking Antibiotic Treatment Strategies and Drug Targets. *Adv. Drug Deliv. Rev.* **2002**, *54*, 1425–1443.
- (5) Stewart, P. S.; William Costerton, J. Antibiotic Resistance of Bacteria in Biofilms. *Lancet* **2001**, *358*, 135–138.
- (6) Hall-Stoodley, L.; Stoodley, P. Evolving Concepts in Biofilm Infections. *Cell Microbiol.* **2009**, *11*, 1034–1043.
- (7) Donlan, R. M. Biofilm Formation: A Clinically Relevant Microbiological Process. *Clin. Infect. Dis.* **2001**, *33*, 1387–1392.
- (8) Høiby Bjarnsholt, T., Givskov, M., Molin, S., Ciofu, O., N. Antibiotic Resistance of Bacterial Biofilms. *Int. J. Antimicrob. Agents* **2010**, *35*, 322–332.
- (9) Cullen, L.; McClean, S. Bacterial Adaptation during Chronic Respiratory Infections. *Pathogens* **2015**, *4*, 66–89.
- (10) Lyczak, J. B.; Cannon, C. L.; Pier, G. B. Lung Infections Associated with Cystic Fibrosis. *Clin. Microbiol. Rev.* **2002**, *15*, 122–194.
- (11) Stone, A.; Saiman, L. Update on the Epidemiology and Management of Staphylococcus Aureus, Including Methicillin-Resistant Staphylococcus Aureus, in Patients with Cystic Fibrosis. *Curr. Opin. Pulm. Med.* **2007**, *13*, 515–521.
- (12) Dasenbrook, E.; Checkley, W.; Merlo, C.; Konstan, M.; Lechtzin, N.; Boyle, M. Association between Respiratory Tract Methicillin-Resistant Staphylococcus Aureus and Survival in Cystic Fibrosis. *JAMA* **2010**, *303*, 2386–2392.
- (13) Ratjen, F. A. Cystic Fibrosis: Pathogenesis and Future Treatment Strategies. *Respir. Care* **2009**, *54*, 595–605.
- (14) Ciofu, O.; Hansen, C. R.; Høiby, N. Respiratory Bacterial Infections in Cystic Fibrosis. *Curr. Opin. Pulm. Med.* **2013**, *19*, 251–258.

- (15) Ciofu, O.; Tolker-Nielsen, T.; Jensen, P. Ø.; Wang, H.; Høiby, N. Antimicrobial Resistance, Respiratory Tract Infections and Role of Biofilms in Lung Infections in Cystic Fibrosis Patients. *Adv. Drug Deliv. Rev.* **2015**, *85*, 7–23.
- (16) Carpenter, A. W.; Schoenfisch, M. H. Nitric Oxide Release: Part II. Therapeutic Applications. *Chem. Soc. Rev.* **2012**, *41*, 3742–3752.
- (17) Riccio, D. A.; Schoenfisch, M. H. Nitric Oxide Release: Part I. Macromolecular Scaffolds. *Chem. Soc. Rev.* **2012**, *41*, 3731–3741.
- (18) Barraud, N.; Hasset, D. J.; Hwang, S. H.; Rice, S. A.; Kjelleberg, S.; Webb, J. S. Involvement of Nitric Oxide in Biofilm Dispersal of *Pseudomonas Aeruginosa*. *J. Bacteriol.* **2006**, *188*, 7344–7353.
- (19) Barraud, N.; Kelso, M. J.; Rice, S. A.; Kjellerberg, S. Nitric Oxide: A Key Mediator of Biofilm Dispersal with Applications in Infectious Diseases. *Curr. Pharm. Des.* **2015**, *21*, 31–42.
- (20) Keefer, L. K. Fifty Years of Diazeniumdiolate Research. From Laboratory Curiosity to Broad-Spectrum Biomedical Advances. *ACS Chem. Biol.* **2011**, *6*, 1147–1155.
- (21) Hetrick, E. M.; Shin, J. H.; Stasko, N. A.; Johnson, C. B.; Wespe, D. A.; Holmuhamedov, E.; Schoenfisch, M. H. Bactericidal Efficacy of Nitric Oxide-Releasing Silica Nanoparticles. *ACS Nano* **2008**, *2*, 235–246.
- (22) Nair, L. S.; Laurencin, C. T. Biodegradable Polymers as Biomaterials. *Prog. Polym. Sci.* **2007**, *32*, 762–798.
- (23) Khan, S.; Tøndervik, A.; Sletta, H.; Klinkenberg, G.; Emanuel, C.; Onsøyen, E.; Myrvold, R.; Howe, R. A.; Walsh, T. R.; Hill, K. E.; et al. Overcoming Drug Resistance with Alginate Oligosaccharides Able To Potentiate the Action of Selected Antibiotics. *Antimicrob. Agents Chemother.* **2012**, *56*, 5134–5141.
- (24) Pritchard, M. F.; Powell, L. C.; Menzies, G. E.; Lewis, P. D.; Hawkins, K.; Wright, C.; Doull, I.; Walsh, T. R.; Onsøyen, E.; Dessen, A.; et al. A New Class of Safe Oligosaccharide Polymer Therapy to Modify the Mucus Barrier of Chronic Respiratory Disease. *Mol. Pharm.* **2016**, *13*, 863–873.
- (25) Alnaief, M.; Alzaitoun, M. A.; Garcia-Gonzalez, C. A.; Smirnova, I. Preparation of Biodegradable Nanoporous Microspherical Aerogel Based on Alginate. *Carbohydr. Polym.* **2011**, *84*, 1011–1018.
- (26) Draget, K. I.; Taylor, C. Chemical, Physical and Biological Properties of Alginates and Their Biomedical Implications. *Food Hydrocoll.* **2011**, *25*, 251–256.
- (27) Sun, J.; Tan, H. Alginate-Based Biomaterials for Regenerative Medicine Applications. *Materials.* **2013**, *6*, 1285–1309.
- (28) Lee, K. Y.; Mooney, D. J. Alginate: Properties and Biomedical Applications. *Prog. Polym. Sci.* **2012**, *37*, 106–126.

- (29) Roberts, J. L.; Khan, S.; Emanuel, C.; Powell, L. C.; Pritchard, M. F.; Onsøyen, E.; Myrvold, R.; Thomas, D. W.; Hill, K. E. An in Vitro Study of Alginate Oligomer Therapies on Oral Biofilms. *J. Dent.* **2013**, *41*, 892–899.
- (30) Hengzhuang, W.; Song, Z.; Ciofu, O.; Onsøyen, E.; Rye, P. D.; Høiby, N. OligoG CF-5/20 Disruption of Mucoid *Pseudomonas Aeruginosa* Biofilm in a Murine Lung Infection Model. *Antimicrob. Agents Chemother.* **2016**, *60*, 2620–2626.
- (31) Powell, L. C.; Pritchard, M. F.; Ferguson, E. L.; Powell, K. A.; Patel, S. U.; Rye, P. D.; Sakellakou, S.-M.; Buurma, N. J.; Brilliant, C. D.; Copping, J. M.; et al. Targeted Disruption of the Extracellular Polymeric Network of *Pseudomonas Aeruginosa* Biofilms by Alginate Oligosaccharides. *npj Biofilms Microbiomes* **2018**, *4*, 13.
- (32) Klinger-Strobel, M.; Lautenschläger, C.; Fischer, D.; Mainz, J. G.; Bruns, T.; Tuchscher, L.; Pletz, M. W.; Makarewicz, O. Aspects of Pulmonary Drug Delivery Strategies for Infections in Cystic Fibrosis – Where Do We Stand? *Expert Opin. Drug Deliv.* **2015**, *12*, 1351–1374.
- (33) Marshall, B.; Petren, K.; Elbert, A.; Rizvi, S.; Fink, A.; Ostrenga, J.; Sewall, A.; Loeffler, D. 2015 Cystic Fibrosis Foundation Patient Registry Report. *Cyst. Fibros. Found. Patient Regist.* **2016**, 1–94.
- (34) Chmiel, J. F.; Aksamit, T. R.; Chotirmall, S. H.; Dasenbrook, E. C.; Elborn, J. S.; LiPuma, J. J.; Ranganathan, S. C.; Waters, V. J.; Ratjen, F. A. Antibiotic Management of Lung Infections in Cystic Fibrosis. I. The Microbiome, Methicillin-Resistant *Staphylococcus Aureus*, Gram-Negative Bacteria, and Multiple Infections. *Ann. Am. Thorac. Soc.* **2014**, *11*, 1120–1129.
- (35) Davies, K. M.; Wink, D. A.; Saavedra, J. E.; Keefer, L. K. Chemistry of the Diazeniumdiolates. 2. Kinetics and Mechanism of Dissociation to Nitric Oxide in Aqueous Solution. *J. Am. Chem. Soc.* **2001**, *123*, 5473–5481.
- (36) Keefer, L. K.; Nims, R. W.; Davies, K. M.; Wink, D. A. Diazeniumdiolates as NO Dosage Forms. *Methods Enzymol.* **1996**, *268*, 281–293.
- (37) Ahonen, M. J. R.; Suchyta, D. J.; Zhu, H.; Schoenfisch, M. H. Nitric Oxide-Releasing Alginates. *Biomacromolecules* **2018**, *19*, 1189–1197.
- (38) Kirchner, S.; Fothergill, J. L.; Wright, E. A.; James, C. E.; Mowat, E.; Winstanley, C. Use of Artificial Sputum Medium to Test Antibiotic Efficacy Against *Pseudomonas Aeruginosa* in Conditions More Relevant to the Cystic Fibrosis Lung. *J. Vis. Exp.* **2012**, e3857.
- (39) Reighard, K. P.; Schoenfisch, M. H. Antibacterial Action of Nitric Oxide-Releasing Chitosan Oligosaccharides against *Pseudomonas Aeruginosa* under Aerobic and Anaerobic Conditions. *Antimicrob. Agents Chemother.* **2015**, *59*, 6506–6513.
- (40) Mao, S.; Zhang, T.; Sun, W.; Ren, X. The Depolymerization of Sodium Alginate by Oxidative Degradation. *Pharm. Dev. Technol.* **2012**, *17*, 763–769.
- (41) Coneski, P. N.; Schoenfisch, M. H. Nitric Oxide Release Part III. Measurement and Reporting. *Chem. Soc. Rev.* **2012**, *41*, 3753–3758.
- (42) Hetrick, E. M.; Schoenfisch, M. H. Analytical Chemistry of Nitric Oxide. *Annu. Rev. Anal. Chem.* **2009**, *2*, 409–433.

- (43) Cramton, S. E.; Ulrich, M.; Götz, F.; Döring, G. Anaerobic Conditions Induce Expression of Polysaccharide Intercellular Adhesin in *Staphylococcus Aureus* and *Staphylococcus Epidermidis*. *Infect. Immun.* **2001**, *69*, 4079–4085.
- (44) Breed, R. S.; Dotterrer, W. D. The Number of Colonies Allowable on Satisfactory Agar Plates. *J. Bacteriol.* **1916**, *1*, 321–331.
- (45) Lu, Y.; Slomberg, D. L.; Schoenfisch, M. H. Nitric Oxide-Releasing Chitosan Oligosaccharides as Antibacterial Agents. *Biomaterials* **2014**, *35*, 1716–1724.
- (46) Lu, Y.; Shah, A.; Hunter, R. A.; Soto, R. J.; Schoenfisch, M. H. S-Nitrosothiol-Modified Nitric Oxide-Releasing Chitosan Oligosaccharides as Antibacterial Agents. *Acta Biomater.* **2015**, *12*, 62–69.
- (47) Lutzke, A.; Pegalajar-Jurado, A.; Neufeld, B. H.; Reynolds, M. M. Nitric Oxide-Releasing S-Nitrosated Derivatives of Chitin and Chitosan for Biomedical Applications. *J. Mater. Chem. B* **2014**, *2*, 7449–7458.
- (48) Damodaran, V. B.; Reynolds, M. M. Biodegradable S-Nitrosothiol Tethered Multiblock Polymer for Nitric Oxide Delivery. *J. Mater. Chem.* **2011**, *21*, 5870–5872.
- (49) Wold, K. A.; Damodaran, V. B.; Suazo, L. A.; Bowen, R. A.; Reynolds, M. M. Fabrication of Biodegradable Polymeric Nanofibers with Covalently Attached NO Donors. *ACS Appl. Mater. Interfaces* **2012**, *4*, 3022–3030.
- (50) Palmer, K. L.; Mashburn, L. M.; Singh, P. K.; Whiteley, M. Cystic Fibrosis Sputum Supports Growth and Cues Key Aspects of *Pseudomonas Aeruginosa* Physiology. *J. Bacteriol.* **2005**, *187*, 5267–5277.
- (51) Schobert, M.; Jahn, D. Anaerobic Physiology of *Pseudomonas Aeruginosa* in the Cystic Fibrosis Lung. *Int. J. Med. Microbiol.* **2010**, *300*, 549–556.
- (52) Fung, C.; Naughton, S.; Turnbull, L.; Tingpej, P.; Rose, B.; Arthur, J.; Hu, H.; Harmer, C.; Harbour, C.; Hassett, D. J.; et al. Gene Expression of *Pseudomonas Aeruginosa* in a Mucin-Containing Synthetic Growth Medium Mimicking Cystic Fibrosis Lung Sputum. *J. Med. Microbiol.* **2010**, *59*, 1089–1100.
- (53) Hrabie, J. A.; Klose, J. R.; Wink, D. A.; Keefer, L. K. New Nitric Oxide-Releasing Zwitterions Derived from Polyamines. *J. Org. Chem.* **1993**, *58*, 1472–1476.
- (54) Keefer, L. K. Nitric Oxide (NO)- and Nitroxyl (HNO)-Generating Diazeniumdiolates (NONOates): Emerging Commercial Opportunities. *Curr. Top. Med. Chem.* **2005**, *5*, 625–636.
- (55) Bansil, R.; Turner, B. S. Mucin Structure, Aggregation, Physiological Functions and Biomedical Applications. *Curr. Opin. Colloid Interface Sci.* **2006**, *11*, 164–170.
- (56) Wang, Y.; Lai, S. K.; Suk, J. S.; Pace, A.; Cone, R.; Hanes, J. Addressing the PEG Mucoadhesivity Paradox to Engineer Nanoparticles That “Slip” through the Human Mucus Barrier. *Angew. Chemie Int. Ed.* **2008**, *47*, 9726–9729.
- (57) Lai, S. K.; Wang, Y.-Y.; Hanes, J. Mucus-Penetrating Nanoparticles for Drug and Gene Delivery to Mucosal Tissues. *Adv. Drug Deliv. Rev.* **2009**, *61*, 158–171.

- (58) Hassett, D. J.; Sutton, M. D.; Schurr, M. J.; Herr, A. B.; Caldwell, C. C.; Matu, J. O. *Pseudomonas Aeruginosa* Hypoxic or Anaerobic Biofilm Infections within Cystic Fibrosis Airways. *Trends Microbiol.* **2009**, *17*, 130–138.
- (59) Worley, B. V.; Schilly, K. M.; Schoenfisch, M. H. Anti-Biofilm Efficacy of Dual-Action Nitric Oxide-Releasing Alkyl Chain Modified Poly(Amidoamine) Dendrimers. *Mol. Pharm.* **2015**, *12*, 1573–1583.
- (60) Hall-Stoodley, L.; Costerton, J. W.; Stoodley, P. Bacterial Biofilms: From the Natural Environment to Infectious Diseases. *Nat. Rev. Micro.* **2004**, *2*, 95–108.
- (61) Field, T. R.; White, A.; Elborn, J. S.; Tunney, M. M. Effect of Oxygen Limitation on the in Vitro Antimicrobial Susceptibility of Clinical Isolates of *Pseudomonas Aeruginosa* Grown Planktonically and as Biofilms. *Eur. J. Clin. Microbiol. Infect. Dis.* **2005**, *24*, 677–687.
- (62) Borriello, G.; Werner, E.; Roe, F.; Kim, A. M.; Ehrlich, G. D.; Stewart, P. S. Oxygen Limitation Contributes to Antibiotic Tolerance of *Pseudomonas Aeruginosa* in Biofilms. *Antimicrob. Agents Chemother.* **2004**, *48*, 2659–2664.
- (63) Kim, H. Bin; Jang, H.-C.; Nam, H. J.; Lee, Y. S.; Kim, B. S.; Park, W. B.; Lee, K. D.; Choi, Y. J.; Park, S. W.; Oh, M.-D.; et al. In Vitro Activities of 28 Antimicrobial Agents against *Staphylococcus Aureus* Isolates from Tertiary-Care Hospitals in Korea: A Nationwide Survey. *Antimicrob. Agents Chemother.* **2004**, *48* (4), 1124–1127.
- (64) Sletmoen, M.; Maurstad, G.; Nordgård, C. T.; Draget, K. I.; Stokke, B. T. Oligoguluronate Induced Competitive Displacement of Mucin-Alginate Interactions: Relevance for Mucolytic Function. *Soft Matter* **2011**, *8*, 8413–8421.
- (65) Nordgård, C. T.; Nonstad, U.; Olderø, M. Ø.; Espevik, T.; Draget, K. I. Alterations in Mucus Barrier Function and Matrix Structure Induced by Guluronate Oligomers. *Biomacromolecules* **2014**, *15*, 2294–2300.
- (66) Nordgård, C. T.; Draget, K. I. Oligosaccharides as Modulators of Rheology in Complex Mucous Systems. *Biomacromolecules* **2011**, *12*, 3084–3090.

CHAPTER 5: SUMMARY AND FUTURE DIRECTIONS

5.1 Summary

Cystic fibrosis is an autosomal disease that causes a deficiency in chloride secretion, ultimately disrupting mucociliary clearance and the removal of pathogenic bacteria. Chapter 1 discussed the pathophysiology of CF, current treatment methods, and the potential utility of NO-based therapies. In healthy patients, the regulation of salt concentration via the CFTR protein allows the ASL to function as an innate defense barrier in airways.¹⁻³ However, in the case of CF, a defective CFTR results in ASL dehydration, abnormal mucus accumulation, persistent bacterial infection, and chronic inflammation that altogether causes respiratory decline and irreversible lung damage.^{4,5} Current treatment methods focus on rehydrating the ASL to improve lung function and eradicating bacteria to disrupt the vicious cycle of chronic infection and lung degradation. Limitations to these current treatments, including bacterial adaptations and antibiotic resistance, motivate the development of non-traditional, novel therapies for the treatment of CF.⁶ Nitric oxide represents an attractive alternative to conventional drugs due to its antimicrobial activity and mucolytic action. Inhalation of NO gas demonstrated efficacy in small animal studies and proved safe for healthy adults at low concentrations that require multiple repeat exposures and high clinical oversight (i.e., hospitalization).^{7,8} While effective, the inconvenience and high costs associated with gaseous NO administration warrant the development of a new delivery system that could directly deliver NO to the lungs.

As an alternative delivery system, Chapter 2 focused on modifying high and low molecular weight alginate with small molecule alkyl amines for subsequent NO donor formation. The resulting NO-releasing alginate possessed diverse and tunable NO-release kinetics (0.5-13 h half-lives) dependent on the structure of the precursor alkyl amine and alginate molecular weight. Bactericidal activity against planktonic and biofilm forms of *P. aeruginosa* and *S. aureus* was dependent on both the NO-release kinetics and molecular weight of the alginate system. Nitric oxide-releasing alginate possessing slow, sustained release properties (i.e., DETA- and DPTA-modified alginate) was found to be more efficacious against bacterial biofilms, requiring lower concentration of NO-releasing alginate to elicit biocidal action. Further, low molecular weight alginate exhibited antibacterial activity at lower concentrations versus their high molecular weight counterparts. The results indicate the potential utility of the alginate biopolymer as a NO-delivery scaffold with tunable release kinetics and antibacterial activity.

Chapter 3 evaluated the impact of NO-releasing alginate on mucus rheology. Treatment of mucus with NO-releasing low molecular weight alginate reduced both the viscosity and elasticity of the mucus. The reduced viscoelasticity was found to be dependent on NO-release kinetics and dose of treatment. Of the NO-releasing alginate biopolymers, the hybrid Alg5-PAPA-DPTA/NO was most effective, possessing the necessary NO flux and sustained release to substantially reduce the viscoelasticity. Increasing the alginate dose improved efficacy, with high concentrations (~80 mg/mL) reducing mucus viscosity and elasticity most significantly. All of the NO-releasing alginates investigated were more effective at reducing viscoelasticity than chitosan, which suggesting a benefit for using a negatively charged biopolymer over a cationic scaffold. The NO-releasing alginate also exhibited a greater effect than *N*-acetyl cysteine (NAC), a common mucolytic agent, thereby requiring a lower NO dose to achieve the same reductive effect.

Lastly, Chapter 4 demonstrated the use of NO-releasing alginate as a biocidal agent against a broad-spectrum of CF-relevant pathogens (i.e., *Pseudomonas aeruginosa*, *Burkholderia cepacia* complex, *Staphylococcus aureus*, and methicillin-resistant *S. aureus*). Distinct alkyl amine functional groups allowed for tunable NO storage (0.1-0.3 $\mu\text{mol/mg}$) and release kinetics ($t_{1/2}$ 0.2-0.4 h) when measured in biological media that mimics components of CF mucus (i.e., artificial sputum media). Following treatment with NO-releasing alginate, it was determined that aerobic biofilms required greater NO doses to achieve killing versus that for anaerobic biofilms. The hybrid alginate biopolymer, Alg5-PAPA-DPTA/NO, exhibited the most potent antibacterial action (NO dose $\leq 520 \mu\text{g/mL}$) regardless of growth conditions. This low dose surpasses that required of either tobramycin ($\geq 2000 \mu\text{g/mL}$) and vancomycin ($\geq 1000 \mu\text{g/mL}$). A time-kill study with *P. aeruginosa* demonstrated that the NO-releasing hybrid alginate achieved biofilm eradication faster than tobramycin and at lower concentrations than the mono-substituted biopolymers (i.e., alginate modified with only PAPA or DPTA). Overall, the results of this study suggest the use of NO-releasing alginate in treating biofilm-based infections in CF.

5.2 Future Directions

The results presented in the previous chapters highlight the potential of biopolymer-based NO delivery as a dual-action therapy for CF. While these studies clearly demonstrate both the reductive antibacterial and mucolytic activity of NO-releasing alginates, substantial work remains to fully develop NO-based therapeutics for CF.

5.2.1 Combination therapy with current CF treatments

Combination therapy is often used for treating pulmonary infections in CF.^{9–11} While the success of this approach using combinations of conventional antibiotics against multidrug-resistant pathogens is debated, co-administration of these therapies with NO may be of benefit due to NO's multi-mechanistic antibacterial action and ability to degrade biofilm exopolysaccharide (EPS) matrices.^{12–14} Thus, assessing the utility of NO-releasing alginate as a co-administered CF therapy is an essential next step.

Simultaneous treatment of *P. aeruginosa* biofilms with the small molecule NO donor sodium nitroprusside (SNP) and tobramycin has previously been reported to improve biofilm eradication compared to single agent treatment.¹³ Reduced presence of biofilms in airways was also observed when antibiotics (i.e., tobramycin or ceftazidime) were co-administered with inhaled NO gas (5–10 ppm for 8 h per day) for CF patients. A recent study by Howlin et al. showed that pretreatment of *P. aeruginosa* biofilms with low doses of NO (~450 nM NO generated from 500 µM SNP) increased biofilm susceptibility to either tobramycin or a tobramycin-ceftazidime combination.¹² While the results of these initial studies are promising, a systematic evaluation on the effect of NO when used in combination with antibiotics is still necessary. In addition, elucidating the influence of both the biopolymeric scaffold used for NO delivery and the NO-release properties is greatly needed. The possible effects of NO-releasing alginate (i.e., synergistic, additive, indifferent, or antagonistic) with a broader range of antibiotics (e.g., tobramycin, vancomycin) should be evaluated using combination bactericidal antibiotic tests (i.e., checkerboard assays). Assays should be performed using both planktonic and biofilm forms of CF-relevant strains (e.g., multi-drug resistant *P. aeruginosa*, MRSA) to test the broad-spectrum activity of alginate-based NO therapy when combined with other antibacterial agents.

Combination time-kill assays performed alongside the checkerboard assays should facilitate quantitative determination of the effect of each antibiotic agent in conjunction with NO as a function of time. Comparison with the single agent time-kill assays will allow for a better understanding as to how NO release influences the overall effect of the NO-based therapy when co-administered with antibiotics.

5.2.2 Biophysical characterization of biofilms and CF sputum

The impact of NO-releasing alginates on mucus viscoelasticity was also evaluated using human bronchial epithelial (HBE) mucus, and the influence of key biopolymer properties (i.e., size, charge, NO-release kinetics, and dose) was examined in Chapter 3. Future studies should evaluate the ex vivo efficacy of Alg5-PAPA-DPTA/NO, the most effective biopolymer, on CF sputum – a truly representative medium containing other key mucus components such as DNA. Parallel plate rheology should be used to determine the bulk changes in elasticity and viscosity. A comparison with rhDNase I (i.e., Pulmozyme), the most commonly used mucolytic agent employed for treating CF, should be carried out to fully ascertain the relative utility of NO-releasing alginate as a mucolytic therapy. Combination treatments using both NO-based therapy and rhDNase I should be investigated to identify any potential synergistic, additive, indifferent, or antagonistic activity between the two treatment regimens. The ability of NO-releasing alginate to reduce the size of mucins and DNA can be evaluated using electrophoretic separation of CF sputum following treatment. Additionally, confocal microscopy of CF sputum samples treated with alginate should be used to examine how these materials alter mucin and DNA networks, providing insight on how the biopolymeric scaffolds with and without NO interact with the 3D networks.

The ability of the NO-based therapeutic to alter the 3D structure of the biofilm EPS matrix is also of interest. Rheological studies (e.g., sand-blasted parallel plate, cone and plate, and multiple particle tracking rheology) should be conducted to evaluate the impact of NO-releasing alginate on the viscoelastic properties of the biofilm EPS matrix. Comparison with other NO-releasing biopolymers (e.g., chitosan), non-NO-releasing biopolymer controls, and conventional antibiotic treatments (e.g., tobramycin, vancomycin) should be carried out and benchmarked.

As mucociliary clearance is a crucial aspect of the host defense in the airways, particularly in removing inhaled pathogens, characterization of how alginate-based NO delivery systems impact mucus transport should be performed. Optical coherence tomography (OCT) is a high-resolution imaging technique that can be used to monitor mucus flow and ciliary beat frequency on airway epithelium *in vitro*.^{15,16} Human bronchial epithelial cell cultures grown over approximately 6 w develop cilia and secrete mucus that accumulates over time.¹⁶ As the cells are cultured in a circular dish, the accumulated mucus is transported in a rotational pattern. Mucus flow imaging and analysis should be performed in cross-sectional slices moving across the center of the spiral for untreated culture, and cultures treated with non-NO-releasing (control) and NO-releasing alginate. The ciliary beat rate should be measured to determine how NO release affects the rate of mucus clearance.

5.2.3 Biopolymeric scaffolds for improved nitric oxide storage and release

While alginate represents an attractive material for use in pulmonary delivery due to its low toxicity and water solubility, it is limited by a relatively lower NO payload compared to other macromolecular scaffolds (e.g., dendrimers with total NO ~1 $\mu\text{mol/mg}$). Developing alternative modification strategies for alginate (e.g., modifying the hydroxyl moieties on the biopolymer backbone) and/or employing other biopolymeric delivery systems with greater NO payloads could

facilitate lower therapeutic doses to eradicate biofilms and reduce mucus viscoelasticity. In this regard, a library of NO-releasing biopolymeric systems should be created and evaluated as potential CF therapeutics.

Hyaluronic acid (HA), an anionic biopolymer found throughout the body composed of alternating β -*N*-acetyl-D-glucosamine and 1,4-linked β -D-glucuronic acid units (Figure 5.1A),¹⁷⁻²⁰ represents a potential alternative to alginate as a NO delivery scaffold. In nature, HA is found in abundance in biological fluids and tissues, and is water soluble at molecular weights up to 2.5 MDa.^{17,19} It is an essential component of the extracellular matrix (ECM) in cartilage tissues, synovial fluid, umbilical cords, and the vitreous of the eye.^{18,19} High molecular weight HA plays multiple roles within mammalian tissue, including water homeostasis, cell proliferation, and wound repair. Low molecular weight HA has been reported to have angiogenic, pro-inflammatory, and immunostimulatory properties.¹⁷⁻²⁰ As a consequence of these molecular weight dependent roles, HA has been used for a wide range of biomedical applications, including tissue engineering, drug delivery, and wound dressings. The biopolymer backbone allows for versatile modification chemistries due to its functional groups (i.e., carboxylic acid, primary and secondary alcohols).¹⁷ For example, carbodiimide chemistry can be utilized to impart secondary amine functionalization on the carboxylic acid moieties of HA with various alkyl amine functional groups to tune NO release properties. Similar to alginates, molecular weight may also influence the NO-release properties of HA. While HA is commercially available in a range of molecular weights (~6-1000 kDa), oxidative degradation could be explored to obtain even smaller biopolymer sizes (i.e., <6 kDa), similar to alginate and chitosan.^{21,22}

Another potential biopolymer system of interest is the cyclodextrin (CD) family, which are cyclic oligosaccharides comprised of α -D-glucopyranose units joined together by α -(1-

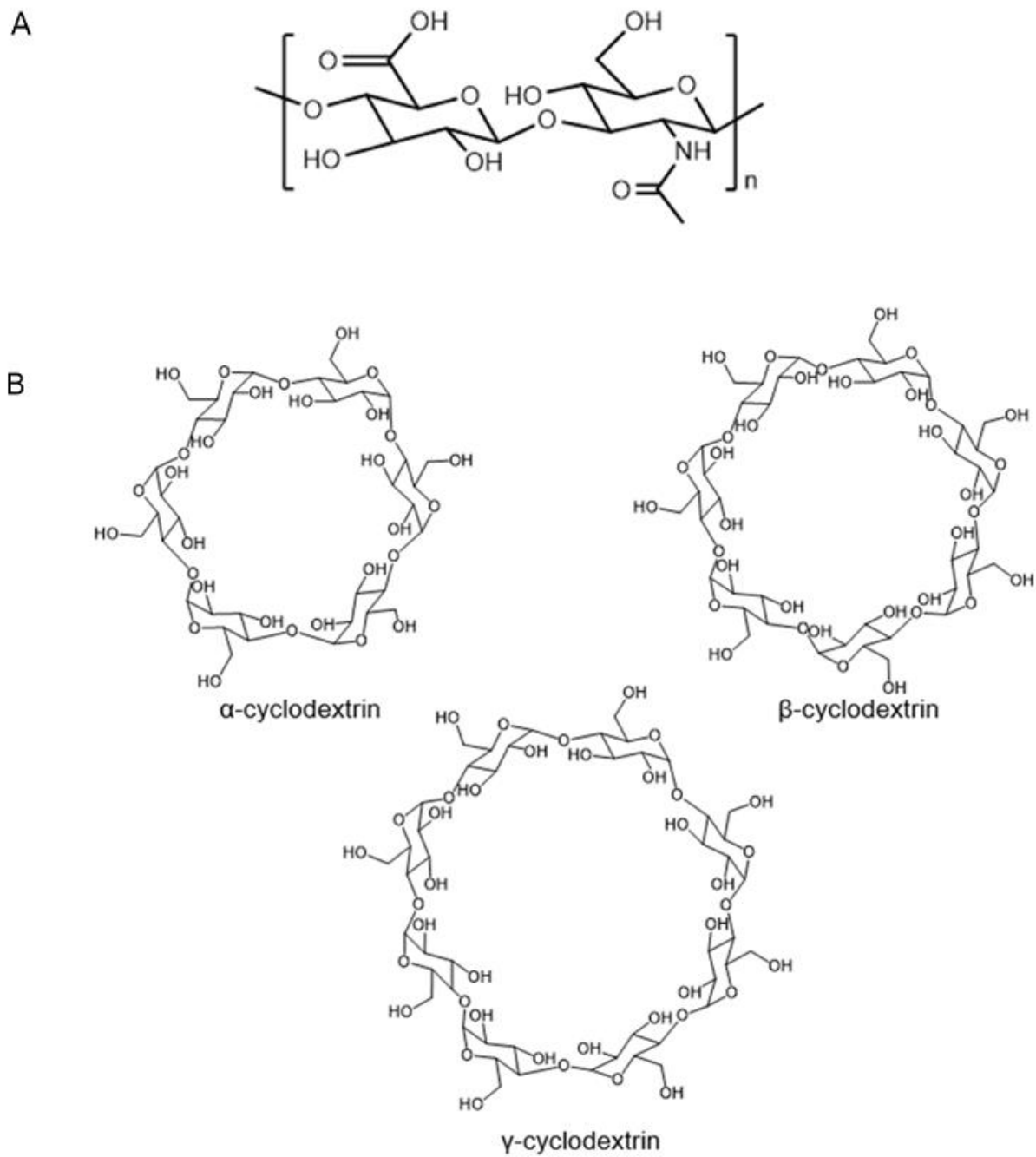


Figure 5.1 Structures of (A) hyaluronic acid and (B) cyclodextrin biopolymers.

4) linkages,²³⁻²⁷ and are highly water soluble, biodegradable, and biocompatible. Due to steric effects, α -, β -, and γ -CDs exist in nature with 6, 7, or 8 D-glucose units, respectively (Figure 5.1B). Their cyclic structure provides a hydrophobic central cavity that is attractive for the encapsulation of poorly water-soluble drugs (e.g., doxorubicin).²³⁻²⁵ A hydrophilic exterior provides enhanced water solubility. Of importance, the exterior hydroxyl groups are easily modified with functional groups ideal for NO storage and release capabilities.²⁸ The overall amphiphilicity may allow for co-delivery of different therapeutic agents used in CF (e.g., antibiotics such as rifampicin and ciprofloxacin) with NO for possible synergistic activity.

The hydrophilicity, NO-release profiles, antibacterial and mucolytic activity, and cytotoxicity for these biopolymers can be further controlled using additional surface modifications.²⁸ For example, modification with functional groups such as PAPA can minimize interactions with mucus components while amine-terminated modifications such as DPTA or SPER could promote such interactions and mitigate NO's mucolytic effect. Elemental (CHN) analysis, along with ¹H and ¹³C NMR, should be used to confirm the structure and composition of the resulting materials. The mucolytic potential and antibacterial efficacy of the NO-releasing biopolymers should be evaluated and compared to alginate and chitosan systems using previously reported methods.

5.3 Conclusion

The work presented in this dissertation describes the potential of nitric oxide (NO) as a dual-action CF therapeutic. Alginate was selected as a macromolecular scaffold for NO storage and release due to its inherently low toxicity, biocompatibility, water solubility, and ability to modulate mucus viscoelasticity. Low molecular weight (~5 kDa) alginates with high initial NO

flux and sustained release capabilities significantly altered mucus viscoelasticity at a lower concentration than the conventional mucolytic agent NAC. Further, each alginate biopolymer, regardless of the alkyl amine modification, also showed greater efficacy for reducing mucus viscoelasticity relative to the positively charged chitosan oligosaccharides, demonstrating the benefits of using a negatively charged NO delivery biopolymer for CF applications. Nitric oxide released from the alginate biopolymers also exhibited greater biocidal activity against the biofilms of four CF-relevant pathogens compared to commercially used antibiotics, indicating NO's potential as a dual-action therapeutic agent. The results of the studies presented here suggest that the use of NO-releasing alginates as a single-agent therapeutic may be an attractive alternative to currently employed therapies which must be used in combination. To further develop NO-releasing alginate as a dual-action therapeutic, additional characterization of the impact of NO-releasing alginate on biofilm rheology and mucociliary clearance should be performed. The observations derived from the previous chapters will also aid in the design of other novel NO-releasing biopolymers with potential to improve NO payloads and prolong release under CF-relevant conditions.

REFERENCES

- (1) Hassett, D. J.; Cuppoletti, J.; Trapnell, B.; Lymar, S. V.; Rowe, J. J.; Sun Yoon, S.; Hilliard, G. M.; Parvatiyar, K.; Kamani, M. C.; Wozniak, D. J.; et al. Anaerobic Metabolism and Quorum Sensing by *Pseudomonas Aeruginosa* Biofilms in Chronically Infected Cystic Fibrosis Airways: Rethinking Antibiotic Treatment Strategies and Drug Targets. *Adv. Drug Deliv. Rev.* **2002**, *54*, 1425–1443.
- (2) Samet, J. M.; Cheng, P. W. The Role of Airway Mucus in Pulmonary Toxicology. *Environ. Health Perspect.* **1994**, *102 Suppl*, 89–103.
- (3) Button, B.; Cai, L. H.; Ehre, C.; Kesimer, M.; Hill, D. B.; Sheehan, J. K.; Boucher, R. C.; Rubinstein, M. A Periciliary Brush Promotes the Lung Health by Separating the Mucus Layer from Airway Epithelia. *Science.* **2012**, *337*, 937–941.
- (4) Stoltz, D. A.; Meyerholz, D. K.; Welsh, M. J. Origins of Cystic Fibrosis Lung Disease. *N. Engl. J. Med.* **2015**, *372*, 351–362.
- (5) Boucher, R. C. New Concepts of the Pathogenesis of Cystic Fibrosis Lung Disease. *Eur. Respir. J.* **2004**, *23*, 146–158.
- (6) Høiby Bjarnsholt, T., Givskov, M., Molin, S., Ciofu, O., N. Antibiotic Resistance of Bacterial Biofilms. *Int. J. Antimicrob. Agents* **2010**, *35*, 322–332.
- (7) Miller, C.; McMullin, B.; Ghaffari, A.; Stenzler, A.; Pick, N.; Roscoe, D.; Ghahary, A.; Road, J.; Av-Gay, Y. Gaseous Nitric Oxide Bactericidal Activity Retained during Intermittent High-Dose Short Duration Exposure. *Nitric Oxide* **2009**, *20*, 16–23.
- (8) Miller, C.; Miller, M.; McMullin, B.; Regev, G.; Serghides, L.; Kain, K.; Av-Gay, Y. A Phase I Clinical Study of Inhaled Nitric Oxide in Healthy Adults. *J. Cyst. Fibros.* **2012**, *11*, 324–331.
- (9) Ciofu, O.; Tolker-Nielsen, T.; Jensen, P. Ø.; Wang, H.; Høiby, N. Antimicrobial Resistance, Respiratory Tract Infections and Role of Biofilms in Lung Infections in Cystic Fibrosis Patients. *Adv. Drug Deliv. Rev.* **2015**, *85*, 7–23.
- (10) Speert, D. P. Advances in Burkholderia Cepacia Complex. *Paediatr. Respir. Rev.* **2002**, *3*, 230–235.
- (11) Aaron, S. D.; Vandemheen, K. L.; Ferris, W.; Fergusson, D.; Tullis, E.; Haase, D.; Berthiaume, Y.; Brown, N.; Wilcox, P.; Yozghatlian, V.; et al. Combination Antibiotic Susceptibility Testing to Treat Exacerbations of Cystic Fibrosis Associated with Multiresistant Bacteria: A Randomised, Double-Blind, Controlled Clinical Trial. *Lancet* **2005**, *366*, 463–471.
- (12) Howlin, R. P.; Cathie, K.; Hall-Stoodley, L.; Cornelius, V.; Duignan, C.; Allan, R. N.;

- Fernandez, B. O.; Barraud, N.; Bruce, K. D.; Jefferies, J.; et al. Low-Dose Nitric Oxide as Targeted Anti-Biofilm Adjunctive Therapy to Treat Chronic *Pseudomonas Aeruginosa* Infection in Cystic Fibrosis. *Mol. Ther.* **2017**, *25*, 2104–2116.
- (13) Barraud, N.; Hassett, D. J.; Hwang, S. H.; Rice, S. A.; Kjelleberg, S.; Webb, J. S. Involvement of Nitric Oxide in Biofilm Dispersal of *Pseudomonas Aeruginosa*. *J. Bacteriol.* **2006**, *188*, 7344–7353.
- (14) Reighard, K. P.; Hill, D. B.; Dixon, G. A.; Worley, B. V.; Schoenfisch, M. H. Disruption and Eradication of *P. Aeruginosa* Biofilms Using Nitric Oxide-Releasing Chitosan Oligosaccharides. *Biofouling* **2015**, *31*, 775–787.
- (15) Oltmanns, U.; Palmowski, K.; Wielpütz, M.; Kahn, N.; Baroke, E.; Eberhardt, R.; Wege, S.; Wiebel, M.; Kreuter, M.; Herth, F. J. F.; et al. Optical Coherence Tomography Detects Structural Abnormalities of the Nasal Mucosa in Patients with Cystic Fibrosis. *J. Cyst. Fibros.* **2016**, *15*, 216–222.
- (16) Oldenburg, A. L.; Chhetri, R. K.; Hill, D. B.; Button, B. Monitoring Airway Mucus Flow and Ciliary Activity with Optical Coherence Tomography. *Biomed. Opt. Express* **2012**, *3*, 1978–1992.
- (17) Burdick, J. A.; Prestwich, G. D. Hyaluronic Acid Hydrogels for Biomedical Applications. *Adv. Mater.* **2011**, *23*, 41–56.
- (18) Khanlari, A.; Schulteis, J. E.; Suekama, T. C.; Detamore, M. S.; Gehrke, S. H. Designing Crosslinked Hyaluronic Acid Hydrogels with Tunable Mechanical Properties for Biomedical Applications. *J. Appl. Polym. Sci.* **2015**, *132*, 1–7.
- (19) Kogan, G.; Šoltés, L.; Stern, R.; Gemeiner, P. Hyaluronic Acid: A Natural Biopolymer with a Broad Range of Biomedical and Industrial Applications. *Biotechnol. Lett.* **2007**, *29*, 17–25.
- (20) Stern, R.; Asari, A. A.; Sugahara, K. N. Hyaluronan Fragments: An Information-Rich System. *Eur. J. Cell Biol.* **2006**, *85*, 699–715.
- (21) Mao, S.; Zhang, T.; Sun, W.; Ren, X. The Depolymerization of Sodium Alginate by Oxidative Degradation. *Pharm. Dev. Technol.* **2012**, *17*, 763–769.
- (22) Lu, Y.; Slomberg, D. L.; Schoenfisch, M. H. Nitric Oxide-Releasing Chitosan Oligosaccharides as Antibacterial Agents. *Biomaterials* **2014**, *35*, 1716–1724.
- (23) Wang, X.; Deng, L.; Cai, L.; Zhang, X.; Zheng, H.; Deng, C.; Duan, X.; Zhao, X.; Wei, Y.; Chen, L. Preparation, Characterization, Pharmacokinetics, and Bioactivity of Honokiol-in-hydroxypropyl- β -cyclodextrin-in-liposome. *J. Pharm. Sci.* **2011**, *100*, 3357–3364.
- (24) Anand, R.; Malanga, M.; Manet, I.; Manoli, F.; Tuza, K.; Aykaç, A.; Ladavière, C.;

- Fenyvesi, E.; Vargas-Berenguel, A.; Gref, R.; et al. Citric Acid- γ -Cyclodextrin Crosslinked Oligomers as Carriers for Doxorubicin Delivery. *Photochem. Photobiol. Sci.* **2013**, *12*, 1841–1854.
- (25) Lu, B.; Li, L.; Wu, J.; Wei, L.; Hou, J.; Liu, Z.; Guo, X. Synthesis of a Dual PH and Temperature Responsive Star Triblock Copolymer Based on β -Cyclodextrins for Controlled Intracellular Doxorubicin Delivery Release. *New J. Chem.* **2016**, *40*, 8397–8407.
- (26) Szejtli, J. Introduction and General Overview of Cyclodextrin Chemistry. *Chem. Rev.* **1998**, *98*, 1743–1754.
- (27) Crini, G. Review: A History of Cyclodextrins. *Chem. Rev.* **2014**, *114*, 10940–10975.
- (28) Davis, M. E.; Brewster, M. E. Cyclodextrin-Based Pharmaceuticals: Past, Present and Future. *Nat. Rev. Drug Discov.* **2004**, *3*, 1023–1035.

Calculation of % Modification for Alg5-PAPA-DPTA

The % PAPA modification was first determined from the hybrid scaffold by integrating the ^1H NMR peak at 0.83 ppm corresponding to the methyl terminal group of PAPA (I_{methyl}):

$$\% \text{ PAPA} = \frac{I_{\text{methyl}}}{3} \times 100 \% \quad (\text{eq. 1})$$

From the ^1H NMR spectra, PAPA modification for the alginate hybrid scaffold was found to be 43%. The % N from the PAPA modification was then determined from the % PAPA value as follows:

$$\% N_{\text{PAPA}} = (\% \text{ PAPA} \times \text{theoretical \% } N_{\text{PAPA}}) \times 100 \% \quad (\text{eq. 2})$$

Where theoretical % N_{PAPA} is the theoretical % N value corresponding to 100 % PAPA modification (i.e., 9.6 %) and was determined following the equation below:

$$\text{theoretical \% } N_{\text{PAPA}} = \frac{\# \text{ of } N \text{ in PAPA} \times \text{mass of } N}{\text{MW of PAPA-modified Alg monomer}} \times 100 \% \quad (\text{eq. 3})$$

The % N_{PAPA} was found to have a value of 4.1%. Next, the % N from the DPTA modification was calculated by subtracting the % N_{PAPA} from the total % N for the hybrid alginate as determined by CHN.

$$\% N_{\text{DPTA}} = \% N_{\text{total}} - \% N_{\text{PAPA}} \quad (\text{eq. 4})$$

Using the equation, % N_{DPTA} was found to be 7.1%. The % DPTA modification of the scaffold was determined using the equation below:

$$\% \text{ DPTA} = \frac{\% N_{\text{DPTA}}}{\text{theoretical \% } N_{\text{DPTA}}} \times 100 \% \quad (\text{eq. 5})$$

Where the theoretical % N_{DPTA} (i.e., 14.1 %) was determined following eq. 2 for the DPTA modification. From the equation, the hybrid scaffold had 50% DPTA modification, giving an overall 93% total modification of the scaffold.

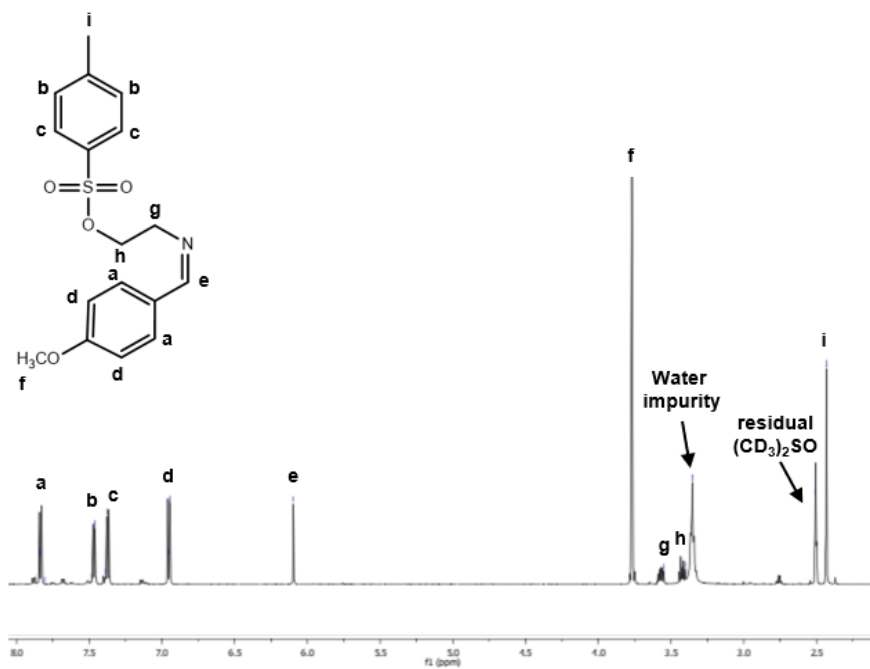


Figure A.1 Representative ¹H NMR spectra of tosyl-modified ethanolamine Schiff base (TES).

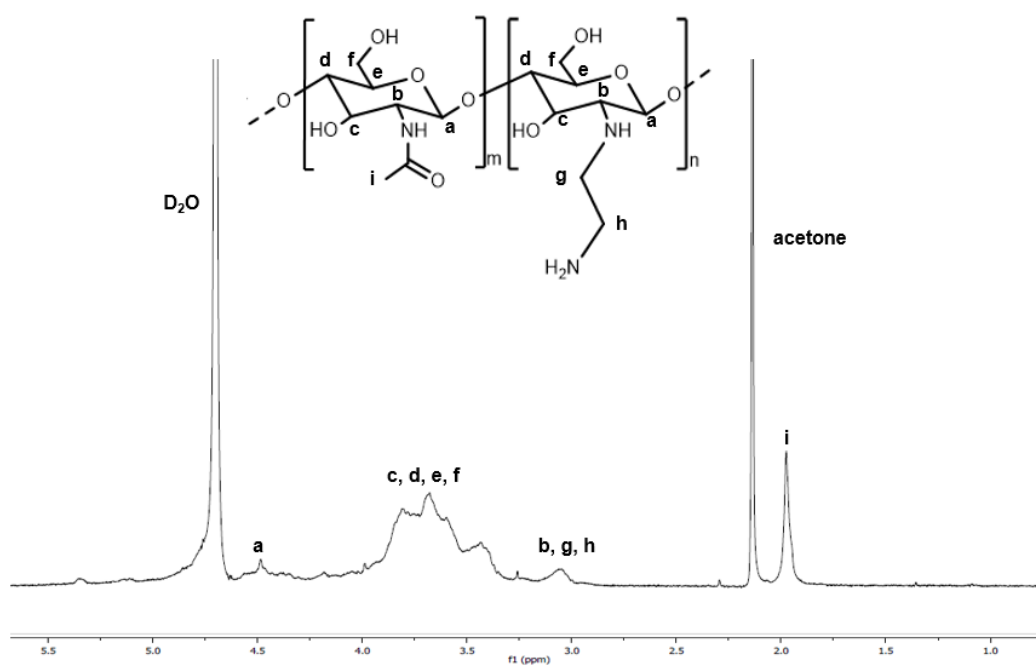


Figure A.2 Representative ^1H NMR spectra of COS-EA.

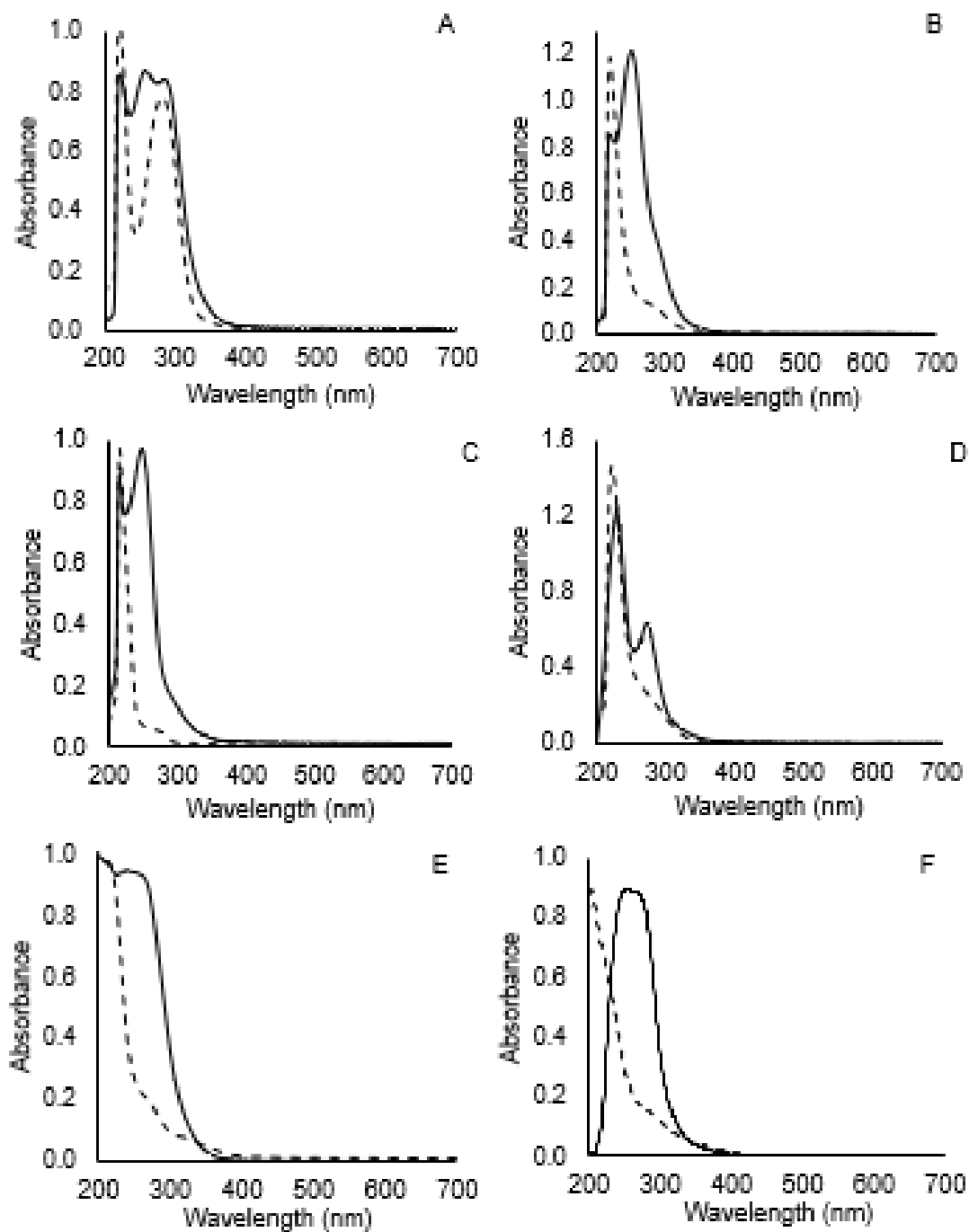


Figure A.3 Representative UV-vis spectra for secondary amine- (dash) and *N*-diazoniumdiolate-modified (solid) (for (A) Alg5-DETA, (B) Alg5-DPTA, (C) Alg5-SPER, (D), Alg5-PAPA, (E) Alg5-PAPA-DPTA, and (F) chitosan oligosaccharides (COS-EA).

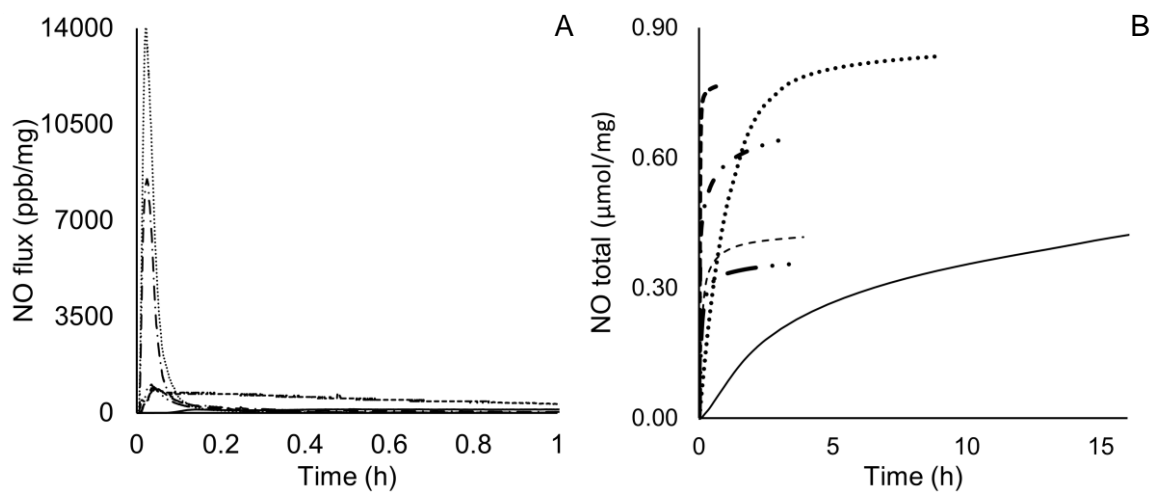


Figure A.4 (A) Real time NO-release profiles for the first 1 h and (B) plot of total NO release vs. time for representative biopolymers Alg5-DETA/NO (—), Alg5-DPTA/NO (— —), Alg5-PAPA-DPTA/NO (— ■ —), Alg5-PAPA/NO (▪), Alg5-SPER/NO (— ■ ■), and COS-EA/NO (•) measured via chemiluminescence in PBS pH 6.5.

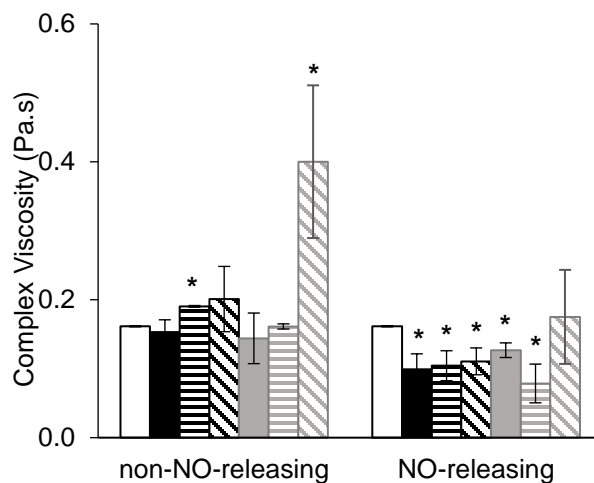


Figure A.5 Complex viscosity of 3 wt% HBE mucus following treatment with Alg5-DETA (black solid), Alg5-DPTA (black horizontal), Alg5-SPER (black diagonal), Alg5-PAPA (gray solid), Alg5-PAPA-DPTA (gray horizontal), and COS-EA (gray diagonal). Values presented as the mean standard deviation of the mean for $n = 3$ experiments. Asterisks (*) indicate significant differences ($p < 0.05$) relative to untreated sample (hollow).

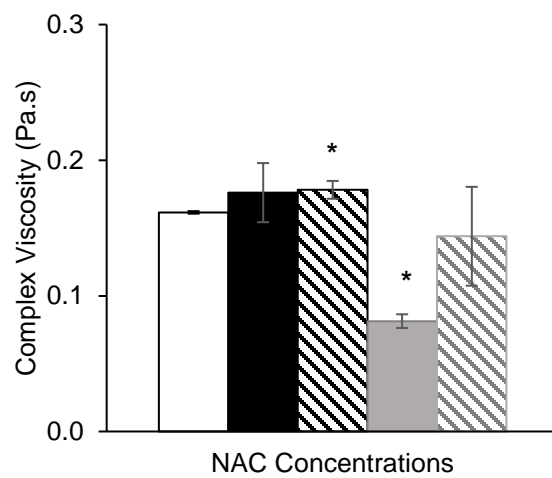


Figure A.6 Complex viscosity of 3 wt% HBE mucus following treatment with NAC 0.1 wt% (black solid), NAC 0.2 wt% (black diagonal), NAC 10 wt% (gray solid), and NAC 20 wt% (gray diagonal). Values presented as the mean standard deviation of the mean for $n = 3$ experiments. Asterisks (*) indicate significant differences ($p < 0.05$) relative to untreated sample (hollow).